COMBUSTION MODELING IN THE RISER OF FLUIDIZED BED COMBUSTOR FOR THAR COAL AND ITS BLENDS FOR EMISSION CONTROL

JAWWAD ABDULLAH BUTT

02-282162-001

BAHRIA UNIVERSITY, KARACHI CAMPUS

COMBUSTION MODELING IN THE RISER OF FLUIDIZED BED COMBUSTOR FOR THAR COAL AND ITS BLENDS FOR EMISSION CONTROL

JAWWAD ABDULLAH BUTT

02-282162-001

A thesis submitted in fulfillment of the

requirements for the award of the degree of

Doctor of Philosophy (Environmental Science)

Department of Earth and Environmental Sciences

BAHRIA UNIVERSITY, KARACHI CAMPUS

NOVEMBER 2023

Approval for Examination

Scholar's Name: Jawwad Abdullah Butt Registration No. 20455

Programme of Study: PhD in Environmental Sciences

Thesis Title: Combustion Modeling in the Riser of Fluidized Bed Combustor for Thar Coal and its Blends for Emission Control

It is certify that the above scholar's thesis has been completed to my satisfaction and, to my belief, its standard is appropriate for examination. I have also conducted plagiarism test of the thesis using HEC prescribed software and found similarity index 13 % that is within the permissible limit set by the HEC for PhD degree thesis. I have also found in a format recognized by the BU for the PhD thesis.

Principle Supervisor's Signature: _____

Date: 07 November 2023 .

Name: Professor Dr. Yasmin Nergis

Author's Declaration

I Jawwad Abdullah Butt hereby state that my PhD thesis titled "Combustion Modeling in the Riser of Fluidized Bed Combustor for Thar Coal and its Blends for Emission Control" is my own work and has not been submitted previously by me for taking my degree from this university Bahria University or anywhere else in the country/world.

At any time if my statement is found to be incorrect even after my graduation, the University has right to withdraw/cancel my PhD degree.

Name of Scholar: Jawwad Abdullah Butt

Date: 07 November 2023

Plagiarism Undertaking

I, solemnly declare that research work presented in the thesis title

Combustion Modeling in the Riser of Fluidized Bed Combustor for Thar Coal and its Blends for Emission Control

Is solely my research work with no significant contribution from any other person. Small contribution/help wherever taken has been duly acknowledged and that complete thesis has been written by me.

I understand zero tolerance policy of HEC and Bahria University towards plagiarism. Therefore, I as an Author of the above titled thesis declare that no portion of my thesis has been plagiarized and any material used as reference is properly referred/ cited.

I undertake that if I am found guilty of any formal plagiarism in the above tilted thesis even after award of PhD degree university research the right to withdraw / revoke my PhD degree and that HEC and the university has the right to publish my name on the HEC/University website on which name of scholars are placed who submitted plagiarized thesis.

Scholar/ Author`s Sign: _____

Name of the Scholar: Jawwad Abdullah Butt

DEDICATION

This thesis is dedicated to my late Father, beloved Mother, who worked very hard throughout their life, supporting me to complete my education, and the rest of all my family, for always believing in me, inspiring me, and encouraging me, to reach higher to achieve my goals.

ACKNOWLEDGEMENT

All praises for Allah, the Most Beneficent, and Ever Merciful. Who is the entire source of knowledge and wisdom endowed to mankind and who guides me in the darkness and helps me in difficulties. I am thankful to Almighty ALLAH, who gave me the potency, courage, wisdom, knowledge and empowered me to carry out this research work and complete the thesis for my Ph.D. Peace and blessings of Allah be upon the Holy Prophet, Muhammad (SAW), who exhorted his followers to seek knowledge from cradle to grave.

I am obliged to thank my Honorable Supervisor Prof. Dr. Yasmin Nergis (Sr. Professor and Head of ERC, Bahria University Karachi Campus Pakistan) whose guidance, interest and cooperation with me throughout the research and entire phase of my studies. I would like to thank Prof. Dr. Ahmad Hussain (Professor and Dean Faculty of Engineering and Applied Sciences, DHA Suffa University, Karachi-Pakistan) who's constructive ideas, guidance, technical support and encouragement regarding the experimental studies, design and modeling of the CFBC riser. I would also like to thank Dr. Salma Hamza (Head of Department E&ES, Bahria University Karachi Campus Pakistan) for her administrative guidance and cooperation. My sincere thanks to all staff of Environmental Research Center, Bahria University Karachi Campus for their support and cooperation in experimental work.

I am also thankful to all my family and friends, who have been always with me in the time when I needed them, especially for their encouragement and moral support.

Lastly, I feel overwhelmed by the blessings, love and trust given by my parents and the endless support given by my family members.

ABSTRACT

Pakistan has faced a prolonged shortage of energy for the past several years. However, Pakistan is blessed with enormous coal reserves (185 billion tonnes), it is needed to utilize the latest technology for coal combustion. The research study aims to evaluate the physicochemical characterization of low-rank Thar coal to understand the combustion behavior and model the combustion performance in a circulating fluidized bed riser by using ANSYS FLUENT software. Computational fluid dynamics (CFD) analysis of Thar coal has been done to minimize emissions and improve combustion efficiency. This study also examines the physicochemical characteristics of rice husk biomass and its blends with Thar lignite coal for combustion and determines the influence of these blends' proportions on pollution. Thermo-chemical characteristics of Thar coal were determined from a large number of Thar coal samples from Block II, and pyrolysis properties were determined with the chemical configuration of coal ashes as per standard methods. Using the Thermogravimetric (TGA) analysis, the pyrolytic heating rate and temperature were established, which have a significant effect on the pyrolysis of Thar coal. Kinetic constraints (frequency factor and activation energy) were obtained by curve-fitting the TGA data. Using these kinetic constraints, a one-step global model was used to forecast the pyrolytic transformation. In the co-combustion, it was found that rice husk contains a higher content of volatile matter, lowest in moisture and sulfur, and has higher ash contents. The blends of coal with rice husk in weight fractions of 90:10 (CRh-1), 80:20 (CRh-2), and 70:30 (CRh-3) were also characterized. The analysis revealed that 70:30 (CRh-3) contained the lowest elemental sulfur, NOx, and SOx emissions. A CFD model was developed to simulate the hydrodynamics of gas-solid flow in a circulating fluidized bed riser using the

ANSYS FLUENT software. The effect of several exit shapes of the riser was studied using a mathematical parametric investigation of the two-phase gas-solid stream hydrodynamics of a CFB riser. The CFD model for the gas segment and the viscosity of static particles in the solids segment with a k-e turbulence model displayed virtuous mixing performance. These outcomes were found to be beneficial for the additional progress of gas-solid flow modeling in the riser. For combustion modeling, the FLIC code was found to be precise in simulating coal bed combustion, and the FLIC code's outcomes were imported into the FLUENT database. The maximum temperature inside the compartment, according to the FLUENT results, was around 1440K (1166^{o}C), at the primary burning sector in the bed center. The peak value in the center-oriented riser/combustor was 3.3 m/s, as determined from velocity contours. The CO and CO_2 mass fraction contours showed that it is concentrated in the center geometry, and a lower CO concentration was found in the parallel geometry. The contours indicate the amount of NOx at the highest level of around 31 ppm, while the parallel geometry establishes the lowest level at around 15 ppm. The Circulating Fluidized Bed Combustor is found to be the most advantageous and effective technology for producing power from Thar lignite coal while simultaneously reducing SOx and NOx emissions.

TABLE OF CONTENTS

CHAPTER-4 RESULTS AND DISCUSION

LIST OF TABLES

LIST OF FIGURES

LIST OF ABBREVIATIONS

CFD	Computational Fluid Dynamics
FVM	Finite Volume Method
2-D	Two Dimensional
CO	Carbon Monoxide
CO_2	Carbon Dioxide
SO_2	Sulfur Dioxide
SO_X	Oxide of Sulfur
SO_3	Sulfur Trioxide
NO_X	Oxide of Nitrogen
NO	Nitric Oxide
NO_2	Nitrogen Dioxide
O_2	Oxygen
GWh	Gigawatt hours
MW	Megawatt
ASTM	American Society for Testing and Materials
TWh	Terawatt Hour(s)
TGA	Thermogravimetric Analysis
mm	millimeter
Ad	As-determined
AR	As-received

ADL	Air-Dry Loss
DAF	Dry Ash Free
USEPA	United States Environmental Protection Agency
FLIC	Fluid Dynamic Incinerator Code
FLIC	Solid Bed Combustion Simulation
CFBC	Circulating Fluidized Bed Combustion
EMMM	Eulerian Multiphase Mixture Model
MTM	Mixture Turbulence Model
TL	Thar Lignite
RH	Rice Husk
FCC	Fluid Catalytic Cracking
H_2	Hydrogen
H_20	Dihydrogen Monoxide (Water)
HCN	Hydrogen Cyanide
NH_3	Ammonia
SiO_2	Silicon Dioxide
Al_2O_3	Aluminum Oxide
Fe_2O_3	Ferric Oxide
Na_2O	Sodium Oxide
CaO	Calcium Oxide
MgO	Magnesium Oxide
K_2O	Potassium Oxide
HCL	Hydrochloric Acid
HNO_3	Nitric Acid
Mt	Metric ton
P	Pressure
T	Temperature

H	Hydrogen
N	Nitrogen
S	Sulfur
ppm	Part Per Million
mg/Nm^3	Milligrams Per Cubic Meter
SEQS	Sindh Environmental Quality Standards
NoGL	No Guideline Limits Available
CRh-1	Coal-Rice Husk (90:10)
CRh-2	Coal-Rice Husk (90:20)
CRh-3	Coal-Rice Husk (90:30)
RFO	Residual Furnace Oil
RLNG	Regasified Liquefied Natural Gas

LIST OF SYMBOLS

d	Diameter (m)
V	Volume (m^3)
α	Volume Fraction
ρ	Density of Fluid (kg/m^3)
v	Velocity (m/s)
p	Pressure (Pa)
$\bar{\bar{\tau}}$	Stress-strain Tensor (Pa)
$\vec{g}$	Acceleration due to Gravity (m/s^2)
F	Force (N)
μ	Viscosity (kg/m. s)
h	Specific Enthalpy (J/kg)
q	Heat Flux (J)
Sq	Source Term (kg/s)
ΔH^0	Standard Enthalpy
KIs	The Fluid-solid and Solid-Solid Exchange Coefficient
τp	Particulate Relaxation Time (s)
Re	Reynolds Number

egs	Coefficient of Restitution
g0,ls	Radial Distribution Co-efficient
Cfr,ls	Coefficient of Friction Between the lth and Solid Phase Particles
Θs	Solid Phase Granular Temperature (m^2/s^2)
g0	Radial Distribution Function
μs	Solid Shear Viscosity (kg/m. s)
μs,col	Collision Viscosity (kg/m. s)
μs,kin	Kinetic Viscosity (kg/m. s)
μs,fr	Frictional Viscosity (kg/m. s)
λs	Bulk Viscosity (kg/m. s)
ϕ	Angle of Internal Friction (deg)
KΘs	Diffusion Co-efficient (kg/m.s)
YΘs	Collisional Dissipation of Energy (J)
Φls	Energy Exchange Between Lth Solid Phase and sth solid Phase (J)
$\vec{U}$ q	Phase-weighted Velocity (m/s)
εq	Dissipation Rate (m^{-2}/s^{-3})
Gk,q	Turbulence Kinetic Energy (m^2/s^2)
τF,pq	Characteristic Relaxation Time (s
ΓØ	Diffusion Co-efficient for ϕ
∇	Gradient
Gk	Generation of Turbulence Kinetic Energy due to the Mean Velocity Gradients

Gb	Generation of Turbulence Kinetic Energy due to Buoyancy
Ciε	Constants
m/s	Meter per second
σk	Turbulent Prandtl Numbers For k
σε	Turbulent Prandtl Numbers For ε
β	Coefficient of Thermal Expansion
Prt	Turbulent Prandtl Number
ppmv	Parts Per Million Volume
Yi	Mass Fraction of Species
N	Total Number of Phases
R	Rate of Reaction
T	Temperature (K)
K	Rate Constant
v'	Stoichiometric coefficient of reactant
k-ε	*K*-epsilon
%	Percent
kcal/Kg	Kilo Calories per Kilogram
CR_h	Coal-Rice Husk
A	Intensity Element (min^{-1})
E	Pyrolytic Procedure's Initiation Energy (J/mol)
R	Globally Gas Constant (J/mol K)
w_o, w, w_f	Primary, Definite and Ending Weights (mg)
β	Heating Frequency

Fr_R	Froude Number
R	Radius
$\bar{u}_{st}$	Cross-Section Normal Velocity
kJ/mol	Kilojoules Per Mole
wt%	Weight percent
vol %	Volume percent

LIST OF APPENDICES

CHAPTER 1

INTRODUCTION

1.1 Background of the Study

Pakistan's energy requirements are enormous, and the prolonged power scarcity is one of the main concerns for the constituency (EIU, 2017). The ambition for fast economic growth, the key to rapid industrialization combined with increasing urbanization and development in technology are responsible for increasing the demand for power or energy (Moti et al., 2012; Mal et al., 2021). In the current perspective, all over the world, fossil fuels bring about 80% of energy supplies (Gielen et al., 2019).

Electricity makes a significant contribution to economic growth, and the power sector is a critical component of any economy. Delivering appropriate, consistent, and reasonable electric power is important for economic growth, humanoid wellbeing, improved living ethics, and long-term environmental goals (Nazar et al., 2021). The usage of energy has enlarged due to numerous innovations and modernizations of communal usage made in the previous era. Hence, nearly all humanoid events are more energy dependent (NTDC, 2021). For developing countries, the energy mandate has been enlarged due to an increase in trade, efficient cultivation, increased business, and better transport. Pakistan is reliant on energy imports due to a lack of investment in native assets such as natural gas, hydropower, biomass, and lignite coal (PES, 2021).

Pakistan's major energy source has been driven by indigenous and imported fossil fuels for decades. To meet energy demand, gas and oil made up three-quarters of the total energy mix. Natural gas has remained an important source of primary energy; however, as local natural gas assets are rapidly depleted, dependency on imported LNG and oil is increasing, putting a strain on foreign exchange reserves (IEP, 2022). Coal has long been utilized in power generation and other industries, such as brick kilns and cement plants. Several developing economies rely on coal for electricity production and supply because it is safe, cheap, and reliable. As a result, it is critical to ensure that coal is used effectively and with the least amount of environmental impact (Zhang, 2021). In the near future, Pakistan is likely to serve as a global energy and trade corridor because of its strategic location (Farooqui, 2014). Thus, with additional social, political, and economic aspects, Pakistan must make sure its power provisions fulfill the requirements of the state, not merely for sustaining financial development but also for underneath global and regional economic advantages (Raheem et al., 2016).

Sustainable delivery of power to meet the present and upcoming industrial and domestic requirements in Pakistan will depend on full-scale energy production from altered resources to create major inputs to the supply chain. Present power production has an enormous economic load on the country’s budget because of the import of oil to maintain the present energy mix, and the condition is amplified by the fast decline of gas resources (Naseem, 2015). Pakistan has a significant coal deposit to fulfill the country's future coal needs. Coal-fired power plants have displaced a significant amount of oil and gas in the industrialized division. To meet the predictable requirement, exploiting local assets, such as the Thar coalfield, a 100,000 MW production capability asset, might be the feasible answer (Masih, 2018).

Moreover, to meet energy demand, fossil energy sources are used and various pollutants are generated. These pollutant gases cause different effects on the environment, including the greenhouse effect, climate change, and global warming (Atimtay, 2003; Abdeshahian et al., 2016; Bariani et al., 2020). The severe energy crisis also causes advers economic and social impacts. This directly affected industrial, commercial, and population

activities (Naseem, 2015). In countries like India, Pakistan, and Bulgaria, burning native lignite with biomass or high-quality coals could help to reduce energy production rates and low discharges, allowing for more energy to be delivered at a reasonable cost. As assets become depleted, the grade of coal is declining; therefore, more lignite, bituminous, and sub-bituminous coals are being burnt in power plants (Zhang, 2021). The environmental effects of energy schemes contain local, regional, and worldwide emission pollution from the burning of fuels, climate change, and effects on the veracity and stability of diverse environments. Pakistan has enormous coal reserves and needs to recognize the latest technology concerning coal and biomass. Co-combustion is receiving too much attention in electricity production and control of pollution (Siddique et al., 2013; Mal et al., 2021). Coal with biomass co-combustion has a high capability to fulfill the energy requirement. Circulating fluidized bed technology might be applied for the consumption of Pakistani coal or co-combustion to reduce the prevalent energy crises (Shahzad et al., 2015). For developing nations, such as Pakistan, where lignite assets are abundant and power demand is increasing quickly, consuming local lignite might also support generating jobs and improve the local economy (Zhang, 2021).

Research data on Thar coal and other coal from Pakistan is relatively limited. This study is aimed at adding new knowledge for the efficient utilization of Thar coal with minimal environmental effects.

1.1.1 Global Energy Overview

Universally, energy is widely recognized as one of the most important aspects of communal well-being and a necessary part of long-term growth. When it comes to supplying consumers with clean, sustainable, and inexpensive energy, a stable energy resource and demand are critical factors for any government (IEP, 2022). Energy reliability is define by the World Energy Council as the management of primary energy sources from both internal and external sources, the consistency of the energy structure, and the ability to meet current and future demand (NTDC, 2021). Following a slight incline in 2020, the worldwide electricity mandate was enlarged by 6% in 2021. It was the largest annual rise (nearly 1500 TWh) and the highest % increase since the economic downturn in 2010. A

rapid economic recovery, along with more intense climate conditions than in 2020, as well as a colder-than-average winter, increased global electricity demand. The industrial division subscribed to the maximum demand growth, trailed by the commercial and facilities division and then the residential division (IEA, 2022). Coal has played and contributed an important role in our daily survival. As per the International Energy Agency (IEA), coal delivers 28% of worldwide prime energy requirements and generates above 37% of global electricity (IPCC, 2018; IEA, 2020). The global energy mix is shown in figure 1.1.

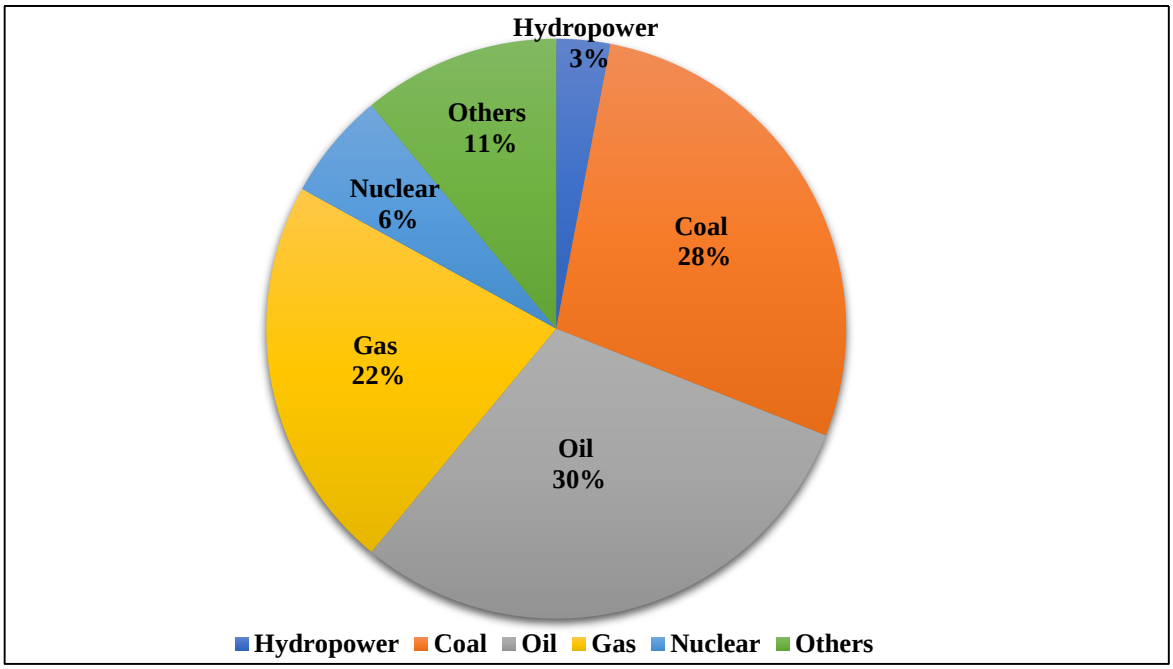

Figure 1 Global Energy Mix (IEA, 2020)

In general, coal is the best available and most inexpensive energy fuel, with the potential to develop into the most consistent and simply available energy or power source. It's also able to make essential input to global energy security (Zhang, 2021a). The harmful effects of coal on the surrounding environment are due to the emission of different pollutants like SO_X, NO_X, CO, CO_2, and particulate matter, and some heavy metals (Diego, 2015). The present's use of coal makes it a challenge to reduce air pollutants from the coal power plant. Therefore, it's essential to make a control mechanism or tools to decrease these harmful coal emissions (Zheng, 2011). Possible reductions in greenhouse gas

emissions, especially carbon dioxide, are significantly gaining attention worldwide (Diego, 2015). Clean coal technology will be significantly more expensive. As such, it's unlikely to deliver a parsimoniously feasible solution for CO_2 and other contamination from coal-based power production. In numerous portions of the world, there is rising stress on the better arrangement of renewables such as wind and solar power. Though both are reliant on weather and hence, inherently irregular in their processes. This means that there is a requirement for a protected backup source of power to recompense for small or fluctuating stages of output from renewables and deliver constancy to the network (Mills, 2021). Considering all the above facts and challenges, current research is focused on mechanisms or modeling that especially reduce emissions.

1.1.2 Energy Status in Pakistan

The World Energy Council has Pakistan ranked 99th out of 110 countries in terms of energy security for 2020 (NTDC, 2021). Pakistan imports one-third of its energy in the form of RLNG, oil, and coal. Currently, imported fuel is utilized to produce energy for 47 percent of the installed capacity. In the current economic environment, Pakistan is in a position of energy uncertainty. Great dependence on foreign fuel for secure energy sources not only upsurges the foreign bill but also places Pakistan vulnerable to constantly varying international and geopolitical factors (NTDC, 2021).

According to Pakistan's Economic Survey for 2019–20, the connected power production volume touched 37,000 MW in 2020 (Bhutta, 2020). The total demand from industrial and residential domains is estimated to be around 25,000 MW; however, the transmission and supply volume is stuck at around 22,000 MW (Rehman, 2020). At peak demand, this indicates a shortage of around 3,000 MW. This additional 3,000 MW cannot be delivered, although the country's maximum demand is met by the country's installed capacity of roughly 37,000 MW. As per the economic forum, the energy panel forecasts that electricity demand in Pakistan in 2025 will be around 44 GW and in 2030 will be around 65 GW (Shabbir, 2018) as shown in figure 1.2.

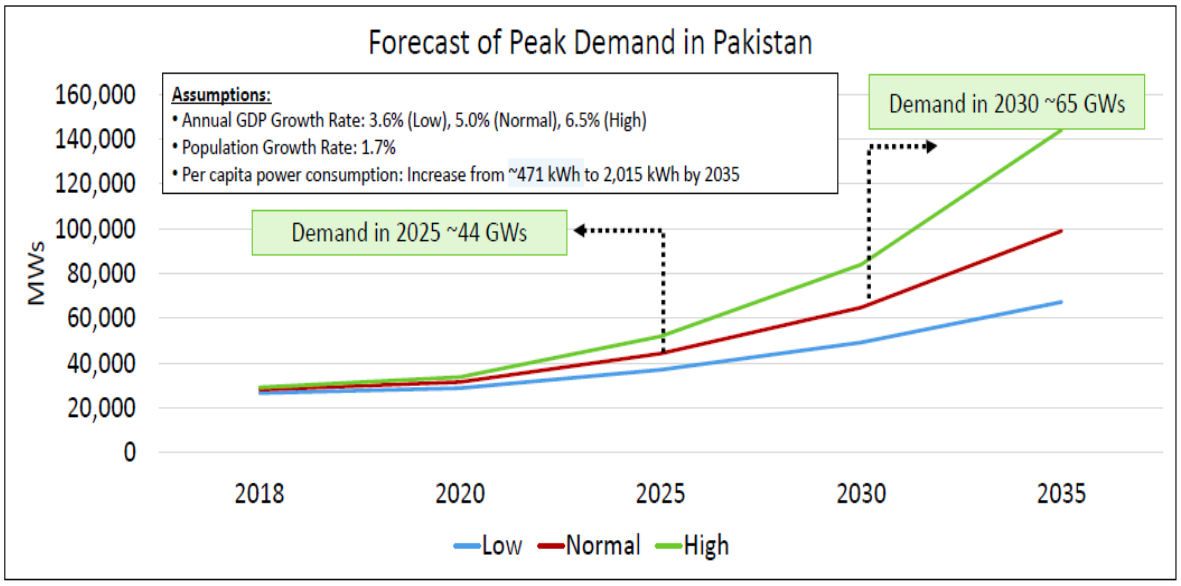

Figure 1.2 Pakistan Power Peak Demand Forecast (2018-2035) (Shabbir, 2018)

Underneath these situations, Pakistani people have been forced to recognize the planned power load shading for many hours per day in different areas of Pakistan. The electricity load shading has begun problems in the public's daily lives and the growth of cultivation, which requires electricity for agronomy. The industry has also borne an enormous loss because of power load shading, initiating joblessness, and the elevated price of finished goods (Ali et al., 2018). Pakistan is rich with energy resources, including fossil fuels, non-renewable gas reserves, oil reserves, and coal reserves, as well as renewable energy resources like hydropower, wind energy, solar, etc.

Pakistan's fuel mixture has contained nearly 70% of all power generation using thermal bases such as gas and furnace oil since past eras. Pakistan's fuel mix has transformed intensely after the Chinese-sponsored power ventures that have been ongoing since 2017. As per Arif Habib's limited research (AHL, 2021), power generation decreased through the calendar year, 2020 compared to last year, due to reduced requests due to the besieged economy combined with the effects of the COVID-19 epidemic. Major contributor's shares during the calendar year 2022 are revealed in Table 1.1 and Figure 1.3.

In the current energy mix, the hydro share has deteriorated in 2022 as compared to last year. Presently, thermal has the main share in electricity production (NTDC, 2022). Pakistan's dependency on the total energy mix of natural gas was reduced because of deteriorating natural gas assets and the start of RLNG. The noteworthy development of RLNG usage in the energy mix has facilitated a better stream to numerous power plants. The portion of coal and renewable energy has progressively improved over the years. The fuel-wise break-up as of May 2022 is shown in Table 1.1 and Figure 1.3, as well as the projected fuel-wise break-up of 2025 (NTDC, 2022).

Table 1.1: Fuel-wise Installed Capacity breakup 2022 (NTDC, 2022)

Fuel	**Installed (MW)**	**Percentage Share (%)**
Hydel	10,251	24.7
RLNG	9,884	23.8
RFO	5,958	14.3
Coal	5,332	12.8
Gas	3,536	8.5
Nuclear	3,647	8.8
Wind	1,985	4.8
Solar	600	1.4
Bagasse	364	0.9
Total	**41,557**	**100.0**

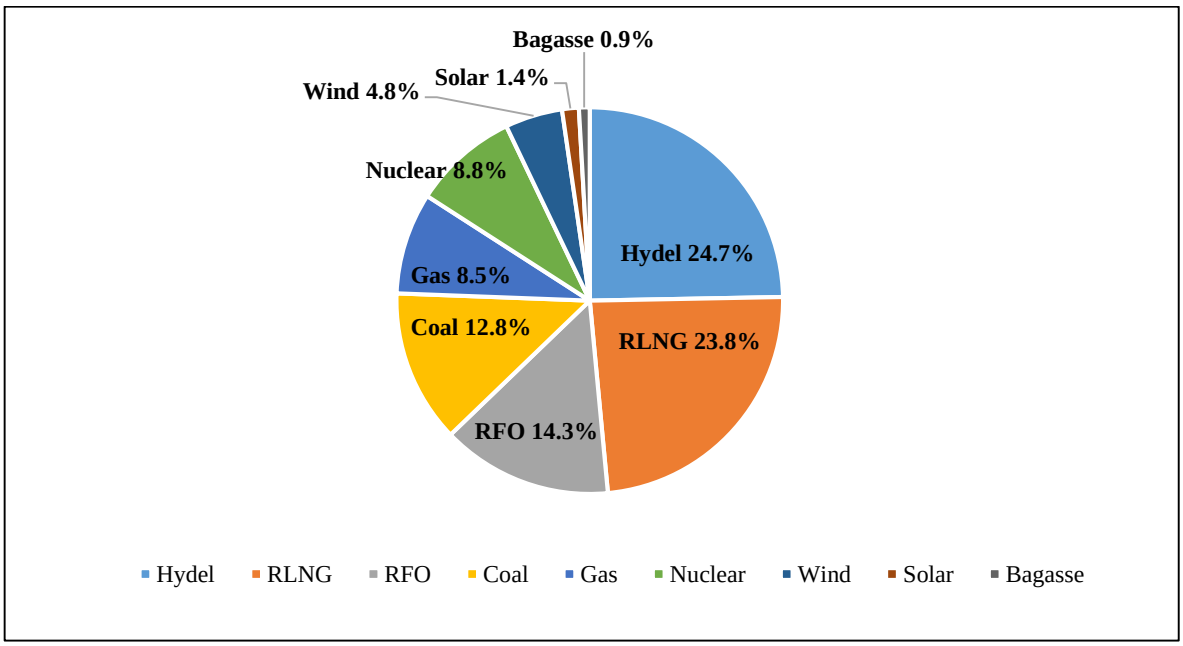

RLNG = Regasified Liquefied Natural Gas

Figure 1.3: Pakistan Fuel Wise Break-Up as of May 2022 (NTDC, 2022)

Pakistan projected a fuel-wise break-up in 2025, as shown in Figure 1.4, and electricity consumption sector-wise, as shown in Figure 1.5.

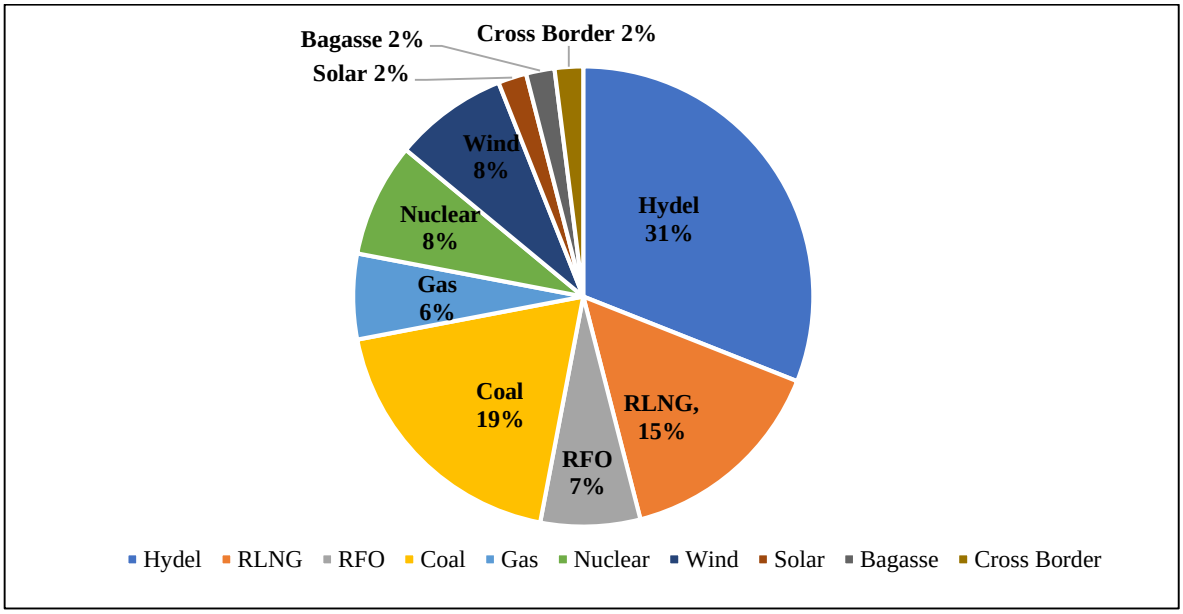

RLNG = Regasified Liquefied Natural Gas

Figure 1.4: Pakistan Fuel Wise Break-Up Projected 2025 (NTDC, 2021)

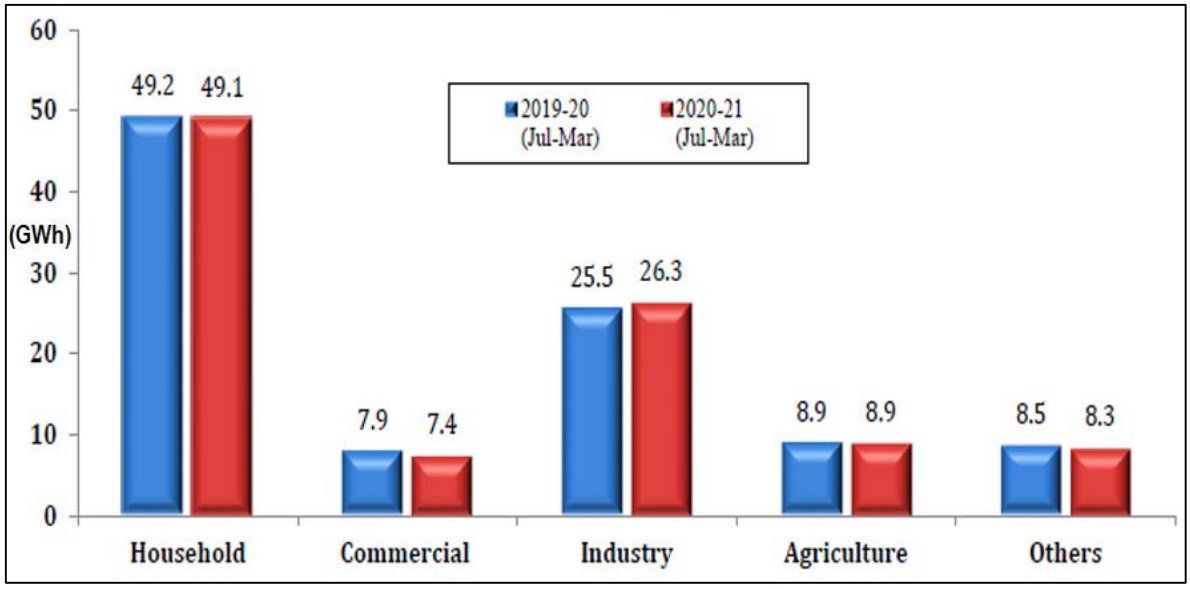

Figure 1.5: Share in Electricity Consumption (GWh) Pakistan 2019-2021 (NTDC, 2021)

1.1.3 Coal as a fuel

Coal is the most extensively formed mineral on earth and still produces over a third of the world's electricity. It has been mined for over 100 years, and possibly 300 billion tons (Bt) have been produced (Chapman, 2022). Thermal coal is the fuel that produce around 37% of worldwide electricity supplies (World Coal Association, 2021). Coal has persisted as an important energy source for various years, particularly as emission reduction technologies are progressively applied (Manook, 2021). Hence, the easy availability of coal remains the main problem in determining coal's role in the energy mix. Coal categorization and classification schemes vary in detail all over the world. There are four main grades of coal in a directive of quality: anthracite, bituminous, sub-bituminous, and lignite. The features of low-quality coal, especially lignite, might contain a low calorific value, ash fusibility, low volatile matter, high moisture, ash, and sulfur content (Chapman, 2022; Zhang, 2021).

A built-in supply-demand dynamic pushed coal and natural gas prices to multi-year highs in the 2nd quarter of 2021. Unexpected weather-related measures, along with strong economic reclamation, resulted in more coal and gas demand than projected (IEA, 2022).

More than half of the increase in world electricity demand is covered by coal. Coal-fired electricity production reached a new record, growing by 9%, and the fastest increase since 2011. Subsequent to a slight decline in 2020, the world's power demand expanded by 6% in 2021. A rapid economic recovery, along with more intense climate conditions than in 2020, as well as a colder-than-average winter, increased global electricity demand. The industrial division saw the greatest increase in demand, followed by the business and facilities division, and finally the residential division. Coal came back in 2021 because of the strong development in power demand, negative renewable circumstances, and rising gas charges. Overall thermal power production rose by nearly 6% (980 TWh) in 2021, the maximum development since 2010, as shown in Figure 1.6. Following a decline in 2019 and 2020, coal-fired electricity production increased by around 9%, reaching a record high. In 2021, coal helped to meet more than half of the additional demand, outpacing renewable energy for the first time since 2013. Higher gas prices have caused gas-fired electricity to expand by 2% globally, countering a dip in 2020. (IEA, 2022).

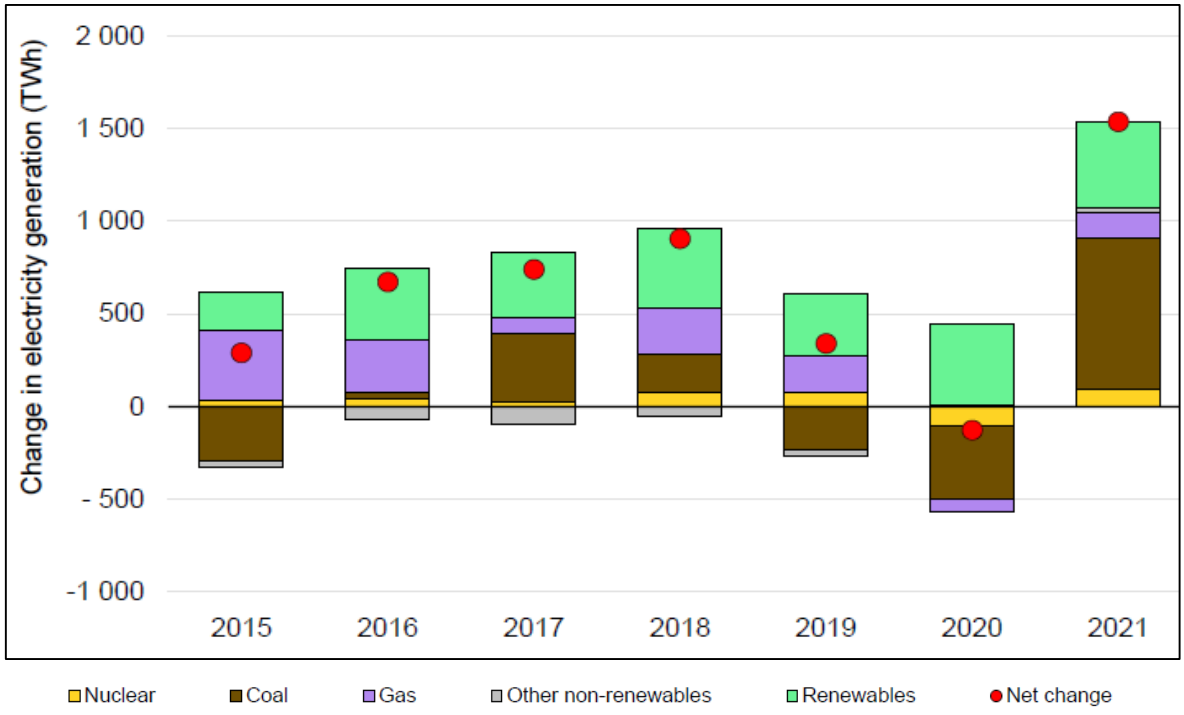

Figure 1.6: Global change in electricity generation, 2015-2021 (IEA, 2022)

Coal remnants are energetic, and their demand is on track to rise in 2021, pushing worldwide coal demand above 2019 levels when total production was 7921 million tonnes (Mt). The common thermal coal at 6175 Mt and 739 Mt of lignite were produced (IEA, 2020). More than 80% of the development is focused on Asia. As the major user of coal, China alone is predicted to account for over 50% of worldwide development (IEA, 2021a). Coal is the preferred energy fuel for power production all over the world. The easy availability of coal in the vicinity and continuously elevated prices of oil and natural gas make electricity from coal-fired plants more economical, attractive, and feasible (BP, 2020; Moti et al., 2012). Coal provides around one-third of worldwide electricity generation and contributes a vital character to industries such as iron and steel. Coal plays a vigorous part in power production globally. Power plants that run on coal presently fuel 37% of worldwide electricity, retentive coal's place as the solitary largest basis of power globally (WCA, 2021).

According to the International Energy Agency (IEA), in the coal forecast for 2021, an all-time-high production of 8,111 Mt will occur in 2022. The major growths are projected in India (+163 Mt), China (+57 Mt), Russia (+16), and Pakistan (+12 Mt). Pakistan's coal assets are recorded at around 3 billion tonnes (BP, 2020), containing mostly lignite and sub-bituminous coal in the Thar Basin, which might contain 175 billion tonnes of lignite coal overall. Nevertheless, the moisture content of coal is high, and the heat value is low. Pakistan experiences similar challenges as other developing states in Asia. Whereas Pakistan depends, at least in part on coal to meet its increasing energy requirements. In 2020, coal consumption rose to 23 Mt in Pakistan (+5% from 2019). Pakistan has added the erection of 5 GW of coal-based power plants constructed in recent years. Consequently, expect coal consumption in Pakistan to be ~67% higher in 2024 than in 2021, increasing to 42 Mt with the majority of the increase stemming from new power plants fired by local Thar lignite coal (IEA, 2021b).

As compared to other countries, Pakistan's reliance on coal power is comparatively less. Consuming coal as well as hydro and renewable energy, which are currently accessible energy bases in Pakistan for production, is the utmost necessary way of

obtaining constant power. Electricity production from coal has been constantly improving in relation to productivity development, process control, and emission reduction. Though the challenging target of sustainable growth requires the delivery of consistent, inexpensive, and environment friendly power. To attain this objective, it is necessary to introduce highly efficient coal-fired power production technologies with minimum emissions. Research and development efforts are paying attention to efficiency enhancement to meet the goals of sustainable development; coal-biomass co-combustion, carbon capture technologies, and sequestration are being used (Rehman, 2017).

1.1.4 Coal Reserves in Pakistan

Pakistan has wide reserves of coal. These coal reserves vary from different low-rank coal-like sub-bituminous and lignite, found all over Pakistan as well as Azad Kashmir. Overall, Pakistan's coal assets are more than 185 billion tonnes as shown in Table 1.2, of which only 175.5 billion tonnes are reserves from Thar coal. Thar coal mine is located in Sindh's south-eastern corner and encompasses an area of 9000 square kilometers (IEA, 2009). Pakistan possesses the world's seventh-largest lignite coal deposits, which can provide 100,000 megawatts of power every year for the next 200 years (EIU, 2017).

Table 1.2: Coal Reserves in Pakistan (Raza et al., 2022)

Region	**Coal Reserves (Billion Tonnes)**
Azad Kashmir (Kotli)	0.009
Khyber Pakhtoon Khaw (Hangu/Orakzai, Gulla Khel/Karak, Mansehra)	0.091
Baluchistan (Chamalong, Sor Range/Degari, Musakhel Abegum Mach-Kinri, Duki, Khost-sharig-Harnai, Ziarat, Pir Ismail,)	0.217
Punjab (Makerwal, Central Salt Range, Eastern Salt Range)	0.235
Sindh (Lakhra Thar, Sonda, Thatta, Haji Coal, , Jherruck, others)	184.623
Grand Total	**185.175**

The coal portion is 12.8% of the overall mounted volume, and it's still used as a source of energy generation. The provincial coal production and its imports are specified underneath for fiscal year (FY) 2020-2021, as shown in Table 1.3.

Table 1.3: Coal Production for fiscal year (FY) 2020-2021 (Tonne) (PES, 2021)

Province	**FY-2020**	**FY-2021**
Punjab	1,072,120	526,190
Sindh	4,414,296	3,747,144
Balochistan	3,086,576	2,060,624
Khyber Pakhtunkhwa	257,240	41,212
AJ&K	272	205
Import	16,421,787	12,183,161
Total	**25,252,291**	**18,558,536**

1.1.4.1 Thar Coal Reserves

Thar coal reserves total estimated areas of about 9000 sq. km. The depth of total reserves is about 155-200 meters, and the total estimated reserves are about 175 billion tonnes. The collective thickness of the coal seam is about 24 meters. The total area of drilled twelve blocks (I–XII) is 1192 sq. km. Coal reserves at each block are approximately 2.0 billion tonnes. Each block can produce electricity of approximately 4000-5000 MW of electricity for 30 years (TCEB, 2021).

Figure 1.7: Thar Coal Field Location Map (PPIB, (2017)

In Sindh Province, one enormous coalfield was revealed, namely the Thar coalfield. The coalfield is close to the Indian border and accounts for nearly all of Pakistan's coal assets. The assets available are sufficient for coal power generation (JICA, 2013).

1.1.4.2 Coal Based Power Projects

Pakistan has signed power production schemes under a mega venture called the China-Pakistan Economic Corridor (CPEC, 2017). Pakistan's energy production strategy (GoP, 2015) objects to an enhancement in an electricity production facility that guarantees the development of local assets and pursues win-win conditions for all investors. The construction of coal power plants in different regions of Pakistan is in progress to utilize Thar coal assets.

Table 1.4: Power Projects under China-Pakistan Economic Corridor (CPEC, 2017)

Power source	Power project
Coal power plants	2x660 MW Port Qasim coal-fired power plant 2x660 MW Sahiwal Coal-Fired power Plant 4x330 MW Engro Thar Coal-Fired Power Plant and Surface Mine in Block II of Thar Coal Field 2x660 MW Rahimyar Khan Coal power Plant Thar coal Block I and 2x660 MW Mine Mouth Power Plant 2x660 MW Hubco Coal Power Plant 300 MW Gaddani Power Plant at District Lasbela Baluchistan 660 MW HUBCO Coal Power plant 300 MW Salt Range Mine Mouth Power Plant including Mining 2x660 MW Thar Mine mouth Coal-Fired Power Plant by oracle 2x660 MW Muzaffargarh Coal-Fired Power Plant

Following are the Thar coal-based power project.

Table 1.5: Thar Coal Based Power Projects in 2017 (TCEB, 2017)

Block	Investment Firm	Total Coal Potential of Block Billion Tonne	Power projects Initiated/ Planned MW
Block-I	SSRL (China-Pak)	3.657	2X660 Phase-I 2X330
Block-II	SECMC Pakistan	1.584	Phase-II 2X330 Phase-III 4X660
Block-III	Asia Power UK	2.007	2X660
Block-IV	Harbin Electric China	2.572	2X660
Block-V	UCG Project	1.394	2X50 Phase I: 8-10 MW
Block-VI	Oracle Coalfields (UK)	1.423	2X330

Table 1.6: List of Coal Projects up till 2030 (NTDC, 2021)

Name of the Project	Fuel Type	Installed Capacity (MW)	Nominal Capacity (MW)
Lucky Electric Power	Local Coal	660	607
Thar TEL	Local Coal	330	300
Thar-I (SSRL)	Local Coal	1,320	1,214
Thal Nova	Local Coal	330	300
Jamshoro Coal (Unit-I)	Imported Coal/Local Coal	660	629
Gwadar Power Plant	Imported Coal/Local Coal	300	273
Siddiqsons Power Plant	Local Coal	330	304

1.1.4.3 Thar Coal Block-II

As per the existing setup and promising geology, Thar coalfield has been distributed into twelve blocks (I–XII). Thar Block II has total lignite assets of two billion tonnes. At present, only Block II is in an operating phase and is relatively important for energy production (Hina et al., 2018). The map of Block II is shown in Figure 1.8.

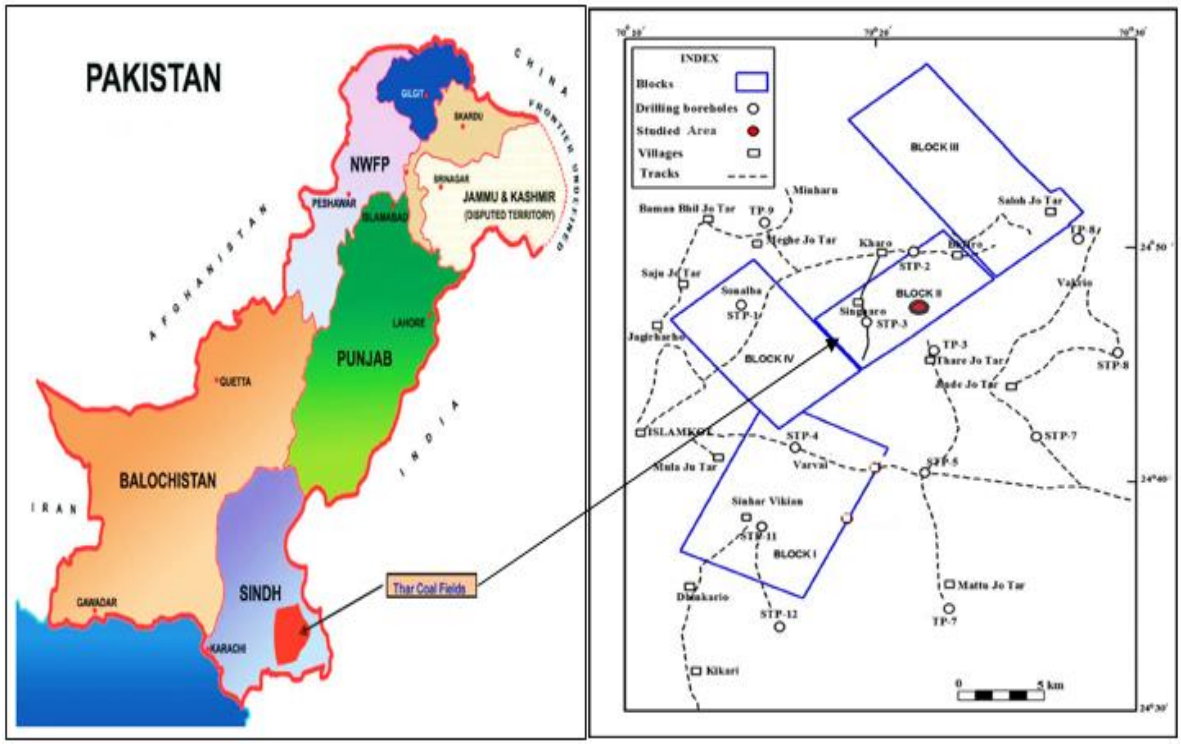

Figure 1.8: Map of Thar Block II

Sindh Engro Coal Mining Company (SECMC) has been given a 95.5 square kilometer (km^2) tract near the coalmine known as Thar Block II by the Sindh Coal Authority (SCA) for the study and extension of the block's coal potential. SECMC built a 660 MW (2330 MW) mine-mouth power station as part of Block II. (Hagler Bailly, 2014). Nonconformity in coal quality affects the whole power generation process, which is again associated with numerous cost elements in a complex way (Mohanta, 2015).

1.1.5 Thermo Gravimetric Analysis (TGA)

It is necessary to identify the thermal activities of fuels to assess their suitability for combustion. Thermo gravimetric analysis is widely used in the investigation of the effects of reactive atmospheres, proximate analysis, and the definition of thermal consistencies and decomposition of constituent kinetics (Hussain, 2015). Thermo gravimetric analysis (TGA) is another well-known approach for examining thermal actions and kinetics in the coal pyrolysis process. It calculates the sample's mass loss as a function of temperature and time (Hussian, 2006). The motivation for the thermal reactions that occur during the pyrolysis of Thar coal and the acquisition of kinetic data based on TGA information related to kinetics and thermal actions plays a significant role in the competent design, modeling, and operation of boilers (Vuthaluru, 2003; Usto et al., 2021).

1.1.6 Coal Blends

Coal blends are used for low-grade coals to increase their ignition performance, enhance the flexibility of fuel types, and comply the conditions of emission regulation (Arenillas, et al., 2004; Cebrucean et al., 2020). Biomass blending continues to raise the combined fuels' burning temperature, indicating the devolatilization of coal (Bampenrat et al., 2021). Numerous power plants have mixed coals to regulate the configuration of the fuel and to deliver a reliable feedstock for power production. Further explanations for mixture coal contain a shortage of high-quality coal; the rate of the fuel; to ease coal transference difficulties; to decrease fouling and slagging and reduce discharges of

contaminants. Coal mixture is a physical procedure planned mostly to affect fuel chemistry (Zhang, 2021).

Biomass is a renewable and environmentally friendly energy source that is mostly derived from agronomic waste (Saini et al., 2015; Abaide et al., 2019). Biomass is a composition of organic substances like crop waste (wheat straw, rice husk, bagasse, etc.), wood and forest wastes, animal waste, organic parts of industrial and metropolitan wastes, etc., that have been consumed for power generation for several years because of the lower ignition temperature with quick ignition due to elevated volatile substances and reactive char (Shahbaz et al., 2020; Khan, 2007). Every year, about 0.30 tons of biomass residue are produced in the country, with an estimated electricity production of 166.72 TWh/year. (Irfan et al., 2020a).

Both coal and biomass are carbon-containing substances, instigating from flora, and have similar fundamental elemental components (Boerrigter and Reinhard, 2006). The co-burning of coal and biomass is an attractive fuel for all thermal transformation processes. Slight consideration has been given to the system that these combinations of biomass and low-quality coal thermally relate to and convert in the co-transformation situation (Li, et al., 2014; Aboyade et al., 2013). Methods like combustion, gasification and pyrolysis might be used to produce electricity from coal-biomass blends (Chieng and Kuan, 2020). The combustion method is the most widely used worldwide (Cardozo et al., 2016).

Co-combustion represents the simultaneous burning of more than one fuel for power generation in a similar plant (Tchapda and Pisupati, 2014; Argus, 2021). Co-combustion shows a high combustion rate for changing biomass into energy in coal-burning power plant with additional significant environmental advantages like low CO, CO_2, NOx, and SOx emissions compared to those released by the burning of neat coal (WEC, 2004). Due to those advantages, co-combustion of coal with biomass has more potential to meet electricity demands. Furthermore, using biomass in conjunction with coal to generate electricity could make the system more sustainable (Kanwal et al., 2021).

Responses taking place in the burning region become more complex once coals of diverse grades are co-fired or mixed. While a combination of lignite with biomass or higher-grade coal might improve burning conditions, reduce gaseous discharge pollutants, and mitigate some operative complications, it does not constantly decrease problems with grinding, flame constancy, ash deposition, etc. For developing nations, such as Pakistan, where lignite assets are abundant and power demand is increasing quickly, consuming local lignite might also support generating jobs and improve the local economy (Zhang, 2021).

1.1.6.1 Rice Husk Biomass

All over the world, rice is the main crop made of rice husks through the rice milling practice in huge volumes and comprises a small content of sulfur and other pollutants (Gautam et al., 2020). Rice husk comprises organic and inorganic substances. Around 134 Mt of rice husk are produced annually around the world, with roughly 90% of it being burned in the open air or dumped into lakes and rivers (Quispe et al., 2017). Pakistan produces millions of tons of biomass each year. The accessibility of agronomic biomass like rice husk is certain to be a byproduct of agronomic production (Mirani et al., 2013). In Pakistan, rice is the most important farmed crop. Pakistan comes in 10^{th} in the ranking of rice production. Pakistan produced 7.410 million tons of rice altogether, spread across 3.034 million hectares of land (Khan et al., 2022). Rice husk, a derivative from rice mills, has a yearly production capacity that is very high. Thus, they are a suitable and attractive basis for energy production in such constituencies, as they have an admirable potential to be used in co-firing systems (Shahzad, 2015). Rice is mostly grown in Pakistan's Punjab and Sindh interior provinces. Sindh, Pakistan, produces roughly 23110 tons of rice husk every year (World Bank, 2016; Iqbal et al., 2018). Rice husk is obtained by breaking the rice grain from its husk, and it accounts for 20% of the rice's weight (Mohiuddin et al., 2016). Due to its ease of transport and low cost, rice husk is taking on too much popularity as boiler fuel (Hussain, 2015). According to estimates, the CFBC power plant can produce 5360 MWh of energy annually while using 6968 tons of RH fuel; the cost of producing electricity through CFBC is around Rs. 4/kWh, making it more practical and affordable to

produce electricity (Memon et al., 2017) and suitable for power generation at the district level.

1.1.7 Fluidized Bed Technology

Fluidization is a two-phase technique in that a discrete solid substance is suspended upstream of gas flowing over the fluidized grate. The level of solid units suspended inflowing gas forms fluidized beds (Trinks et al., 2004). Fluidized-bed methods have functioned commercially since the 1920s, with the introduction of the Winkler coal gasifier in Germany (Cocco et al., 2014). The fluidized bed (FB) technique has been widely practiced in the energy division and engineering chemistry for undertaking heterogeneous procedures for transforming numerous feedstocks into heat or chemicals. FB technology is very flexible towards the materials characteristics to be processed, i.e., moisture, feedstock heating value, density and particle size, sulfur content, etc. (Leckner et al., 2015), and possesses greater performance in expressions of heat (Blaszczuk et al., 2014) and mass transfer (Miccio et al., 2021; Di Natale et al., 2013). In specific, gasification and combustion have been established and conceded in the previous five decades using solid fuels in the form of coarse granules, powders, and pellets made from fossil and renewable sources (Basu, 2006). The utmost significant features of FB from other technologies are fuel flexibility, greater heat transfer, the capability to simply transfer solids, and the capability to proceed with wide particle size material circulation (Trinks et al., 2004). There is also the opportunity to undertake additional sub-processes, e.g., heterogeneous catalysis, particle drying and $NO_X/SO_2/CO_2$ capture (Miccio et al., 2021; Liu et al., 2014).

1.1.7.1 Fluidized Bed Boilers Types

The construction of fluidized beds is distributed into two main types (Iannello et al., 2020), Bubbling (Stationary) Fluidized Bed (BFB) and Circulating Fluidized Bed (CFB).

In a BFB, the bed media is prepared of elements normally 0.5–1.0 mm in size, Group B of the Geldart grouping (Blaszczuk et al., 2014), and is fluidized from the lowest

part with a velocity variable from 1 to 3 m/s (Miccio et al., 2021). Under these circumstances, the bed solid is completely fluidized and acts like a boiling liquid (Yang, 2003).

In CFBs, the bed material is normally a lesser particle size (e.g., 0.2–0.5 mm) and fluidized with superficial velocities up to three to five times (5–10 m/s) greater than in BFBs (Miccio et al., 2021). A downstream component is then, compulsory to discrete (a cyclone) and recirculate these particles. (Gómez and Leckner, 2010; Puig et al., 2010). Figure 1.9 shows the types of fluidized beds.

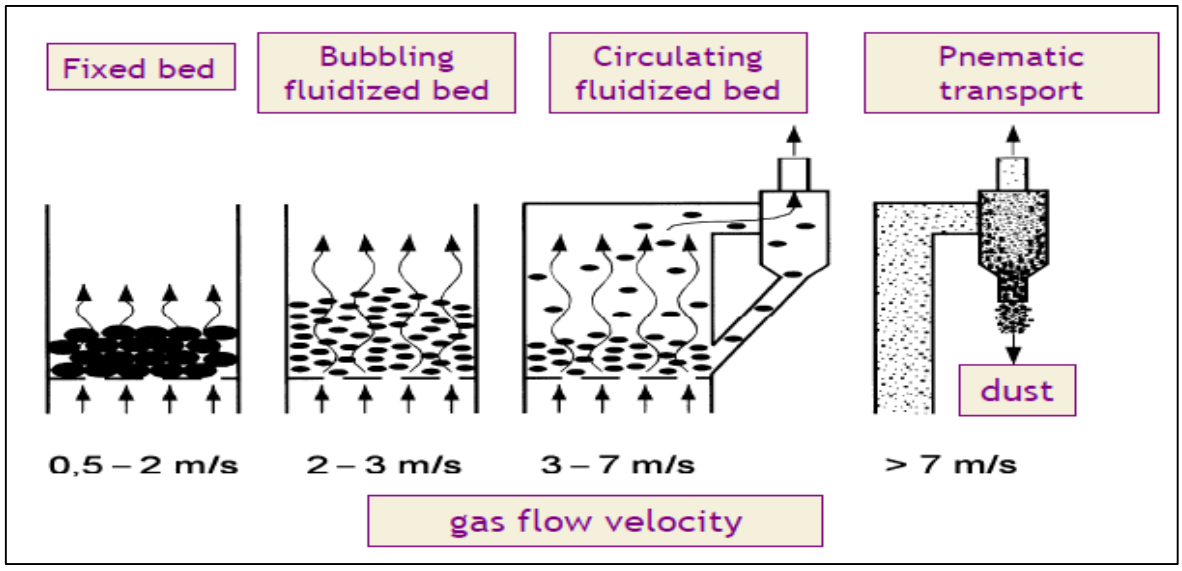

Figure 1.9: Types of Fluidized Bed

1.1.7.1.1 Circulating Fluidized Bed Combustion (CFBC)

In recent years, CFBCs have been extensively used for power generation because of their superior burning efficiency and relatively better control of emission gases (Liu et al. 2020a; Khan et al., 2011). The increasing application of fluidized bed combustion technology all over the world has led to improving the design and reducing emissions through further experiments and modeling (Göğebakan, 2006). CFB methods have been used widely in the fields of energy, metallurgy, and chemical engineering, among others.

As a type of complicated engineering device, the approach and process of CFB will be influenced by several factors (Liu et al., 2022).

Coal combustion discharge, different levels of emission gases within the combustion chamber, and the technology of CFBC are vital (Kishore et al., 2021). Combustion techniques in the riser can considerably reduce the excessive cost. For burning low-class coal with biomass, different waste, and mixtures, CFBC is gaining broad research concern because of its economic and valuable engineering potential (Xie et al., 2013). The improvement and different behavior in CFBC applications required a modern and more creative test strategy, investigation, structure, and logical simulations. Due to that, various CFBC uses show an inimitable test to understand the variation and support between phases in the CFBC risers. CFB design is highly complex in terms of scaling-up difficulty, operational circumstances, and elevated affectability of the flow to scale (Kishore et al., 2017; Almuttahar et al., 2008; Hartge et al., 2009).

In the 19th century, the major use of the fluidization invention retreated, whereas fluidization was consumed as a fraction of the calcining heater (Benyahia et al., 2000). During the 20th century, more improvements and arrangements made CFBC a novelty. The fluidized bed technique provides a very small history of unique functions and productivity. For more than 20 years, the major fluidization advancement has been used for various additional processes as well as coal combustion, waste incineration, catalytic processes, and paralysis for energy production (Yang et al., 2003). In the chemical and process industries, different kinds of reactors are functional to assist in the chemical mixing of gases, solids, liquids, and chemical reactions to get several products (Gidaspow et al., 1992). For CFBC design and process, it is essential to recognize the profile of the CFBC. The Circulating Fluidized Bed Boiler is shown in Figure 1.10.

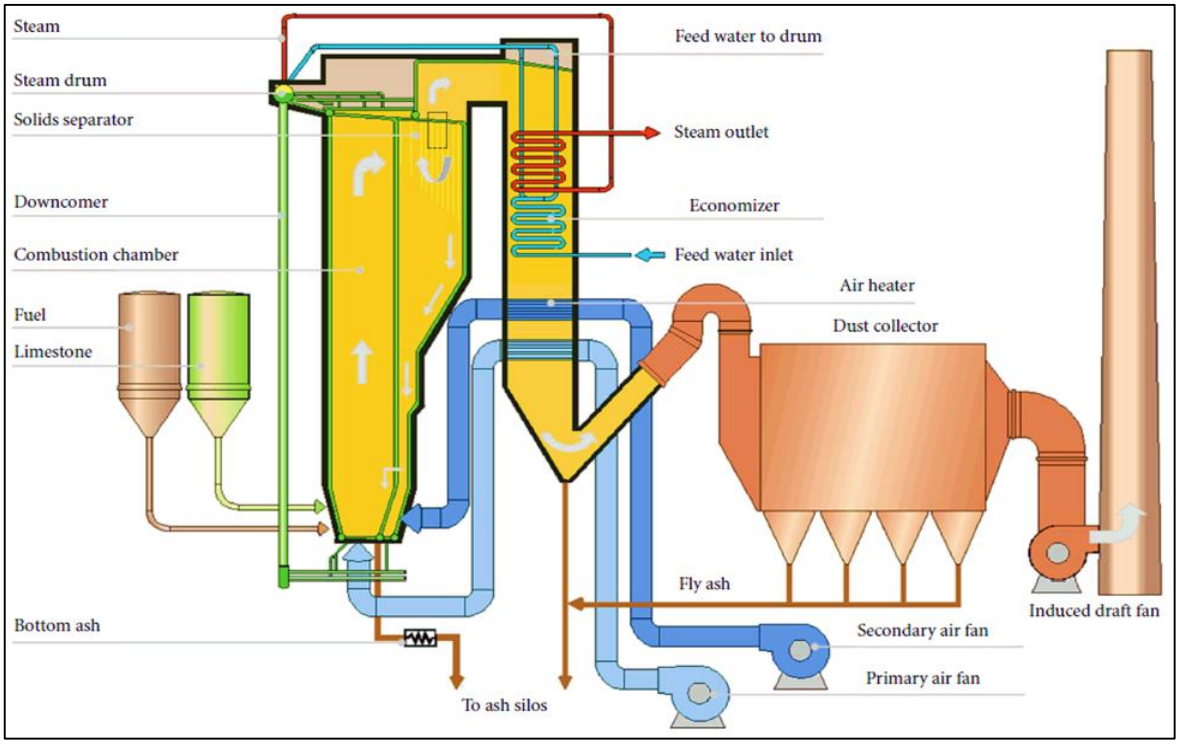

Figure 1.10: Cross-Section of the Circulating Fluidized Bed Boiler (Liukkonen et al., 2010)

The CFBC boiler is a fluidized bed boiler that is believed to be the second generation. It is divided into two parts: one is fluidized, and the other is a cyclone (the gas-solid separator). The boiler's principal combustion air passes through an air supply or grate at the bottom. To ensure complete combustion, supplementary air is injected at a high altitude above the grate. The solids in the bed are finely separated as the boiler is raised. As a result, the bed temperature in the range is nearly identical, but the temperature is extracted together with its height (Sahu et al., 2015). The technology of mixing limestone with fuel into CFBC boilers gives great desulphurization efficacy while avoiding the use of pulverization machinery in plants (Kishore et al., 2021). Commercial CFBC has confirmed many operational benefits, including a wide turn-down fraction, fuel flexibility, less NO_X emission, elevated sulfur retention efficiency, and elevated burning efficiency (Chang et al., 2021; Seveille et al., 2005; Gomez and Leckner, 2010; Kaushal et al., 2007). CFBC is an ignition engineering element consumed as an element of energy generation (Emami et al.,

2019; Singh et al., 2013; Nguyen et al., 2012; Yang et al., 2004). The following are some advantages of CFBC:

a. Higher thermal efficiency.
b. Ease of ash removal.
c. Quick erection and commissioning of the equipment.
d. Automated operation and lesser human involvement make it safer even in extreme temperatures.
e. Can be operated with a considerable size of coal particles as well.
f. A quick thermal equilibrium is established between coal and air.
g. The use of limestone or dolomite reduces the sulfur content escaping into the atmosphere.
h. Low-temperature operation reduces the formation of nitrous oxides and limits air pollution.

1.1.8 CFB Riser and combustion Process

When the fresh coal is injected into the CFBC riser, the following main process occurs:

a. Heating and drying
b. Devolatization and volatile combustion
a. Burning of char

An essential fact of coal burning is that it is similar to whatever the burning machine. It engages the thermal decomposition of the coal matrix, releasing volatiles, followed by the subsequent burning of the char and volatiles in the presence of oxygen (Basu, 2015; Abdullah, 2007).

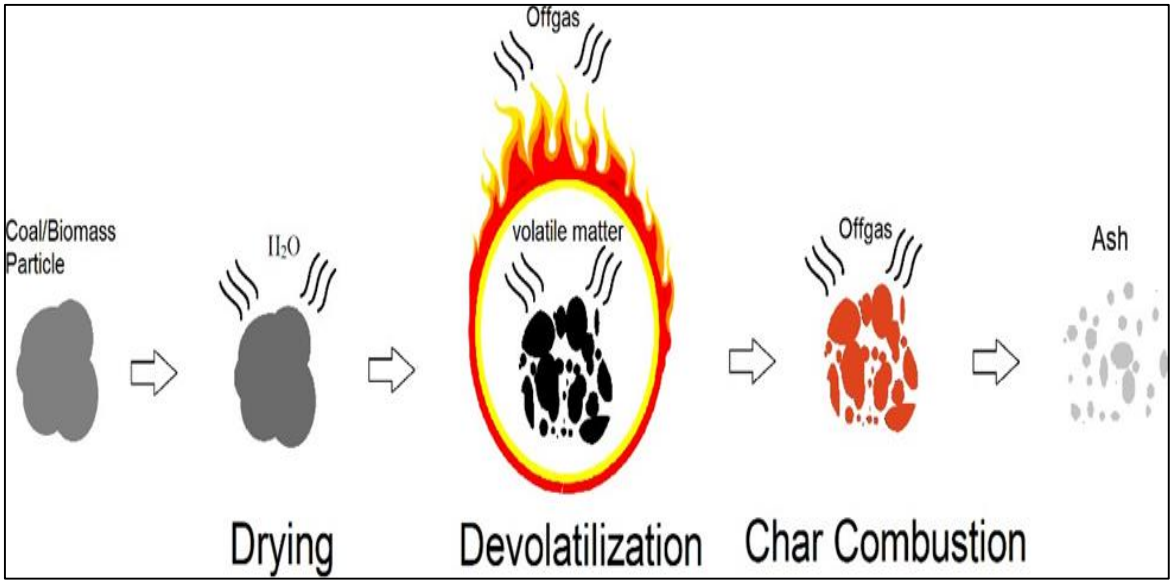

Figure 1.11: Stages of the coal particle burning (Basu, 2015)

The coal-burning procedure is a complex procedure in which surface reaction kinetics and diffusional mass transference are combined. The burning of solid coals could be characterized by the above three steps. The procedure is concise visually in Figure 1.11. Especially, devolatilization and char burning tend to happen at a similar period for some coals (Levendis et al., 2011; Magalhães et al., 2019). After the completion of the steps, the remaining residual is inorganic ash.

CFB boiler performance is influenced by the combination of particles and gas. A good combination rate gives an efficient circulation of reactants, while an inadequate combination can lead to CO emissions and hydrocarbons (Kishore et al., 2021). Hence, a sufficient understanding of the combined activities is essential to ensuring good burning efficiency and emission management. Understanding the combination characteristics is also helpful for the justification of computer simulations of CFB risers (Hussian, 2006). A vertical riser with a square cross-section is widely practiced in a CFB for industrial use to pass on the ascending co-current flow of particles and gas (Kishore et al., 2017; Meer et al., 2000). Because of the variety of arrangements and their multifarious impacts on the solid-gas two-phase flow, there has been little research on the intake and outlet effects on the hydrodynamics in risers or combustors, but an apparent categorization and comprehension

have not been gained. As a result, understanding the hydrodynamic characteristics of riser inlet sections is critical (Liu et al., 2020b). The riser outlet geometry of a CFB has been shown to have a significant impact on the component's hydrodynamics. To manage the emissions efficiently, mainly to minimize emissions of imperfect burning products, it is essential to know the effects of diverse variables/factors on the emission actions (Yuan et al., 2019; Hussian, 2006; Harris et al., 2003).

1.1.9 ANSYS Fluent Software

ANSYS is a unique, powerful tool utilized extensively for basic to highly complicated systems and mechanisms to get highly precise results without fabricating a model for design analysis. A simple CFB combustion riser will be modeled using ANSYS Fluent software for the computational fluid dynamics (CFD) combustion analysis of Thar coal reserves. This study is to examine the burning performance of low-grade Pakistani coals from Thar in a CFB riser by using ANSYS software to minimize investment and operating costs, minimize emissions of various fuel mixtures, and increase the burning efficiency.

1.1.10 Features of ANSYS Fluent Software

ANSYS Fluent deals are greatly accessible to help resolve multifarious, large-model CFD simulations rapidly and cost-efficiently. The ANSYS simulation tool can solve multiple models in a single file, which ultimately reduces the simulation time. It is also evident that the results obtained from this tool have high accuracy when likened to the real model. Therefore, this tool is selected for combustion analysis (Patra, 2013).

The following are the features of the ANSYS Fluent Model:

a. Geometry (Geometry of the reactor with its dimensions)
b. Mesh Flexibility (To solve flow problems using unstructured mesh)
c. Multiphase Flow (Diverse fluids model in a single field)
d. Reaction Flow (Combustion, surface, and finite rate chemical modeling)

e. Turbulence Effects (Turbulence effect in an extensive range of flow regimes)
f. Data and Post-processes Export: (Post processes their records in the FLUENT model. To visualize the data, you can use contours, vectors, and path lines, among other things.).

1.2 Research Hypothesis

Pakistan's energy needs are immense compared to the previous two eras, and the government's primary concern is the ongoing power shortages brought on by the country's increasing industrialization and urbanization. The ongoing electricity crisis has negative impacts on the economy, business, industry, and society. Due to the import of oil necessary to maintain the current energy mix and the rapid depletion of gas supplies, current energy generation imposes a significant financial burden on the nation (Raheem et al., 2016). The answer may be as simple as producing electricity up to predicted demand using local resources like the Thar coalfield, which has the seventh-largest lignite coal reserves in the world. With about 185 billion tonnes of native coal reserves, of which only 175.5 billion tonnes come from Thar coal, Pakistan has more than enough to cover the country's ongoing and sustainable energy needs (NTDC, 2021). According to Pakistan's energy mix in 2022, only 12.8% of the country's total power was produced utilizing coal (NTDC, 2022). A coal base energy power plant generates several emissions pollutants. The environment is affected by these polluting gases. Modeling of CFB risers for various coals is available in the literature, but this type of modeling study is not presented for Thar coal. Therefore, the study was designed to concentrate on modeling, specifically reducing emissions for Thar coal-based power plants.

Thar coal has undergone computational fluid dynamics (CFD) analysis to reduce emissions and increase combustion effectiveness. In addition, this study looks at the physicochemical properties of rice husk biomass and how it interacts with Thar lignite coal when burned, as well as how the ratios of these mixtures affect pollution. The most advantageous and efficient technique for generating electricity from Thar lignite coal is the Circulating Fluidized Bed Combustor, which also reduces SOx and NOx emissions.

1.3 Research Gap/Novelty Statement

a. Numerous studies on combustion modeling of CFBC risers using ANSYS FLUENT software are available in the literature for different coal categories. But to date, a complete model that reflects the burning of low-quality lignite coal, especially from Thar coal Pakistan, and its emissions data is not presented.
b. Very limited literature is available on the rice husk and coal blends combustion properties with emission data from Pakistan.
c. Different researchers worked on Thar coal for different selected properties, but no compiled data is available for Thar coal physicochemical, thermal, combustion, and emission characteristics on one platform.

1.4 Problem Statement

a. The prolonged energy shortage is one of the key issues of Pakistan, and energy issues are mainly due to the historical trend of higher oil prices and the depletion of natural gas assets.
b. Pakistan has the world's seventh-largest reserves of lignite coal and can produce thousands of megawatts of electricity each year for long periods, only limited energy is generated from Thar coal (IEP, 2022).
c. Due to incomplete combustion, no proper estimation data of CO, CO_2, SO_2, NO_X, and other emission pollutants are available for Thar coal and their co-combustion with rice husk biomass.
d. These emission pollutants are the primary sources of acid rain, smog, and greenhouse gases, which cause global warming and climate change.
e. No proper combustion modeling study was carried out for Thar lignite coal.

1.5 Objectives of the Study

The main research/study objectives are:

a. The physiochemical characterization was done to understand the combustion behavior of selected Thar coal and rice husk.
b. Thermogravimetric Analysis (TGA) was done to understand the devolatization behavior of Thar coal.
c. To use the ANSYS FLUENT code to make a computational fluid dynamics (CFD) model of the riser geometry and to perform a two-phase flow CFD model of the riser to estimate the pollutant gases produced as a result of the combustion process, including a parametric study to minimize pollutants.

1.6 Significance of the Study

The significance/outcome of the prospective research are:

a. ANSYS FLUENT Computational fluid dynamics (CFD) modeling has been done to minimize emissions and improve combustion efficiency for Thar lignite coal.
b. Model with ANSYS code will reduce investment and working costs for developing experimental test rigs built for such studies.
c. Cost-effective and beneficial by reducing long-term experiments, and will help design and improve equipment performance.
d. Without hazards or possible industrial accidents, or experimental difficulty, CFD will provide consumers to adjust equipment settings and parameters safely.
e. This study helps to find out new thermo-chemical characterization and emission data for Thar lignite coal co-blended with rice husk biomass.
f. This research work compiled the Thar coal physicochemical, thermal, combustion, and emissions characteristics on one platform.
g. This study of Thar coal is an important reference for future researchers and power plants and also helps to reduce power/electricity shortages and environmental pollution by reducing emission gases.

CHAPTER 2

LITERATURE REVIEW

This section critically assesses the literature on coal's thermal and physical properties. The combustion procedure's thermochemistry has been thoroughly investigated. This section reviews the literature on energy and coal status, Thar coal reserves and quality, coal blending, circulating fluidized beds (CFB) technology, hydrodynamics of CFB riser, computational fluid dynamics (CFD), and modeling, combustion, and emission gases chemistry specifically in CFB. The research also acknowledges various investigators concerning diverse methods and modeling of combustion in riser has been deliberated. The influence of operational constraints on burning and emissions has also been studied by numerous scientists. There are various studies in the literature that model CFB risers for different types of coal, but none have been given a model for Thar coal. Determining how to predict particularly decreasing emissions for Thar coal-based power stations was the focus of the study. Research data on Thar coal from Pakistan is relatively limited.

2.1 Energy Overview

Presently, the worldwide requirement for power is enlarged due to industrial growth, and humanoid progress is the scientific community's practice of speeding up components of environmental variability around the world (Barca, 2011). Established states have a larger power demand than lesser established nations because of the huge socio-

economic growth at local and countrywide levels (Barca, 2011; Raza et al., 2022). An energy disaster is defined as an increase in energy asset amounts or an excessive deficit in the supply of energy resources. Generally, it refers to a shortage of power, natural gas, oil, and other natural assets (Akbar et al., 2021). The energy demand is incessantly growing in the world, resulting in a disaster for energy. The deficiency of energy is challenged by the majority of the states, and therefore it is harshly distressing their financial evolution and social revolution. Several opinions and concepts may make connections between energy and financial development (Naseem and Khan, 2015). Energy is the measured economy backbone and acting a significant part in the socio-economic growth of a country. If there is not adequate energy, industrial development will not grow, it is vital for running trades and production parts, for residential and commercial usage and transport, etc. In brief, energy is vigorous for running all the capital, and energy disasters straight affect all the divisions of the economy, such as agronomy division, trade division, joblessness, poverty, lesser GDP, and advanced price increases (Akbar et al., 2021; Abbasi et al., 2021).

Technologies that are effective in energy production and environmental friendly are attentive at present all over the world because of inadequate fossil assets. Amongst numerous transformation machinery such as thermochemical, thermal, chemical, and biochemical procedures. Thermochemical transformation of coal/biomass is effective and eco-friendly. The usage of energy has enlarged significantly because of numerous developments and modernizations of communal usage made in the last era. For emerging countries in particular, there is an essential requirement for consistent and inexpensive energy. In these states, energy claims have increased due to developments in trade, efficient agronomy, enlarged businesses, and better transportation (Maitlo et al., 2019).

2.1.1 Pakistan Energy Overview

Pakistan is an emerging country that is part of the South Asian region (Mengal et al., 2019). Electricity is critical to every nation's prosperity, but Pakistan has declared itself an energy-scarce country because of rapid urbanization and improved human living ethics (Procter, 2017) and is reliant on foreign fuels for electricity production (Sáez-Martnez et

al., 2016). Pakistan spent roughly 60% of its foreign cash on fuel imports, which included oil, coal, and natural gas (Kanwal et al., 2020). Power, cement, and brick kiln manufacturing are the three main coal consumption divisions. Pakistan gets coal from South Africa and Indonesia, and it is 66 percent dependent on them. Such reliance on foreign coal and a lack of management capability for discovering local coal resources for power generation are both problematic. As an outcome, Pakistan's electricity consumption is increasing on a daily basis (Rehman et al., 2018; Raza et al., 2022).

Presently, Pakistan is facing the foulest energy disaster in its history. Pakistan has energy-restricted rising economies, and its energy requirements are met by enormous volumes of oil imports, as in most other non-oil manufacturing states. Pakistan’s energy structure is not well established and is supposed to be unachieved. Despite populace development, economic evolution, and enlarged demand through the previous decades, no thoughtful efforts were made for energy generation. Furthermore, electricity theft and transmission sufferers due to the obsolete structure have deteriorated the condition (Rehman et al., 2021).

The manufacturing, financial, engineering, and trade events of Pakistan are severely exaggerated due to the present energy disaster. As manufacturing continues to close, the employees will become unemployed (Abbasi et al., 2021). In Pakistan, maximum manufacturing is not self-capable of producing power and is also troubled with weighty taxes and an expensive energy stream with a constant disturbance, which outcomes in a loss of productivity, particularly in the textile sector, whose exports are limited to a very small level and are closing down or, moreover, shifting to neighboring states (Naseem and Khan, 2015).

Pakistan had significant electricity and gas shortages at the start of this decade. During the peak summer months, several parts of the state, primarily rural areas, saw 8-12 hours of daily shutdowns, and during the peak winter months, many regions of the state experienced short gas pressure or supply (Malik et al., 2019). Consequently, Pakistan has decreased its energy deficiencies; nevertheless, it nowadays faces physical tasks like

enhancing energy safety by dropping the portion of foreign fuels and using local assets like coal to lower the price of energy (Ahmed et al., 2019).

After wasting about 60% of the energy during production, transmission, and distribution, the housing estate purchases around half of the overall electricity sold on the grid. As a result, Pakistan consumes roughly 18% of its primary energy (Aized et al., 2018). Although it is significant to achieve the elementary requirements of a populace. Pakistan cannot afford to rely on imported fuels to meet its domestic energy needs, with half of these fuels prone to being misplaced during manufacturing and transfer (Tahir and Ayaz, 2018).

Pakistan is reliant on imported energy due to a lack of speculation in its natural assets like hydro, natural gas, and lignite coal. This energy restriction developed from a two-hundred-year-old energy mix shift when power generation was more reliant on imported oil than hydropower. As natural gas assets have diminished and LNG has been introduced, Pakistan's reliance on natural gas has decreased in term of energy (NTDC, 2021).

Hence, native energy resources are to be observed properly for attaining long-term electricity viable goals. Pakistan has risen to sixth place in terms of coal resources with the discovery of the Thar coalfield, since it has a potential of 175 billion tonnes, with a large capacity to create power in the future (Akhtar et al., 2018). The energy produced by Thar coal can provide Pakistan with power in all areas of the economy, providing answers to the country's power requirements. The advancement of Thar coal for electricity production is a temporal need that has a long-term relationship with expanding populations and rapid industrial development (Fatai et al., 2004; Raza et al., 2022). Hence, local coal assets need more attention for connecting via up-to-date technologies and will contribute a vital part to the overall energy mix for power generation. Pakistan has enormous stocks of Thar lignite coal that involve important deliberation for development ever since it is realistic for electricity generation and economical for the coal mine. Although efficacy is a significant performance constraint that might be efficiently accomplished with the use of the latest

equipment. Nonetheless, the Thar coalfield can alleviate existing energy crises and fulfill prospective power competitions, and it confirms the constancy and safety of Pakistan's power division (Raza et al., 2022).

Pakistan generates the majority of its electricity from natural gas, coal, and oil (Valasai et al., 2017). However, oil assets and natural gas will run out soon if new oil fields and natural gas are discovered (Bhutto and Karim, 2005). Currently, the coal reserve offers an appropriate choice for electricity generation. In comparison to the existing assets, local coal production is rather limited. As a result, the coalfield has an enormous ability to supply current and future energy needs, ensuring Pakistan's electricity security (Bhutto and Karim, 2005).

2.1.1.1 Pakistan's Power Production Capacity, Consumption and Energy Mix

The hydro portion of the entire power production has deteriorated in 2021, as associated with its portion last year. Presently, thermal has a major portion of power production. Furthermore, its fraction portion in 2021 has enlarged as compared to 2020. The noteworthy development of coal and RLNG utilization in the energy mix has facilitated better provision to numerous power plants. (NTDC, 2021).

Table 2.1: Installed Capacity (NTDC, 2021)

Year	2019-20 (July-April)	2020-21 (July-April)
Installed Capacity (MW)	35,972	37,261

Table 2.2: Electricity Generation Share (GWh) (July-April) (NTDC, 2022)

Electricity Generation in (GWh)				% Share		
Source	**FY2020**	**FY2021**	**FY2022**	**FY2020**	**FY2021**	**FY2022**
Thermal	65,317	71,178	74,862	61.43	62.52	60.9
Hydel	30,136	31,730	29,181	28.34	27.87	23.7
Nuclear	8,101	8,218	15,182	7.62	7.22	12.4
Renewable	2,768	2,715	3,709	2.60	2.38	3.0
Total	106,322	113,842	122,934	100	100	100

FY: Fiscal Year, GWh: Gigawatt hours

There has been no significant change in the way electricity is used. The share of agronomy in electricity usage will remain stable in 2021 (July-April). However, the share of an industry that uses power has increased, indicating that economic activity is reviving.

Table 2.3: Electricity consumption share (July-March) (NTDC, 2022)

Sector	Units sold (GWh)		% Share	
	2020-21	2021-22	2020-21	2021-22
Household	41,508	42,055	49.1	47
Commercial	6,246	6,648	7.4	7
Industry	22,280	25,160	26.3	28
Agriculture	7,558	8,151	8.9	9
Others	7,008	7,347	8.3	8
Grand Total	**84,600**	**89,361**	**100**	**100**

GWh: Gigawatt hours

2.2 Coal Overview

Coal is one of the most significant natural energy assets in emerging states because of its lower price than other power production assets. It has accumulated industrial rebellion and regularly delivers energy to numerous states around the globe. The main usage of coal is the production of power via burning (Zaigham and Nayyar, 2005; Ali, 2019). The coal was molded over millions of years by the anaerobic deterioration of organic materials underneath the earth at high pressure and temperature, frequently in infested ecological circumstances. The configuration of coal in common comprises Hydrogen, Carbon, Oxygen, Sulfur, Nitrogen, and certain metals (Lu et al., 2004). Coal is a sedimentary rock, and it has enormous uses in various industries; however, it is commonly used for energy and power production all over the globe (Vejahati and Gupta, 2010).

Coal is the most extensively formed mineral on earth and still generates over a third of the world's electricity. Coal has been intensively mined for over 100 years, and possibly

300 billion tonnes (Bt) have been formed. Defining outstanding economic coal assets is inspiring. There is an extensive variety of worldwide reserve cataloging schemes, and all the main coal-producing states stand by such a scheme. This provides stockholders and operators with the assurance that the finances of a coal reserve are precise and dependable (Chapman, 2022).

Coal is a worldwide trade and the principal mined product on Earth; it originated in 70 nations and is vigorously mined in 50 of them. Coal is readily accessible from an extensive variety of bases in a well-supplied international market. It might be transported to demand centers rapidly, securely and simply by ship and rail (Chapman, 2022). Thermal coal is the fuel basis for around 37% of worldwide electricity provisions (World Coal Association, 2020). Metallurgical coal, mainly for steel manufacture, contains around 15% of worldwide coal usage. Numerous reserve reports of worldwide coal assets do not distinguish between thermal and metallurgical coal.

Despite the ongoing energy revolution, coal can continue on an important energy basis for several years, particularly as emission reduction machinery, is progressively applied (Manook, 2021). Hence, the long-standing accessibility of coal remains an important matter in significant coal's part in the energy mix. Fewer emission machinery such as carbon capture, utilization, and storage (CCUS), is measured as very imperative in attaining worldwide emission goals, somewhat for the reason that its flexibility for usage with diverse machins such as power generation or hydrogen manufacture (Kaplan, 2021; Kelsall, 2020).

Related to older coal-based power production arrangements, modern high efficacy, fewer emissions CDFB and HELE power plants persist as attractive schemes in some economies. They can deliver cleaner, reasonable power and are proficient in flexible cyclical and low-load processes (Mills, 2021). Numerous states support our proposal to develop new coal-fired power-producing capacity. This might be to substitute obsolete coal power plants or to deliver enough power to populations where energy deficiency is communal (Baiyu, 2020). Coal-based power schemes projected or in progress are inspected

through a sequence of case studies of states where coal is observed as a feasible selection for producing inexpensive, consistent electricity. Each reflects the encouragement of government strategies and environmental guidelines and inspects the gauge and category of machinery that might be organized in the future (Mills, 2021).

2.2.1 Coal and its Chemical Structure

Coal is a black rock created by deceased plants. As the result of subversive pressure over millions of years, deceased plants were transformed into peat, lignite, bituminous, and anthracite coal, correspondingly from earliest to eldest (Tomeczek, 1994). The chemical configuration of the coal mostly relies on its creative deceased plants and the circumstances throughout the carbonization procedure. Chemical configuration is extremely multifarious, and its diverse nature does not permit division into equivalent portions. There are numerous kinds of functional groups and clusters connected to peripheral points (Özer, 2019).

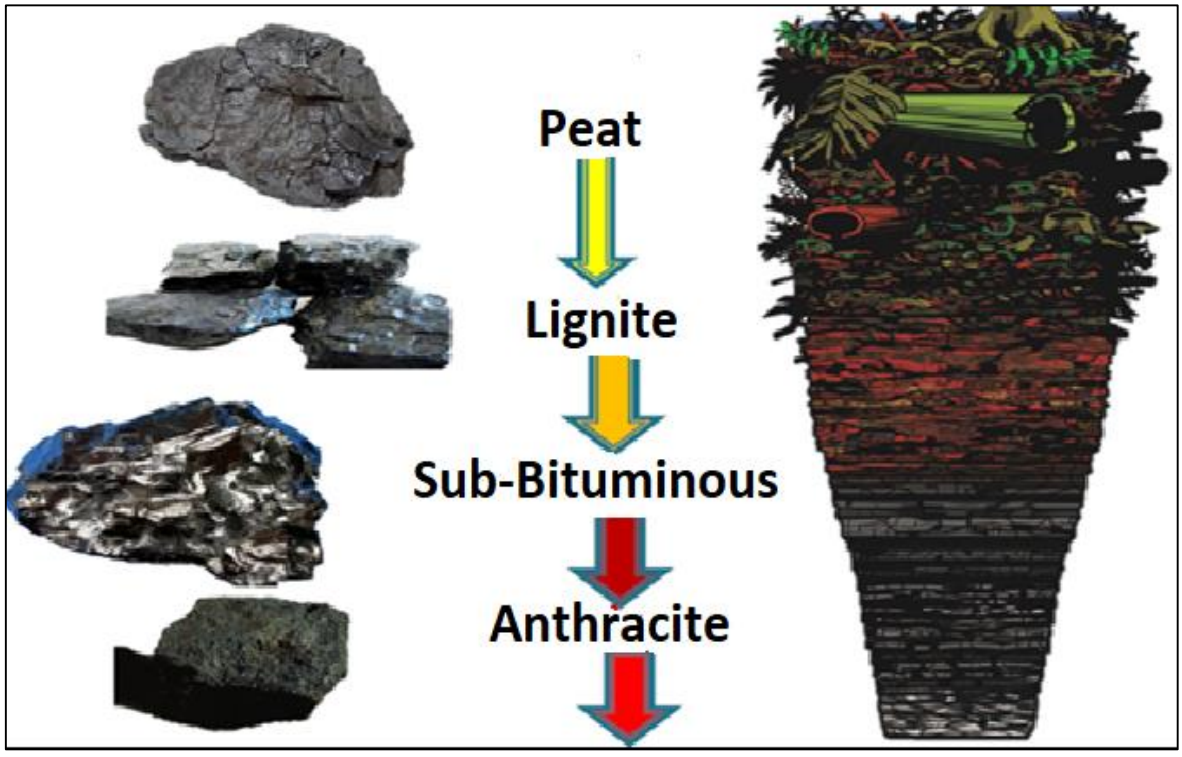

Figure 2.1: Coal Types

2.2.2 Coal Classification

Types of coal were recognized on the substances of carbon, moisture quantity, volatile matter, ash and nature of coke (Kurose et al., 2004). The coals are categorized on the basis of carbon% into four main types, such as lignite, sub-bituminous, bituminous, and anthracite, on a dried basis (Demirbaş, 2003).

Over eras, coal ordering systems transformed with the latest coal samples and the progress of the latest investigational approaches. The leading kinds of coals are anthracite, bituminous, sub-bituminous, and lignite. Anthracite is the hoariest coal with the maximum heating value. It has less moisture and volatile matter. There are three subcategories of anthracite: anthracite, semi-anthracite, and meta-anthracite. Its small quantity of volatile matter makes its ignition problematic. For this reason, anthracite coals are not appropriate for power production solicitations. In power plants, bituminous and sub-bituminous coals are the most communal coals used for burning. Bituminous coal has heating values like anthracite and sufficient volatile matter for its dissolute ignition and burning. Lignite coals are the newest coals and comprise several residual wooded configurations from their plant genes. Its lower heating value and higher moisture mark it as the minimum preferred among the other coals (Özer, 2019).

In modern years, ASTM standards (D388−19a) and the Van Krevelen diagram are the most widespread coal cataloging arrangements. The Van Krevelen diagram (Figure 2.2) demonstrates the atomic C, O, and H fractions of every organic constructed solid fuel. It also delivers a perfect appearance for the aged coal.

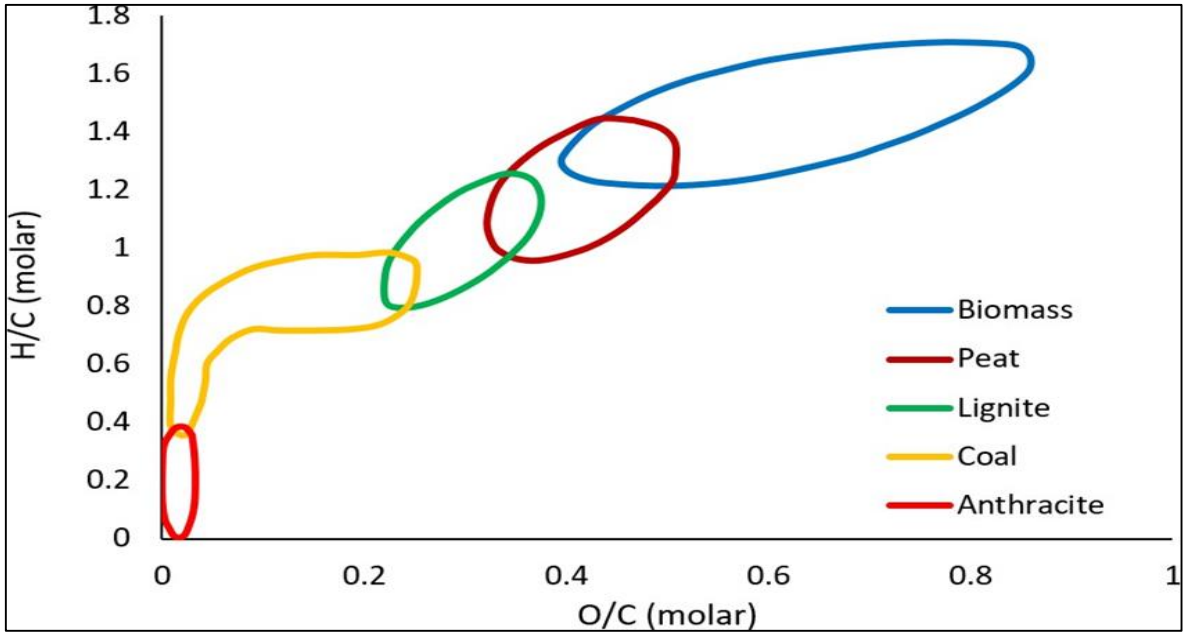

Figure 2.2: Van Krevelen diagram for various solid fuels

2.2.3 Coal Conversion Process

Coal alteration is characterized into two subdivisions: Combustion and Pyrolysis reliant on the contented of the gas part to which coal is revealed in Figure 2.3 (Özer, 2019).

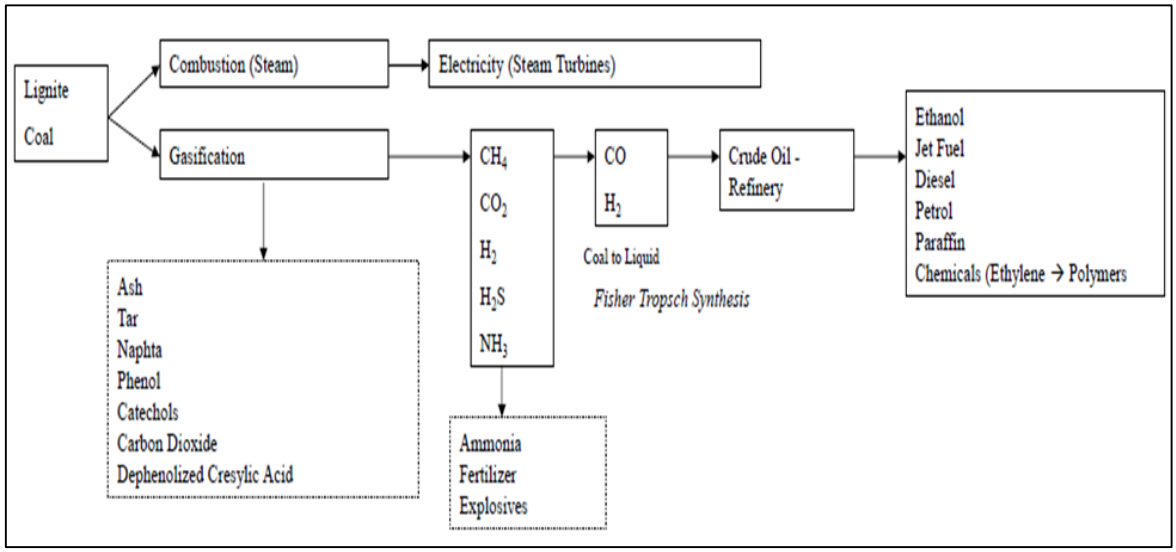

Source: Mr. Johannes Van Heerden, Syngas and Coal Technology, R&D, SASOL

Figure 2.3: Uses of Lignite Coal

2.2.4 Combustion

The chemical reaction of combustion is a self-sustaining exothermic reaction between a fuel and an oxidizer. For the combustion of hydrocarbon coals, oxygen serves as the oxidizer. It has an initial energy obstruction, much like all other reactions. As a result, the type of burning yield depends on the fuel and the combustion sites. Burning reactions are imperfect when there is insufficient time or oxygen. Improper combustion of hydrocarbons causes the generation of CO, coupled with CO_2 and H_2O. Depending on the physical formalism of the fuel and oxidizer at the time of the burning reaction, burning processes can be classified as homogenous or heterogeneous. Homogeneous reactions take place all at once. The burning of a mixture of natural gas and air is the most frequent instance. There are two or more steps to heterogeneous reactions (Özer, 2019).

Char burning may be precisely controlled by chemical kinetics or dispersion rate, depending on the temperature and heating rate. Figure 2.4 shows the three char burning regions. At lower temperatures, char-burning is ordered by chemical kinetics, at moderate temperatures by O_2 pore dispersion, and at higher temperatures by O_2 majority dispersion. Another way to segment them is to evaluate the time scales of chemical kinetics and dissemination.

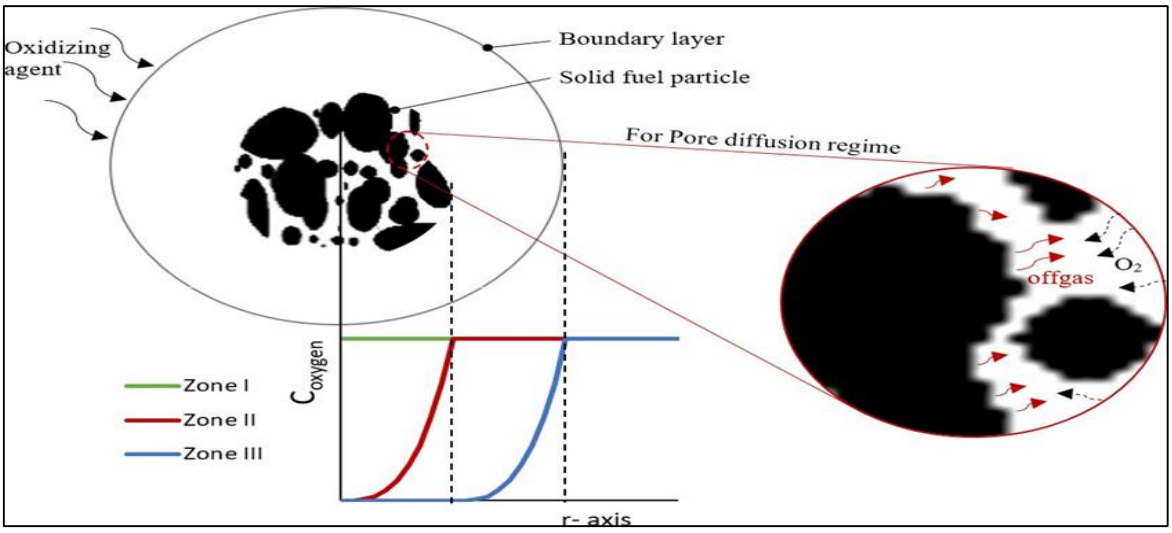

Figure 2.4: Rate-regulatory systems for heterogeneous char oxidation (Smith et al., 1994)

Zone I is mentioned in the kinetic limited circumstance. O_2 molecules diffuse into the element midpoint and meet carbon molecules at a higher rate than the burning rate. Meanwhile, O_2 molecules are not spent quickly; O_2 deliberation is continuous in the boundary layer and the particle. On the contrary, zone III has a higher reaction kinetic rate than the dispersal rate. Burning responses are so fast that a higher flow rate of vent gas does not permit O_2 molecules to spread the element. In the circumstances of zone II, kinetic and dispersal rates are so close to each other that the reactant gas is spent in the element but does not spread its midpoint (Özer, 2019).

Riaza et al. (2014) examined the burning and ignition performance of a single element of four different grade coals by consuming a drop tube furnace with laminar flow that is heated by electricity. Outcomes indicated that burning performance diverges relies on the coal grades. Char and volatile exhaustion periods are aggregated linearly with carbon and volatile substances in the coal, correspondingly.

Additionally, Khatami and Levendis (2016) stated cinematography pictures of numerous coal categories gained with DTF investigation at 1400 K wall temperature and inert flow circumstances. Conferring to the cinematography, burnout periods and the propensity of the coal to have different burning stages raises as coal grade rises.

Magalhaes et al. (2019) stated the burning and fragmentation performances of Soma and Tunçbilek lignites below higher heating and temperature circumstances. Cinematography, together with to drop tube furnace, revealed that Soma lignite elements disjointed widely in the devolatilization period. At that time, instantaneous devolatilization and char oxidation happened for the resulting fragments. Unexpected rise in the external area of Soma lignite because the fragmentation affected in smaller burnout period. Whereas, Tunçbilek lignite, which has a parallel elemental composition with Soma lignite, presented char oxidation and devolatilization in the directive.

2.2.5 Pakistan Coal Reserves

Pakistan's total coal assets are currently estimated to be around 185 billion tonnes containing recently discovered assets of Thar coal containing lower to moderate contents of sulfur. As per the Geological Survey of Pakistan, the coal assets of Sindh are expected to be about 185 billion tonnes (BTs), out of which more than 175.5 BTs are in the Thar coalfield. The accessibility of coal assets in Pakistan was previously recognized as a freedom; however, its economic worth was significant in 1980, when coal assets were found in the Sonda and Lakhra parts of Sindh. The coal assets of Pakistan have enlarged in the Thar coalfield in the Tharparkar district of Sindh. Afterward detection of the Thar coalfield, Pakistan has currently come to be the sixth leading coal deposited state in the world. Despite the global trend toward countries with large coal reserves, the Thar coalfield in Pakistan was not discovered earlier (Ali, 2019).

Moreover, to Thar coal assets, there are lignite coal assets situated in several districts of Pakistan, i.e., Lakhra, Sonda Indus East, and further parts of Sindh. Bituminous and sub-bituminous coals might be consumed for power production and their assets in huge volumes are situated in diverse coalfields in the Baluchistan and Punjab provinces of Pakistan. Further coal assets presented in the KPK and AJK areas of Pakistan are being extracted in lesser quantities, according to the geological survey of Pakistan. The coal assets of Pakistan are referenced as: Azad Kashmir and Gilgit-Baltistan, 9.0 MTs; Khyber Pakhtunkhwa, 91 MTs; Punjab, 235 MTs; Balochistan, 217 MTs; and Sindh, 184.6 BTs (Ullah et al., 2019). Measured assets are 7,775 MT, indicated assets are 19,412 MT, inferred assets are 44,524 MT, and hypothetical assets are 114,293 MT, according to the Hydrocarbon Development Institute of Pakistan (HDIP) (HDIP, 2014; Valasai et al., 2017).

Pakistan has impartially huge native coal assets that are enough to fulfill the energy necessities of the state on a continuing, maintainable basis. The local coal invention is probable to rise in the mining activity at Thar coalfield in coming years. Currently, brick kilns regularly use native coal, and cement plants use a lesser amount (NTDC, 2021).

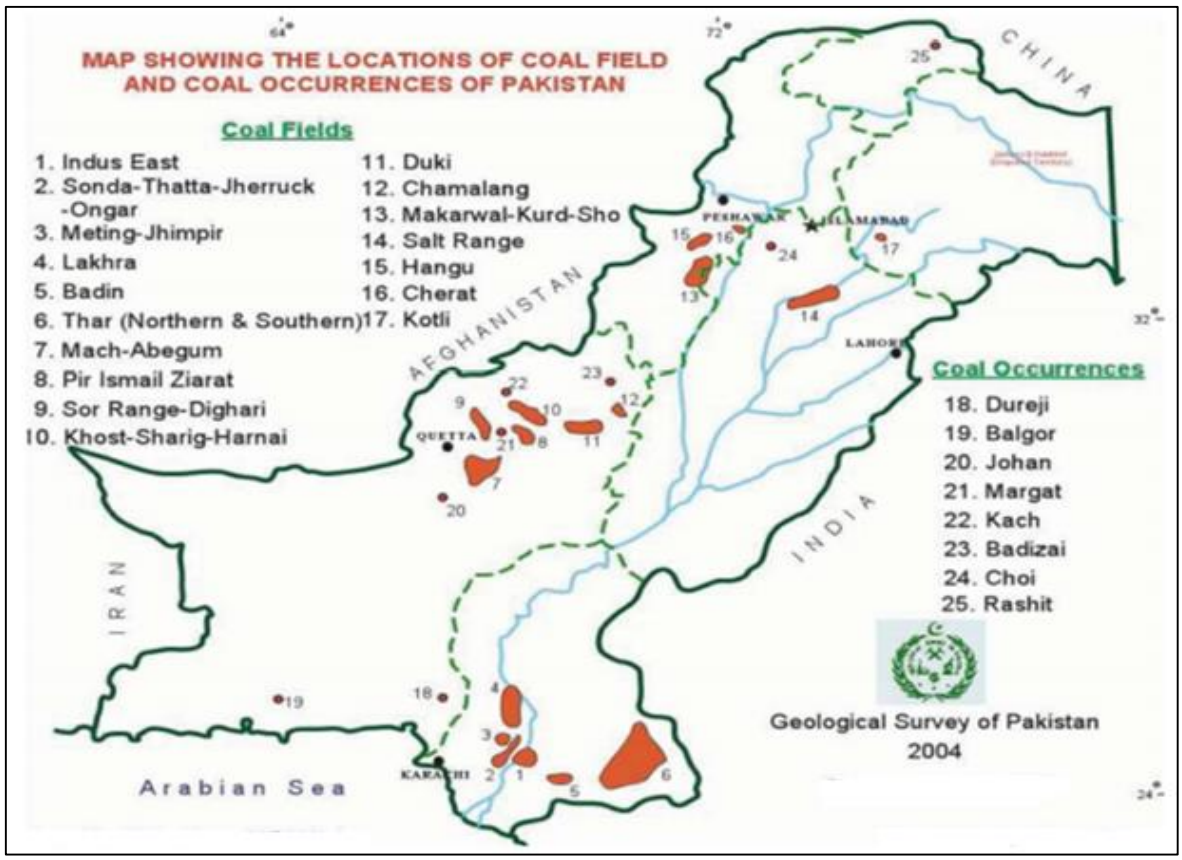

Figure 2.5: Location of coalfields in Pakistan (Malkani, 2012)

2.2.5.1 Thar Coal Field

The Thar coalfield is situated in the eastern portion of Sindh province, Pakistan, about 400 km from the province capital, Karachi. The Thar lignite coalfield was exposed in 1994. Thar coalfield covers around 9,600 sq. km. 65 kilometers (E-W) and 140 kilometers (N-S) of the Sindh desert. Thar coalfield has borders on the north, east, and south with India. Thar coalfield is deliberated to be the 7th biggest lignite coal reserve in the world. It lies among latitudes 24˚ 30' N to 25˚ 0'N and longitudes 70˚ 10' E to 70˚ 30' E (Nergis et al., 2018) as shown in Figure 2.6.

An enormous coalfield, having an asset value of around 175 billion tonnes, has been exposed at Thar, and 12 blocks have been established (Blocks I to XII). The worth of coal has been inspected by chemical analyses, and the quality of the coal was demarcated from

lignite B to A (Hagler Bailly, 2014). With the massive energy scarcity and the absence of any dependable and supportable indigenous energy assets in the country, the Thar coal mining development offers incredible development prospects. The consistency of this energy reservoir, as well as the venture's potential for reliability, make it one of the most relevant and long-term development goals for ending the energy crisis and bringing energy security to the state.

Figure 2.6: Thar Coalfield Location Sindh, Pakistan (JICA, 2013)

Thar coal has a lower overall sulfur level, making it an ideal fuel for thermal power generation. The Thar coalfield is surrounded by a sand dune that stretches to a depth of almost 80 meters and remains in the eastern area of the desert, leading to a structural platform (Ahmad et al., 2015). Shallow granite basement rock has comparatively underlain this platform. The Thar coalfield area's comprehensive geology is revealed in Figure 2.7. It is made up of a basement composite, the coal-bearing Bara formation from the Paleocene to the early Eocene, alluvial deposits from the recent past, and a modern sand dune. All the geological information has been obtained during drilling. Many coal seams are existing in

the zone. Thar coal color is normally brown to brownish-black and a little debarred and cleared. Resins in a range of colors, from dark brown to greenish-yellow, are currently available. Pyrite exists as fine grains (JICA, 2013). Apart from the assets' low sulfur content, heating value, and manufacturing capacity, the assets' massive size (175 billion tonnes), makes them a more capable asset that can serve the state for a minimum of two centuries (Masih, 2018).

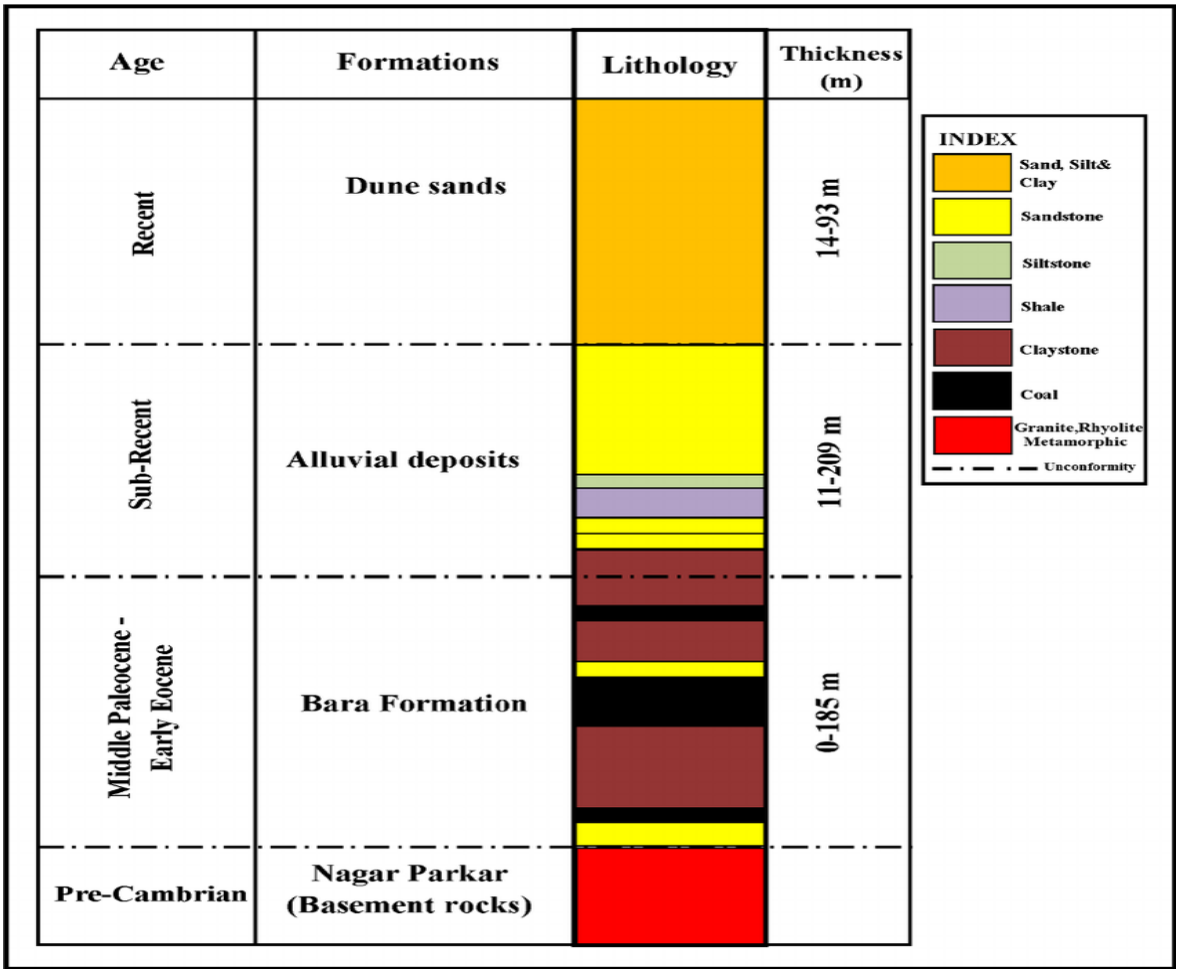

Figure 2.7: General Geology of Thar Coalfield (Ahmad et al., 2015)

The Thar lignite coal has a capacity of 175 billion tonnes, which necessitates special care while connecting with contemporary technologies. In general, conservative boilers depreciate coal and emit large amounts of NOx. Hence, because of decreased

environmental risks and increased electricity production efficiency, CFBC technology has been established and is used by contemporary productions and power locations (Raza et al., 2022). The practice of the CFBC technique is used for a variety of solid fuels, such as petroleum coke, municipal trash, and lignite coal. Because it has the potential to co-fire a variety of solid fuels, it is a techno-economically feasible selection for Pakistan (Luecke et al., 2004; Zhang et al., 2010). CFBC mechanization has numerous benefits, i.e., it increases ash, moisture, and sulfur content. Because SOx can be removed within the boiler by simply injecting limestone, and NOx cannot be removed because the furnace temperature is lower, i.e., 800–900 °C, the contaminating SOx and NOx discharges are ultimately minimized with Lignite's coal. Separate bag house filters for boilers to catch particulate matter, a dust annihilation system, and a distinct Continuous Emission Monitoring System (CEMS) for boilers are all available (Balat, 2007). CFBC technology is currently in use all over the world (Balasubramanian et al., 2021).

2.2.5.2 Thar Coal Reserves and Recourses

Coal reserves and resources for Block I -XII are concise in Table 2.4.

Table 2.4: Coal Resources and Exploration

Block	Allocated Investors	Exploring Agency	Classification system	Period	Total Drill Holes	Area (km^2)	Resources (million tonnes)			
							Measured <0.4km	indicated 0.4-1.2km	inferred 1.2-48km	Total
l	Sino Sindh Resources	GSP Rheinbraun Engineering (Germany)	GESCR	1994-1995	41	122	6020.42	1,918.06	1,028.43	3,566
			USGS	2003	30	40	588.035	403.351	11.934	1,003
ll	Sindh	GPS	GESCR	1994-1995	26+17	55	640	944		1,584
	Engro	Engro	USGS	2010	113	79.6	1,216	1021	114	2,351
		Engro	JORC-AusIMM	2010	113	79.6	425	1392	423	2,240
Ill-A	Couger	GSP	GESCR	1995-1996	41	99.5	412.75	1,337.01	258.28	2,008
Ill-B		GSP	GESCR	2007-2008	14	76.8	225.94	938.91	288.33	1,453
IV		GSP	USGS	1996-2001	42	82	684.09	1,711.28	176.14	2.571
V	UCG Project	CNCGB	USGS	2005-2006	35	63.5	637	757	-	1,394
Vl	Oracle Coalfield	CNCGB	GESCR	2005-2006	35	66	762	893	-	1,655
		Oracle	JORC	2008	7	66	653.000	770	-	1,423
Vll		DRD	USGS	2008-2009	52	100	572.28	1,514.51	89.15	2,175
Vlll		DRD	USGS	2008-2009	58	100	882.81	2,131.36	21.68	3,035
lX		DRD	USGS	2009-2010	50	100	661	2,048	152	2,862
X		DRD	JORC	2011	45	100	857.8	1,365.59	747.23	2,870
Xl		DRD	USGS	2012	31	101.46	315.6	1,014.28	282.17	1.612.05
			JORC				449.38	669.04	467.37	1,585.79
Xll		DRD	USGS	2012	31	100.74	510.01	1,755.85	79.74	2,345.60
			JORC				737.17	1,309.33	243.90	2,045.50
Total						**1432**				**39780**

Source: Thar Coal Energy Board (TCEB, 2017)

2.2.5.3 Thar Coal Quality

Coal qualities of Thar Block-I to XII are concise in Table 2.5.

Table 2.5: Coal Qualities for Thar Blocks I to XII

Block	Area (km^2)	Total Reserves (Billion tonnes)	Moisture (%)	Ash (%)	Volatile Matter (%)	Sulfur (%)	Heating Value (As Received) (Btu/lb.)	Fixed Carbon (%)
I	122.0	3.56	43.13	6.53	30.11	0.92	6,398	20.11
II	79.6	2.24	47.89	7.37	25.15	1.12	5,008	19.68
III-A	99.5	2.00	45.41	6.14	28.51	1.12	6,268	19.56
III-B	76.8	1.45	47.42	9.30	25.49	1.15	4,808	16.79
IV	82.0	2.47	43.24	6.56	29.04	1.20	5,971	21.13
V	63.5	1.39	46.82	8.92	30.24	1.20	5,682	13.26
VI	66.1	1.65	46.80	5.89	29.34	0.90	5,727	16.6
VII	100.0	2.17	48.27	8.03	25.30	1.16	5,440	25.30
VIII	100.0	3.03	49.57	7.78	24.32	1.44	5,302	18.10
IX	100.0	2.86	48.60	5.92	29.03	0.96	5,561	15.73
X	100.0	2.87	48.99	6.35	30.79	1.17	4,840	13.54
XI	101.0	1.61	49.97	8.07	24.16	1.61	5,228	17.26
XI	100.0	2.34	50.82	5.71	25.00	1.11	5,459	17.26

Source: Mines and Minerals Development Department, Government of Sindh and JICA (2013)

2.2.5.4 Thar Block II

Thar Block II is located in the District Thar Parker in the eastern region of Sindh Province, Pakistan, at latitudes of 24º 43' 38" - 24º 50' 18" and longitudes of 70º 17' 36" and 70º 26' 16". Thar block II has total lignite assets of two billion tonnes, making it one of the 12 blocks in Pakistan's Thar coalfield and the only one that is currently being mined (Hina et al., 2018). It is near the villages of Singharo-Bitra, 20 km from Islamkot City. Thar Block II is shown in Figure 2.8.

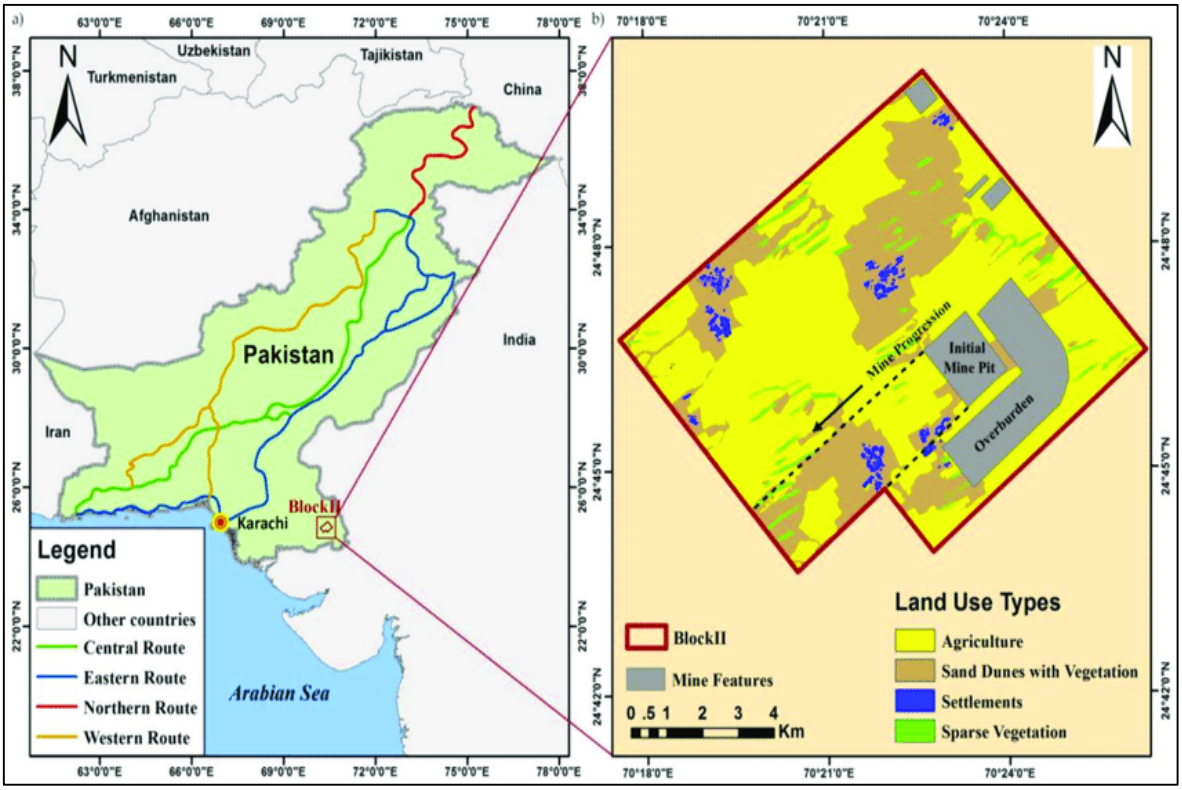

Figure 2.8: Location of Block II (Hina et al., 2018)

Thar Block II covers 95.5 square kilometers (km^2) in the vicinity of the coalfield. Sindh Engro Coal Mining Company (SECMC) was in charge of exploring and expanding the block's coal resources.

Within Block II, SECMC is constructing a 660 MW (2330 MW) mine-mouth power plant (Hagler Bailly, 2014). The climate of Thar Block-II is subtropical. Temperatures generally go as high as 50°C in summer and as low as 2°C in winter. Following are some significant aspects of Thar Block-II geology. The ground altitude varies from 80 to 100 meters Above Mean Sea Level (AMSL), overstrain width fluctuates from 130 to 150 m, the core lignite layer has a width of 18 m, accumulative lignite width fluctuates from 22 to 32 m, and three aquifers are existing in the area (Hagler Bailly, 2014). As per Cambridge Energy Research Associates (CERA) assessments, Block-II will enormously advantage entrepreneurs, local customers, and the economy of the state by decreasing the power production rate and providing continuous electricity (Masih, 2018).

2.2.5.5 Thar Block II Coal Quality

Coal quality is currently acknowledged as having a practical and often important effect on coal burning, particularly in numerous parts of the power plant process. The constraints of rank, ash content, moisture, and sulfur are considered defining features in burning (Choudry et al., 2010). Hagler Bailly Pakistan described Thar Block-II coal quality as lignite.

SRK UK, Sino Coal China, RWE Germany, Hagler Bailly Pakistan, and NCGB China, among others, have all accompanied investigations to pattern the reliability of the Thar coal assets and found that fresh coal contains 45.71% of moisture, volatile matter is 25.00%, ash is 9.69%, and fixed carbon is 19.6% (Shaikh, 2016).

Thar coal's usual calorific value (11.6 MJ/kg) differs from related types of lignite coal assets in other states, such as Hungary lignite (7.1 MJ/kg) and Rhineland lignite (Germany), and makes the Thar coalfield relatively affordable (Choudry et al., 2010).

According to the Environmental and Social Impact Assessment (ESIA), GHG gas production from the Block-II power plant might exceed 4.9 million tonnes per year (Hagler Bailly, 2014). Carbon emissions from lignite are estimated to be 101,000 kg per Tera-joule of heat input using the IPCC Tier 1 procedure (Masih, 2018). A chemical study of raw coal ash revealed a higher % of silicon dioxide and aluminum oxide, low calcium oxide and ferric oxide, and a little amount of manganese oxide and sulfur oxide (Choudry et al., 2010).

2.3 Thermogravimetric Analysis (TGA)

TGA is a unique and most common method used to study thermal measures and kinetics in the course of coal pyrolysis (Arenillas, et al., 2004). It delivers a mass loss measurement of the sample as a function of temperature and time. The disparity of fuel form for the duration of thermochemical transformation has been widely deliberated for an enormous range of petroleum in TGA apparatus. The appropriateness of the substantial for

burning relies on the different appearances of the fuels, such as water substances, heating rates, and feed dimensions. A range of fuels can be mixed and burned (Boerrigter and Reinhard 2006). Thermogravimetric is the thermal deprivation method that mostly relies on the circumstance in which it happens, e.g., the inert circumstance is desirable for pyrolysis, limited oxidizing or reducing for gasification, and additional oxidizing for burning. Thermogravimetric analysis is extensively proceeding in the study of the effect of reactive atmospheres and proximate analysis and defines the thermal constancies and disintegration of constituent's kinetics (Hussain, 2015). TGA deals with a measurable sympathetic of the pyrolysis course under fine, precise laboratory circumstances. Nevertheless, the TGA technique only delivers facts about the loss of total mass sample relative to temperature and does not essentially relate to the chemical complex in the solid waste's thermal deprivation (Vuthaluru, 2004).

Burning is deliberated as an addition to pyrolysis. Many scholars studied the pyrolysis method for a range of resources like biomass, coal, and mixtures via TGA and described their remarks for mass loss and de-volatilization performance of these constituents (Hameed et al., 2020; Sonobe and Worasuwannarak, 2006; Damartzis et al., 2011; Chen and Kuoh, 2011; Wang et al., 2012; Hass et al., 2001; Hussain, 2006).

While further investigators studied the burning procedures via TGA, acquired in oxidative circumstances (Yorulmaz and Atimtay, 2009; Shen, et al., 2009; Sonibare, et al., 2005; Mortaria, et al., 2010; Safi et al., 2004). TGA is also used to define the kinetic constraints of a range of coal and biomass resources (Munir et al., 2009; Tiwari and Deo, 2012; Mehrabian et al., 2012). Moreover, aspects distressing the thermal and kinetic disintegration of resources have been the subject of the attention of numerous investigators, who resolute the burning kinetics of remaining char in the pyrolytic procedure (Cai and Chen, 2012; Senneca et al., 1999; Otero et al., 2008).

German lignite coal's TGA was examined by Hassaid et al. (2022). In a temperature range of 30–1000 °C, 5 mg of the sample of coal of the designated size was heated at a rate of 5–10 °C/min in air, oxygen, and nitrogen. They discovered that low-rank lignite undergoes two distinct stages of oxidation. The majority of the coal content undergoes

oxidation in the first step at low temperatures (between 220 and 400 °C), perhaps as a result of the more reactive aliphatic CH content, and at higher temperatures (between 420 and 520/580 °C).

Thermogravimetric analysis was used by Patel et al. (2022) to assess the thermal breakdown characteristics of Indian lignite coal. TG curves of lignite at various heating rates of 5, 7, 10, 15, 20, 30, and 50 °C/min in an oxidizing environment. The weight loss of the lignite sample took place throughout a wide temperature range, from 125 to 900 °C, demonstrating a temperature-dependent weight loss. The breakdown began at over 125 °C and lasts until about 900 °C. Between 200 °C and 400 °C, the rate of decomposition was extremely high, and it gradually decreased as the temperature increased. The modification in heating rate has no impact on an asymptotic yield at the 900 °C final temperature. During the disintegration, lignite lost about 60% of its weight.

Usto et al. (2021) characterized Thar lignite coal with Thermogravimetric Analysis (TGA) to examine the burning performance of treated coal. It was perceived that the burning properties of treated Thar lignite coal at 5–10 °C/min, a little amount of mass loss was observed up to the temperature of 150 ^{o}C due to volatile loose and from temperature 330 ^{o}C to 520 ^{o}C mass of coal was rapidly reduced, about 75% coal mass lost.

Yuan et al. (2021) studied the co-burning features of coal and biomass mixtures (20, 40, 60, 80, and 100 % wt.) by thermo gravimetric analysis. All the samples functioned under an oxidative environment, with a heating rate of 20 ^{o}C/min. Established on numerous burning indices, 20% was an optimal % for the co-burning of coal biomass mixtures. With the decreasing biomass fraction in the mixtures, the activation energy value and pre-exponential aspect improved.

Bampenrat et al. (2021) investigated the thermal characteristics and kinetic limits of coal/biomass combination blends (75:25, 50:50, and 25:75 % wt.) at 5, 10, 20, and 40 K/min using the Thermogravimetric method. Thermal degradation of biomass happens in 3 to 4 phases, according to the findings: moisture and light volatile elimination (up to 463 K), char burning (663-823 K), volatile oxidation (423-663 K), and inorganic oxidation (423-663 K) (803-953 K). During the burning process, lignite, on either has only two principal

peaks, which correspond to moisture loss (up to 433 K) and disintegration/oxidation (433-833 K).

The thermal profiles of Thar lignite coal were examined by Wahab et al. (2020) under conditions of dry air and a dynamic heating rate of 25 °C/min. Two heating zones were created within the chosen heating profile. The temperature in the first heating zone was increased from ambient to 110 °C at a rate of 15 °C/min. The temperature was again ramped up at a rate of 25 °C/min until it reached the final temperature of 950 °C, where an additional hold-up 10 min was allowed to assure full combustion. The apparent activation energy "Ea" (kJ mole1) and the order of the average and peak rate of conversion for Thar coal were both found to be 23.1.

Mehdi et al. (2020) examined the thermal act of lignite and rice husk, as well as their combinations, using pyrolysis and burning operations. The results of the burning investigation revealed that the thermal constancy of lignite decreased as rice husk increased. The slow decay of lignite in blends was seen in the TG curve, which showed that the weight degradation rate decreased from 330 °C to 950 °C. Over a wide temperature range of 180-950 °C, the loss of carbon atoms typically occurs at a slower pace.

Rizvi et al. (2015) studied two heating rates of 10 and 40 °C/min, a non-isothermal TGA of Thar coal was investigated under reaction situations containing O_2 21−30%/N_2 70−79% and O_2 21−30%/$CO_2$70−79% to study their particular kinetics reaction at these four changed burning circumstances. More reactivity of the Pakistani Thar lignite coal was perceived at a higher O_2 concentration of 30% and heating rate of 40 °C/min.

Sarwar et al. (2014) used a TGA to describe the Thar coalfield and discovered that the chemical reactivity of Thar coal was identified at the basic de-volatilization portion (257–412 ^{0}C) and secondary de-volatilization portion (741–900 ^{0}C).

Sarwar et al. (2012) looked into a different study for Thar block V. Thermal disintegration of Thar coal is a diverse heterogeneous method containing an amount of equivalent and repeated reactions, according to kinetic studies of oxidation and de-volatilization of the samples. The average activation energy and burning processes for

pyrolysis are 35.50 and 34.27 kJ/mol, respectively. It is classified as reactive coal because it has lower activation energy values.

Table 2.6: Summary of previous related TGA studies

References	Year	Hydrodynamics	Coal Type	Heating Rate
Hassaid et al.	2022	Yes	Lignite	5–10 °C/min
Patel et al.	2022	Yes	Lignite	5, 10, 15, 20, 30, & 50 °C/min
Usto et al.	2021	Yes	Lignite	5–10 °C/min
Yuan et al.	2021	Yes	Lignite	20 °C /min
Bampenrat et al.	2021	Yes	Lignite	5, 10, 20 and 40 K/min
Wahab et al.	2020	Yes	Lignite	15 °C /min to 25 °C /min
Mehdi et al.	2020	Yes	Lignite	40 °C/min
Rizvi et al.	2015	Yes	Lignite	10 and 40 °C/min
Sarwar et al.	2014	Yes	Lignite	10 °C/min
Sarwar et al.	2012	Yes	Lignite	10 °C/min

Therefore, as such TGA permits investigators to precede their research on a small laboratory scale, other than at a level of the plant. The thermal transformation procedures and make their remark on the operative constraints disturbing the transformation and kinetic performance of these thermal procedures.

2.4 Coal Blending with Biomass

Since ancient times, biomass has been the primary source of energy. Biomass energy has been used since the beginning of time. Even at this early stage, biomass has been the primary source of domestic energy in several developing countries (Kumar et al., 2015). Sweden is the world leader in the production of biomass energy. Sweden is one of the wealthiest countries in the world in terms of GDP per capita (Johansson et al., 2004; Irfan et al., 2020a). Biomass is a renewable energy source that is both ecologically friendly and safe to use (Irfan et al., 2019b). Diverse biomass assets, combined with crop residues, result in lower greenhouse gas emissions.

The total mounted capability of biomass electricity has surpassed 130 GW worldwide (REN21, 2019). Latent biomass assets used for electricity generation in Pakistan include animal waste, forest remnants, agronomic residues, and urban solid trash. All of these assets combined produce 230 billion tons of biomass each year (Iqbal et al., 2018).

Co-firing coal with biomass to make energy has been vigorously investigated and implemented for over two decades. Numerous information have been printed by the IEA Clean Coal Centre (IEACCC), covering all features of co-firing coal with biomass, and those available in the previous decades are; Zhang (2019) support apparatuses for co-firing coal with biomass; Dooley and Mason (2018) supply restraint budgets for biomass co-firing; Barnes (2012) Sympathetic pulverized coal, biomass and waste burning; Fernando (2012) co-firing high proportions of coal with biomass, etc.

Numerous developing economies rely on coal for safe, reasonable, and consistent power production and supply. Hence, it is vigorous to guarantee that coal is used proficiently with the least environmental effects. Firing native lignite coal with biomass or high-quality coals in states like Pakistan, India, and Bulgaria might support reducing the price of power generation and possessing producing power at high efficacy with fewer emissions to deliver energy at a reasonable value (Argus, 2021). Adding lignite to biomass or using higher-quality coals could also help lower fuel prices. Coal configurations, like proximate and ultimate analysis information and the calorific value, continue additive afterward blending (Dong, 2021). It's more difficult to predict the impact of a physical structure on a mix of factors like slog capacity, swelling, ash fusion temperature, and burning characteristics. Blending fraction, furnace and grinder performance, burning characteristics, and ash cotent are the most important factors to consider while burning lignite mixes at power plants. Small-fraction lignite blends (less than 15%) could be accepted without plant modification at coal-fired power plants (Zhang, 2021).

Co-combustion allusions, which link coal and a variety of biomasses, can play a significant role in coal partial substitution (Zhang and Meloni, 2020). Biomass co-combustion also offers a cost-effective, secure, renewable, and long-term solution to the environmental challenges produced by the massive usage of coal. As a result, not only may

CO_2, SOx, and NOx emissions be reduced, but also the discharge of gases such as ammonia, organic acids, methane, hydrogen sulfide, and their compounds can be limited, and several researchers have highlighted the compensation associated with co-combustion. (Williams et al., 2001; Sweeten, 2003). Biomass usage is an alternative energy asset that progressively gains attention because of its low cost and easy accessibility as a by-product (Shahbaz et al., 2020).

As an alternative to developing dedicated biomass-fired power plants, the complementary utilization of biomass as fuel, mainly with extremely resourceful coal-utilizing power plants (Sahu et al., 2014; Hupa, 2005). Carbon impartiality is one of the mainly vital rewards related to utilizing biomasses as they are likely to attract a similar quantity of CO_2 for the period of their life cycle as they release CO_2 after burning (Munir et al., 2010). Co-combustion has a number of potential advantages, such as a decrease in CO_2 discharges from fossil fuels, a less complicated and therefore potentially cost-effective change in biomass and coal with elevated efficiency, and under controlled environmental circumstances (Shahzad, 2015).

Further co-combustion-related studies done by different researchers describe the benefits of co-combustion, such as Xu et al. (2009) and Shen et al. (2012), which found that the combination of coal with biomass, known as co-combustion, is a capable tool to attain higher transfer efficacy burning methods. The main remunerations of co-firing are that the combined value constraints like heating value and sulfur and ash are retained.

The co-burning of coal and sludge can result in a change in the sludge's energy, according to Liang et al. (2022). The boiler temperature was increased, and the sludge moisture content was decreased given a continual mix ratio. The boiler exits temperature design by around 108K when the moisture content is reduced from 80% to 20%, thus increasing the degree of fuel burnout. Additionally, this difference caused the thermal NOx content to increase while maintaining the fuel NOx level. The NOx output rose by 32.9% when the moisture content dropped to 20%.

In N_2/O_2 and CO_2/O2 atmospheres, Qi et al. (2021) calculated the ignition and burning characteristics of single elements of two biomass remnants (wheat and maize

straw) and three coals (anthracite, bituminous, and lignite coals). They stated that the biomass and lignite elements burned equivalently, whereas the bituminous coal and anthracite elements burned heterogeneously.

According to Bhattacharyya et al. (2021), co-pyrolysis of coal with sawdust is a practical option for using low-grade coal to produce pyrolytic oil. By lowering the stimulation energy and Gibbs free energy, co-pyrolysis of coal with sawdust promotes an increase in the degree of thermal deprivation in low-temperature sections. Consequently, co-pyrolysis using waste biomass is an acceptable way to manufacture solid, liquid, and gaseous products since low-rank coal has a low heating value and is more thermally constant.

Using a Thermogravimetric analyzer, Guo et al. (2020) investigated the co-burning of biomass pellets and the two types of coal. They discovered that raising the biomass pellet fraction enhanced the extreme burning ratio and burning index while lowering the exhaustion temperature, implying that coal's burning performance might be improved.

Maitlo et al. (2019) prepared a numerical CFD model of gasifier flow to simulate coal and biomass mixtures. Pakistani Thar lignite coal and sugarcane bagasse were used as feedstock for gasification. Different fraternization structures were implemented to attain the best performance through the co-gasification procedure. The best combination ratio was observed at a combination ratio of 35:65 on a weight basis. At the optimal combination fraction, the carbon conversion efficiency (CCE) and cold gas efficiency (CGE) were 87% and 99.8%, correspondingly.

Sasongko et al. (2017) determined that blending coal that has a greater heating value than lignite coal and is similarly more ecologically pleasant might be attained by co-burning of coal and rice husk. Investigational results recommended that by rising the co-burning temperature from 200-400 °C, the heating value of blend coal could rise by 14.5-17.7%. Solid fuel 30% combination is suggested for making a coal mixture as the rising biomass ratio would decrease the heating value of blend coal. The mixture of coal that was

formed from this study was similar in bituminous coal heating value, hence appropriate for power plants whereas being further environmentally pleasant.

Anukam et al. (2016) deliberate the impact of blending on the transformation efficacy of the co-gasification procedure of coal and corn stover. They found that the utmost appropriate blend was 90% corn stover/10% coal since a change was autonomously attained at a temperature that is in between that of coal and corn stover. Though, outcomes also displayed that the fitness of coal and corn stover for co-gasification relies on a numeral aspect which comprised the configuration and properties of together feedstocks and the fraction of combination as well as the working circumstances of the gasifier.

Zuo et al. (2015) used isothermal thermo gravimetric analysis at 900, 950, and 1000 °C to investigate the isothermal gasification responsiveness of coal char (CC) and biomass char (BC) mixed at mass fractions of 1:3, 1:1, and 3:1 under CO_2. They observed that with a rise in BC combination fraction, there were a rise in gasification amount and a limitation of the gasification period. This could be due to the great homogeneity of carbon structures in CC and the specific surface area of BC, which was previously related to BC. The BC combination fractions of 75 percent had the lowest activation energy (123.1 kJ/mol). All mass fraction of the blended char produced synergistic results, which grew in size as the gasification temperature increased.

According to Tchapda and Pisupati (2014), the reason for the composition of the feedstock can influence the conversion actions during the initial stages of fuel de-volatilization and char gasification. They also investigated the impact of the temperature profile next to the height of the bed and discovered that a rise in temperature next to the riser height supported minimal oxidation and reactions.

Related to this Wei et al. (2013) observed that higher coal char substance (~45%) is mixed with biomass of less coal (~20%) with mass fractions of 80:20, 90:10, 100:0 and in categorize to make superior quality gas. It was observed that with the rise of the coal fraction, the temperature raised notably and additional burnable gases similarly CH_4, CO were produced.

In inconsistency with above Ataei et al. (2012) studied a reduction in efficiency for the blends of together, rice husk and bagasse, when coal 50% blend with rice husk and bagasse was co-combustion.

Further to the above, Seo et al. (2010) found that co-firing less volatile coal with high volatile biomasses improves the burning with an added advantage of a decline in CO_2 release to the atmosphere.

Prins et al. (2007) studied that the configuration of creator gas was mostly pretentious by the fraction of biomass in the co-burning procedure. Biomass and coal change in configuration; the biomass mostly holds 45% oxygen and 50% carbon with small ash, while coal holds 5-20% oxygen and 60-85% carbon, relying on the coal grade (bituminous–lignite). Different biomasses consumed as a fuel in co- burning in diverse mass fraction has been described in the literature.

Whereas, a few other researchers like Kazuhiro et al. (2007) described the outcome of coal and biomass blending in diverse fractions for co-combustion and monitored the variation in the configuration of produce gas with modification in mixture fraction at 900°C temperature. The study of the resulting produce gas illustrated higher hydrocarbons (0.8-2.9), reduction in H_2 from 47.9 to 37.5 (vol %), while enhancement in other gases like CO (22.1-23.9), CO_2 (26.1 to 33.7), CH_4 (2.6-4.6) were observed.

Cordero et al. (2004) found that due to the reduction of fuel-nitrogen and sulfur in the ash withholding, a clear reduction of SOx and NOx discharge for co-burning of coal and straw was studied. Further to above a raise in desulphurization was studied when blending coal with multiple types of biomasses throughout combustion.

Additional investigators Pan et al. (2000) utilized two diverse natures of low-grade coal in combination with biomass and studied the effects of the combination on co-combustion. They suggested at least 40 wt% for refuse coal and 20 wt% of pinewood chips for low-grade coal to obtain an improved conversion, with the fluidized bed.

In recent periods, a study is ongoing to discover more effectual usage of biomass energy and numerous technical investigations have been conceded on this tool to increase full remunerations deprived of impairing the environment. Due to the lowest investment cost, lowest electricity production rate, accessibility of all assets, and delivery of widespread employment prospects, it is of vigorous significance for energy-ravenous developing countries (Iqbal et al., 2018).

Table 2.7: Summary of previous related coal blends studies

References	Year	Hydrodynamics	Coal Blends	Char Combustion	Emissions
Liang et al.	2022	Yes	Yes	Yes	Yes
Qi et al.	2021	Yes	Yes	Yes	Yes
Bhattacharyya et al.	2021	Yes	Yes	Yes	Yes
Guo et al.	2020	Yes	Yes	Yes	No
Maitlo et al.	2019	Yes	Yes	Yes	No
Sasongko et al.	2017	Yes	Yes	Yes	No
Anukam et al.	2016	Yes	Yes	Yes	No
Zuo et al. (2015)	2015	Yes	No	Yes	No
Tchapda and Pisupati	2014	Yes	Yes	Yes	No
Wei et al.	2013	Yes	Yes	Yes	Yes
Ataei et al.	2012	Yes	Yes	Yes	No
Seo et al.	2010	Yes	Yes	Yes	Yes
Prins et al.	2007	Yes	Yes	Yes	No
Kazuhiro et al.	2007	Yes	Yes	Yes	Yes
Cordero et al.	2007	Yes	Yes	Yes	Yes
Pan et al.	2002	Yes	Yes	Yes	No
Liu et al.	2000	Yes	No	Yes	Yes

2.4.1 Co-Combustion of Rice Husk

Pakistan is a cultivation state, generating all the main crops like rice, maize, wheat, cotton, and sugarcane. Production of the rice crop is estimated at 6160 million tons, with an

increasing rate every year. Rice hulls engage two phases of the paddy milling process. Initially, 12.5% of the hull is separated, which is utilized as fuel in brick kilns and rice mills, whereas in the next step, the residual of the husk beside certain shattered parts of rice is eliminated. This rice husk component is consumed as fuel and animal feed. Because it is less expensive and easier to transport, rice husk captivates too much admiration as a boiler fuel (Hussain, 2015). There are only a few studies in the literature that look at biomass energy's potential, mostly in Pakistan.

According to Nazar et al. (2021) rice husk is a suitable fuel for the boiler, much like coal and furnace oil. They were working on a boiler that produces 370 tons of steam per day at a temperature of 281 and 15 bar pressure. The quantity of fuel needed to generate 370 tons of steam was altered for each fuel, including rice husk, furnace oil, and coal. The efficiency of coal-fired boilers, furnace oil, and rice husk was found to be 87 percent, 80 percent, and 64.8 percent, respectively. This proved that using rice husk as boiler fuel was an efficient and affordable energy source.

Using different fractions on the thermal foundation of coal and biomass assumed as 50:50, 60:40, 70:30, 80:20, 90:10, and 100:0 by mass proportion leftovers from rice husk, poplar sawdust, sunflower residues, and pine nutshells, Kanwal et al. (2021) formed coal and biomass combinations. According to the study, burning coal and biomass together can greatly help in lowering emissions of hazardous gases, increasing burning efficiency, and reducing the amount of particulate matter released into the environment.

Rice husk combustion in a rectangular fluidized bed combustor was studied by Chokphoemphuna et al. (2019). Among the investigated excess air fractions, excess air (EA)= 60% produces the best burning performance of 99.2 percent. The lowest CO, CO2, O2, and NOx emissions are also produced while burning at EA=60 percent; they are 236.8% Vol, 2.55 ppm, 13.53 percent Vol, and 110.2 ppm, respectively.

Siddiqi et al. (2018) used Thermogravimetric analysis for burning and pyrolysis concert of Pakistani lignite (PL) and rice husk (RH) mixtures of 50PL/50RH, 40 PL/60RH

and 30 PL/70RH underneath oxygen and nitrogen atmosphere circumstances. The thermal constancy of lignite was discovered to be declining with the increase of rice husk in the burning investigation. They discovered that 50PL/50RH is suitable for power generation due to its high heating value, low ash content, volatile matter, and ignition theme in comparison to other samples, and lower costs than imported coal. This will finally outcome in a benefit to decreasing contamination and production of NOx.

Akhtar et al. (2018) investigated the coal and rice husk combination and boiler temperature on gaseous discharges and exhaustion in a drop tube boiler vessel. It was observed that the combination proportion facilitated decreased discharges of NO and SO_2 associated with Lakhra coal. A decrease in NO and SO_2 discharges was establish to be 8 and 17.8% by growing the combination fraction from 5 to 15%.

Jaffri, (2018) found that the H_2S volatilization is greater for Rice husk and Bagasse (18 bar) and less for Rice husk and Bagasse (6 bar) at a higher pressure in the course of gasification. She also predicted that the SO_2 volatilization is lesser for rice husk and Bagasse (12 and 18 bar) at higher pressure.

Wang and Li (2018) investigated a two-dimensional riser model made for an exploratory fluidized bed bench. A numerical simulation for the burning reaction of various portions of coal and rice husk has been prepared using Fluent software. The results show that when rice husk fraction increases, burning temperature and nitrogen oxide volume drop concurrently, and the influence is gradually reduced. According to this simulation, a reasonable amount of rice husks is around 30%.

Quispe et al. (2017) studies the energetic latent of agronomic residues, concentrated on rice husk. The assessment defines straight burning and fast pyrolysis tools to convert rice husk into energy seeing its physicochemical properties. Furthermore, the use of rice husk is environmentally rigorous and sustainable.

In a 100 kW CFBC, Sathitruangsak and Madhiyanon (2017) investigate the burning characteristics of coal and rice husk and their co-burning. The discharge of volatiles was

discovered to be ignited mostly above the bottom bed, and the burning of rice husk may not be sustained without the assistance of an external heat source. The use of more rice husk during co-burning resulted in increased CO outputs. Even though rice husk makes up about half of the coal, nitrogen, and NOx emissions increased as more rice husk was used in the mix of fuel.

Anshar et al. (2016) assert that the use of rice husk as a fuel for energy plants could ease the shortage of electrical energy, lower the consumption of fossil fuels, and diminish negative environmental effects.

According to Mohiuddin et al. (2016), rice husk produces 47.36 cents/kWh of energy per unit, compared to coal's 55.22 cents/kWh, which results in an annual power output of 1,328 GWh assuming 70% of the leftover rice husk is used. They estimated that 225 tons of rice husk produce 10 MW of electricity per day.

As per Shah et al. (2016), biomass fuels such as rice husk and sugarcane bagasse can be considered as appropriate fuels for power generation and can be delivered as an environmental friendly fuel for power generation.

Shahzad et al. (2015) studied the fluidized bed burning performance of coal and biomass due to its important contribution to heating systems and power plant processes. This burning performance has been considered by numerous investigational methods along with dissimilar kinetic models.

Bhutto et al. (2011) focused on the issues and tasks involved in the efficient and actual use of biomass as energy in Pakistan. Rice husk energy is largely determined by its configuration; proximal and final analyses.

Mahar (2010) analyzed a variety of tools for converting agricultural biomass to energy and found them to be the most reasonable, environmentally sound, and cost-effective options. Organic substance in the rice husk further concerted methods of energy will be useful.

Mirza et al. (2008) investigated Pakistani biomass energy use and evaluated the various options for generating electricity in rural areas using biomass. They discovered that biomass is an environmental friendly and cost-effective fuel source with great potential for demand in Pakistan.

Table 2.8: Rice Husk Production in Sindh, Pakistan

Province	District	Rice Mill	Rice husk Production (Tons/yr.)
Sindh	Larkana	Abadghar Rice Mill Larkana	650
Sindh	Qambar Shahdadkot	Memon Rice Mill Kamber	760
Sindh	Qambar Shahdadkot	Mumtaz Rice Mill Mirokhan	800
Sindh	Larkana	Dastagir Rice Mill Badah	800
Sindh	Qambar Shahdadkot	Hamid Rice Mill Wagan	800
Sindh	Qambar Shahdadkot	Tunio Rice Mill Mirokhan	800
Sindh	Larkana	Khshtkar Rice Mill Larkan	800
Sindh	Qambar Shahdadkot	Mughari Rice Mill chamber	800
Sindh	Larkana	Amanullah Rice Mill Larkana	900
Sindh	Qambar Shahdadkot	Bismilah Rice Mill Nasirabad	960
Sindh	Larkana	Husnain Rice Mill Ratodero	2400
Sindh	Qambar Shahdadkot	Faiz Masan Rice Mill Nasirabad	1120
Sindh	Qambar Shahdadkot	Mohammadi Rice Mill Nasirabad	1120
Sindh	Larkana	Jawad Rice Mill Larkana	1120
Sindh	Qambar Shahdadkot	Ubaidullah Rice Mill Kamber	1120
Sindh	Qambar Shahdadkot	Aziz Rice Mill Wagan	1120
Sindh	Qambar Shahdadkot	Abidullah Rice Mill Mirokhan	1200
Sindh	Qambar Shahdadkot	Madina Rice Mill Mirokhan	1200
Sindh	Larkana	Bismilah Rice Mill Ratodero	1440
Sindh	Larkana	Masha Allah Rice Mill Ratodero	1600
Sindh	Qambar Shahdadkot	Aaquib Rice Mill Kamber	1600
Total			**23110**

Source: (World Bank, 2016; Iqbal et al., 2018)

Kwong et al. (2007) confirmed that gaseous contaminants like CO, CO_2, SO_2, and NOx, might be decreased in the coal burning with rice husk. Madhiyanon et al. (2009) investigated the 120 KWth cyclonic fluidized bed combustor burning with bituminous coal and rice husk. They studied the influence of additional air fraction and fuel mixtures on emissions and burning efficacy. CO discharges were observed up to a reasonable level, while NOx releases seemed higher due to elevated bed temperature.

For the recapture of energy from various biomass resources, different thermochemical transformation techniques such as CFB boilers and gasifiers have been confirmed, explored, and used (Sharma et al., 2014; Lee et al., 2019; Tareen et al., 2020). The rice husk production in Sindh province, Pakistan is shown in Table 2.6.

Biomass and agricultural wastes converted to bioenergy can also contribute to alleviating the energy crisis and reducing broad reliance on fossil fuels developed assets (Danish et al., 2015). Nevertheless, widespread and consistent data on the rice husk characteristics relating to the strategy of such schemes is missing. For proper design and modeling, a complete indulgence of the rice husk is required.

2.5 Circulating Fluidized Bed Combustor (CFBC) Technology

Numerous options are available for power generation from coal, whereas pollution in the air is related to it. The selection of converting to less-ash, low-sulfur coal is one of the modest selections; however, it might be objectionable because of the non-obtainability of low-ash or low-sulfur coal at a realistic rate. A low NOx burner is a recognized tool; however, it cannot comply with the emission conditions for most world countries, and it might enhance the loss of carbon in the boiler. On the other side, CFBC has proven itself to be more cost-beneficial (Basu and Debnath, 2019). The essential assets of fluidized combustion permit them to limit the release of both SO_2 and NOx under the limits fixed by the environment-control authorities without pretreatment of coal or extra tools like special burners, vent gas desulfurization or catalytic converters (Basu, 2015). In 2016, above 3000

CFB boilers were in commercial production with a total mounted capability of above 90000 MW amongst over 100 items is 300 MW (Cai et al., 2017). CFBs have been studied intensively during the past two decades to continuously improve the industrial process and are being used in many countries (Hussain, 2018; Jia et al., 2010). The CFB technology was initially used for the ignition of coal because of its unique capability to run low-quality and high-sulfur coal. A wide range of experimental studies have been done to date on the viability and performance of the CFBC of various fuels. A CFB boiler is producing steam by combustion of fossil fuels in a combustion compartment worked underneath a distinctive hydrodynamic circumstance (Basu and Debnath, 2019). The combustion compartment of a CFB boiler contains a huge portfolio of non-burnable items that are elevated and exited by high-velocity burning gas over the boiler. The main segment of solids that exits the boiler is arrested by a solid-gas partition and is re-circulated back nearby the bottom of the furnace at a level acceptable to the base of the furnace (Basu, 2015).

2.5.1 Circulating Fluidized Bed Boiler Features

The combustor chamber of a CFB boiler comprises a huge number of granulated solids, termed bed materials. Bed ingredients might be prepared by the following:

a) Gravel or sand (burning small-ash fuels boilers).
b) Limestone (boiler combustion with high-sulfur coal or for sulfur discharge control).
c) Fuels Ash (boilers combustion with medium or high ash fuels for no sulfur retaining).

Remarkably, combustion fuel elements are found only a slight portion (1–3 %) of the whole bed ingredient mass in the CFB boiler. Therefore, fuel element mass, particularly for low-ash selection, does not essentially have the main characteristics of bed constituents in the hydrodynamics (Basu, 2015).

2.5.2 Boiler Description

The boiler might be divided into two units:

a) Solid circulating circle
b) Convective unit.

The first unit contains:

- Riser or furnace of a CFB
- Solid-gas divider (cyclone)
- Solid reprocess section (loop seal)
- Heat exchanger external (optional)

The second unit is called the convective unit, where the superheater, re-heater, air preheated, and economizer rivet the residual heat from the vent gas. The furnace bottom portion is usually smaller than the higher portion, and it is conical in cross-section. This support retaining more separated particles with good fluidization (Basu and Debnath, 2019).

Fuel is commonly introduced from the bottom unit of the furnace. It is occasionally introduced into the loop seal where the fuel goes in the furnace beside the reverted hot solid. The fuel combusts, although combined with hotbed solids. Limestone is introduced to arrest sulfur in the bed at an upper height. The prime burning air comes into the furnace via an air supply or grates at the bottom of the furnace. To complete the combustion, the secondary air is introduced at a certain altitude beyond the grate. The temperature of the bed is almost constant between 800 and 900 °C; however, heat is removed along with its height. The majority of the elements at the exit of the furnace are arrested in the gas-solid divider and are reused back nearby the bottom of the furnace (Basu and Debnath, 2019; Hussian, 2015; Basu, 2015). CFB technology is currently discovering uses in biomass combustion. Biomass is a renewable source with nearly zero or very small net CO_2 that releases energy, and carbon is stable through biomass growth (Chen et al., 2003; Hussian, 2006).

Solids and Gas vessels are of key importance in many large-scale manufacturing processes (Ersoyet al., 2004). When the solid particles are homogeneously mixed in the bed, the procedure might be observed as isothermal, particularly for char particles (Gomez and Leckner, 2010). The riser, where the main flow transformation of fuel particles happens, is the main part of the furnace. A CFB is considered to have a high solid recirculation ratio over the bed and a great superficial gas rate (Hussain, 2018).

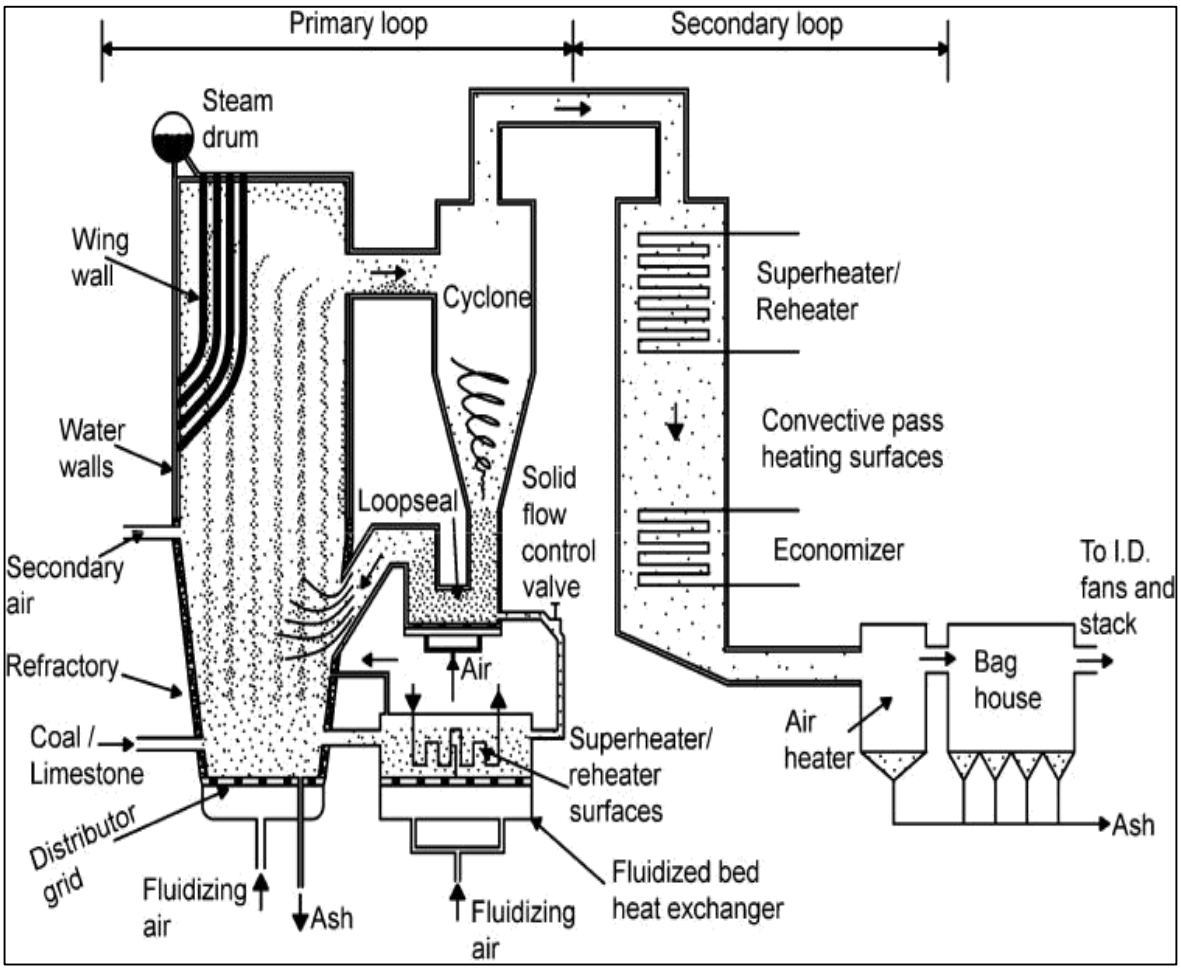

Figure 2.9: Schematic diagram of a CFBC boiler (Basu, 2015)

Moreover, the greater sand heat transfer in the fluidized bed allows the fuel (solid) to be gasified at a comparatively lower working temperature. The great performance of CFBC made it widespread worldwide (Hussain, 2018; Collot et al., 1999; Hussian, 2015).

2.5.3 Advantage of the CFBC

From a literature survey (Kishore et al., 2021; Basu and Debnath, 2019; Hussain, 2018; Basu, 2015; Breault, 2006; Vatanakulet et al., 2005; Hussian 2006; Meer et al., 2000), numerous advantages of CFBs have been recognized and listed below:

2.5.3.1 Fuel and load flexibility

Due to outstanding solid/gas mixing and fuel suspension, a CFBC conveys the fuel quickly to the burning temperature. It permits an extensive range of fuels to be combusted under an extensive variety of working circumstances. Fuel flexibility is mainly huge in comparison with other pulverized fuel combustors (Breault, 2006).

2.5.3.2 Combustion Efficiency

Associated with bubbling FBCs, the combustion ratio in a CFBC is greater, and solids mixing is fast. A noteworthy descending gesture of solids beside the boundary of the oxygen-rich riser bases an inside movement and thus increases the fuel holding and burnout period. Burning competencies up to 98-99% are considerably higher than for bubbling FBCs and similar to those of pulverize fuel combustors (Hussian, 2006).

2.5.3.3 Sulfur Elimination

In-bed detention of SO_2 is attained in CFBCs by adding dolomite or limestone as a sorbent to the furnace. Aimed at 90% imprisonment, a CFBC needs stoichiometric volume around 1.5-2.5 times that of sorbent, while others need around 2-3.5 times. For this benefit of CFBCs, they might use minor sorbent elements (Meer et al., 2000).

2.5.3.4 Nitrogen Oxide Formation

Low entire additional air and air staging in CFBCs forbid the creation of NOx, nearby the base permit only partial NOx in the higher portion. In addition, the lower the

temperature of burning in the riser, the greater the oxidation of nitrogen. NOx discharge in CFBCs is around a third of PFCs and half of BFBs (Basu, 2015).

2.5.3.5 Heat Producing and Transference

The strong cross-mixing of gas and solids in CFBCs produces fast dispersal and heat transfer to the furnace walls. It is projected that the grating heat discharge ratio is around 5 MW/m^2 is around 4-fold that of BFBCs and parallel to the rate of PFCs (Meer et al., 2000).

2.5.3.6 Fuel Intake

The fuel intake structure is easy in a CFB boiler because of its comparatively few intake points. It needs fewer grate areas for a certain thermal yield. The worthy lateral mixing commonly allows the usage of one fuel entrance for commercial CFBCs, besides around 25 for BFBs. This evades the requirement for proper feeding tools and comparable peripheral combustion that is practiced in PFCs. The above benefits highlight the prospective of CFBCs wherever commercial and environmentally friendly limitations are significant. Acknowledgment of this prospective has permitted CFBCs to capture a main and growing stake in the marketplace for commercial burning of fossil fuels. An estimated comparable price to PFCs would make CFBCs inexpensive because of their environmentally friendly benefits (Vatanakulet et al., 2005). Extensive ranges of investigational studies have been completed to date on the viability and performance of the CFBC of numerous diverse fuels and by different modeling.

2.5.4 Combustion Phases in CFB

Burning is a multifaceted procedure containing sequential heterogeneous and homogeneous reactions. The important procedure stages contain drying, devolatilization, gasification/char burning, and gas stage reactions.

Fuel inserted into a fluidized bed goes through the subsequent consecutive proceedings.

- Heating and drying
- Devolatilization and volatile burning
- Char Burning

These procedures are presented qualitatively in Figure 2.10, which also illustrates the directive of the magnitude of the interval engaged by every phase (Basu, 2015).

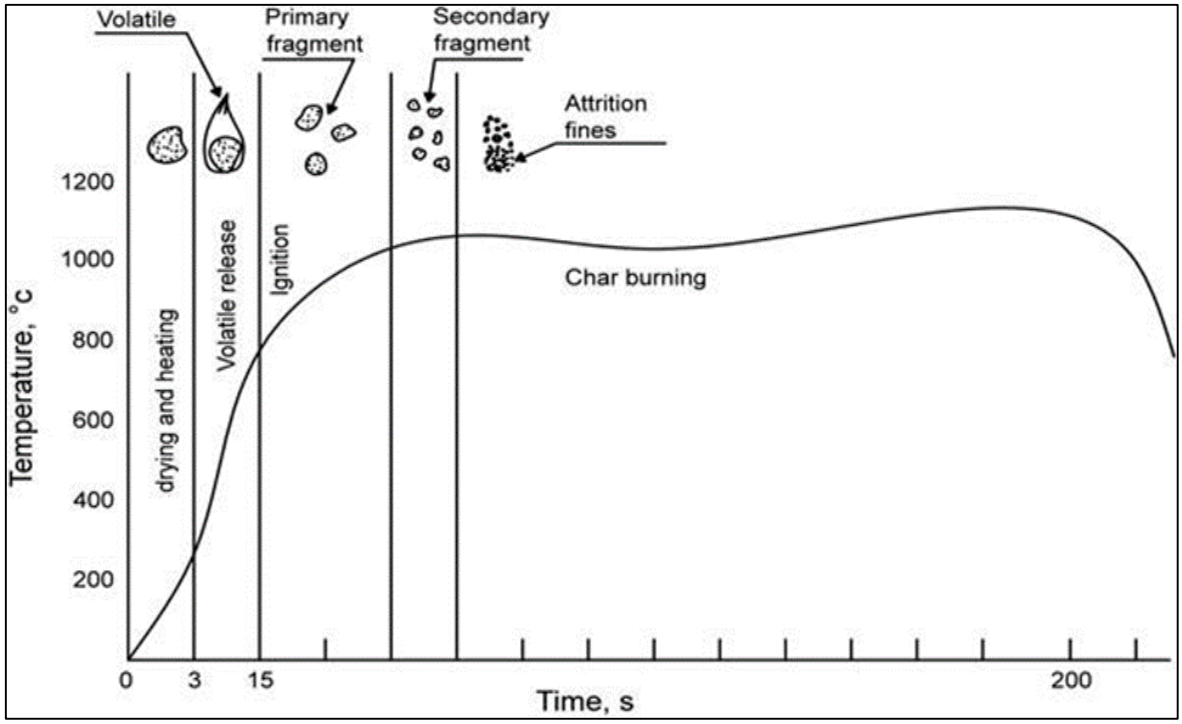

Figure 2.10: Order of procedures in the burning of a coal particle (Basu, 2015)

The furnace or riser of a CFB boiler is normally made of evaporator tubing, which absorbs a segment of the burning heat. Another unit is named the convective unit, where the economizer, superheater, re-heater, and air pre-heater absorb the residual heat from the vent gas. The lower portion of the riser is normally less than the greater portion, and it is tapering in a cross-section. This supports upholding virtuous fluidization, either with larger or more separated elements. Lower segment walls are aligned with the refractory up to the near secondary air entrance or overhead. Beyond this level, the riser is unchanging in cross-section and bigger than the lower section of the riser. The solid-gas strainer and the non-

mechanical controller for solid reuse are situated nearly downstream of the riser (Basu and Debnath, 2019).

Fuel is usually inserted into the lower segment of the riser. The fuel ignites while assorted with hotbed solids. The primary burning air passes through the riser over an air supply or grid at the riser bottom. The secondary air is inserted at a selected elevation above the grid to complete the burning process. Bed solids are finely mixed through the elevation of the riser. Therefore, the bed temperature is approximately constant in the range of 800–900 °C; however, heat is extracted from its elevation. The majority of the particles that exit the riser are arrested in the gas-solid extractor and sent back nearby to the base of the riser. Finer solids produced throughout burning and desulfurization might leave the riser, evasion over the gas-solid separators, but they are held by an electrostatic precipitator or bag house situated further downstream (Basu, 2015).

2.5.4.1 Heating and Drying

Char burning typically begins in the fluidized bed at 1-3% of the weight of the total solids. As bed components, the leftover solids are incombustible, like ash. As a result, as soon as a fuel element is introduced into a CFB combustor, a substantial amount of hot solids that cannot be burned immediately overtake it. The coal element next is warmed to bed temperature by these hot elements. Depending on a number of factors, including the size of the fuel particle, the heating system's temperature can vary from 100 to 1000 °C/s or more. The heating fraction of large and fine coal particles in a CFB is only partially known (Basu and Debnath, 2019; Basu, 2015).

2.5.4.2 Devolatilization and Volatile Burning

Devolatilization (or pyrolysis) is the procedure of discharging an extensive verity of condensable and non-condensable gaseous products of fuel. The volatile matter contains several hydrocarbons that are discharged in different phases. Figure 2.5.4.2 shows a diagram of how the ingredients of a coal element are discharged in steps. The initial stable

discharge commonly happens at about 500–600 °C, and another discharge happens at about 800–1000 °C (Basu and Debnath, 2019).

The amount of heating, the beginning and ending temperatures, the contact time at the final temperatures, the category of coal, the particle size, and the pressure can all affect the real yield of volatile matter and its configuration. Despite the fact that proximate analysis can approximate the volatile matter constrained under typical conditions (Basu, 2015).

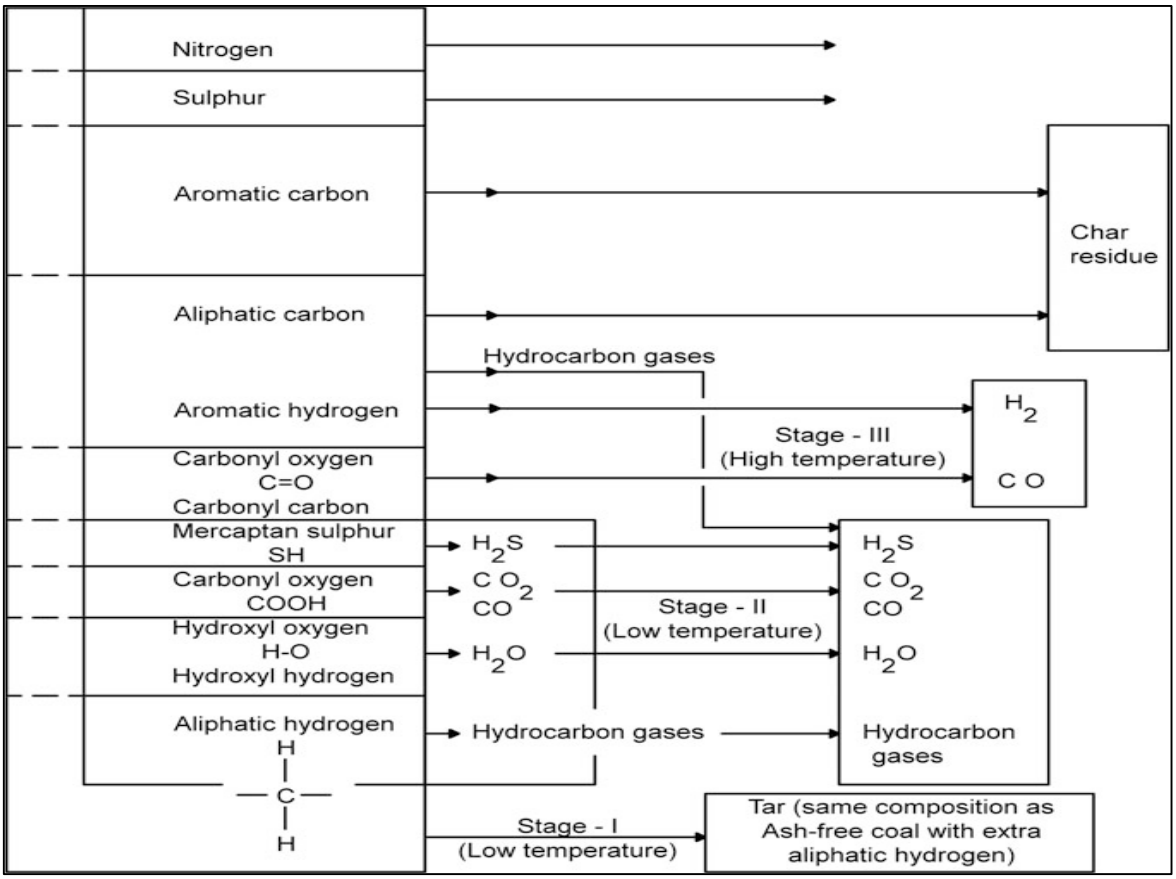

Figure 2.11: Order of volatile discharge (Basu, 2015)

2.5.4.3 Char Burning

Char is the devolatilized form of the coal element. The burning of char normally begins after the discharge of volatiles, and it proceeds for the longest period. Sometimes there is an intersection of the two procedures. Throughout the burning of a char element, oxygen is conveyed to the bed particle surface. At that time, the O_2 moves into an oxidation state with the carbon on the char exterior to form CO_2 and CO (Basu and Debnath, 2019).

The char, which is actually highly permeable, has a huge quantity of interior holes of changing dimensions and tortuosity. Opening wall zones are numerous orders of magnitude superior to the outside surface zone of the char. Under advantageous circumstances, oxygen disperses into the holes and oxidizes the carbon on the internal walls of the pores (Basu and Debnath, 2019; Basu, 2015).

2.5.4.4 Regions of CFB Riser

The furnace is distributed into three different regions from the burning point of view.

- Lower region
- Upper region
- Cyclone

The burning efficacy of CFB risers relies on numerous aspects, but it might be parallel to that of pulverized coal boilers (Lockwood, 2013). Flexibility for diverse kinds of fuels and properties is one of the main benefits of CFB boilers. The process is likely to involve an extensive variety of particle densities, shapes and sizes, heating values and chemical configurations (Oka, 2003; Walter and Epple, 2017). Hence, CFB boilers are extremely appropriate to burn a large variety of coal/biomass and additional fuels (Peters et al., 2020).

The burning air inserted into a boiler riser is separated among primary and secondary air. The lower region is fluidized by primary burning air that establishes merely 40-80 % of the stoichiometric volume. A minor quantity of fluidizing air is inserted into the loop seal.

Therefore, they might also be considered as a portion of the primary air. The lower portion of the furnace works below sub-stoichiometric or O_2 poor circumstances. The lower unit obtains coal from the feeder and unburned char elements that are reverted to the lower bed by the loop seal. More devolatilization and limited burning happen in this O_2 poor region (Basu and Debnath, 2019; Basu, 2015).

A furnace's lower section is noticeably thicker than its upper section. As a result, it also functions as a standalone container for hot solids, supplying the furnace with a thermal "fly roll". As the boiler's capacity increases, the ratio of primary to secondary air improves, carrying more hot solids to the higher part of the furnace to increase the top part's capacity for absorbing heat. At the border between the riser's bottom and higher portions, secondary air is introduced. Occasionally, a portion of the secondary air may be injected close to the grating when staged burning is not necessary, such as when using less volatile coal (Basu, 2015).

2.6 Hydrodynamics of CFB Riser

Hydrodynamics participate in a fundamental function that is not considered the process of a CFB. It assists in understanding the numerous characteristics of CFB solid-gas suspension actions under a variety of circumstances (Hussain, 2015). It presents a sympathetic way to ascertain in what way gases might be transferred from one section to another and produce gases at the outlet of the riser (Lim et al., 2012). The movement of reaction gases is determined by the hydrodynamics of the riser.

2.6.1 Performance and Design Modeling Effects on Hydrodynamics of CFB Riser

2.6.1.1 Influence of Burning Temperature

Around 850°C temperature, CFB furnaces are functional. The burning heat is preferably retained in the 800–900°C range since, mostly at this temperature, fuel ash does not fuse. Around 850°C the sulfur detention reaction is optimal. Hence, air nitrogen in the combustion process is not willingly changed into NOx. The continued process at a

temperature above 900 °C might carry an abundant rise in sorbent and limestone ingesting for decreased levels of sulfur (Basu, 2015).

2.6.1.2 Influence of Grate Heat Discharge Level

The heat burning volume that might be out of the cross-section per unit of the furnaces is an essential design standard of the boiler. The task of the mass stream rate of burning air transient over the furnace (Waters, 1975). The volumetric temperature discharge amount is not usually used for the scheme of CFB boilers, as the elevation of the boiler is normally determined by the temperature constraint of the boiler walls. For greater depth or breadth, the boiler would be greater to facilitate broad fraternization of the secondary air and the volatiles.

2.6.1.3 Influence of Fuel

Fuels influence a major part of the scheme and process of CFB boilers. For initial strategies, the proximate, ultimate, and heating rates of the fuel are prerequisites. The heating rate depends on the coal intake ratio. Cyclone and downstream constituents are identify by the ultimate analysis. Adding the normal size of bed ingredients in boilers without sorbent manages the bed heat transmission and hydrodynamics, which are significantly affected by the fuel ash compositions (Basu and Debnath, 2019).

2.6.1.4 CFB Performance Modeling

A combustor CFB performance model helps to describe the association between strategy and operative constraints and its performance. It also expresses the designer's intention to plan boiler height and further measurements that will permit the boiler to fulfill the burning and emission necessities. The combustor performance may usually be referred to by:

- Loss of carbon (unburnt)
- Circulation of carbon, volatiles, and O_2 beside the tallness and through the cross-section of the boiler.

- Stack emission gas configuration at the departure of the cyclone, particularly the discharge of NOx and SO_2.
- Heat discharge and configuration of absorption in the boiler
- Solid waste produced

The symmetrical constraints comprise the boiler measurements, its structure, and those constraints that cannot be simply altered without any hardware changes to the boiler. Process constraints contain course constraints and feedstock features (Basu, 2015).

Several significant studies on the hydrodynamics of CFB have been reported by numerous researchers, e.g. (Basu and Debnath, 2019; Khan et al., 2009; Hussain, 2018; Hussain, 2006). Ziqu et al. (2018) stated that the coal preheating burning method has been shown to be an effective method to burn semi-coke and anthracite. Liu et al. (2019a) have recognized the load response rate of a CFB boiler, and it was observed that the relative load alteration rates surpass 2.0%/min. Hussain et al. (2018) studied that the CFB riser at the top has a dilute region of the riser is at the lowest in the dense zone of the riser. In the warm CFB combustor, the burning performance of low-grade coals was assessed and their emission performance was understood. Thar coal is a capable selection for the power generation sector in Pakistan.

Hence, a virtuous awareness of the solid-gas movement in the riser of a fluidized bed part is extremely significant. Till now, inadequate data has been offered concerning some significant operative factors and the CFB riser design (Bolkan et al., 2003). Understanding the flow system is necessary for the effective scale-up and design of the CFB riser (Lim et al., 2012). Fluidization bed systems have been widely categorized and recognized as bubbling, fixed beds, turbulent, slugging, etc. Many scholars hypothesized that the gradient pressure at an axial position in a CFB's furnace is proportional to the suspension density (Youchou and Kwauk, 1980; Monceaux et al., 1985) which was verified by a number of researchers (Arena et al., 1990; Feugier et al., 1986). Further numerous researchers' work on CFBC in the last decades.

To decrease the auxiliary power ingesting and increase the consistency of an extensive circulating fluidized bed (CFB) furnace was considered by Liu et al. (2020). They found that the lesser bed pressure descent process attained only by decreasing the coal particle size is not favorable to the SO_2 and NOx discharge controller, and the pollutant controllers' price will rise. Together with the net coal consumption, the effect of fluidization state optimization on the gross power resource rate can be calculated.

Sun et al. (2022) applied a cluster-based drag model into an extensive range of working situations containing the high-density CFB risers and attains a worthy agreement with the investigational statistics. Slight deviations of the simulation outcomes, which are still suitable, are further expected to be established in the wall of the riser or denser bottom, where the clustering result is considered severe.

In order to simulate the mass transference process in a solid-liquid CFB riser, Zhang et al. (2021) suggested the Two-Equation Turbulent (TET) model. In order for the planned model to be able to confirm, the combined model is identified and simulations are accompanied for a riser comprising an impulse tracer test method. Since the turbulent Schmidt number is demonstrated to be variable but not continuously distributed throughout the riser, the use of a continuous turbulent Schmidt number for the conventional model is called into question.

Wang et al. (2021) simulate a high-density circulating fluidized bed (HDCFB) in a two-fluid model expedited with the kinetic theory. The cogency of the model is initially confirmed by associating the numerical outcomes with the capacities in relation to solid holdup, gas pressure and velocity in numerous circumstances. Then, the special effects of solid circulating rate and superficial gas velocity on cluster development and related gas-solid flow are calculated.

Liu et al. (2020) examined mathematically the working features of a coal-gasification reactor of 60 m high engineering circulating fluidized bed (CFB) established on the Eulerian-Eulerian methodology. The outcomes illustration that each of the three working constraints has a abundant influence on diverse performance constraints, like

H_2/CO ratio, average bed temperature, the operative syngas yield, and the solid mass circulation rate. The forecast facts were then interrelated to deliver support for improving the processes of large-scale CFB coal gasifier.

According to Dwivedi et al. (2019), the effectiveness of the gas-solid interaction increases as the surface gas velocity in CFB structures grows. Particle size distribution is also having an impact on the effectiveness of the gas-solid interaction. In CFB schemes, the gasification is disturbed by the coal feeding ratio and solid movement rate. Larger riser diameter and smaller particle size is a necessary form for increased solid movement ratio. The velocity inside the riser increases as a result of pressure rise inside the connecting valve.

Vivekananda et al. (2019) studied that in a CFB, the loop seal is a significant constituent that re-circulates the solids arrested by the cyclone to the bottommost of the riser and evades the straight stream of gas from high-pressure riser to the low-pressure cyclone. The stream of a solid element within the loop seal was considered intricately, and numerous scheme and operational constraints of the loop seal were examined in detail via CFD.

Hussain et al. (2018) investigated that voidage beside the riser elevation is disturbed by the geometry of the CFB riser. The burning performance of low-ranking coal from Duki and Chamalung from Baluchistan, was also discovered in a CFB Combustor. The impact of the fluidizing air on the burning behavior was studied and their consequence on emissions was recognized. The CFB riser temperature was rapid to about 900°C. This increase in temperature has produced a rise in the volume of discharge gasses which affects the interruption density.

The simulation of CFB boiler 30 MW is executed at five diverse primary and secondary air deliveries by Wijayanto et al. (2018). The outcomes in the sand volume portion, velocity, and pressure from dissimilar circumstances were equated. They perceived that the primary and secondary air delivery in a CFB boiler has a momentous consequence on fluidization performance.

Frank (2018) suggested that the CO_2 footprint decrease is a serious matter for power plants. This is why CFB has come to be the tool of selection to achieve objectives on environmental enactment and struggles to raise the portion of renewables in the perspective of the energy evolution.

Major riser dimensions for the CFB boiler operating with the 210 MW thermal capacity power plant using lignite coal were decided upon by Kishore et al. (2017). They focused on the thorough procedure that is indicated regarding the design of the upper and lower riders of the CFB boiler. Additionally considered are the pressure drop, profiles over the furnace bed, and the hydrodynamic limitations.

Cai et al. (2017) briefly reviewed CFB technology improvement and précised that CFB plays a significant part in the operation of low-rank coal. They also concluded that the emission decline is through higher efficiency de-sulfurization by limestone addition into the furnace and less NO*x* burning; very small release of NO*x* and SO_2 in the furnace might be recognized by accumulative the solid flow ratio and improving the bed eminence.

Vyas and Jani (2017) presented work containing a CFD model of the burning compartment of the CFBC boiler by taking into account three diverse types of nozzle range, which are arrowhead type nozzle, mushroom type nozzle and pigtail type nozzle. They observed that the CFBC boiler is one of those applications in which airflow performance has to be forecasted before the real installation of the plant.

Kumar et al. (2016) assessed the performance guarantee test of CFBC boilers using coal as fuel. He observed that there are numerous damages in the boiler structure which decline the efficacy of the boiler and rise operational rate. Productivity enhancement is attained by calculating diverse readings by analysis data and it is assessed that the real value of boiler efficacy is 82.45% and projected value efficacy is 84.00% by perceiving all constraints. He also concluded that by the used flue gas constraints to produce energy as a by-product consuming a distinctive principle termed Magneto Hydro Dynamic (MHD).

Tora and Dahliquest (2015) studied that in CFBC temperature circulation and inner mass inside a combustor is the main aspect of a good burning process as it controls the contact among the materials of reacting and facilitates to decrease of unnecessary products formation. They found that the CFD ANSYS Fluent model is a device to assist the process operator to manage uniform mass transfer and heat by permitting the process operator to regulate the working circumstances to well fit the applied fuel.

Daood et al. (2014) studied Pakistan's biggest Tharparkar lignite coal Sindh in CFB and observed block-VIII coal combustion in a 50 kWth furnace pilot-scale experimental facility. It was observed that in the common fuel to air ratio (1.16), NOx maximum discharges at 6% O_2 levels were 165 ppmv were noticed. Meanwhile, air-staging at 22% level found highly reduction of NOx, 60% was attained to lower discharges of NOx to 65 ppmv at 6% O_2. Unusually greater sulfur level of inherent SO_2 was discharged between 1380 ppmv to 1550 ppmv @ 6% O_2. 99.92% carbon exhaustion was gained stoichiometric ratios for 1.16; close the flame as related to 99.56% carbon exhaustion for stoichiometric ratios 0.9 in the flame area.

Akhtar et al. (2013) assessed the burning properties of indigenous coal mixtures in a CFB. The special impact of variable the feed ratio and primary air on vent gases were studied. It was observed that CO and NOx releases increase with the coal particles in the mixture. A mixing fraction of 40% is observed to be optimal to achieve a higher CFBC temperature by attaining the least amount of SO_2, CO and NOx.

Gungor, (2012) studied that; CFB combustor well-designed might burn coal with great efficacy and within satisfactory volumes of gaseous releases. The unreacted reduction core model was assumed for desulphurization. He also observed that operative bed velocity has a progressive consequence on SO_2 release. Air-staging intensely affects the concentration and spreading of sulfur combinations in the burning chamber of fluidized beds. Adding limestone with a great ratio of fines into the combustor reasons high sulfur retentions.

Khan et al. (2011) carry out a study of comprehensive parameters performed on the radial heat movement. He studied fabricated CFB combustor by burning makarwal coal. A comprehensive radial heat profile was also studied in the investigational runs. It was observed that radial temperature transfer factor rises in bed heat, solid flow rate and density of suspension.

Another research by Khan et al. (2009) stated that hydrodynamics participates in a significant function in describing the process of CFB. It guides to sympathetic of solid and gas flow in the CFB riser in various circumstances. With the development in the research of fluidization systems and hydrodynamics, a comprehensible image of flow formation can be estimated in CFB. Riser flow is generally defined by two sections, the top of the column and the bottom.

In another study, a dynamic 2D model was also developed by Gungor, (2007) because of the CFB hydrodynamic performance. The CFB riser was studied in two sections of the lower zone of a riser in an unstable fluidization system and modeled in detail. The simulation model obtains and describes the radial and axial allocation of pressure and velocity drop for solid and gas phase, solid phase circulation for particle size and fraction number of solids.

Abdullah (2007) had been done a comprehensive trial research study on the reduction of sulfur and nitrogen oxides in a CFB combustor by low-quality indigenous coal burning. Finding outcomes from this study have shown that the process can flame indigenous low-quality coal with elevated burning efficiency and therefore can be utilized in the power generation sector. The major working parameters observed were secondary air ratio, excess air factor, bed temperature, solids flow velocity and gas velocity. A broad model of coal-burning was prepared, which incorporated associate models of burning reactions, temperature movement and hydrodynamic performance characteristics of a CFB.

Ngampradit et al. (2004) offered a model with decreasing core of different fuel mixtures (bagasse, sludge, bark) and to forecast the dimension change alongside a riser of

CFBC. Gas release models were consumed to estimate the kinetic rates of SO_2, NO and N_2O transformation to forecast the discharge to the environment.

Huilina et al. (2000) focused on a stable condition model for CFB coal-fired boiler depends on heat movement, burning and hydrodynamics. Model forecasts the temperature of emission gas, different gases CO, H_2O, CO_2, O_2 and SO_2 as well as coal concentration circulations in radial and axial positions. Experimental figures were produced with a small circulation ratio and validated with the model.

Further studies reviewed, multi-control pollutant, pairing temperature with the transfer of radiative heat models, combustion of coal modeling in CFBCs are additional done by different researchers. Another main advantage of CFB is the decreasing volume of reverted vent gas, as a result of circulating solids used for cooling (Czakiert et al., 2010). Due to the significance of CFB in industry and their complex fluid dynamics, more and more research on CFBs is being carried out.

2.7 ANSYS FLUENT Software and CFD Modeling

FLUENT is a single, extensively used CFD package. ANSYS FLUENT software comprises an extensive variety of physical modeling abilities that are used for turbulence, model flow, heat transfer, and reaction for engineering application CFD problem solving in three major phases. These are pre-processing, solver, and post-processing (Patra, 2013).

2.7.1 Pre-processing

This is the first step in any CFD problem-solving process. It mainly contains planning and structuring the territory. It involves the description of the geometry of the area, grid preparation of physical or chemical occurrences that require to be modeled, fluid properties description, and condition of suitable boundary environments at cells. The flow difficulties like velocity, temperature, pressure, etc. are distinct at nodes intimate every cell. The precision of a CFD result is determined by the figure of cells in the grid. Geometry and mesh-producing software ANSYS FLUENT proceeds to draw multifarious geometry.

When computational territory geometry has been meshed in ANSYS, it is introduced into the commercial CFD code from ANSYS, Inc.

2.7.2 Solver

Afterward, the geometry has been completed; the subsequent phase is to do the flow designs. Designs are made to get the result of the governing equations. Flow designs and the outcomes presented in the CFD solver. FLUENT, CFX, and POLYFLOW, etc. are specific varieties of solvers. A finite-volume-based ANSYS FLUENT CFD solver can resolve heat transfer, chemical reactions, and fluid flow in complex geometries and control both structured and unstructured mesh.

2.7.3 Post-Processing

This is the last phase in CFD analysis, and it contains the association and explanation of the forecast flow statistics and the creation of CFD images and simulations. Graphs and numerous imagining systems might be working to assist in understanding solution physics. The outcomes are offered in the arrangement of contour plots, x-y plots, e.g., velocity and temperature contours, velocity vector designs, and animations incorporated into plotting software in ANSYS Fluent.

2.7.4 Statistical Procedure

For the execution of the model in ANSYS FLUENT, the processes are; create and mesh the geometry model using ANSYS FLUENT software, import geometry, describe the solver model, describe the turbulence model, Outline the species model, explain the resources and the chemical reactions, describe primary and secondary segment, describe the boundary conditions, initialize the calculations, post-processes the results. CFD Process flow chart shown in Figure 2.12 as prepared by Rajat Walia (2022).

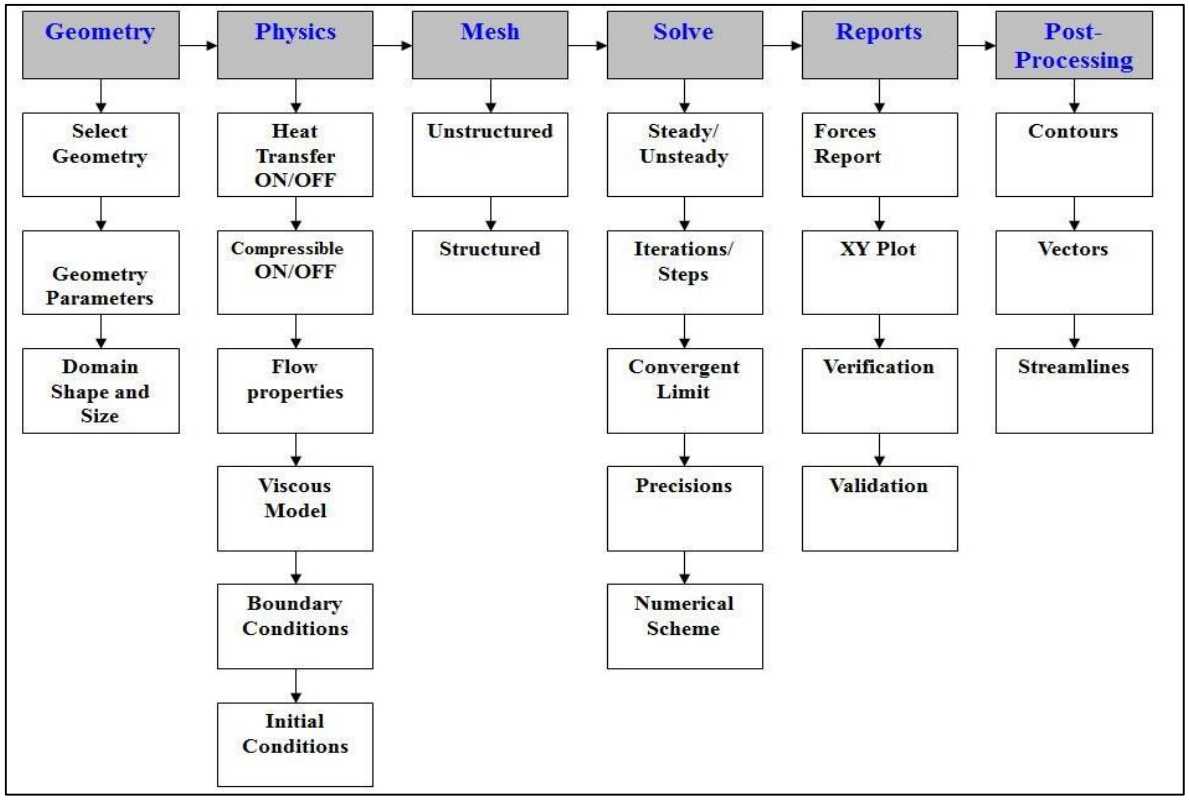

Figure 2.12: CFD Process (Rajat Walia, 2022).

2.8 Computational Fluid Dynamics (CFD)

With modern developments in computer supremacy, the Computational Fluid Dynamics (CFD) model has come to be an authoritative instrument for various geometry and course schemes. Coal burning is one of the meadows that takes benefit of the CFD model described by various researchers (Salahi, 2012). In the earlier few years, the usage of CFD codes is shown to be of great potential in studying CFBC structure (Tillman, 2000; Wankhede and Adgulkar, 2008). The period required to run these codes is also compact because of innovative mathematical techniques and upgraded hardware tools. While studying the burning course, simple flow simulations comprised of equations of mass, energy, and motion are resolved along with sub-simulations of chemical species transport, reaction, turbulence, char burnout, radiation energy transport and fuel element de-volatilization (Banerjee and Hughes, 2020). The early progress of computational fluid

dynamics (CFD) models of CFB combustors is attentive to small-scale structures (Adamczyk et al., 2014; Basu, 2015). A complete CFD model of a CFB boiler essential consists of hydrodynamics, combustion models, and wall heat transfer models (Xu et al., 2019). The majority of the progress in numerical models for CFB combustion at a great level has been imperfect in hydrodynamics (Xie et al., 2018; Liu et al., 2019b).

The pre-processor, solver, and post-processor are the three parts of a CFD code (Kumar et al., 2017). The abundant latent of CFD depends on its post-processing, which delivers both quantitative and qualitative information. An additional benefit of CFD stances in consuming compassion studies is delivering the tractability to modify constraints and response values, which is simply difficult in a research laboratory or ground experimentation. To confirm whether the model of concentration is sufficiently completed, the CFD model is confirmed with investigational records (Gera et al., 1998). Enormous numbers of CFD models were initiated in furnaces for power generation. Various schemes primarily prepared for coal burning have been altered to relate to co-firing. The co-burning of biomass and coal has been suggested for the past few years as being beneficial on both an environmentally friendly and cost-effective basis, alongside local farmer's employability of giving biomass fuel and therefore facilitating sustainable improvement. CFD is a powerful implement in the progress of coal and biomass co-firing machinery for improved sympathy, a study of unaccustomed situations, strategy, optimization, and troubleshooting of burning procedures (Cebrucean et al., 2020). There are a variety of commercially available CFD models, and the suitability of the replacement models for biomass burning is the most important factor to consider while selecting a code (Kumar et al., 2017). CFD modeling methods are attractive and broad in the thermochemical adaptation zones, especially in biomass combustion and gasification (Patra, 2013).

Numerous studies have been written about CFD modeling of coal-burning methods and several of these writing proposes drawing upgrading and maximizing functions depending on individual computational recreations (Salahi, 2012).

Mal et al. (2021) examined the performance of the Multi-Opposite Burner **(**MOB) gasifier of fraternization the low-grade Thar coal and biomass. MOB gasifier modeled with commercial CFD software ANSYS FLUENT with Euler- Lagrangian Basis for study the properties of biomass gasification combined with Thar lignite. It was determined that the fraternization of coal with biomass has noteworthy effects on the syngas configuration, temperature, and char alteration.

Prokhorova and Piralishvilib, (2020) investigated that the CFD model sufficiently forecasts the inside temperature of the combustion compartment and the configuration of gas combination that is made as an outcome of pulverized coal burning, as well as axial and radial distributions of those constraints. It is found that the CFD outcomes deviate from investigational statistics at distances from the inlet of over 1 meter. Results indicate an over-prediction of the maximum in-furnace temperature of around 100 K.

Hashmi et al. (2021) deliberate the strategy and modeling of a carbon-capturing membrane which is used in an IGCC power plant to arrest carbon dioxide from its flue gases. The modeling and strategy of the membrane are completed by consuming CFD software specifically the Ansys workbench. The strategy and modeling are completed by two simulations, one defines the strategy and assembly and the second one determines the operational mechanism of the membrane.

To better understand the burning process inside the boiler when employing various types of sub-bituminous coals, Noor et al. (2020) performed a CFD simulation of flow and burning in a full-size power plant furnace. The forecasted results show that the types of coal have an impact on temperature delivery, O2 velocity, and CO species circulations. Three acceptable coals were employed for the burning. They discovered that coal with a high heating value releases more energy during combustion, leading to higher furnace temperatures. The fuel fraction may also be a significant factor in temperature delivery.

Hyunbin et al. (2020) have studied CFD mesh sensitivity and comparison of the forecast burning constraints with real parameters of the tangential-fired boiler. They

recommended that the usage of a coarse mesh might be suitable in assessing the key performance constraints influenced by main process variables such as fuel properties and air distribution. Though, satisfactory mesh quality is mandatory if a comprehensive flow outline is desirable, particularly for ash deposition study.

Peters et al. (2020) found that the CFD codes deliver a shortcut to contract the comprehensive info in CFB risers. Numerous numerical investigations have been dedicated to the gas-solid flow in CFB in directive to recognize the actual and statistical composite.

Madejski and Mondinski, (2019) investigated commercial steam boilers with numerical modeling by using of Computational Fluid Dynamic method. They estimate the existing burning method quality by a simulation of the coal-burning method in a commercial boiler. The pulverized coal flow performance throughout the burners was studied, and the velocity and temperature circulation in the burning compartment were reproduced in the simulation. Investigation of diverse fuels and their burning procedure impact was carried out by using developed models. The authentication of the simulation outcome was completed by evaluating the results from the model by using ANSYS FLUENT software. They found that assessment of the outcome confirms the accurate modeling of the burning process as well as the excellent quality and precision of the outcome in the boiler.

In their 2019 study, Daryus et al. used the Standard (STD) k- and Renormalization (RNG) k- turbulence models to examine CFD simulations on a 2D solid-gas fluidized bed. Using inquiry statistics to verify the simulation results, it is shown that the lowest fluidization velocity is 0.4 m/s. They also found that both models originate from the turbulent regime at fluidization speeds of 0.60 m/s and higher. The volume component of the solid in the RNG k- model is thought to be more accurate because it has a more intricate model.

Kumar and Sathyabalan (2018) developed a CFD model using FLUENT for the forecast of burning activities of a 500 MWe imaginatively fired boiler. The velocity and temperature profiles were observed. The temperature at the boiler vent is in close

concurrence with the device rate. The model analyses the figures attained from the plant below the limited load and parallel for the complete load process. A PDF (Probability Density Function) chart was created for the estimation of density, temperature, and proportion of composition of dissimilar variety with a particular assortment portion approach. Burning performance simulates by using the Lagrangian-based Discrete Phase model and single-step de-volatilization model.

The impacts of the momentum fraction and velocity differential among primary and secondary airflow on boiler efficiency were investigated by Zixiang et al. (2018), who used a three-dimensional computational fluid dynamics model to simulate a lignite-fired boiler. They found that coal burning performance is also affected by the velocity variance between primary and secondary air, and a big velocity variance is advantageous in boiler operation.

A 225 MWe front wall boiler was the subject of a CFD simulation by Pawe (2018). To describe the gas phase burning process, he employed the mixture fraction approach and took into account the element heating, char burning, devolatilization, radiative heat transfer, turbulent flow, and char burning. He values the area of high corrosion risk inside the boiler and predicts where ash deposition may occur by looking at the temperature, velocity, and distribution of burning materials.

Kumar et al. (2017) investigates a widespread assessment of CFD functions in FBC structures depending on co-firing has been carried out. Fundamental fluid stream models, diverse methods, and extra burning and physical simulations utilized in CFD are offered and it is reviewed that CFD simulations afford acceptable outcomes, whereas validating them in the majority of the research.

Tian et al. (2016) used CFD methods to make a thorough image of the circumstances within the boiler, and the consequence of the working environment, coal variety, and boiler design in those environments. They described equations leading CFD models of pulverized coal burning, with attention in sub-models required for de-volatilization, burning, and heat transmission. The utilization of the models is argued with indication to illustrations of brown coal-fired boilers by CFD modeling.

Sudheer and Nagaraj (2016) prepared a 2D model and studied pressure and temperature in the CFBC boiler with the inline influence of flue gas movement through the process of refractory. CFD simulation study was done on full scale to realize the flow and performance of internal vent gases of the CFBC loop. ANSYS software was used to set up and solve the model. Pressure and temperature results were observed at different velocities. In this study, coal combustion analysis in a circulating fluidized bed had been carried out with fluent software at different three fluidizing velocities. They found that at fluidizing velocity of 8m/s, all parameters including pressure and temperature are better for combustion. Hence, 8m/s fluidizing velocity is appropriate for fluidized bed combustion as related to 6m/s and 7m/s.

Zhang et al. (2015) used the Eulerian CFD model to investigate the impacts of the operating temperature, air/coal mass proportion, and steam/coal mass fraction on the mole fractions of gaseous species ejected by the CFB coal gasifier. Furthermore, the effects of working temperature, air/coal proportion, and steam/coal fraction on the leaving gas configuration, as well as anticipated tendencies, were statistically deliberate. These limitations are realistic and consistent with literature conclusions, demonstrating the utility of the Eulerian multiphase model in simulating coal gasification methods in CFB gasifiers. Coal gasification in a CFB reactor was also studied using CFD simulation and parametric analysis.

A widespread CFD modeling investigation was carried out by Al-Abbas (2012); he studied integrating the burning of crushed dry lignite coal in numerous burning situations. The obtainable investigational outcomes from 100 kW lignite firing lab-scale units were chosen for the confirmation of these simulations. The results illustrated logical concurrence with the quantitative and qualitative amounts of temperature allocation contours and species application reports at the mainly strong burning places within the furnace. In the course of utilization of Computational Fluid Dynamics (CFD), it is found that the stoichiometry, recycled flue gas, and resident time speeds are related parameters to maximize the drawing of furnaces.

Kumar and Pandy (2012) studied that coal and air are introduced at the bottom with different velocities whereas captivating coal particles as a solid bed at different diameters. In the 2D CFB combustor, a discrete phase model is used for burning processes with single injection with ANSYS FLUENT software at three different fluidizing velocities 4m/s, 5m/s, and 6m/s. It was perceived that the deviation in extreme temperature is inconsequential for all three fluidizing velocities. He concluded that several parameters are significant in fluidized bed combustion, such as pressure and temperature. It has been also noticed that all the factors pressure and temperature are fine for burning at 6m/s fluidizing velocity. Hence, a 6m/s fluidizing velocity is appropriate for fluidized bed combustion as related to 4m/s and 5m/s.

Peng et al. (2012) study hydrodynamic performance in a CFB riser was established by spending the CFD model. A novel technique to identify the inlet boundary circumstances that see the inlet air-jet result was projected in the study to pretend solid-gas two-phase movements in CFB risers additional precisely. A CFD model recognized on the Eulerian- Eulerian method attached with the kinetic concept of granulated movement was assumed to pretend the movement spending the planned inlet boundary circumstances. Model outcomes were likened to investigational figures and found that a worthy contract between the mathematical outcomes and investigational figures was perceived underneath diverse working circumstances, which designates the value and precision of the CFD simulation with the planned inlet boundary conditions.

Hartge (2009) worked on a simulation of the fluid mechanism in the riser of a CFB that has been executed by CFD. The two-fluid model (TFM) method is implemented to characterize the fluid mechanism elaborate in the stream. The computational application is able by the commercial FLUENT software. The effort demonstrated here contains two main portions. Both portions contain a design study, where numerous mixtures of granular temperature creation, methods for solids part turbulence, drag relationships, turbulence models, and solid-solid compensation factors are established.

Various CFD investigations on thermochemical biomass renovation together with burning courses in fluidized beds, furnaces, and fixed beds were studied by Wang and Yan (2008). They declared that CFD can be employed as a controlling device to forecast thermochemical courses as well as to propose thermochemical furnaces. They also found that CFD has taken part in dynamic structure drawing as well as examination of the allocation of yield, temperature, ash, flow, and NOx release as well as outcomes are acceptable and have prepared worthy covenants with the investigational statistics in numerous circumstances.

CFD simulation of air and fluid catalytic cracking (FCC) elements in the furnace of a high concentration CFB implemented by Almuttahar (2008). The application of precise inlet circumstances was found to be precarious for the effective model of hydrodynamics.

A Eulerian CFD model using granular movement addition is applied to pretend a solid-liquid fluidized bed studied by Cornelissen et al. (2007). The mathematical models are assessed qualitatively by the literature available and quantitatively by evaluation with fresh investigational numbers. The mesh size special effects, time phase, and merging conditions are examined. The Eulerian CFD models for water fluidization are established on FLUENT software and provide outcomes, which are usually in realistic quantitative and worthy qualitative covenant with investigational outcomes.

Deviation of velocity curves beside the riser column was argued by Hussain and Nasir (2005) with the geometry of riser outcome on bed hydrodynamics in a higher area of a CFB riser column. They found that the velocity curve beside the riser elevation is inclined by the departure geometry. The riser inlet geometry outcome on slide velocity is important for around 600 mm distance in the lesser area of the riser column.

Williams et al. (2002) accomplished a broad study about the present state of coal-burning modeling. Their key tenacity was to plan the latest development in the use of CFD models for the valuation of coal circles in furnaces/boilers or using NOx reduction equipment and in this course, their key point was coal-burning sub-models. The solicitation

of these sub-models to two burning circumstances, a drop duct boiler and a squat NOx flam jet has been considered.

Huilin et al. (2000) investigated CFD on a coal-fired CFB boiler with a stable state model based on hydrodynamics, heat transmission, and combustion. This model forecasts the temperature of vent gas like O_2, CO, SO_2, and CO_2 as well as char volume allocations in both the radial and axial positions beside the boiler containing the upper and bottom regions. The model was authenticated alongside investigational statistics produced in a 35 t/h commercial boiler with a small rotation fraction.

2.9 Pollutant Productions

Pollutants might be categorized into two main modules:

- Unburnt pollutants.
- Pollutants that are formed by burning.

The unburnt contaminants contain different gases and char elements. These contaminants are generally caused by poor burning, which is an outcome of a low burning temperature, an inadequate combination of fuel with burning air, and also a too short residence time for the burnable gases in the burning region. They might be probable for all fuel types, depending on the boiler design and the process circumstances of the firing schemes. Normally, lesser discharges of these contaminants might be understood by accompanying the burning in such circumstances that higher burn-out efficacies might be attained. This needs effective mixing of the burning air with the combustible material, a high burning temperature, and satisfactory holding time in the burning region. Staged burning has been found as an active mode of confirming high burning efficacy and accordingly discharges. Another type comprises nitrogen, ash and sulfur-associated discharges, as these are not the products of inadequate burning. These contaminants are closely associated with the properties of coal/biomass, and are produced through burning. These are SOx, PM, and NOx (NO, NO_2 and N_2O). Heavy metals and acid gases might also be released. The creation of these types might be affected in a positive way by air-fuel

stoichiometry and further burning constraints and methods. Heavy metals might exist in a higher range in different fuels.

2.9.1 Coal Combustion and Emissions

Enhancing a combustion structure necessitates improved combustion efficacy, fuel investments, and a decrease in combustion emissions. Coal is a numerous fuel asset that is comparatively cost-effective to generate and transform into valuable energy. However, generating and consuming coal affects the environment. Numerous major discharges outcome from coal burning, such as SO_2, which causes acid rain and breathing diseases. NOx causes breathing diseases and smog. Particulate Matter, cause haze, smog, and lung infection. CO_2 is the main greenhouse gas formed from coal burning. Fly and bottom ash are residues made by coal burning (Kazanc, 2013).

2.9.1.1 Nitrogen Oxides Emissions

2.9.1.1.1 NOx Sources and Formation

NOx might happen through three diverse mechanisms, i.e., thermal NOx, fuel NOx, and prompt NOx (Miller and Bowman, 1989; Downmore et al, 2015). Thermal NOx is a consequence of high-temperature (>1500°C) disconnection and elemental nitrogen chain reactions with oxygen from the air through burning. NOx formation and demolition mechanisms are significant in CFBC. Nitrogen oxides (NOx) and nitrous oxide (N_2O), are generally refer to as nitrogen dioxide (NO_2) and nitrogen oxide (NO). Releases of NOx play a significant role in the atmospheric responses that produce dangerous smog (ground-level ozone), particulate matter (PM), and acid rain. These releases of NO_X mix with hydrocarbons (HC) by photochemical reaction and form ozone, which causes eye irritation and lung problems in metropolitan atmospheres. NOx discharges also contribute to misty air contamination in our natural built areas **(**Basu, 2015; Khan, 2007). The contrivance of NOx creation and demolition is significant in CFBC. (Aho et al., 1995; Barisic et al., 2005; Jong, 2005; Shehzad, 2012) investigate that nitric oxide (NO) is made over oxidation of the air nitrogen and fuel-bound nitrogen. Nitrogen oxides released from coal-fired furnaces

comprise three key gases; NO, NO_2, and N_2O, which are signified by the term NO_X, and these contribute to acid rain and certain local pollution. The term NO_X usually characterizes NO as NO_2 set up at less than 5% for coal burning (Basu and Debnath, 2019).

Burning air nitrogen might be oxidized to thermal NO_X; however, this reaction is important and can be obtained at temperatures greater than 1540°C (Morrison, 1980). Hence, it is merely an inconsequential provider (<10%) to the NO_X produced in CFB boilers, which are calculated to burn fuel between 800-900°C. Over sequences of reactions, the nitrogen in char is crumbled to NO. In a similar serial reaction, by the oxidation of volatile nitrogen, NO is made (Sarofim and Beer, 1979). A portion of the NO made overhead is also declined back to nitrogen (Basu, 2015).

The developments revealed in the literature for NOx releases recommend that the NOx is created from fuel nitrogen (Demirbas, 2005; Leckner and Karlsson, 1993; Khan, 2007). Though certain investigators have also specified a major quantity of rapid NOx creation (Miller and Bowman, 1998; Khan, 2007). Fluidized bed structures are usually operated at 815-925^oC, and at that temperature, the fuel nitrogen is controlled (Kaynak et al., 2005). In a CFB boiler, the tool of creating N_2O is less assumed in term of emission when coal is burned. In the circumstance of coal burning, HCN is formed from coal volatiles, increasing the probability of N_2O creation. The amount of demolition of N_2O, nevertheless, rises with the reaction heat (Amand and Andersson, 1989).

Various scientists observed that the maximum NOx discharges are generated from the fuel nitrogen (Lecknar et al., 2004; Lyngfelt and Leckner, 1999; Hamalainen et al., 1994).

Skreiberg et al. (2019) investigated kinetics-limited optimal situations for NOx decrease, revealing the effect of fuel and procedure circumstances. This advanced information can be additionally used to decrease. They found that CFD simulations were appropriate for examining the NOx decrease degree in an actual plant.

Khan et al. (2008) investigates that NO is the main type as related to NO_2; however, in the occurrence of oxygen, the vent gas route NO is gladly oxidized to NO_2. The dispersal of the nitrogen among the residual char and the volatiles is approximately related to the coal volatile matter.

DeMartini et al. (2004) and another scientist, Zabetta et al. (2005), observed that the maximum nitrogen in biomass fuel is at the volatile level (around 70%). Diverse scientists have described different fuel NOx proportions in biomass (Werther et al., 2000). Nitrogen bound with char burns to produce N_2O, NO, and NO_2, as stated by Leckner et al. (2004).

The decline of NO in CO and char was studied by Nussbaumer et al. (2003). Nevertheless, this consequence was not important in the case of biomass because of the lesser char content. In the circumstances of co-firing coal and biomass, a catalytic NO decrease might also be found. Higher unburned carbon also caused fewer NOx discharges, which endorses the catalytic decline by char.

Werther et al. (2000) studied ammonia as the decreasing mediator for NO for the period of coal burning. High nitrogen matters found in biomass have a higher NOx for the duration of biomass burning, as stated.

Bauman and Moller (1991) studied that in the course of the de-volatilization of coal, mixtures of nitrogen are made in fewer fractions at the lesser temperatures (700 K) (Moller et al., 1988). Whereas at upper temperature (900 K-1200 K), additional nitrogen mixtures will be discharged in the course of the de-volatilization of the char with a low nitrogen content related to the coal (Solomon and Collect, 1978).

2.9.1.1.2 Influences of Operational Parameters on NO_X Emission

The contrivance of NO_X released from CFB containers is under control for a lesser level of discharge (Yuan et al., 2019). Either deprived of the enactment of air, the nitrogen oxide (NO) in a CFB boiler is increasingly abridged to nitrogen by the inflammable carbon in the boiler. A small amount of carbon monoxide (CO) or ammonia (NH_3) is established in the boiler to support this decrease (Basu, 2015). Some of the significant explanations in a

CFB boiler (Basu, 2015) are that the amount of nitrogen dioxide (N_2O) enlarged beside the elevation of the CFB boiler, although the amount of nitrogen oxide (NO) decreased constantly. At lower burning temperatures, the release of N_2O is preferred as compared to the release of NO_2. Additional air raises the NO_X; however, its influence on N_2O release is insignificant. Rather than its fixed carbon, the nitrogen particle of the fuel disturbs the discharge of N_2O. Re-flowing of char might raise the N_2O amount as it creates greater char area availability, which helps NO decline (Oka and Anthony, 2004; Basu, 2015).

Chang et al. (2021) worked on a complete CFD model for a 630 MW pulverized-coal boiler comprising coal burning, flow, and NOx creation, targeting to resolve the problematic of declining burning constancy and growing NOx discharge in the less-load process. Simulation outcomes show that, under low-load circumstances, the residual airflow cycle still persist at the upper part of the boiler, nevertheless of how to regulate the angle planning of burners.

Emami et al. (2019) concentrate on diverse physical mechanisms of NO_x creation. Results show that the exit temperature and NO_x value decline, whereas the excess air ratio rises. Also, the burning air temperature, rises and the thermal NO_x value rises intensely. Additionally, the NO concentration at the boiler exit is at an extreme value at a swirl angle of 55 ºC and a steady increase in the NO_x value is noticed as the burning fuel temperature rises.

Sheikh et al. (2019) found that pressure, temperature, and excess oxygen are the significant operational constraints influencing NOx discharges. It’s strongly dependent on the temperature of the bed, a higher bed temperature shows elevated NOx discharges. Furthermore, NOx releases are reduced with the rise in pressure, whereas they rise with a higher amount of excess oxygen. Nevertheless, the effect of the operational constraints on NOx discharges was observed mainly depending on the coal type and the quantity of nitrogen existing in it.

Yuan et al. (2019) provided a detailed 3D model of changeable load combustion in a 660 MW supercritical whirling opposed boiler. They discovered that at a boiler load of

30%, a pulverized coal size of 50 lm, and a primary air proportion of 0.2, NOx output is at its lowest. Although the load of the boiler is declining, the burning constancy declines quickly, and the NOx production rises considerably.

Shahzad et al. (2015) studied the special effects of operational circumstances, such as excess air fraction, bed temperature, and primary to secondary air fraction, on productions of NOx, CO, and SO_2 for burning diverse mixtures of coal and wheat straw in a trial-scale test facility under fast fluidized bed conditions. They found that releases of NOx were observed to be reduced with a rise in wheat straw fraction and primary to secondary air fraction. CO and SO_2 discharges were perceived to reduction with a rise in excess air fraction and wheat straw fraction.

Certain investigators (Nussbaumer, 2003; Sanger et al., 2001; Werther et al., 1995) broadly examined the consequence of fuel and air staging on the decrease of NOx creation in CFBs. They found around 50 to 60% decrease in NOx discharges by consuming the staging method.

Gungor (2009) studied a modeling of different pollutant releases such as NOx and SO_2 resultant from burning of coal in three diverse varieties of low-grade Turkish lignite's in CFBC. He perceived that rise of additional air declines SO_2 and NOx productions. Nevertheless, NOx release rises with the operative bed velocity whereas SO_2 release declines. A higher inlet bed pressure rate outcomes in lesser releases of SO_2 and NOx if additional constraints are not changed.

The consequence of flue gas re-flowing on NOx releases was examined by Nussbaumer, (2003) and was observed as unimportant. He found that the primary and secondary air to be added in the upper and lower boiler units separately and was recommended the ratio of Primary air to be 0.6-0.8 in the boiler.

Spinti and Pershing (2003) perceived several effects of the char burning stage in different coal ranks and described that while chars combust in nitrogen-free oxidant the

char-N to NOx transformation was less for bituminous coals (40-50%) and greater for lignite's (50-60%).

A flowing fluidized bed on a pilot scale, the development and decline of NO_X were studied by Diego et al. (1996). Gaseous absorption contours beside the elevation displayed that NOx made in the lowest part of the riser and declined in the higher part of the riser. Whereas, N_2O release in the combustor increased from the lowest to the upper region.

Akhtar (1995) also described that NOx releases increased with the temperature but N_2O was observed to be reduced. The more perceived that NOx releases reduced by amassed the gas velocity and solids movement rate. Nevertheless, these constraints had presented an irrelevant influence on the N_2O release.

Zhao et al. (1994) similarly found the rise in NO_X release with excess air influence, sorbent adding and bed temperature. Further investigators similarly stated a rise in the NO_X releases with the rising excess air influence and bed temperature (Kullendorff and Andersson, 1985).

Commonly in CFB boiler N_2O and NOx releases were from the fuel nitrogen-containing multifarious similar and mixed gas-solids response. Discharge quantity was observed to be associated with the type of fuel used and process constraints such as excess air, temperature, char application and limestone adding in the riser (Eudarson and Allison, 1994).

The air staging technique was employed by Zhao et al. (1994) for regulatory the NOx releases and it was perceived that the NOx decreases suited much effectual with the enlarged secondary air. At enlarged temperatures, NO_X releases were observed to escalation and N_2O releases were reduced (Lundqvist et al., 1991).

Coals with diverse nitrogen substances and volatile matter were studied by Gavin and Dorrington (1993) in a small fluidized bed combustor. Excess air influence, bed temperature, and coal nature were observed as the core constraints affecting the

development of N_2O and NO as related to the coal volatile matter and nitrogen content. Fuel nitrogen oxidation to N_2O and NO changed vice versa with the temperature of the bed.

Leckner et al. (1992) deliberates the consequence of CFB additional air aspect, bed temperature, and intake rate of limestone on the discharges of SO_2 and NO_X from a 165 MW CFB boiler. With the bed temperature and limestone addition, NO was found to escalate, whereas N_2O indicated the opposing actions. NO was observed to decline, and N_2O enlarged with carbon and sulfur matters in the fuel.

2.9.1.1.3 NO_X Remedies

The production of NO_X in a burning method can be reduced to a certain amount through appropriate alterations to the burning method. The alterations comprise the low burning temperature, which prevents nitrogen oxidation in burning air to thermal NO_X. Therefore, temperatures between 800 to 900 °C, the production of thermal NO_X is irrelevant. Hence, NO_X is produced mainly from fuel nitrogen, which declines with temperature (Basu and Debnath, 2019; Khan, 2007).

2.9.1.2 Sulfur Dioxide Emission

2.9.1.2.1 Sulfur Dioxide Sources and Formation

Sulfur content in the coal fluctuates extensively in between 0.1–10.0 % and it might happen in coals in three arrangements, e.g., pyrite, organic and sulfate. The subsequent chemical reactions play a significant role in the creation and arrest of sulfur dioxide (SO_2) in fluidized beds. When coal combusts, the sulfur is oxidized predominantly to SO_2 (Basu, 2015).

$$S + O_2 \longrightarrow SO_2 \qquad \Delta H = -296 \text{ kJ/mol } (\Delta H \text{ is enthalpy of formation})$$

As SO_2 is made by burning fuel-sulfur, the SO_2 formation increases with the increasing sulfur content of the coal. Only the exclusion of SO_2 is essential concerning the emissions in the CFBC. Sulfur is transformed into SO_2 and SO_3 through coal burning,

irrespective of its nature and chemistry. As a lesser amount of SO_3 is made through this oxidation, the elimination of SO_2 is imperative concerning the releases in CFB. Limestone is mixed with fuel for the SO_2 arrest in CFBs. CaO is made from the calcination of limestone, which further reacts with SO_2 to make calcium sulfate ($CaSO_4$). This $CaSO_4$ was mixed with the bottom ash and removed from the CFBC. The procedure of SO_2 preparation and retention proceeds similarly in CFBC (Shehzad, 2015).

SO_2 discharge is reduced for two reasons. In the first phase, the content of sulfur mixtures declines as biomass increases. The second phase is cause by the modification of the transformation proportion. As the biomass ash comprises habitually comparatively higher CaO and MgO, the SO_2 might be absorbed to various levels (Fuertes and Fernandez, 1995; Khan, 2007). The production of sulfur dioxide is usually stated in the volume of the vent gas. Meanwhile, as the coal heating value varies, the sulfur content of a plant with a specified thermal contribution will also diverge. Thus, the SO_2 release is occasionally also stated in terms of contaminants discharged per unit of energy discharged g/MJ or lb/million BTU (Khan, 2007). The remaining SO_2 discharges into the atmosphere. Some portion of the SO_2 might be transformed into SO_3. The creation of SO_3 is contingent on the gas residence period, excess air, temperature, and the existence of catalytic surfaces on the boiler (Basu and Debnath, 2019; Khan, 2007).

2.9.1.2.2 Influences of Operational Parameters on SO_2 Emission

A vigorous 2D model for a CFB riser was established by Gungor and Eskin (2008). This model inspects the influence of diverse operative constraints and coal possessions on bed temperature and the whole CO, SO_2 and NOx discharged from the combustor. In this model, they observed that the additional influence of growing excess air is the reduction of NOx and SO_2 discharges. However, NOx discharge rises with the operative bed velocity whereas SO_2 discharge declines.

SO_2 elimination by the sorbent from the burning of coal alienated by Shimizu et al. (2002). Fine sorbent (limestone) was mixed in a bubbling fluidized bed when coal particles were burnt, so that simply sorbent is entrained to the freeboard. Consuming lesser sorbent

size, the terminal velocity of the sorbent comes to be a lesser amount than the gas velocity caused by low interaction time between the volatile nitrogen and sorbent. N_2O decrease was also perceived between SO_2 eliminations.

Bhutta et al. (2021) studied, using coal as the main fuel, biomass and limestone were combined in diverse ratios to examine the influence on desulfurization through burning. The SO_2 decrease was inclined by fuel assets, burning method, fine/coarse sizes of limestone, and the temperature of the bed. It is disclosed that coal desulfurization was extreme with the limestone fine-sized particles. Co-firing of a reasonable amount of biomass showed a significant reduction in SO_2 emission.

According to Liu et al. (2021a), when the limestone contribution increased by 50%, the SO_2 content in vent gas decreased by 22.56%. As the amount of limestone increased, the level of SO_2 removal gradually decreased. When the limestone flow increased from 0.0275 to 0.0825 kg/s, the SO_2 desulfurization level fell by 68.30%.

Elsukov V. and Latushkina (2020) was found that the upper portion of the cooling compartment, where the designated changeover happens at temperatures of 1500 - 1400 K. It was also found that SO_2 releases increase with a rise in the boiler load and additional air. They also rely on the number of dust structures and their mixture. A technical tool for the SO_2 changeover to calcium sulfate for the process of furnaces with liquid slag elimination is projected. Regime and productive actions are projected to decrease the production of SO_2.

Liu et al. (2020a) found that the small bed pressure drop process attained by dropping the coal particle dimension is not useful to SO_2 and NOx production controller, and the contaminant controller price rises. The consequence of the fluidization state improvement in the gross price of electricity supply might be calculated, and the optimum bed pressure drop might be gained.

The special impacts of limestone particle size on sulphation reactivity at lower SO_2 concentrations are studied by Cai et al. (2019), which boosted capacity enactment. The results of the experiment showed that finer limestone elements had a better final

transformation reactivity and a quicker chemical response ratio. The final calcium transformation and the level of sulphation transformation both decreased with the drop in SO_2 concentration, although even at 250 ppm SO_2, the ultrafine limestone sub-divisions still shown a commendable level of sulphation reactivity.

Krzywanski and Nowak (2016) proposed the artificial neural network (ANN) method, which might overwhelm the deficiencies of the investigational processes and the programmed computing method for solid-fuel burning in CFBC. The ANN model with hyperbolic tangent sigmoid stimulation role was effectively functional to estimate the SO_2 releases from coal burning in numerous CFB boilers working under together air-fired and oxygen-enhanced circumstances.

Downmore et al. (2015) found that the inferences of SOx and NOx discharge depend on the design of FBC schemes and operative circumstances. The design for the exact position of the fuel, secondary air, limestone intake ports and a prearranged size and amount of feed sorbent material into the scheme was found to be critical for the decrease of these emissions. The evaluation hence concludes that there is a close connection between the design and process of FBC schemes with SOx and NOx discharges.

Spörla et al. (2013) determined a widespread compilation and description of transformation rates of fuel sulfur to SO_2 for the burning of lignite underneath air and oxy-fuel circumstances. A significant outcome, with a consequence for industrial use of the oxy-fuel technology, is that additional O_2 levels that are trouble-free in air firing might prime to a noteworthy rise of SO_2 level in oxy-fuel use. Furthermore, in the oxy-fuel process at additional O_2 level under around 5% in the rise of extensive, short-range SO_2 production can arise.

Tarelho et al. (2005) investigated bituminous and anthracite coal in an Atmospheric Bubbling Fluidized Bed Combustion (ABFBC) at a pilot plant capacity with particle sizes ranging from 500 to 4000 m, with and without limestone addition. Limestone addition is effective for in-situ SO_2 elimination via ABFBC, with exclusion efficiencies ranging from

25 to 85%. Overall, as air staging and extra air decrease, the efficacy of SO_2 removal by limestone decreases. The efficiency of SO_2 exclusion by limestone decreases as the bed temperature rises between 825 and 900 °C, and in some cases, a maximum may occur around 825 °C.

Fernandez and Lyngfelt (2001) studied the influence of air staging on the spreading and sulfur complexes attentiveness inside the 12 MW CFB boiler riser. SO_2 concentration was detected in the similar riser with and without air staging. With excessive air staging, around a 30% decline in the sulfur arrest was perceived. In the reducing regions, SO_2 releases were also detected from the sulfated sorbent. The maximum of the coal sulfur was discharged in the condensed lowest region and an elevated H_2S concentration was found underneath the secondary air level.

Wang et al. (1993) examined the influence of Ca/S molar fraction in a CFB combustor burning coal for sulfur detention. Sulfur detention was very low at 1.0 or less Ca/S molar ratio. Nevertheless, retaining efficacy improved ominously consuming the Ca/S molar ratio more than 2.0.

Liu and Gibbs (1998) investigated the impact of limestone adding on SO_2 releases at diverse locations in the riser. However, decreasing SO_2 discharges, limestone adding at any location constantly lead to reduced CO and N_2O discharges with the escalation in NOx releases. SO_2 releases were observed nearly independent of the location at which limestone was intake.

The influence of secondary air addition point, Ca/S molar fraction and bed temperature on NO_X discharges and burning efficacy with a CFB combustor of 0.3 m internal diameter and 15 m height was studied by Asai et al. (1990). They observed that gas residence time by increasing in the secondary combustion zone, pull down NO_X releases (around 50 ppm) besides with elevated sulfur detention efficacy and burning efficacy might be attained. It was also observed that at bed temperature about 850°C was essential for regulatory SO_2 and NOx discharges consuming bituminous coal.

The simulation model used by Rajan et al. (1978) and found that with the bed temperature the decrease in SO_2 is also affected. Extreme sulfur was reserved in the temperature range between 1073-1123 K.

Yang et al. (1977) investigated the sulfur retaining in the course of coal-burning and observed that sulphation occurrence was delayed mostly by the limestone particles plugging possibly by the creation of silicates by reaction with coal ash.

2.9.1.2.3 SO_2 Remedies

In-situ usage of dolomite and limestone is a communal exercise in the CFBC of coal to regulate SO_2 discharges. At the burning temperatures, generally between 800-900 ^oC, the $CaCO_3$ calcines to CO_2 and CaO. The CaO then reacts with the O_2 and SO_2 to create $CaSO_4$. Hypothetically, the creation of $CaSO_4$ needs one mole of Ca for each mole of S discharged through the burning of the fuel. Though the Ca application of the solid sorbent material is generally significantly less, with efficacies characteristically in the range of 25% to 45%. The less use of the sorbent material is mostly due to the comparatively large elements used and obstruction of openings by $CaSO_4$ (Basu, 2015; Khan, 2007).

2.9.1.3 Carbon Oxide Emissions

2.9.1.3.1 Carbon Monoxide Sources and Formation

Carbon monoxide (CO) discharges are the consequence of inadequate burning and are related to the type of unburnt contaminants. CO could be made because of less burning air, dispersal-controlled reactions, and a shorter holding period. They might be measured as a burning efficacy benchmark, while diverse studies stated greater burning efficacies with greater CO release (Gulyurtlu et al., 2004b; Khan, 2007). The discharge of CO from CFB boilers is not usually supposed to be delinquent, as it is generally under the legal limit. The discharge depands on the fuel structure and the burning temperature. In the vent gas, the CO level rises with a lower burning temperature, which is mostly under 800 °C. Discharge

levels are between 15 and 200 ppm at 6 % O_2 dry in CFB, as related to stoker-fired boilers, between 200 and 400 ppm (Basu, 2015).

The lower segment of the CFB combustor functions under sub-stoichiometric circumstances because of the staged addition of burning air, as it is rich in CO. The response, however, favored at higher temperatures, might still happen at comparatively lower temperatures of CFB if adequate CO is present. The staged addition of burning air, which is distinctive of the CFB riser, is therefore not essentially advantageous to effective sulfur imprisonment (Basu and Debnath, 2019).

Gulyurtlu et al. (2004a) reported higher CO releases from inadequate feeding. The greater size of fuel elements is also caused by high CO releases.

Leckner et al. (2004) stated the higher CO release from biomass fuels burning in fluidized beds is due to their greater volatile substances. Similarly, a major quantity of methane created from devolatilization changed into CO_2 and CO. Biomass with higher volatile substances requires additional holding time for comprehensive burning.

2.9.1.3.2 Influences of Operational Parameters on CO Emission

CO releases are frequently the main distress for co-combustion. Discharges in the direction of measurements % have also been described (Khan, 2007; Gulyurtlu et al., 2004). The causes vary from fuel configuration to riser scheme. The greatest evident variance is the elementary fuel configuration variance among biomass and coal. High CO releases can be created from small-scale units because of smaller free panels categorized by lesser holding periods (Khan, 2007).

The burning characteristics of co-firing rice husk with bituminous coal were deliberated in a 120 KW CFB combustor by Madhiyanon et al. (2009). They found that CO releases were reduced with a rise in excess air fraction as well as a rise in rice husk blend fraction.

Mal et al. (2021) found that a rise in feed flow rate declines the mole ratio of CO and rises the mole ratio of CO_2. The extreme mole ratio of CO was detected at 0.344 with 90% rice husk and 10% Thar coal at 1.0 O/C fraction and 0.1 kg/sec feed flow rate.

Noor et al. (2020) concluded that the deliveries of O_2 and CO are thoroughly associated with burning performance in the boiler, which also affects the chimney gas configurations. The temperature and velocity contour are in agreement with the predictable performance of a tangential-fired boiler, and the model was authenticated with boiler performance statistics such as furnace exit gas temperature, O_2, and CO %.

Maitlo et al. (2019) studied the performance of gasification underneath diverse oxygen-fuel fractions at a temperature of 1350 ^oC. The conflicting tendency was detected in the share of CO and CO_2 in contrast to H_2. The H_2O replied with char, which improved the creation of CO in syngas. Moreover, as the O/F fraction improved, the O_2 reacted with char, CO, H_2, and CH_4, producing further proportions of CO_2.

The effects of various inlet parameters, including inlet pressure and temperature, on burning performance in a single-head combustor were empirically explored by Yan et al. (2018). The NO discharge improved while the CO discharge decreased when the inlet temperature or pressure increased. The empirical relationships between the discharges and the input temperature and pressure were discovered experientially by fitting curves to the investigative data.

Li et al. (2008) investigated the effects of coal and chicken litter co-combustion on gaseous emissions in a laboratory-scale CFB combustor. Their studies showed that CO discharges were greater than before with a rise in the blend fraction of chicken litter, but a reducing trend was perceived with the rise in secondary air and bed temperature.

Gungor and Eskin (2008) perceived that by increasing bed operative velocity or additional air proportion, bed temperature declines and CO discharge rises. Bed operative velocity has a greater momentous consequence on CO release than on bed temperature.

Armesto et al. (2003) executed the burning experiments on bituminous coal and sub-bituminous in a CFB boiler and described a minor rise in CO with the escalation in fluidizing airspeed.

Fernandez and Lyngfelt (2001) completed the trials of burning bituminous coal with an average sulfur content in a 12 MW CFB boiler. They found that with the escalation in the Ca/S molar fraction, CO concentration reduced. A similar result was perceived with the air staging.

The co-burning of lignite coal with olive cake was studied by Atimtay and Topal (2004) in a CFB combustor burning at three different weight fractions (25%, 50%, and 75%). They described the escalation in excess air fraction as a severe reduction in CO concentration. A reduction in CO was also perceived with the escalation in bed temperature.

2.9.1.3.3 CO Remedies

Concerning design enhancements, longer freeboards are suggested for coal/biomass burning in FBs, bringing the higher volatile content of coal/biomass into interpretation and growing the entire holding period. Similarly, an interior heat exchanger may be present in the freeboard and splash region in small-scale FBs, which would be detached to retain these units at a higher temperature and hence serve the change of CO to CO_2. Concerning working circumstances, excess air is also described as one of the significant aspects of fuel burnout. The structure load and air staging might also be consumed as working inconstant to raise the fuel holding period in the warm region (Basu, 2015; Khan, 2007).

2.9.1.3.4 Carbon Dioxide Sources and Emission

The devolatilized form of the fuel element is char. In the course of the burning of a charred element, O_2 from the furnace air is conveyed to the external part of the element.

The O_2, with the char surface carbon, comes into an oxidation reaction to create CO and CO_2. The products of carbon burning might be both CO and CO_2, according to the subsequent equations:

$C + O_2 = CO_2$ $\Delta H^0 = -394$ kJ=mol (I)

$C + ½O_2 = CO$ $\Delta H^0 = -111$ kJ=mol (II)

ΔH^0 (Standard Enthalpy)

Deprived of sulfur arrest, a CFB boiler releases a greater volume of CO_2 with sorbent feed. A CFB boiler has a greater perspective for the arrest of CO_2 than another firing. Oxy-combustion, chemical looping, and calcium looping are procedures for the arrest of CO_2 that are efficiently used in CFB systems (Basu, 2015).

2.9.1.3.4.1 CO_2 Remedies

Numerous techniques of detention of CO_2 are efficiently used in the circulating fluidized bed schemes. In CFBC, CO_2 detention by scrubbers could raise the price of power by as much as 80% (Anderson and Newell, 2004), whereas chemical twisting selection might limit this increase in electricity price by 25% (Basu, 2015). Another procedure has the potential to decrease the rate of CO_2 lessening by around $20/ton of CO_2 evaded. Contrasting calcium and chemical looping is a post-burning procedure; however, there is a certain relationship between these two procedures (Khan, 2007).

2.9.1.3.4.2 Carbon Emissions Prediction from 2020 to 2040

The relationship between carbon pollution and a healthy environment is crucial for a country's economic prosperity. Over the last 150 years, human actions have caused carbon releases in the atmosphere. The burning of foreign fossil fuels (coal, furnace oil, and natural gas) over less effective types of machinery is the largest source of carbon emissions in Pakistan, and carbon-absorbing types of gear are absent from present power plants based on fossil fuels. Global warming is caused by carbon emissions. Since it is essential to hold the temperature below 2 °C, widespread usage of carbon arresting strategies combined with

effective power production machinery depending on the local coal will sustainably attain the environmental goal (Raza et al., 2022). From the period 2000 to 2020, carbon discharges were higher because of the widespread consumption of foreign fossil fuel, as revealed in Figure 2.13 (Mirjat et al., 2017).

As shown in Figure 2.14, Raza et al. (2022) looked into and exploited the Thar coalfield's (175 billion tonnes) volume for power generation utilizing current, better, and greener techniques, and forecasted carbon pollution for the years 2020 to 2040.

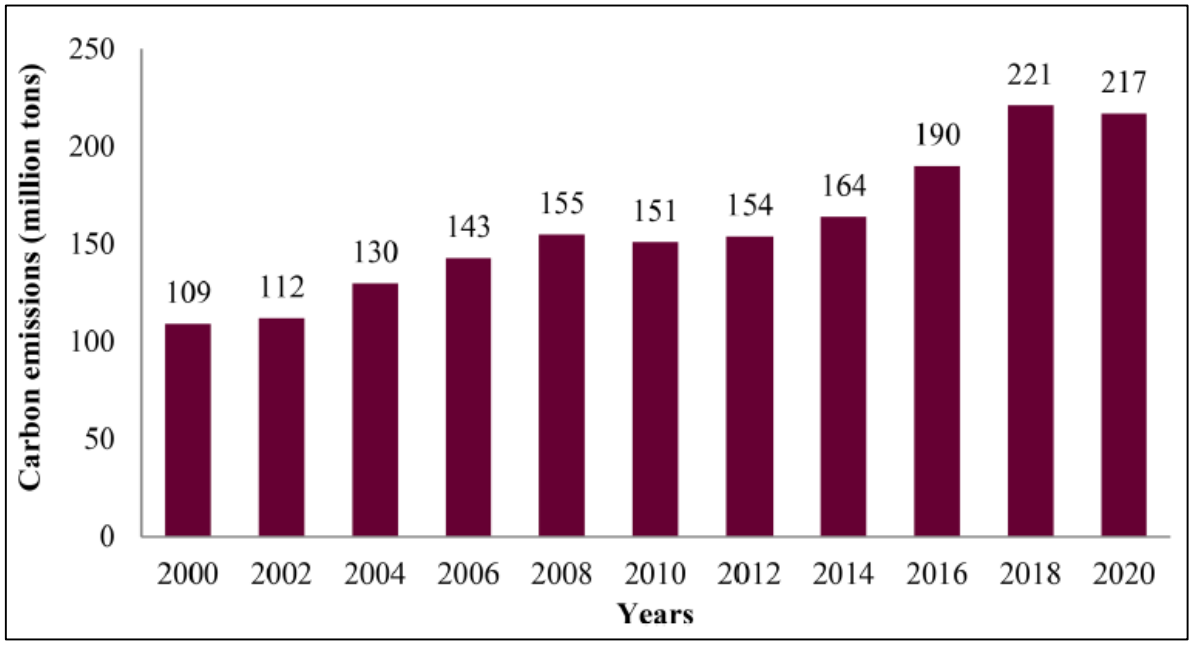

Figure 2.13: Pakistan's annual carbon emissions production from 2000 to 2020 (Mirjat et al., 2017)

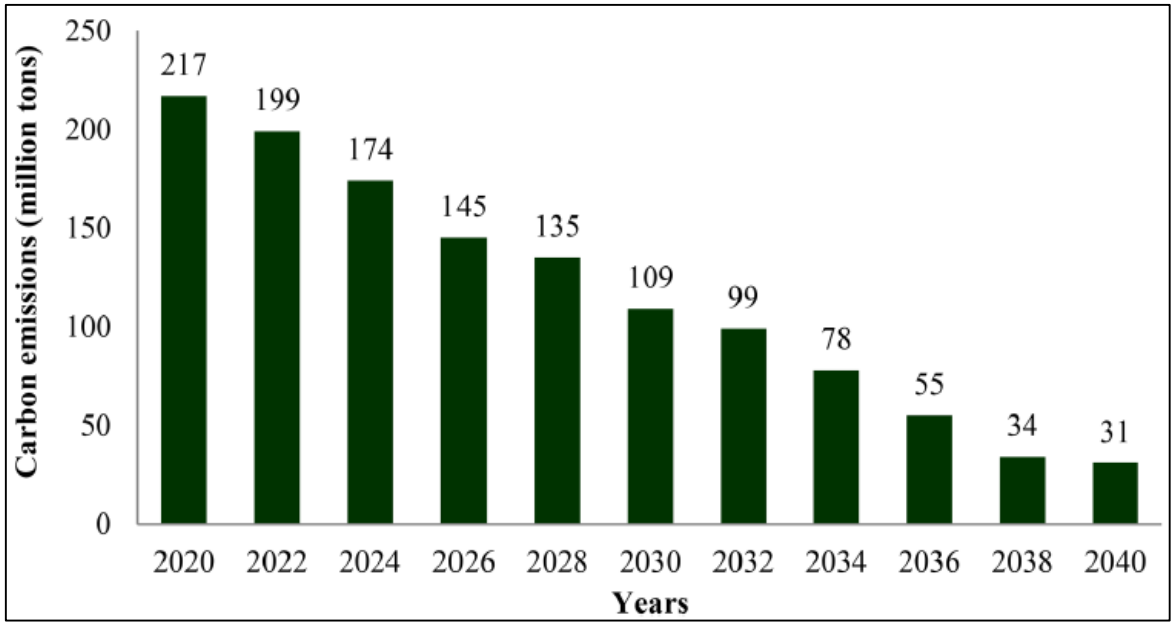

Figure 2.14: Pakistan's annual carbon emissions production projections from 2020 to 2040 (Raza et al., 2022)

2.10 Coal Emissions Control Technology

There is an extensively held statement that it is essential to put an end to the usage of coal to attain net-zero emissions (NZE) (IEA, 2021b). For much of Asia, it is not possible to phase out unrelieved coal in the upcoming eras, as its remnants are the leading basis of energy, due to its small price and ease of accessibility (Greg and Paul, 2022). Numerous Asian states have comparatively fast-growing economies and populations. Hence, the demand for energy and structure is rising. It is considered that Asian states can do tactic NZE, starting with the arrangement of low emission coal technologies (LECT) (BP, 2021). Carbon capture, utilization, and storage (CCUS) is an essential part of Asia's changeover to NZE since coal will persist significantly for numerous years for the present industry, such as power generation and engineering procedures that are tough to stop (Adams et al., 2021). Co-firing coal with biomass and increasing unit efficiency could reduce coal-fired power station discharges. All novel, huge coal plants would accept high efficiency, ultra-supercritical conditions (USC), low emissions (HELE), and best-available contaminant controls. Alternate power production schemes such as those founded on supercritical CO_2 are also possible in the changeover to NZE (Greg and Paul, 2022).

CHAPTER 3

METHODOLOGY

3.1 Characterization of the Thar Block-II Coal

Coal is a mixture of different substances; it shows various physical and chemical properties. Coal composition is described by different analysis proximate, ultimate and ash analysis, as well as burning properties, e.g., heating value and Thermogravimetric analysis (TGA). Thar coal was obtained from Block-II and used in this study. In the current study, 80 samples in three replicates were selected for assessment. The results are the mean value of eighty representative samples from Thar Block-II coalfield, Pakistan. All coal sample analysis for physicochemical parameters were conducted in the Environmental Research Center laboratories at Bahria University Karachi Campus, Pakistan.

3.1.1 Sample Preparation

During the current study, the coal samples were obtained from different agencies. The ASTM procedures were followed in the collection, processing, and analysis of the samples. Coal samples were packed, sealed, and stowed cautiously in a container to avoid any mixing, moisture addition, or loss. The investigational data on the As-determined (Ad) basis was changed to As-received (AR) basis (ASTM D-3180).

The samples were crushed, ground, and pulverized to 60 meshes (250 µm) (ASTM D-2013) and tested for air-dry loss (ADL) in an air-drying oven (ASTM D-3302). Data were collected according to the ASTM standard methods.

- Proximate Analysis (ASTM D-3172-5)
  - ✓ Moisture
  - ✓ Volatile matter
  - ✓ Ash
  - ✓ Fixed carbon
- Ultimate Analysis (ASTM D-3176, D-5373)
  - ✓ Carbon
  - ✓ Hydrogen
  - ✓ Sulfur
  - ✓ Nitrogen
  - ✓ Oxygen
- Calorific Value / Heating Value (ASTM D-2015, D5865)
- Coal Ash Assessment (ASTM D-3682)
- Thermo Gravimetric Analysis (TGA) (ASTM E1131-20)

The leading coal ash mineral constituents are also defined in this study. Thar coal pyrolysis was conceded out by Thermogravimetric analysis (TGA).

3.1.2 Proximate Analysis

The study of the coal configuration (moisture, volatile matter, ash, and fixed carbon) by using approved ASTM methods (D-3172-5) is called proximate analysis.

3.1.2.1 Moisture

The moisture is examined on the air-dried sample. Weight 1 gram of coal sample in a 10-ml crucible and heat for one hour in a preheated Memmert oven (UFB 400) between

104 ^{o}C to 110 ^{o}C. The crucible is then removed, instantly protected with a cover, and cooled in desiccators filled with dry silica gel. This phase is essential to be conceded without any interruption. The percent moisture is calculated by the loss in weight multiplied by 100 (ASTM D-3173).

3.1.2.2 Volatile Matter

All volatile-matter determination is completed in a Vulcan muffle furnace (A550). The muffle is to assure complete oxidation and to deliver circulation over the muffle to eliminate the burning products made through the sample's ignition. The furnace is kept open from the bottom (6-8 mm) to deliver circulation air. The furnace temperature regulator is then tuned to 950^{o}C relentless temperature. Cover the crucible with the residue after the moisture test, then heat at a constant temperature of 950 ± 20 ^{o}C for approximately 7 minutes in a muffle furnace. Take out the crucible devoid of any disruption, cool it rapidly in a desiccator, and weigh it. The decrease in weight after minus the moisture weight. The variance in weightiness is considered a volatile matter (ASTM D-3175).

3.1.2.3 Ash

After the determination of volatile matter, remove the crucible cap. In the muffle furnace, continue the crucible ignition with its matter and steady temperature extent at 450 to 500 ^{o}C for 1 hour. Further heat the crucible at 700 to 750 ^{o}C at temperature for the next 2 hours. Take out the crucible, and cool it in a desiccator, and weigh it. The ash determined by this technique shows the burned coal mineral matter (ASTM D-3174).

3.1.2.4 Fixed Carbon

The fixed carbon value is intended by deducting the sum of the % of moisture, volatile matter, and ash from 100 (ASTM D-3172).

3.1.3 Ultimate Analysis

The information on the elemental configuration of coals (hydrogen, carbon, sulfur, nitrogen, and oxygen) by the ASTM-D-3176/D-5373 method is called the ultimate analysis.

3.1.3.1 Carbon, Hydrogen, Nitrogen and Sulfur Determination

Throughout the current research, a modern and high-tech Elementar CHNS (vario MICRO cube) analyzer is used for the analysis of hydrogen, carbon, sulfur, and nitrogen in coal. The apparatus is built upon a gas chromatographic column and a Thermal Conductivity Detector (TCD). It uses 99.99% pure helium as a carrier gas and oxygen as a fuel. The analyzer is completely computer-companionable fitted with an auto-sampler magazine with 120 positions with a cover ring, and processes the results. The samples were weighed into tin foil dishes with the additive in duplicate. The common principle is the transfer of components in gaseous oxidation products through higher-temperature burning at temperatures over 1000 °C. After gas cleaning and reduction of the made nitrogen oxides to nitrogen, the gas combination is sequentially partitioned into its constituents N_2, CO_2, H_2O, and SO_2 via chromatographic methods of adsorption and desorption in the inert carrier gas flow. The quantifiable determination is conceded out by a common thermal conductivity detector (TCD). In the ultimate analysis, the configuration of coal is stated in %.

3.1.3.2 Oxygen

Oxygen is assessed by subtracting from 100 the sum of the other constituents of the ultimate analysis.

3.1.4 Calorific Value/Heating Value

The heating value of coals was measured using an auto-bomb calorimeter using the ASTM method D-5496.

3.2 Coal Ash Assessment

The main coal ash minerals in coal are silicon dioxide (SiO_2), ferric oxide (Fe_2O_3), sodium oxide (Na_2O), aluminum oxide (Al_2O_3), calcium oxide (CaO), potassium oxide (K_2O), and magnesium oxide (MgO) which were analyzed by the ASTM standard method.

The burning ash residue was investigated by ignited in the air at 750 ^{o}C at a persistent weight. The ash was fused inside lithium tetra borate ($Li_2B_4O_7$), followed by dissolution in hydrochloric acid (HCL) or nitric acid (HNO_3). The solution was analyzed by a Thermo Ice 3000 atomic absorption spectrophotometer (AAS). A further calculation was used for the percent concentration of constituent oxide (ASTM D-3682).

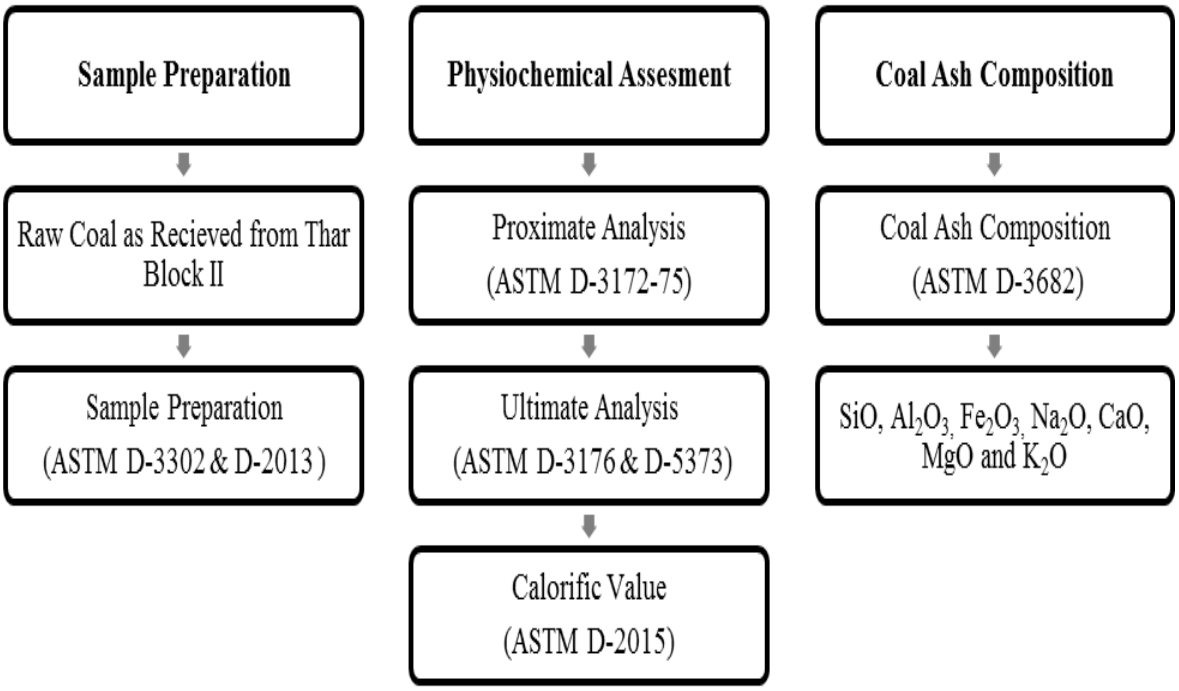

Figure 3.1: Flow chart showing the sequence of coal sample preparation and chemical analysis

3.3 Thermogravimetric Analysis (TGA)

Thar coal pyrolysis was conceded out by Thermogravimetric analysis (TGA). To define the important features of the pyrolytic course, the effects of heating rate, temperature, and particle diameters on pyrolytic qualities, including the profile of thermograms were investigated.

Coal samples were dried out to eliminate free moisture. The dried samples were creased and sieved into numerous size segments. The pyrolysis of coal was conceded out

by a TGA analyzer, Mettler Toledo (TGA/SDTA 851e). The furnace was heated to a fixed temperature of 900 ^{o}C from the ambient temperature at continuous heating rates (5-50 ^{o}C/min). In an inert atmosphere for pyrolysis, purified nitrogen (99.9995% purity) was consumed as the purge gas to deliver and eliminate any contamination. The heat from the heater wall and purge gas radiation across the heater compartment were combined to heat the sample. The sample weightiness was checked constantly by a microbalance as a function of temperature or time.

3.3.1 Kinetic Constraints Determination

Thermogravimetric statistics are consumed in describing the coal and in examining the kinetics and thermodynamics of the conversions and reactions that result from the utilization of coal samples. There were several ways available in the literature at the time that could be utilized to estimate kinetic limitations (Guo et al., 2001).

$$\frac{d\alpha}{dt} = Ae^{-E/RT}(1-\alpha)^{n} \tag{3.1}$$

where A (min^{-1}) is the pre-exponential or intensity element of the pyrolytic procedure, E (J/mol) is the pyrolytic procedure's initiation energy, R (J/mol K) is the global gas constant, T (K) is the total temperature, t is the time, n is the reaction order, and is the section of reactant disintegrated at time t (min).

α is definite in relation to variation in the form of the sample

$$\alpha = \frac{w_{\circ} - w}{w_{\circ} - w_{f}} \tag{3.2}$$

Where w_o, w, w_f are the primary, definite, and ending weights (mg), correspondingly.

To govern the standards of kinetic constraints, the vital technique is used to resolve Equation (3.1).

For continuous heating frequency β :

$$\beta = \frac{dT}{dt} \tag{3.3}$$

Equation (3.1) might be stated by the subsequent equation:

$$\frac{d\alpha}{dT} = \frac{A}{\beta} e^{-E/RT} (1-\alpha)^n \tag{3.4}$$

Reorganizing and take part Equation (3.4), the subsequent appearance image is gained:

$$\frac{1-(1-\alpha)^{1-n}}{1-n} = \frac{A}{\beta} \int_0^T e^{-E/RT}\, dT \tag{3.5}$$

Since there is no exact integral for $\int e^{-E/RT}\, dT$, $e^{-E/RT}$ can be represented as an asymptotic series and integrated without taking into account higher order terms.

$$\frac{1-(1-\alpha)^{1-n}}{1-n} = \frac{ART^2}{\beta E}\left[1-\frac{2RT}{E}\right] e^{-E/RT} \tag{3.6}$$

Expressing Equation (3.6) in logarithmic form

$$\ln\left[\frac{1-(1-\alpha)^{1-n}}{T^2(1-n)}\right] = \ln\left[\frac{AR}{\beta E}\left[1-\frac{2RT}{E}\right]\right] - \frac{E}{RT} \quad (for\ n \neq 1 \tag{3.7}$$

if 2RT/E << 1 is assumed, Equation (3.7) becomes

$$\ln\left[\frac{1-(1-\alpha)^{1-n}}{T^2(1-n)}\right] = \ln\left[\frac{AR}{\beta E}\right] - \frac{E}{RT} \quad (for\ n \neq 1) \tag{3.8}$$

If n=1, the following equation can be used

$$\ln\left[-\frac{\ln(1-\alpha)}{T^2}\right] = \ln\left[\frac{AR}{\beta E}\right] - \frac{E}{RT} \quad (for\ n = 1) \tag{3.9}$$

Thus, a plot of

$$\ln\left[\frac{1-(1-\alpha)^{1-n}}{T^2(1-n)}\right] \ versus\ \frac{1}{T} \quad (for\ n \neq 1) \tag{3.10}$$

or

$$\ln\left[-\frac{\ln(1-\alpha)}{T^2}\right] \ versus\ \frac{1}{T} \quad (for\ n = 1) \tag{3.11}$$

For the suitable value of n, the result is a straight contour with a slope of –E/R. The requirement for appropriate E and A values is that the ending value of n yields the finest E values with the best linear relationship constant.

3.4 Characterization of the Rice Husk

3.4.1 Sample Preparation

Rice husk samples were collected from six distinct locations in Sindh, Pakistan. Rice husk samples weighing roughly 5 kg were collected, sealed in polyethylene bags, and transported to the research facility for physiochemical analysis. Rendering to ASTM methods accompanied sample collection, preparation, and analytical processes. The samples were crumpled, ground, and crushed to 60 meshes (250 µm) (ASTM D-2013) to calculate air-dry loss (ADL) in an air-drying oven (ASTM D-3302). Every residue sample was analyzed in triplicate and reported for characterization and average results. As-determined (Ad) examinational figures were converted to As-received (AR) examinational figures (ASTM D-3180). Samples were performed at the Environmental Research Center Laboratories of Bahria University Karachi Campus, Pakistan.

3.4.2 Proximate Analysis

Proximate analysis was executed in a Memmert oven and a muffle furnace to define moisture content, volatile content, fixed carbon content, and ash content existing in the preferred quantity of agronomy residue sample. ASTM procedures were utilized as the standard examination approach for proximal analysis (D-3172-5). The mass loss of the rice husk sample was used to determine the moisture content in a drying oven at 105-110 ^{o}C. After keeping the sample in a muffle furnace at 900-950 ^{o}C for 7 minutes, the mass loss was measured for volatile materials. Ash contents were determined at 750 ^{o}C by the remains left after heating the sample until the persistent weight was attained.

3.4.3 Ultimate Analysis

The ASTM technique was used to determine the elemental configurations of the rice husk (D-3176, D-5373). The carbon, hydrogen, nitrogen, and sulfur components in rice husk samples were evaluated by ultimate analysis. The carbon, hydrogen, nitrogen, and sulfur contents of dry rice husk samples were determined using an Elementar CHNS Vario MICRO cube analyzer. The apparatus is built upon Thermal Conductivity Detector (TCD) and Gas Chromatographic Column. The analyzer includes an auto-sampler and is fully computer-compatible. The rice husk samples were weighed into tin foil pans in duplicate, together with the addition.

3.4.4 Calorific Value/Heating Value

The ASTM (D-2015) bomb calorimeter was used to assess the heating/calorific value of the rice husk samples.

3.5 Characterization of the Coal and Rice Husk Blends

3.5.1 Coal and Rice Husk Biomass Blending

Samples of a coal-rice husk mixture in various ratios were prepared. Coal was mixed with rice husk at ratios of 10%, 20%, and 30%, respectively. Three different blend samples were created using this method: CRh-1, which contains 90% coal and 10% rice husk; CRh-2, which contains 80% coal and 20% rice husk; and CRh-3, which contains 70% coal and 30% rice husk.

3.5.2. Combustion and Emission Analysis

Co-firing in muffle furnace Volcan USA (Model A-550) and Testo flue gas analyzer (Model-350) were used to measure harmful pollutants such as CO, CO_2, NOx, and SO_2. Samples were heated using a coal and rice husk mixture at a furnace temperature of about 850°C. Co-firing allowed emissions to be released from the muffle furnace's stack. The probe of the exhaust gases analyzer was inserted into the furnace stack's outlet, and

emissions were analyzed using a flue gas analyzer with the capability to analyze CO, CO_2, NOx, and SO_2 emissions as per USEPA Standard Methods (CTM-034 and 6C).

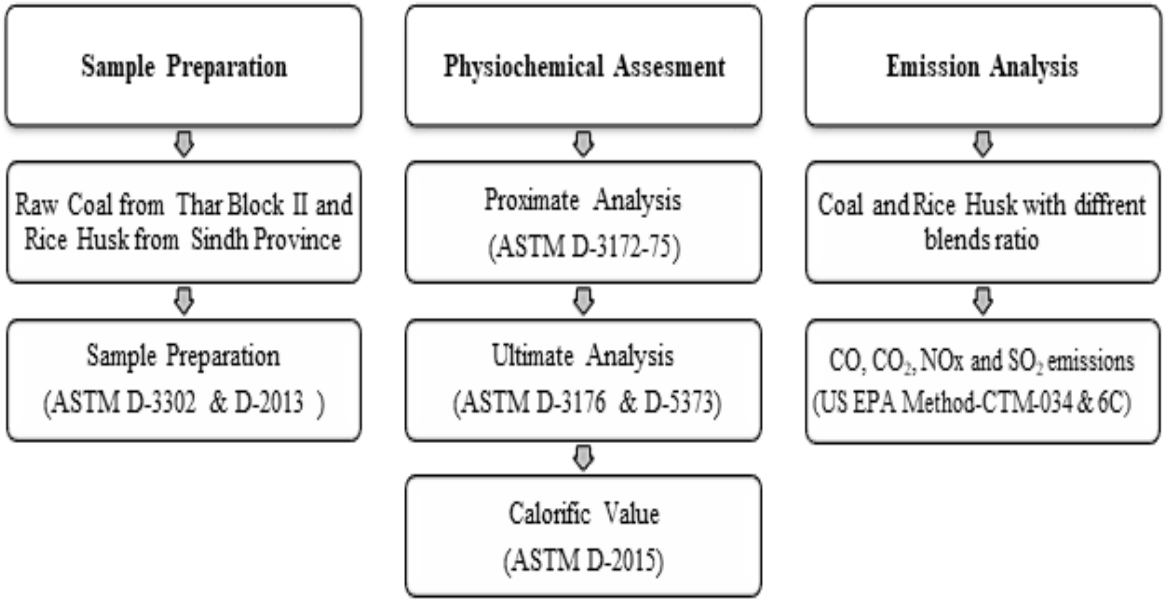

Figure 3.2: Flow chart showing the sequence of coal and rice husk sample preparation and analysis.

3.6 CFB Riser/ Combustor Modeling

3.6.1 Hydrodynamics of CFB Riser/Combustor

The combustion system is based on the principle of Circulating Fluidized Bed Combustion (CFB) using coal as a combusting material. ANSYS software 19.0 includes a broad variety of material modeling capabilities, which are used for industrial applications to model turbulence, reaction, heat transfer, and flow. Models of coal-solid combustors were first created in Solid Works. The models are imported into ANSYS FLUENT to mesh and specify the types of boundary restrictions after being protected as a *.STEP file. The precisely meshed file is subsequently sent as a *.MSH file, is suitable for ANSY FLUENT once this task is accomplished. At a similar time, the bed or solid burning simulation is also completed by utilizing fluid dynamic incinerator code (FLIC) to model the bed burning to

acquire the appropriate constraints to transfer into FLUENT to track the burning gas stream and burning. To model coal bed combustion, FLIC, a code built by the Sheffield University Center of Waste Incineration, is employed (Aliman and Pasek, 2018; Changkook et al., 2007).

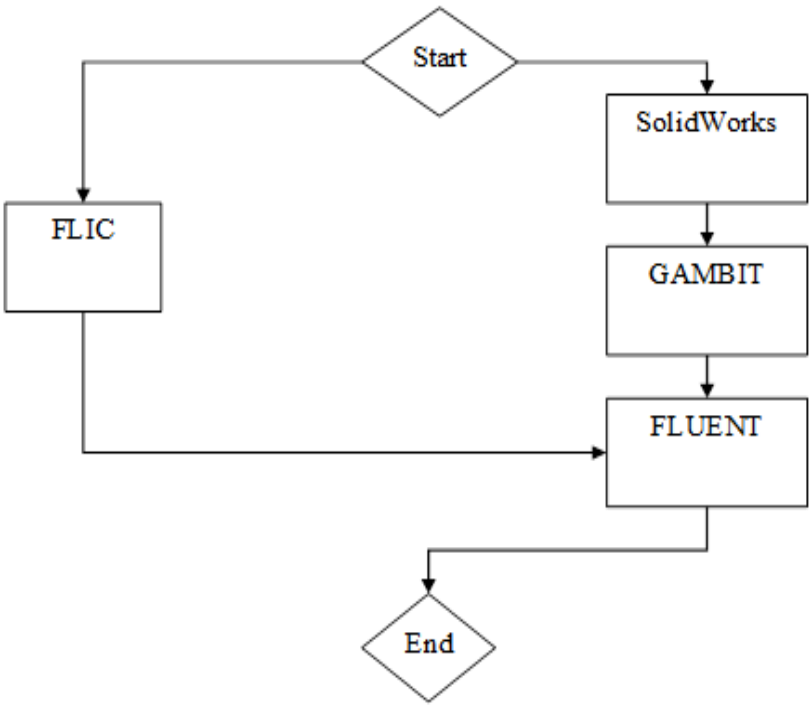

Figure 3.3: Flow diagram of the entire scheme

3.6.2 CFB Simulation

Figure 3.4 demonstrates the diagrams of the CFB simulation. It comprises an airstream blower, a solid intake system, a stainless-steel supply, a rapid Plexiglas column, and primary and secondary cyclones.

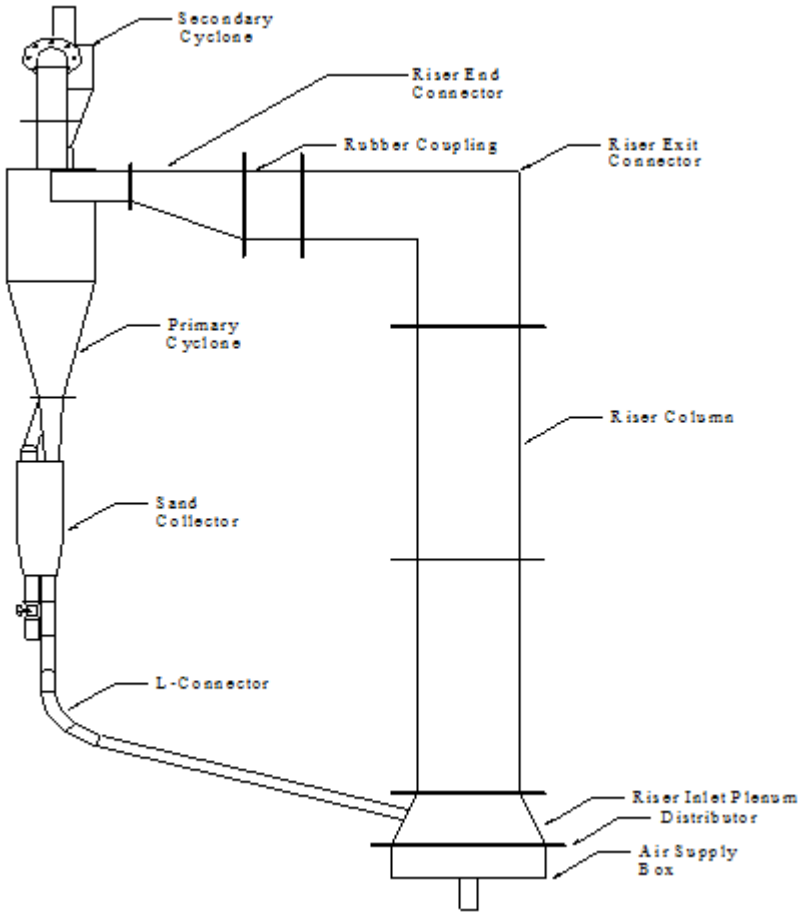

Figure 3.4: Typical CFB Riser geometry

On a riser with quadrilateral dimensions of 2649 mm in height, 265 mm in width, and 72 mm in depth, the 2D simulation work was accomplished. The 2D design was selected to be sympathetic to the flowing outlines in risers with various exit geometries while requiring minimal processing effort (Hussain, 2006). The operative constraints were selected as they were utilized to act in enormous CFBCs. FLUENT, a CFD compendium created and owned by Fluent Inc., prepared a simulation (Fluent, 2013). The solid-gas portions, sand components, and air were utilized in that order. Table 4.10 summarizes the constraints used in the simulation model.

Table 3.1: Parameters used for Simulation work

Constraint	Values Range
Dimensions of Riser	2649 Length x 265 Width x 72 Diameter (mm)
Velocity (Particle)	2 m/s
Velocity (Gas)	3~5 m/s
Particle (sand) properties	Density = 2500 kg m^{-3}
	Diameter= 100 x 10^{-6} m
Air Properties	Density= 1.225 kg m^{-3}
	Viscosity= 1.79 x 10^{-5} kg/m.s
Height of the distributor's sand intake	200 mm
Granular properties	0.95 is the coefficient of particle-particle restitution. Restitution coefficient for particle walls of 0.9
The fraction of sand by volume	Within 10% of the volume percentage of sand, 0.03 utilized as the Algebraic Slip Mixture Model provides reliable predictions.
Multiphase model	Eulerian granular multiphase model

An extensive variety of investigations on the exits of risers have been described in the studies (Yang and Wang, 2020). The curve exits revealed are categorized by the midpoint radius of the bend. Blind T exits are categorized by a special circumstance; the right-angle exit, a roof extension height, wherever the extension elevation is zero. They are widely used in commercial CFBCs. Figure 3.5 illustrates these geometries.

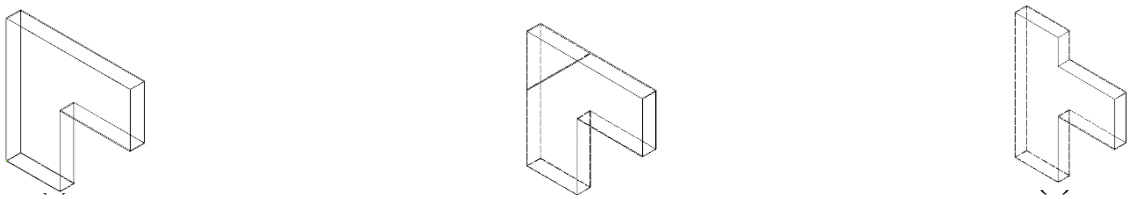

(a) Right angle exit (b) right angle exit with baffle (c) blind T exit

Figure 3.5: Riser Exits

According to Yang and Wang (2020) and Wang (2013), riser departures may have an impact on a CFB's general performance. If additional solids gather nearby the riser exit at that moment, fewer solids exist in the arrival leg, and hence the head of stationary pressure in the arrival leg is lesser. The lesser frequency of solids movement might base the solids size segment in the riser and connective to be a lesser part. However, the solids size segment could be larger if the solids accretion at the riser outlets expanded into these processes. A Core/Annulus (C/A) construction is commonly used in the upward exit area. Inner/outer gesture, first-order secondary flow, tangential acceleration/deceleration, and cavity generation are the four processes that govern solid gesture in riser exits.

3.6.2.1 Inner/Outer Motion

Due to higher density, in the central area of a riser exit, solids might escape to the outer or inner side, reliant on the comparative degrees of their geometry and the hastening caused by gravity “g”, as revealed in Figure 3.6. The solids activity proportion to gravity might be characterized by the subsequent Froude number (Fr_R):

$$Fr_R = \frac{\bar{u}_{st}^2}{g\,R} \tag{3.12}$$

Where

$\bar{u}_{st}$ is cross section average solid velocity near the top of the riser

g is the acceleration due to gravity

R is the average radius of curvature of riser exit

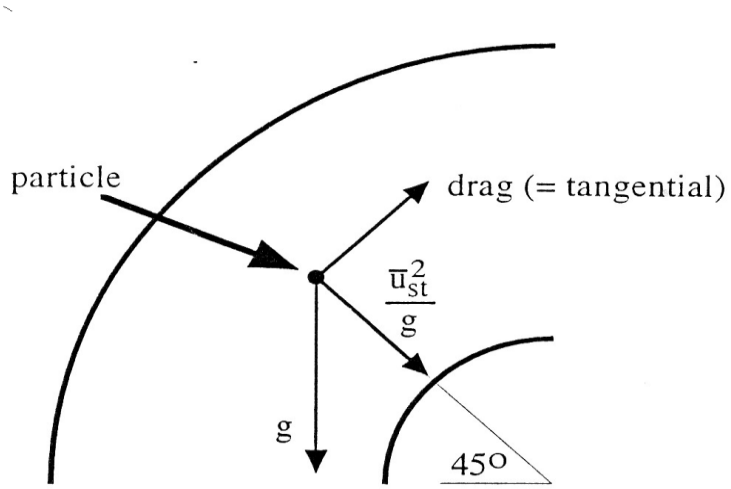

Figure 3.6: Particle motion in exit bend (Meer, 1997)

The Froude number Fr_R is reliant on the cross-section normal velocity of solids nearby the upper of the riser $\overline{u}_{st}$ and on the normal semi diameter of curving R, as demarcated by:

$$R = \sqrt{R_{ei}^2 + R_{eo}^2} \tag{3.13}$$

Here Rei and Reo are the centerline radii of curvature at the inlet and outlet of the riser exit, respectively. The Froude number Fr_R may be expected to be a function of the exit geometry, the superficial gas velocity Us, and the superficial solid mass flow rate Gs.

3.6.2.2 The secondary flow of the first kind

Curves enforce first-order secondary flow in the center passages to the bend's outer wall, as well as steady motion flow near the bend's inner wall. As an outcome, the argument of extreme velocity deceives in the external half of the curve. A higher motion interruption in the center of a riser departure might raise similer crosswise designs. Figure 3.7 demonstrates secondary flow designs in a curve departure with a four-sided cross-sectional.

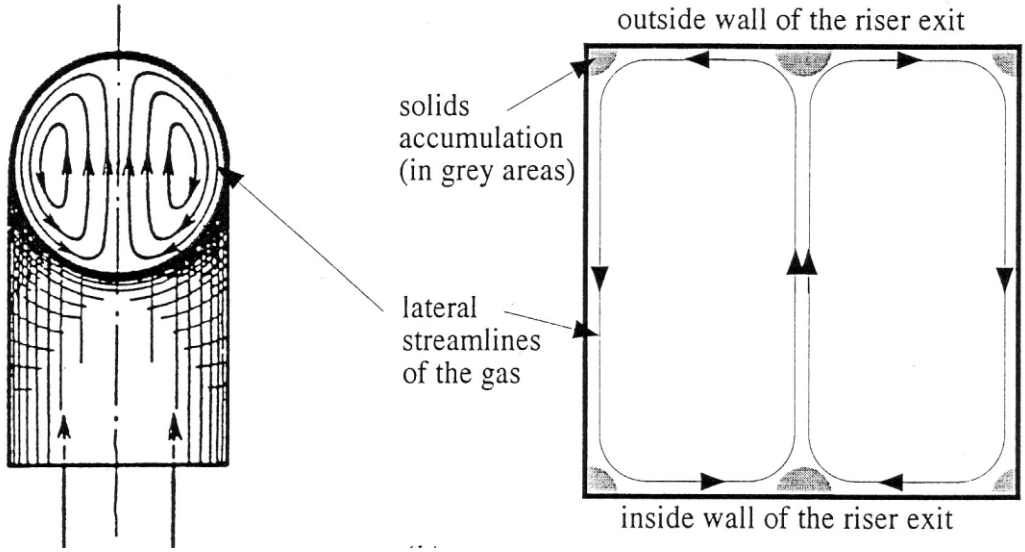

Figure 3.7: Secondary flow of the first kind (Meer, 1997)

It seems that velocity slopes are vast at nearby angles and in the center of the internal and external walls. Because of their higher inactivity, solids might gather in these zones.

3.6.2.3 Tangential acceleration /deceleration

In the riser exits, the gas tangential acceleration or deceleration happens at a cross-sectional area that varies in dimensions from intake to outlet. A rectangular departure with internal perplex flex speeding up followed by slowing down, a blind T departure flex slowing down followed by speeding up, and departures with inadequate dimensions inside and outside enforce a net speeding up or slowing down. While solids might tend to hold their primary velocity because of their higher inactivity, they will slow wherever the gas slows and speediness at gas hastens due to slog among the segments. The outflow of solids is usually proportional to the superficial gas velocity, with a lower outflow for areas of peripheral speeding up and a larger outflow for areas of peripheral slowing down.

3.6.2.4 Cavity Creation

Nearly riser departures might raise cracks or areas wherever solids are disconnected via the core stream. The blind T departure, for example, causes a fracture in the postponement. Solids arriving after the extension may contact the top or, if the expansion is long enough, may slow down due to gas pressure. The resulting accrual of descending motion might increase the solid's reappearance on the riser. Some additional additions to the top might not raise the solids capacity section in the riser and its departure if all solids slow down due to drag. Because two walls shave in this zone, a small hole may appear at the external angle of the right-angle departure. Cavities could also emerge right beneath annulated plate departures and inlet perplexes.

3.6.3 Multiphase Mixture Eulerian Model

The two-dimensional equations for momentum energy, and mass are created in the ANSYS FLUENT modeling. By the Finite Volume Method, the difference equates are discretized and resolved by the modest process. The k-ε was activated by the turbulence model, which has two transportation equivalents for turbulent kinetic energy and rate of dissipation. The FLUENT algorithm quantizes the conservation equations for momentum, energy, and mass using a formless, non-uniform mesh. The k-model specifies turbulent kinetic energy and rate of dissipation, as well as negotiations between turbulent amount determination and computational time.

Table 3.2: FLUENT Models used in the simulation

Model	Setting
Space	2D
Time	Steady
Viscous	Standard k-epsilon turbulence model
Wall Treatment	Standard Wall Function

In the FLUENT processer database, the leading equations were quantized through the finite volume method. The quantization equations, together with the primary and boundary settings, were resolved to attain a geometric result. The Eulerian Multiphase Mixture Model (EMMM) is utilized for predicting the gas-solid stream. For the secondary stage, the EMMM resolves the blend's energy equation, the mixture's conservation equations, and the volume fraction equations, as well as providing a numerical representation of the comparative velocity.

By using the mixture theory approach, the volume of phase q, V_q is defined by

$$V_q = \int_V \alpha_q \, dV \tag{3.14}$$

and

$$\sum_{q=1}^{n} \alpha_q = 1 \tag{3.15}$$

The effective density of phase q is $\hat{\rho} = \alpha_q \, \rho_q$ (3.16)

Where ρ_q is the physical density of phase.

3.6.4 Conservative Equations

FLUENT is offering the typical conservation equation from which the answer is obtained:

The phase q continuity equation is

$$\frac{\partial}{\partial t}(\alpha_q \, \rho_q) + \nabla . (\alpha_q \, \rho_q \vec{v}_q) = \sum_{p=1}^{n} \dot{m}_{pq} \tag{3.17}$$

Where $\vec{v}_q$ is the velocity of phase q and $\dot{m}_{pq}$ characterizes the mass transfer from the p^{th} to q^{th} phase.

From the mass conservation we can get:

$$\dot{m}_{pq} = - \dot{m}_{qp} \tag{3.18}$$

and $$\dot{m}_{pp} = 0 \tag{3.19}$$

Usually, the source term ($\sum_{p=1}^{n} \dot{m}_{pq}$) on the right-hand side of the equation is zero. (3.20)

The momentum balance for phase q yields

$$\frac{\partial}{\partial t}(\alpha_q \rho_q \vec{v}_q) + \nabla.(\alpha_q \rho_q \vec{v}_q \vec{v}_q) = -\alpha_q \nabla p + \nabla.\bar{\tau}_q + \alpha_q \rho_q \vec{g} + \sum_{p=1}^{n}\left(\vec{R}_{pq} + \dot{m}_{pq}\vec{v}_q\right) + \alpha_q \rho_q (\vec{F}_q + \vec{F}_{lift,q} + \vec{F}_{vmq}) \tag{3.21}$$

Where $\bar{\tau}_q$ is the q[th] phase stress-strain tensor

$$\bar{\tau}_q = \alpha_q \mu_q (\nabla \vec{v}_q + \nabla \vec{v}_q^{\,T}) + \alpha_q (\lambda_q - \frac{2}{3}\mu_q)\nabla.\vec{v}_q \bar{I} \tag{3.22}$$

Here μ_q and λ_q are the shear and bulk viscosity of phase q, $\vec{F}_q$ is an external body force. $\vec{F}_{lift,q}$ is a lift force, $\vec{F}_{vm,q}$ is a virtual mass force, $\vec{R}_{pq}$ is an interaction force between phases, and p is the pressure shared by all phases.

$\vec{v}_q$ is the interphase velocity and I can be defined as follows.

If $\dot{m}_{pq} > 0$ (i.e., phase p mass is being transferred to phase q), $\vec{v}_{pq} = \vec{v}_p$; (3.23)

If $\dot{m}_{pq} < 0$ (i.e., phase q mass is being transferred to phase p), $\vec{v}_{pq} = \vec{v}_q$; (3.24)

$$\vec{v}_{pq} = \vec{v}_{qp}$$

The above equation must be closed with appropriate expressions for the interphase force $\vec{R}_{pq}$. This force depends on the friction, pressure, cohesion, and other effects, and is subject to the conditions that

$$\vec{R}_{pq} = -\vec{R}_{qp} \text{ and } \vec{R}_{qq} = 0 \quad (3.25)$$

FLUENT uses the following form:

$$\sum_{p=1}^{n} \vec{R}_{pq} = \sum_{p=1}^{n} K_{pq}(\vec{v}_p - \vec{v}_q) \quad (3.26)$$

Where $K_{pq} = K_{qp}$ is the interphase momentum exchange coefficient.

3.6.5 Turbulence Model

Turbulence modeling in multiphase simulations is complicated by the high number of elements that must be addressed in the momentum equations in interfacial to describe the characteristics of velocity fluctuations. The turbulence model used in the current simulations is the Mixture Turbulence Model (MTM). This model's formula and equation are as follows:

$$\frac{\partial}{\partial t}(\rho_m \kappa) + \nabla .(\rho_m \vec{v}_m \kappa) = \nabla .\left(\frac{\mu_{t,m}}{\sigma_\kappa} \nabla \kappa \right) + G_{\kappa,m} - \rho_m \varepsilon \tag{3.27}$$

$$\frac{\partial}{\partial t}(\rho_m \varepsilon) + \nabla .(\rho_m \vec{v}_m \varepsilon) = \nabla .\left(\frac{\mu_{t,m}}{\sigma_\varepsilon} \nabla \varepsilon \right) + \frac{\varepsilon}{\kappa}(C_{1\varepsilon} G_{\kappa,m} - C_{2\varepsilon} \rho_m \varepsilon) \tag{3.28}$$

Where the mixture density and velocity, ρ_m and $\vec{v}_m$, are computed from:

$$\rho_m = \sum_{i=1}^{N} \alpha_i \rho_i \tag{3.29}$$

$$\vec{v}_m = \frac{\sum_{i=1}^{N} \alpha_i \rho_i \vec{v}_i}{\sum_{i=1}^{N} \alpha_i \rho_i} \tag{3.30}$$

The turbulent viscosity, $\mu_{t,m}$, is computed from:

$$\mu_{t,m} = \rho_m C_\mu \frac{\kappa^2}{\varepsilon} \tag{3.31}$$

and the production of turbulence kinetic energy, $G_{k,m}$, is computed from

$$G_{\kappa,m} = \mu_{t,m} (\nabla \vec{v}_m + (\nabla \vec{v}_m)^T) : \nabla \vec{v}_m \tag{3.32}$$

3.6.6 Mesh Selection

Due to the non-premixed combustion model, randomly spaced gas-solid particles that do not follow any particular pattern, and a vigorously swirling flow inside the combustor/Riser, an unstructured, non-uniform triangle grid or mesh was used.

3.6.7 Boundary Conditions

At the intake, all volume fractions and velocities of mutual segments are definite. The pressure is not definite at the intake since the uncondensed gas segment is a possibility. As shown in Table 4.1, the principal gas velocity and solid segment are being measured. ANSYS FLUENT was used to finish the meshing. For a riser in and out segments in direction, fine meshing was done in direction to examine them in an improved mode. Below relaxation, aspects were adjusted to attain confluence. The confluent tolerance was established at 0.001.

FLUENT uses an iteration calculation technique to determine the key restrictions of the stream within the scheme. The summary of the primary data and primary projected standards kicks off the iterative process, including boundary circumstances, physical situations, and constants. In the next stage, the database estimates the velocity arena from the momentum equations. At that time, the mass balance equations and the pressure equations are resolved. The subsequent stage is to establish further standards of the constraints for both stages. The ending stage is too checked on the conjunction which standard for locked by the operator. The simulation will end and the scheme's results will be displayed if the criterion is met. If this is not the case, definite alteration factors are used to regulate the planned values, and the computation, whose redone using the most recently updated individual constraint values as primary statistics.

The rigidity of particle collisions is measured by the compensation constant. A value of 1 indicates entirely flexible collisions, while a value of 0 indicates completely inflexible collisions. It is applied as an explanation for the energy derivation because of the collision of elements, which is not measured in the conventional kinetic system. The compensation constant is adjacent to unity and uses a 0.95 particle-particle compensation constant and a 0.9 particle-wall compensation constant.

CHAPTER 4

RESULT AND DISCUSSION

4.1 Characterization of Thar Block II Coal

The technique chosen for the burning process was often based on the qualities of the fuel. Thermogravimetric Analysis (TGA), calorific value, and proximate and ultimate analysis are regarded as the most important coal fuel attributes that give the initial impression of specific coal. The coal's moisture, volatile substances, fixed carbon, and ash content are determined by proximate analysis, and its exact elemental fractions of C, H, N, S, and O_2 are determined by ultimate analysis. Heating/calorific value, thermal characteristics, etc. are further important thermal and chemical properties.

The main coal ash minerals in coal are SiO_2, Al_2O_3, Fe_2O_3, Na_2O, CaO, MgO, and K_2O. The investigational data for the As-determined (Ad) was changed to an As-received (AR) basis. The widespread study of the explored reserve is a focus of concern to deliver the solution to energy scarcity through the operative and effective consumption of Thar reserves. Also, the investigation statistics obtained are utilized to assess the probable environmental impact of coal consumption in power plants.

4.1.1 Proximate Analysis

Proximate analysis specifies the fraction % by weight of the moisture, volatile matters, fixed carbon, and ash content. Proximate analysis and heating or calorific values of the samples are presented in Table 4.1 and Figures 4.1 and 4.2. The quality of coal was calculated on an as-received basis.

4.1.1.1 Moisture

The moisture content of Thar Block-II samples is almost high, ranging between 42.06 to 50.62% (Mean 46.26%). The higher moisture content is observed in the Thar coal sample, showing a lower heating value. Moisture plays a significant role in coal quality and usage characteristics. High water content in coal required additional time for heating and impacts the burning and the capacity of vent gases made per energy unit, as well as a lesser calorific value (Sarwar et al., 2014). Moreover, high moisture content trends in more coal consumption, produces enormous vent gas volumes, and requires huge equipment measurements. With the disadvantages of high moisture content, there is also an advantageous feature (Khan, 2007). It supports, limit mandatory fines, and helps radiation heat transmission in the furnace.

4.1.1.2 Volatile Matter

Volatile Matter values observed in Thar Block-II samples range between 25.25 to 35.05% (Mean 28.85%). High volatiles in coal evaluate the ignition and burning efficiency. It supports the initial ignition and reactivity of coal for burning (Akowuah et al., 2012). Additionally, volatiles are subdivided into gases like light hydrocarbons, carbon dioxide, carbon monoxide, hydrogen, and asphalts. The yields rely on the heating rate and temperature of coal to attain complete burning at high efficacy and to guarantee fewer emissions of pollutants from the chimney (Anjum and Khan, 2017). In a furnace, it proportionally increases the fire size, supports easier coal burning, and sets the lowest limit on the furnace dimensions. It also affects secondary air requirements and circulation characteristics.

4.1.1.3 Fixed carbon

Fixed carbon is the hard fuel remaining in the furnace when the volatile matter is extracted. The fixed carbon % in Thar Block-II samples ranges from 15.71 to 24.92% (Mean 18.47%). Thar coal samples contain low fixed carbon. The presence of fixed carbon in coal selects the grade of coal because it turns into a leading heat producer in the course of burning. The greater the heating values and fixed carbon, the higher the rank of coal (Hong and Slatick, 1994).

4.1.1.4 Ash Content

The ash content found in Block-II samples ranged from 4.26 to 10.38% (Mean 6.42%). Ash is the inorganic, unburned portion of coal that is leftward after the whole burning, comprising the majority of the mineral element. Due to the high ash-holding capacity of coal, a capable dust elimination arrangement must be in place to control particulate releases. Moreover, high ash fractions lessen the heating value of the coal (Khan, 2007). The environmental distress of particulate matter is not only limited to its release but also the removal of waste made due to the existence of other toxic materials in the ash (Anjum and Khan, 2017). In furnace ash, burning capability decreases, and a rise in handling rate distresses burning efficacy and boiler productivity. It's also causing slagging and clinkering problems in a furnace.

4.1.1.5 Calorific/Heating Value

The calorific value, similarly named the heating value of the coal in Thar Block-II, ranges between 2027.0 to 3708.9 kcal/Kg (Mean 3030.0 kcal/Kg). Carbon and hydrogen tend to increase the heating value, whereas oxygen declines it.

Table 4.1: Thar Coal Block-II Proximate Analysis As Received Basis (AR)

Number of Samples (N)	Variable	As Received (AR) Basis (%)				Calorific Value kcal/Kg
		Moisture	Ash	Volatile Matter	Fixed Carbon	
80	Min	42.06	4.26	25.25	15.71	2027.0
	Max	50.62	10.38	35.05	24.92	3708.9
	Mean	46.26	6.42	28.85	18.47	3030.0
	Stdev	±2.17	±1.41	±1.98	±1.72	±348.2

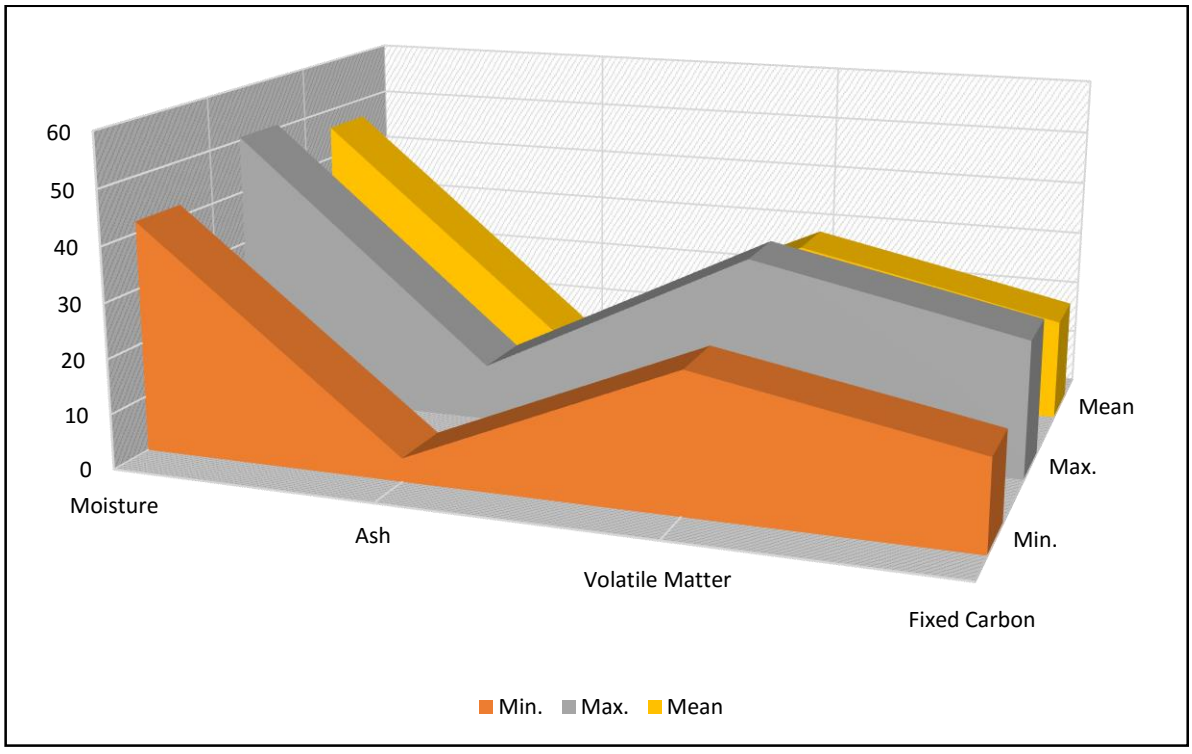

Figure 4.1: Proximate Analysis of the Thar Block-II Coal (%)

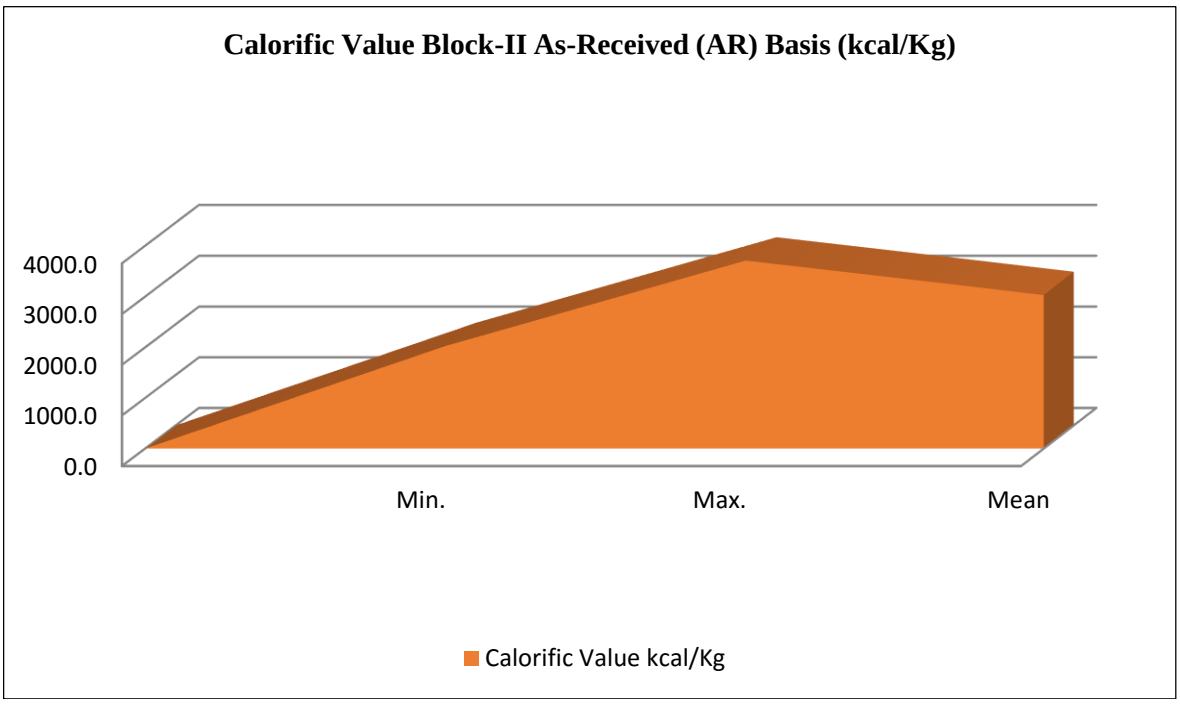

Figure 4.2: Calorific Value of the Thar Block-II Coal

4.1.2 Ultimate Analysis

Table 4.2 and Figure 4.3 show the results of the Thar samples ultimate analysis. Coal quality was determined on an as-received basis. The ultimate analysis illustrates carbon, hydrogen, nitrogen, and sulfur, as well as oxygen %. Those amounts are very vigorous to assess the characteristics of coal for burning and emission purposes. In a furnace, it's beneficial to define the amount of air necessary for burning and the capacity and configuration of the burning gases. This figure is also essential for the design of the flame temperature and the vent dust scheme.

4.1.2.1 Carbon

Carbon value in Thar Block-II samples ranges from 26.71 to 40.79% (Mean 33.76%). Greater carbon content samples comprise more heating values. This is bases on

the discharge of carbon dioxide (CO_2) in the air at a momentous level (Hong and Slatick, 1994).

4.1.2.2 Hydrogen

The hydrogen % in Thar Block-II samples ranges between 5.01 to 8.23% (Mean 6.95%). The Hydrogen/Carbon relation in coal has importance in coal transformation courses.

4.1.2.3 Nitrogen

The nitrogen % are nearly similar in all the Thar Block II samples, ranging between 0.11 to 0.58 (Mean 0.26%). Nitrogen is responsible for NOx creation in coal burning, which is one of the main pollutants in the atmosphere. After the creation of NOx and SOx, they are related to particulate matter ($PM_{2.5}$) (Querol et al., 1998). Adding moisture to these oxides in the atmosphere as a result, precipitation of acid, called acid rain. Most countries are already using low NOx burners to lower the NOx release (You and Xu, 2010).

4.1.2.4 Sulfur

Sulfur values from Thar Block II show ranges between 0.26 to 2.90% (Mean 0.95%). Sulfur is called one of the benchmark contaminants because of the discharges of SOx in the course of burning and its numerous environmental exposures (Nakicenovic and Swart, 2000). The lower-cost technique for decreasing the sulfur in coal and making it environmentally friendly is washing coal before burning it. It decreases up to 50% of sulfur, related to pyrite as well as the usage of limestone (Basu, 2015).

4.1.2.5 Oxygen

The oxygen % found in Thar Block II samples ranges between 33.44 to 49.80% (Mean 41.22%). The higher oxygen % decreases the heat formation capability of coal through impulsive burning. The studied samples comprise higher oxygen and, therefore, lower heating values.

Table 4.2: Thar Coal Block-II Ultimate Analysis As Received Basis (AR)

Number of Samples (N)	Variable	As Received (AR) Basis (%)				
		Carbon	**Hydrogen**	**Nitrogen**	**Sulfur**	**Oxygen**
80	Min	26.71	5.01	0.11	0.26	33.44
	Max	40.79	8.23	0.58	2.90	49.80
	Mean	33.76	6.95	0.26	0.95	41.22
	Stdev	± 3.20	± 0.73	± 0.11	± 0.57	± 3.84

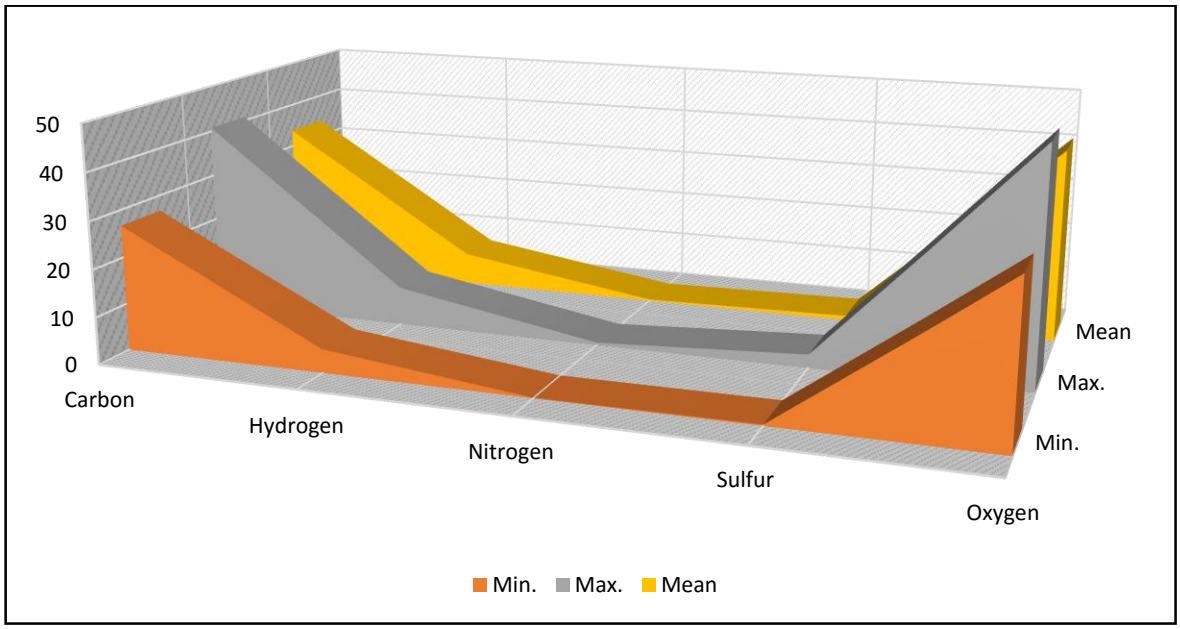

Figure 4.3: Ultimate Analysis of the Thar Block-II Coal (%)

4.2 Assessment of Thar Coal Ash

The assessment of Thar coal Block II ash is shown in Table 4.3 and Figures 4.4 and 4.5. In the coal ash analysis, it can be realized that coal ashes are mostly comprised of inorganic substances, and the major compounds are SiO_2 (Mean 23.59%), Al_2O_3 (Mean 14.52%), and Fe_2O_3 (Mean 11.0%) as well as lower quantities of Na_2O (Mean 5.13%), CaO (Mean 2.76%), MgO (Mean 2.30%) and K_2O (Mean 0.63%) observed. Ash characterizes the larger quantity of mineral substance afterward compelled off in burning. The coal yield ashes and their geochemical properties define the coal quality and its developing circumstances. The assessment of coal ash defines the configuration of coal ash. These facts are beneficial for environmental impact modeling. The configuration of coal ashes depends on the structure of organic matter and inorganic mineral deposits in coal. In the coal-burning course, both organic and inorganic materials will be released and reformed. Some of them will be discharged as volatiles with coal smoke into the air, and other portions will exist in dust, flying ash, and small particles. Selected chemical constituents in the inorganic material of residues are derived from organic material in the coal and will exist as novel parts and mineral constituents in the ashes (Choudry et al., 2010).

Table 4.3: Thar Coal Block-II Ash Analysis

Samples Number (N)	**Variable**	**Coal Ash Analysis Thar Block- I1 (%)**						
		SiO_2	**Al_2O_3**	**Fe_2O_3**	**CaO**	**MgO**	**Na_2O**	**K_2O**
80	Min	12.14	6.41	3.03	0.16	0.09	0.48	0.17
	Max	47.04	25.95	20.93	9.27	6.17	9.85	2.03
	Mean	23.59	14.52	11.00	2.76	2.30	5.13	0.63
	Stdev	±8.44	±5.55	±5.58	±2.55	±1.81	±2.30	±0.79

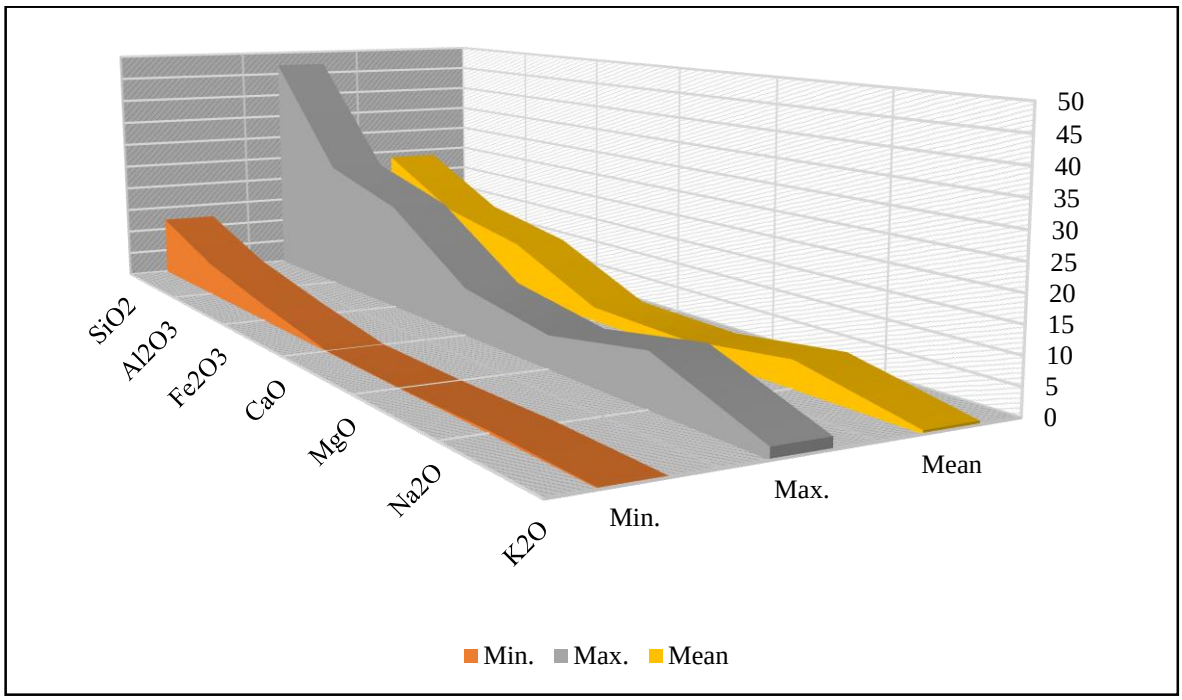

Figure 4.4: Ash Analysis of the Thar Block-II Coal (%)

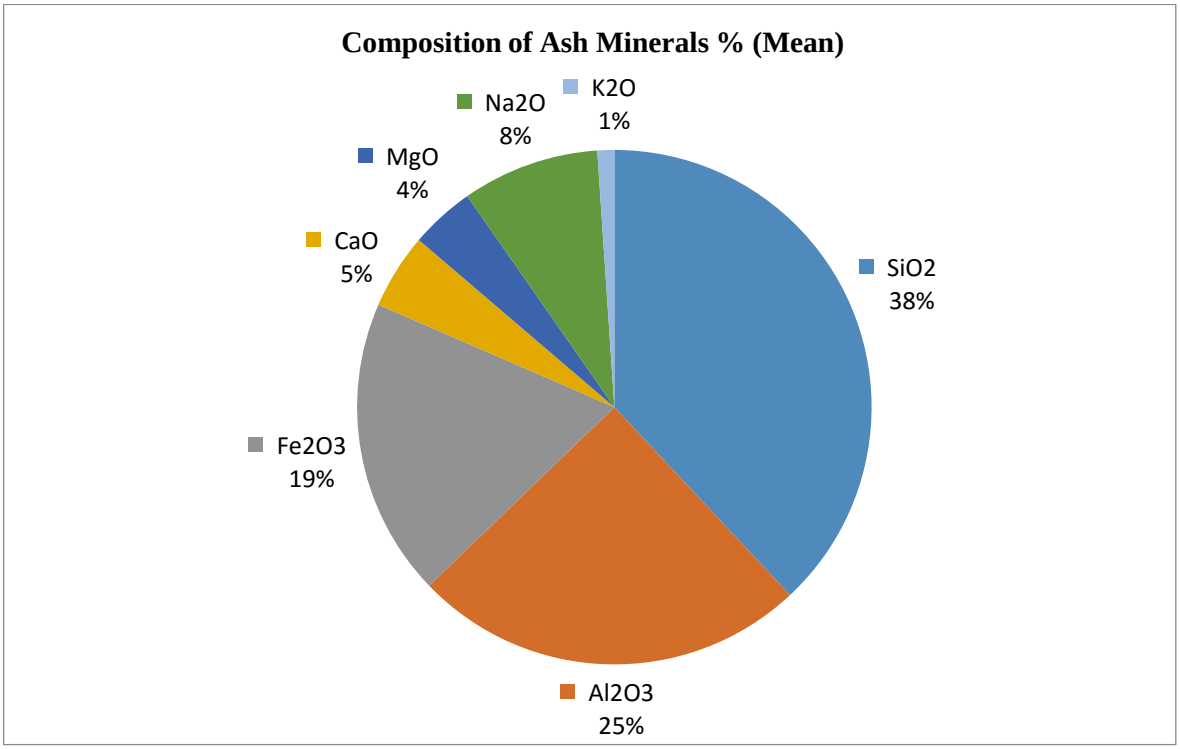

Figure 4.5: Showing the % of Minerals (Mean)

4.3 Thermo Gravimetric Analysis (TGA)

Figures 4.6 and 4.7 show the remaining weight portions of 60 mesh-size coal powder go through pyrolysis for heating rates ranging from 5 to 50°C. It indicated a major mass loss in the key decomposition. At the start, CO and CO_2 were discharged as the major gaseous pollutants, and at the core disintegration time, an enormous volume of gaseous pollutants like CO, H_2, CO_2, and hydrocarbons (i.e., C_2H_6, CH_4 and C_2H_4) were discharged due to major weight loss.

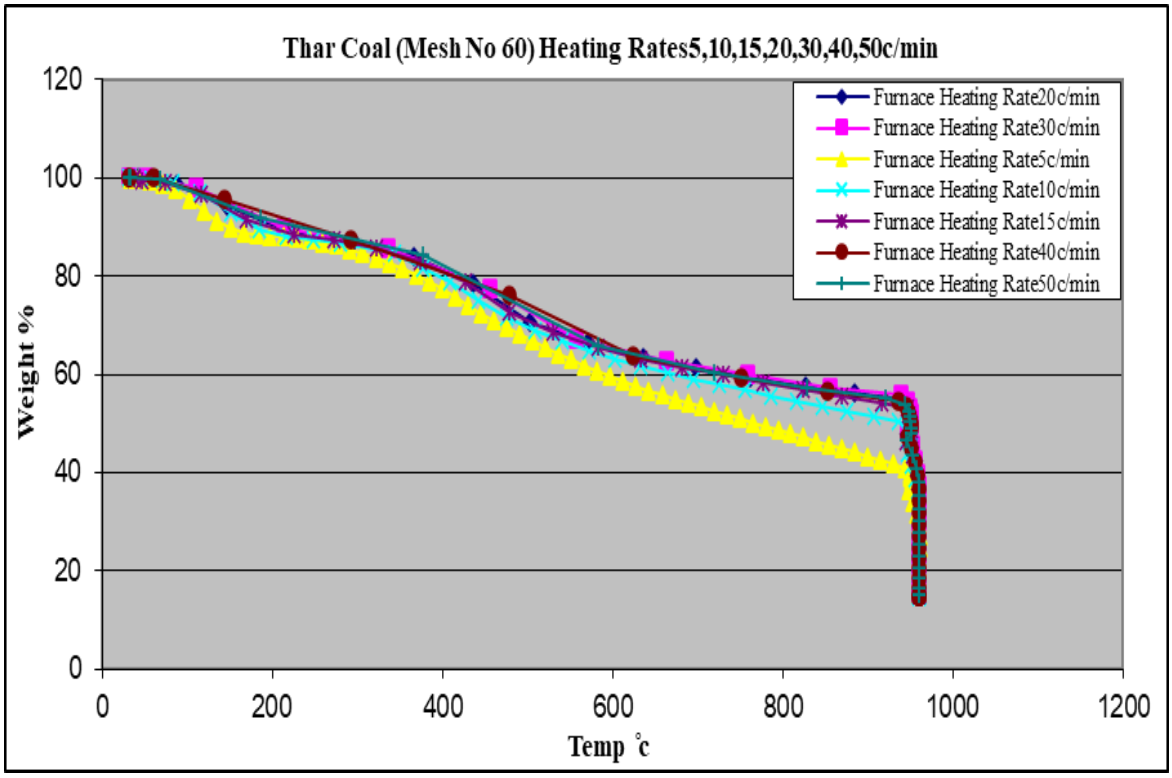

Figure 4.6: Thar Coal 60 Mesh Size TGA analysis (weight loss (%) for diverse heating rates)

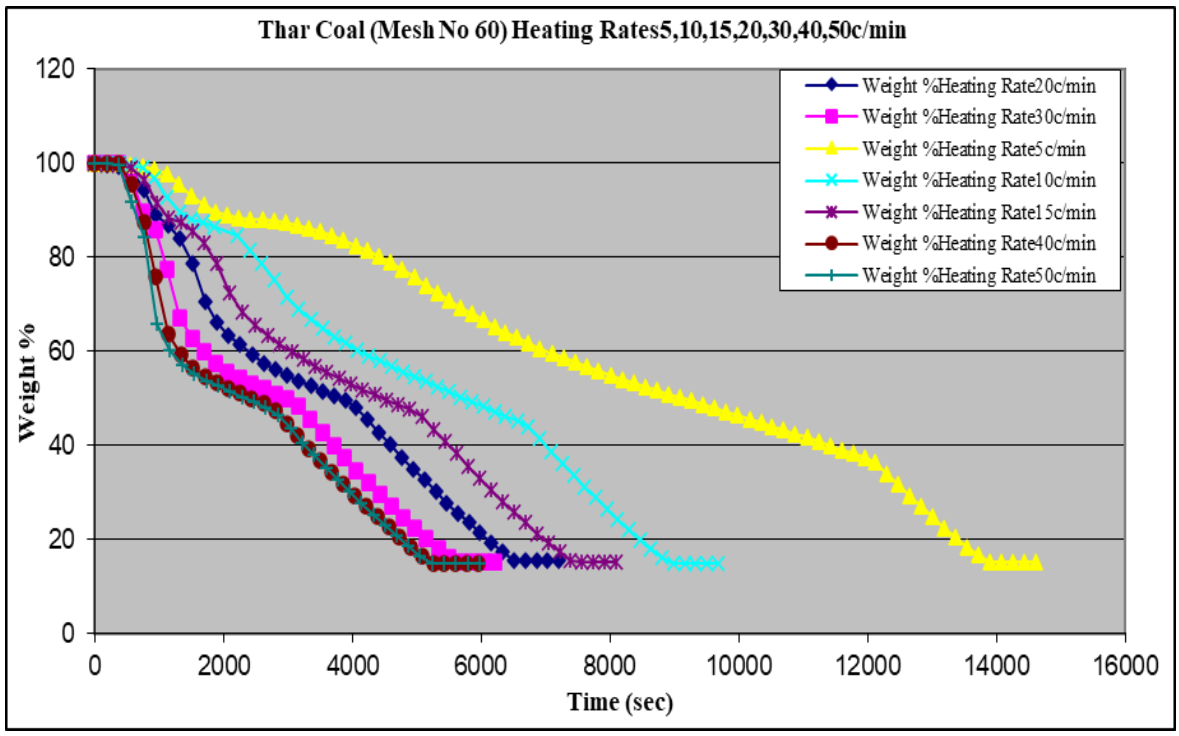

Figure 4.7: Thar Coal 60 Mesh Size TGA analysis (weight loss (%) as a role of time for diverse heating rates)

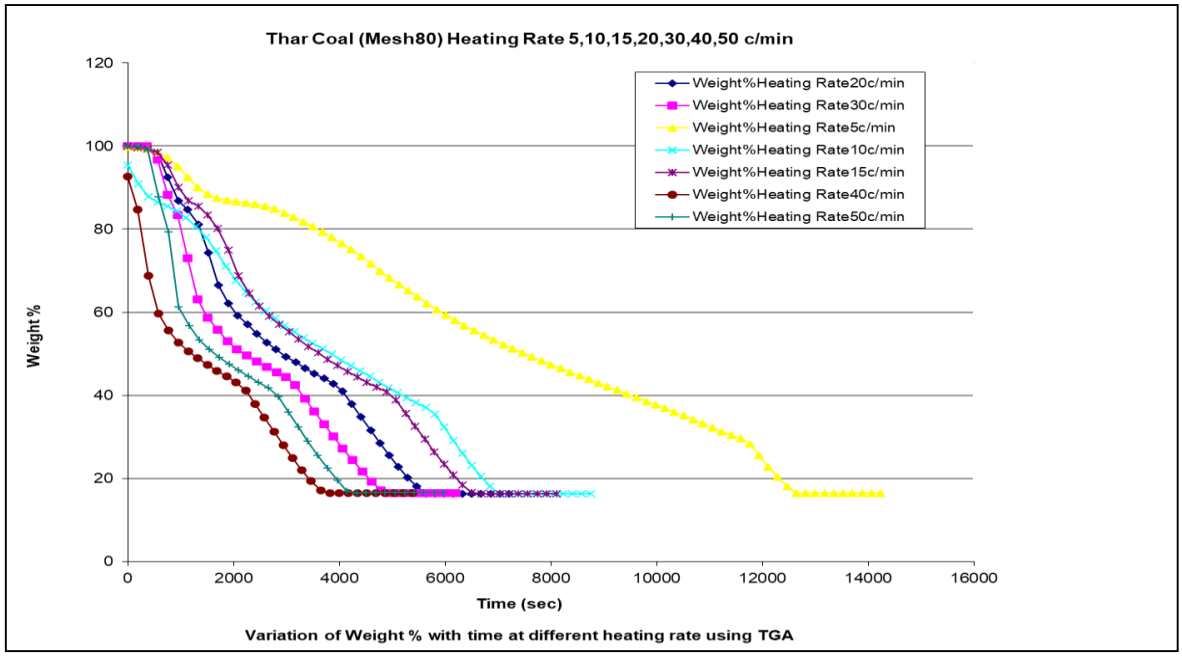

Figure 4.8: Thar Coal of 80 Mesh Size TGA analysis (weight loss (%) as a role of time for diverse heating rates)

Figures 4.8 illustrate the coal pyrolysis of 80 mesh size. It might be recognized that there is an observable lateral change in the thermograms for diverse heating ratios. In addition, the heating ratio has an influence on the overall mass loss. As the heating ratio was greater, a quicker pyrolytic response happened, causing greater pyrolytic transformation in volatile matters. From Figure 4.9, it might be concluded that the pyrolysis reaction is kinetically precise and that's greatly depends on the temperature of the reaction. It is organized by both chemical reactions and heat transmission. For a lesser heating ratio, a comparatively lesser pyrolysis ratio was perceived to cause a lesser transformation fraction.

Figure 4.9 displays the pyrolysis performance for diverse particle sizes. It might be realized noticeably that there occurred distinct stages of reactions that acquired a place in different temperature systems, with noticeable greatest for diverse heating proportions. The heating fraction had effects on not only the extreme degree of pyrolysis and the subject temperature but similarly on the initial and final pyrolytic temperatures. It is as well established that there was an adjacent change to upper temperatures in the course of pyrolysis as the heating amount was greater than before.

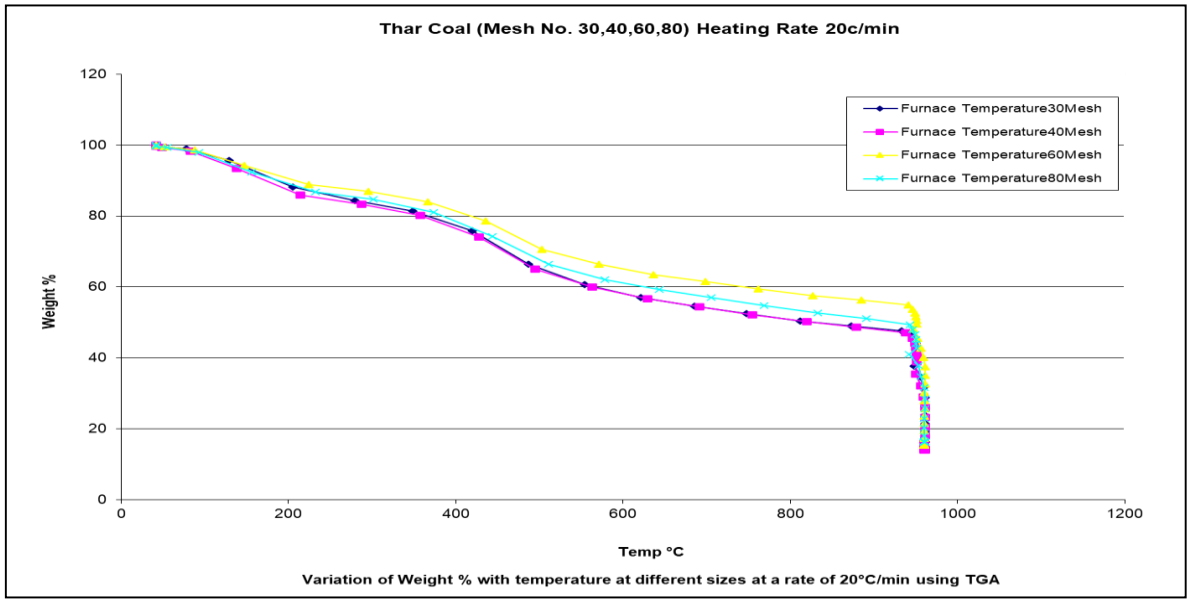

Figure 4.9: Thar Coal Mesh Size from 30-80 TGA analysis (weight loss (%) as a purpose of time for diverse heating rates)

To define the values of the kinetic constraints, the fundamental technique is consumed and a design of $\ln\left[-\frac{\ln(1-\alpha)}{T^2}\right]$ *versus* $\frac{1}{T}$ ($for\ n=1$) ensued in a straight contour of slope (– E/R) for n=1. The dominance of the components in a linear relationship is the requirement for appropriate standards of E and A. The fundamental assumptions are that pyrolysis is a first-order reaction that is entirely kinetically regulated.

By consuming Figure 4.6 statistics from the pyrolysis thermograms, the activation energy (E), the kinetic parameters, and the frequency factor (A) were calculated by Figure 4.10 with elevated correlation factors (all beyond 0.94) and recorded in Table 4.4. For the pyrolysis of Thar coal, the orders of reaction for all the heating rates were first-order reaction mechanisms. The activation energy varied as the heating rate increased, although the frequency factor was dependent on the heating rate, increasing gradually from 6.8 x 10^3 to 6.2 x 10^4 s^{-1}. This suggested that when the heating rate increased, the pyrolytic reaction would occur more quickly and easily. To predict the time-varying contours for the pyrolytic course of changed heating rates, these limitations may be used.

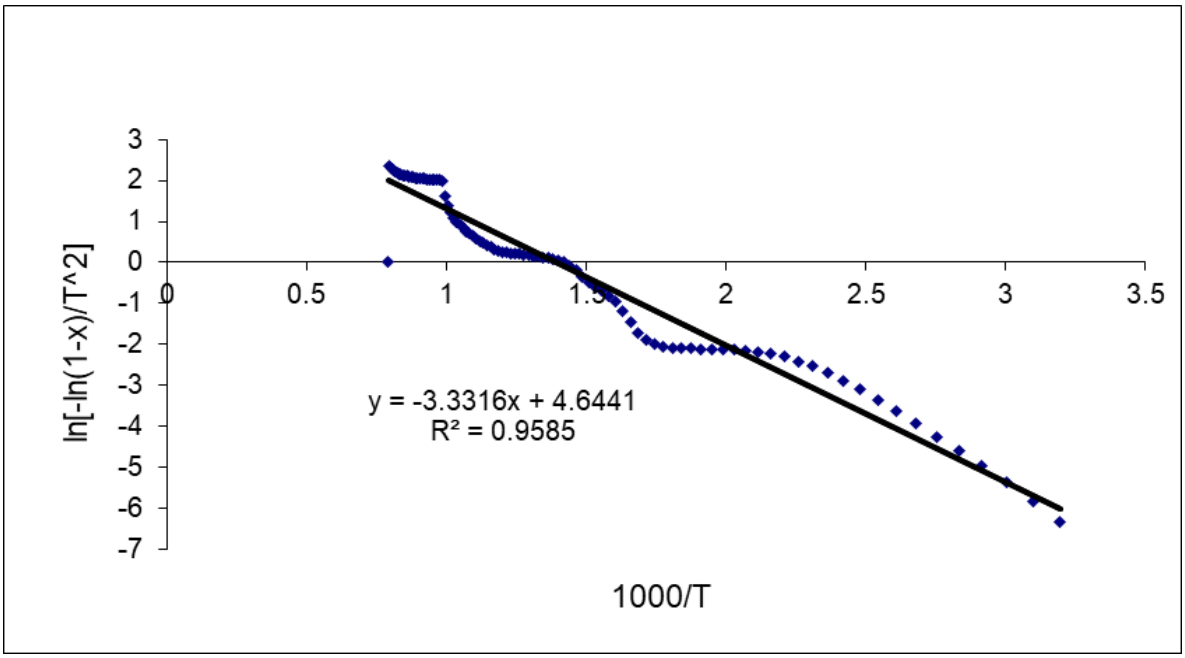

Figure 4.10: Kinetic plot for a typical heating rate

Table 4.4: Thar Coal of 60 mesh size Kinetic Parameters for the Pyrolysis

Heating Rate	Activation Energy (kJ/mole)	Frequency Factor (min^{-1})
5 °C/min	80.16	6.8×10^3
50 °C/min	102.01	6.2×10^4

4.4 Characterization of Rice Husk Biomass

Energy formed from rice husks is mostly contingent on their configuration. The possessions of fuel generally laid the foundation for the tools designated for the burning sequence. The most significant fuel possessions, which deliver the initial imprint of a confident rice husk, are set by proximate, ultimate analysis, and heating value.

4.4.1 Proximate Analysis

Table 4.5 and Figure 4.11 illustrate the rice husk proximate results.

4.4.1.1 Moisture

The moisture content was found to be between 12.76% to 13.50% (Mean 12.98%). The moisture content contributes a vigorous part to the assortment of effective thermal transformation tools. Rice husk moisture content significantly affects its value as a fuel resource. A rise in rice husk moisture content declines its Calorific/heating value and decreases the transformation efficacy and performance of the scheme since a great quantity of energy might be consumed for the evaporation of the fuel moisture during transformation. In addition, management and stowing also contribute to moisture content. Hence, a substantial dry fuel is preferred for burning (Emérita et al., 2020).

4.4.1.2 Volatile Matter

Rice husk has a comparatively higher volatile matter content, ranging from 55.77% to 62.88% (Mean 61.19%). The volatile matter is a vigorous part of the fuel since it defines

the expected impurity of the product gas with condensable vapors in every thermochemical transformation scheme. The fuel volatile content has a prodigious effect on the burning course and the scheme of the burning section (Quispe et al., 2017). Rice husks are a potentially beneficial fuel for gasification and pyrolysis. Due to the high volatile content, less heat is required for reactions, which makes it conceivable to gasify rice husk at lower temperatures (Quispe et al., 2017).

4.4.1.3 Fixed Carbon

Rice husk has a lower fixed carbon. The fixed carbon of the rice husk varies from 9.35% to 14.75% (Mean 10.63%).

4.4.1.4 Ash Content

Rice husk has a relatively higher ash content. The ash content ranged from 14.50% to 16.48% (Mean 15.20%), which is mostly silica as its configuration is around 90-95% in ash. Constant ash elimination in gasification is therefore vital while rice husk is consumed as a fuel. It is favorable from the additional perception that the inorganic composites existing in the agronomy remaining assets with greater ash contents have latent potential to be used as a catalytic agent in thermal transformation technologies, e.g., pyrolysis and gasification (Danish et al., 2015).

Table 4.5: Rice Husk Proximate Analysis As Received Basis (AR)

Variable	Rice Husk Proximate Analysis As Received (AR) Basis (%)				Calorific/ Heating Value kcal/Kg
	Moisture	Ash	Volatile Matter	Fixed Carbon	
Sample 1	12.92	14.75	62.88	9.45	3467.39
Sample 2	12.76	14.69	61.98	10.57	3207.10
Sample 3	12.90	14.50	62.74	9.86	3426.94
Sample 4	13.09	14.81	62.31	9.79	3366.39
Sample 5	13.50	15.98	55.77	14.75	2933.26
Sample 6	12.77	16.48	61.40	9.35	3144.89
Min	**12.76**	**14.50**	**55.77**	**9.35**	**2933.26**
Max	**13.50**	**16.48**	**62.88**	**14.75**	**3467.39**
Mean	**12.98**	**15.20**	**61.19**	**10.63**	**3257.66**

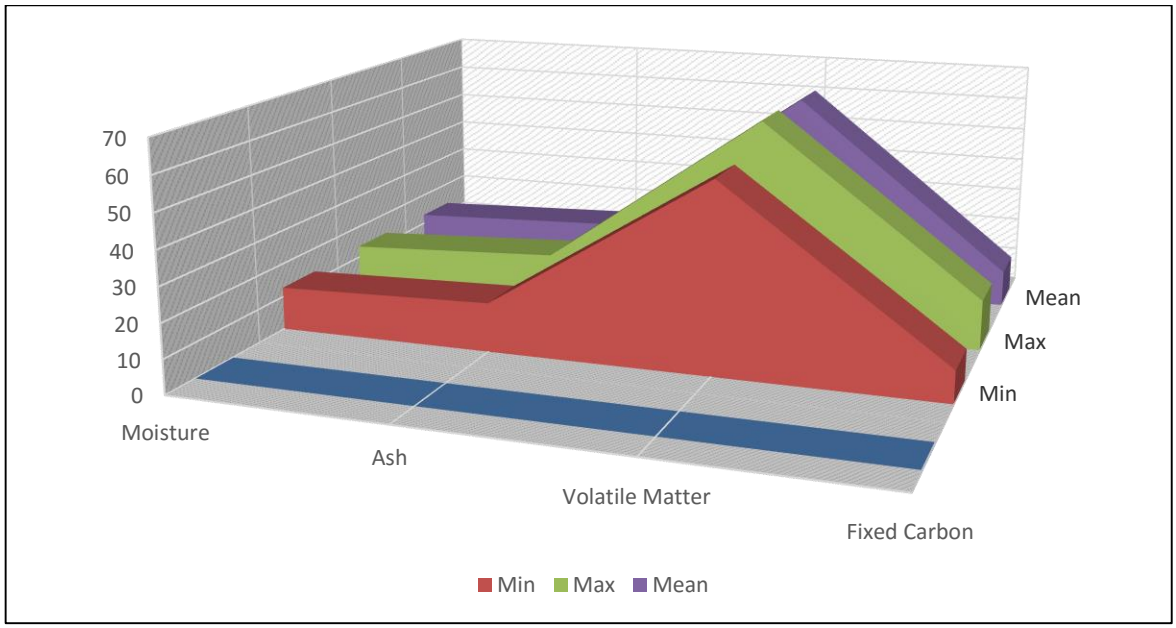

Figure 4.11: Samples (1-6) Min, Max and Mean Proximate Analysis of the Rice Husk (%)

4.4.1.5 Calorific/Heating Value

The heating value of the samples is reported in Table 4.5, and Figure 4.12 shows the heating value of rice husk ranges varied from 2933.26 to 3467.39 kcal/kg (Mean 3257.66 kcal/kg). For the thermochemical modeling transformation scheme, the heating value is an important thermal property. The heating value delivers higher valuations of the fuel. The rice husk sample heating value specified that these within the locality available renewable assets might be converted to a widespread amount of energy products from active transformation tools (Danish et al., 2015).

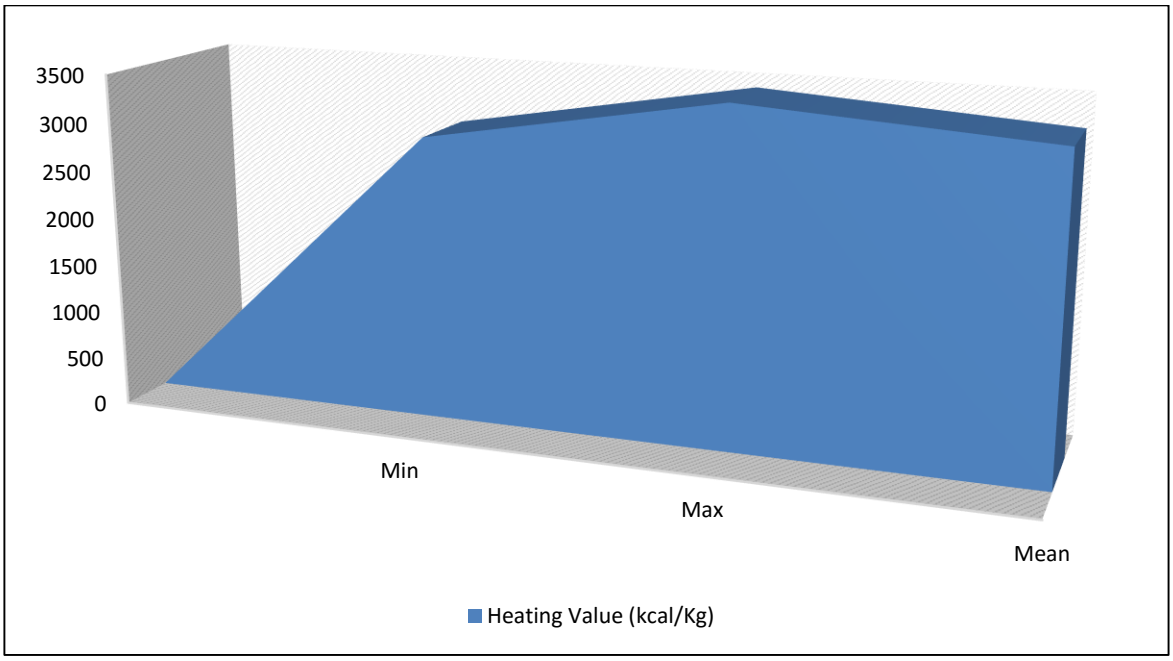

Figure 4.12: Samples (1-6) Min, Max and Mean Heating Value of the Rice Husk (kcal/Kg)

4.4.2 Ultimate Analysis

The ultimate study is mainly significant in assessing the fuel in terms of its pollution potential. The important basic elements of rice husk are carbon, nitrogen, hydrogen, and sulfur. These components are significant in evaluating the suitability of the

fuel and the heat value (Cláudio et al., 2019). Also, deliver statistics on the production of undesirable materials through the combustion process relating to environmental pollution problems. The consequences of the rice husk sample ultimate analysis are revealed in Table 4.6 and Figure 4.12. The percent portion of carbon varied from 32.24% to 41.79% (Mean 37.02%) and hydrogen varied from 5.38% to 5.85% (Mean 5.62%). In rice husk samples, nitrogen and sulfur % were very low, ranging from 0.37% to 1.31% (Mean 0.70%) and 0.02% to 0.19% (Mean 0.11%) correspondingly. The small % of nitrogen and sulfur offer environmentally more suitable fuel properties.

Table 4.6: Rice Husk Ultimate Analysis as Received Basis (AR)

Rice Husk Ultimate Analysis As Received (AR) Basis (%)				
Variable	**Carbon**	**Hydrogen**	**Nitrogen**	**Sulfur**
Sample 1	35.54	5.56	0.53	0.17
Sample 2	34.23	5.78	1.31	0.19
Sample 3	41.35	5.38	0.37	0.07
Sample 4	41.79	5.85	0.43	0.02
Sample 5	32.24	5.71	0.67	0.15
Sample 6	36.88	5.45	0.60	0.08
Min	32.24	5.38	0.37	0.02
Max	41.79	5.85	1.31	0.19
Mean	37.02	5.62	0.70	0.11

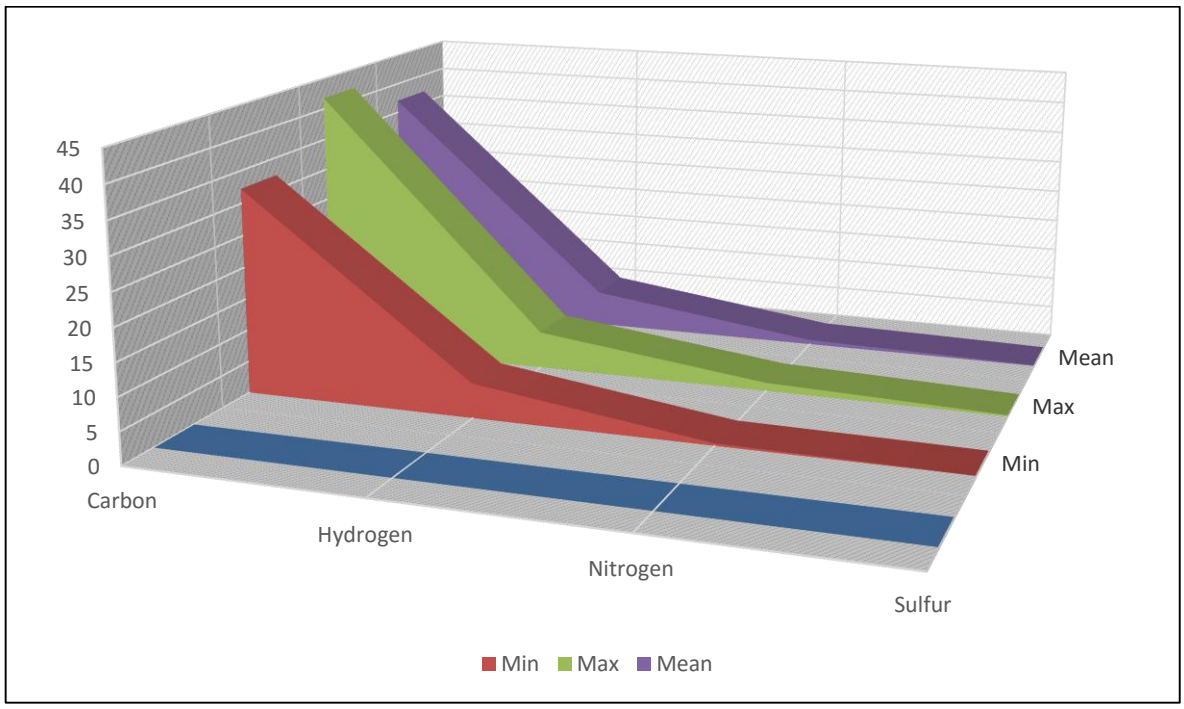

Figure 4.13: Samples (1-6) Min, Max and Mean Proximate Analysis of the Rice Husk

The extensive distinctions in certain of the described physiochemical contents of rice husk perceived are utmost probable because of the diverse approaches and procedures applied for reaping, management, handling, and storing biomass reasonably than to the essential possessions of the rice husk.

4.5 Characterization of the Coal and Rice Husk Blends

Coal-rice husk blend samples were mixed with coal at fractions of 10%, 20%, and 30%, correspondingly. In this method three different samples of blends were made, namely, CR_h-1, which comprises 90% coal and 10% rice husk, CR_h-2, which comprises 80% coal and 20% rice husk, and CR_h-3, which comprises 70% coal and 30% rice husk.

4.5.1 Coal and Rice Husk Proximate Analysis

As shown in Table 4.7, and Figure 4.14 the coal comprises a higher content of moisture (47.30%), fixed carbon (18.12%), and calorific value (3687.60 Kcal/kg), while being lower in volatile matter (29.13%) and ash (5.45%). However, rice husk is the highest in volatile matter (61.98%), the lowest in fixed carbon (10.57%), moisture (12.76%), and higher ash (14.69%).

4.5.2 Coal and Rice Husk Ultimate Analysis

The ultimate analysis of the coal sample gave a higher carbon content 36.73%, Hydrogen 7.53% and sulfur 1.51%, and lower nitrogen 0.58%, as shown in Table 4.8 and Figure 4.15. The rice husk sample offered a lower 34.23% of carbon, 5.78% of hydrogen, 0.18% of sulfur, and higher 1.31% nitrogen. The basic configuration of the rice husk fluctuates depending on its source and environmental circumstances.

4.5.3 Coal- Rice Husk Blended Samples Proximate Analysis

The diverse samples of coal-rice husk blends CR_h-1, CR_h-2, and CR_h-3 were evaluated. CR_h-1 gave a higher moisture content of 43.57%, fixed carbon of 16.20%, and lower ash of 7.0%. CR_h-3 had a higher volatile matter content of 45.02% and a lower moisture content of 34.11%, as revealed in Table 4.7 and Figure 4.14.

Table 4.7: Mean Proximate Analysis of Thar Lignite Coal, Rice Husk and Their Blends

Parameters	**Units**	**Results**				
		Thar Lignite Coal	**Rice Husk Biomass**	**CR_h -1 (90 TL/10 RH)**	**CR_h -2 (80 TL/20 RH)**	**CR_h -3 (70 TL/30 RH)**
Calorific Value	Kcal/Kg	3687.60	3207.10	3424.66	3476.95	3555.37
Moisture	%	47.30	12.76	43.57	38.89	34.11
Volatile Matters	%	29.13	61.98	33.23	38.98	45.02
Ash Contents	%	5.45	14.69	7.0	7.55	8.09
Fixed Carbon	%	18.12	10.57	16.20	14.58	12.78

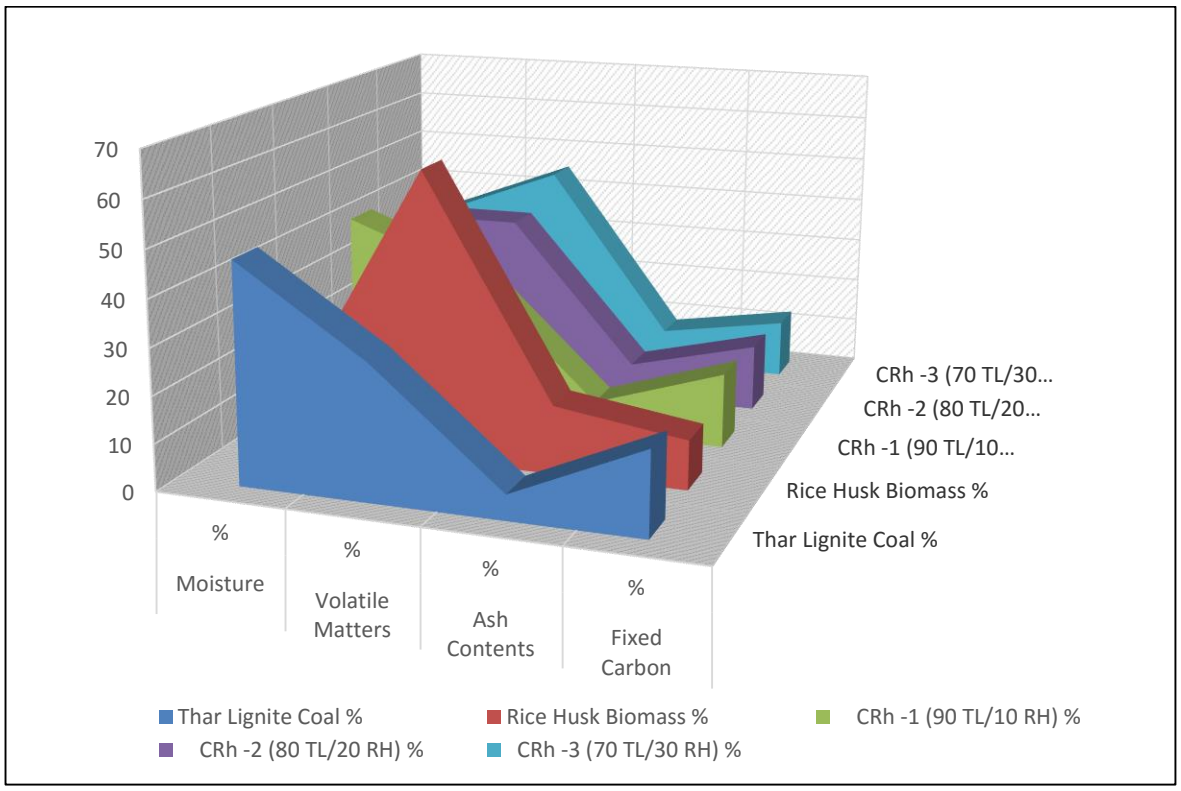

Figure 4.14: Proximate Analysis of Thar Lignite Coal, Rice Husk and Their Blends

4.5.4 Coal- Rice Husk Blended Samples Ultimate Analysis

Coal-rice husk blends ultimate analysis was conceded out, CR_h -1 gave a higher amount of carbon content 36.23% and a lower amount of Hydrogen 6.36%, Nitrogen 0.63%, and sulfur 1.39%. It was examined that the overall % of sulfur reduced in sample CR_h-3 was 0.99%. Whereas hydrogen and nitrogen content are increased, as revealed in Table 4.8 and Figure 4.15.

Table 4.8: Mean Ultimate Analysis of Thar Lignite Coal, Rice Husk and Their Blends

Parameters	Units	Results				
		Thar Lignite Coal	Rice Husk Biomass	CR_h -1 (90 TL/10 RH)	CR_h -2 (80 TL/20 RH)	CR_h -3 (70 TL/30 RH)
Carbon	%	36.73	34.23	36.23	35.73	35.23
Hydrogen	%	7.53	5.78	6.36	6.93	7.50
Nitrogen	%	0.58	1.31	0.63	0.69	0.75
Sulfur	%	1.51	0.18	1.39	1.17	0.99
Oxygen	%	35.38	37.17	35.68	35.90	36.11

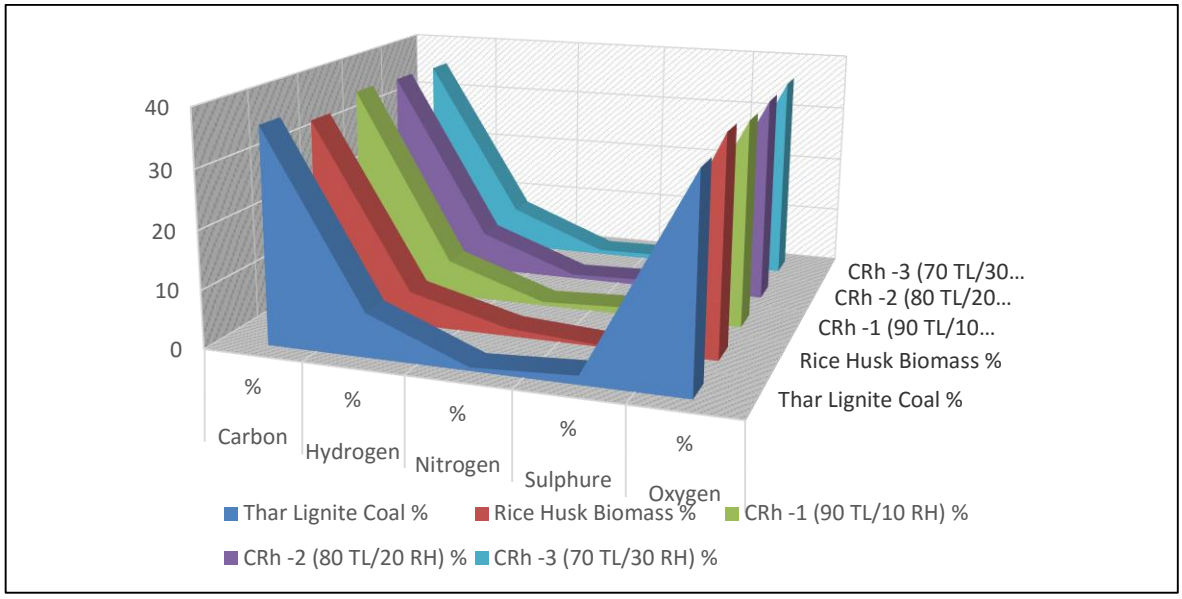

Figure 4.15: Ultimate Analysis of Thar Lignite Coal, Rice Husk and Their Blends

4.6 Coal- Rice Husk Blends Emission Analysis

An emission study is part of a burning system intended to enhance fuel economy, decrease adverse emission discharges, and protect the fuel-burning device. Burning inspection begins with the quantity of exhaust gas concentrations. Flue gases were monitored in a muffle furnace outlet at the lab for co-firing and emissions. A flue gas

analyzer was used for O_2, CO_2, CO, SO_2, and NOx as shown in Table 4.9 and Figure 4.16. Different gases are released in flue gases, which show the consumption of O_2 in the oxidation reactions throughout the burning, which caused the breakdown of carbon bonds and CO_2 production. The sulfur content in coal and biomass reacts with O_2 to form sulfur oxides (SO_2), whereas the nitrogen content reacts with O_2 to form nitrogen oxides (NOx) (Kanwal et al., 2021).

Table 4.9: Emission Analysis of Coal-Rice Husk Different Blends

Component	Unit	CR_h-1 (90 TL/10 RH)	CR_h-2 (80 TL/20 RH)	CRh-3 (70 TL/30 RH)	SEQS Standard mg/Nm^3
O_2	%	5.95	6.41	9.07	NoGL
NOx	ppm	89	69	34	
	mg/Nm^3	167	130	64	1200
SO_2	ppm	828	649	169	
	mg/Nm^3	2167	1698	442	850
CO	ppm	1031	922	789	
	mg/Nm^3	1180	1055	903	800
CO_2	%	4.46	5.45	7.27	NoGL

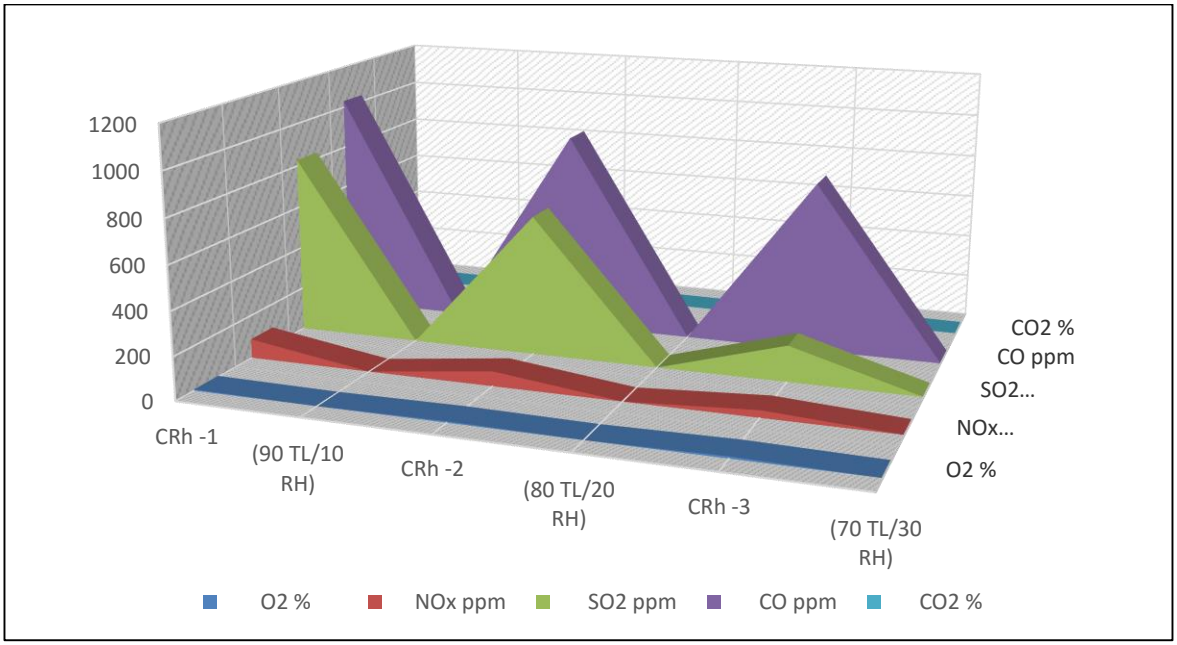

Figure 4.16: Coal-Rice Husk Blends Emission

4.6.1 Oxides of Carbon Emissions

The coal and rice husk emissions analysis from the co-combustion is shown in Table 4.9 and Figure 4.16. The co-combustion of 90:10% (CR_h-1) coal and rice husk biomass showed a CO and CO_2 value of 1031 ppm and 4.46%, respectively. Whereas a 70:30% (CR_h-3) coal and rice husk ratio made CO 789 ppm and CO_2 7.27%. When the CO value was high, the CO_2 value was low. The reduction in CO is because of the transformation of CO into CO_2 with a temperature rise. Also, biomass blending caused less carbon type, resulting in decreased CO discharges with a rise in blending fraction and an increase in furnace temperature. Furthermore, the occurrence of rice husk oxygenates could have helped the conversion of CO_2 from CO; hence, CO discharges might be relatively lesser (Akhtar et al., 2018). If the burning environment is uncontrolled, high CO could be produced because of less burning air, dispersal-controlled reactions, and fewer holding periods.

4.6.2 Oxides of Nitrogen Emissions

The maximum NOx level was reported in CR_h-1 (89 ppm) and the minimum in CR_h-3 (34 ppm), as shown in Table 4.9 and Figure 4.16. Nitrogen Oxides (NOx) are the most significant emissions resulting from the burning of fuels. Characteristically, the main NOx discharges from co-firing are NO and NO_2. NOx discharges rely on the occurrence of nitrogen in the raw material, air (oxygen), and co-firing course circumstances (Kumar, 2015). Furthermore, a 90:10% (CR_h-1) blend of coal and rice husk formed more NOx discharges as compared to 70:30% (CR_h-3). Hence, the blending of coal and rice husk would decrease NOx production from vent gas (Munir, 2011).

4.6.3 Oxides of Sulfur Emissions

SO_2 discharge relies on the occurrence of sulfur content (Mittal et al., 2012). It is estimated that all the existing coal sulfur is transformed into SO_2 discharges in the course

of co-firing. Coal-rice husk blends discharged SO_2 in CR_h-1 (828 ppm), CR_h-2 (649 ppm), and CR_h-3 (169 ppm), respectively, as shown in Table 4.9 and Figure 4.16. Overall, the SO_2 discharges were considerably reduced by increasing the rice husk biomass ratio. This reduction in SO_2 discharges according to the blending proportion might be attributed to the dilution consequence of rice husk in coal. Additionally, the rice husk ash comprises a substantial amount of CaO that might stimulate the fixation of SO_2 as $CaSO_4$ (Akhtar et al., 2018).

4.7 Combustion Modeling in the Riser of Fluidized Bed Combustor

Despite the extensive use of fluidized bed combustors, the progress and strategy of fluidized bed vessels have been experiential. That is because of the intricate stream actions of gas-solid streams in this approach, which makes flow modeling a difficult assignment. The essential delinquent comes across in hydrodynamics modeling of the motion of the two segments: the boundary is indefinite and transitory, and the interface is known individually for a restricted variety of circumstances (Liu et al., 2021b). Because of the mathematical complications of the equations non-linearity and in describing the diffusing and phase boundaries, numerical resolutions are too tough to attain (Zhao, 2021). Nevertheless, CFD is developing as an identical and capable recent device in hydrodynamics modeling. Whereas it is nowadays a benchmark device for single-phase streams, it is in the progress phase for polyphase schemes, like fluidized beds (Taghipour et al., 2003).

Many scientists have used commercial CFD codes to simulate multiphase complications, including Peng et al., (2021) and Jalil et al., (2002), who used ANSYS FLUENT to simulate multiphase complications in a fluidized bed with sand and air. The study was based on numerous velocities. The code's performance improved as the gas velocity increased. Several scholars have simulated in the CFB, two fluids CFD model using the code in CFX of gas-particle flow. The turbulence was demonstrated by the model k-ε turbulence in the gas segment and a model of static particle viscosity in the solid segment. This CFD model displayed a virtuous contract with the trials (Hansen et al.,

2002). A parallel investigation of gas-particle stream actions in the CFB riser unit was completed via FLUENT 19.0. Air and Fluid Catalytic Cracking (FCC) elements were consumed as the solid-gas segments, correspondingly. The outcomes of the computational analysis displayed that the inner and outer strategies have important properties on the complete gas-solid stream designs and bunch creations in the riser (Oloruntoba et al., 2022; Benyahia et al., 2000).

4.7.1 Combustion in Fluidized Bed Riser/Combustor

Through combustion, the capacity of coal solid fuel might be compact, at around 90%. The residual byproduct ash may be dumped or recycled to make further goods, like porcelain or cement. Additional advantages of combustion include the retrieval of energy and the reprocessing of remains for construction products.

Coal is normally conveyed by the retrieval of energy in the system of steam for power production. Combustors might also be planned to adjust processing systems. Coal combustion can vary in dimensions from small units of simply a small amount of tons per day to precise big units with constant regular coal feed capabilities.

Nevertheless, large coal power plants have the potential to be a major cause of environmental contamination. In addition to the discharge of different gases like nitrogen and sulfur oxides and particulate matter, poorly planned or functioning coal power might lead to the unplanned formation and discharge of pollutants gases. The environmentally comprehensive scheme and process of coal power plants entail the use of best environmental performance and superlatively accessible practices to avoid or reduce the creation and discharge of pollutant gases.

4.7.2 Coal Solid Fuel Combustion Mechanism

When a coal solid fuel particle is exposed to a burning, flowing gas stream, it goes through its major phases of mass loss, which are categorized into their parts: drying, devolatilization, and char combustion. However, the comparative importance of each of

these three procedures is specified by the fuel proximate analysis. The case of coal has comparatively less water and volatiles but more fixed carbon (char) as compared to others. For pulverized coal particles, drying, devolatilization, and char burn happen serially, and the char combust duration carries on much longer than the devolatilization and drying phases. For bigger particles, drying, devolatilization, and char burning occur simultaneously.

4.7.3 Coal Solid Fuels Drying

Moisture in the coal might occur in two ways, either as free water or as bound water. Coal, being nonporous, has very little free water but mostly bound water. When heat is fed to the fuel, heat is transferred and emitted to the particle's external parts. For a crushed particle, the moisture is evaporated and forced out of the particle quickly prior to the volatiles being discharged. For relatively large fuel particles, such as coal in furnaces, convective flow is not usable. This is because of the temperature gradients inside the particle: moisture is progressing from inside the particle, but volatiles are being removed nearby the external casing of the particle. Because of the higher pressure in the coal apertures during the devolatilization of the external film of the particle, certain moisture is forced to the center of the particle until the pressure builds up throughout the particle. Therefore, dehydration of huge solid fuel particles primarily comprises the inner movement of the water vapor besides the outer flow. A pyrolysis film begins at the external edge of the particle and slowly transfers to the inner side, discharging volatiles and establishing char. The moisture released decreases the mass and heat transference to the particle; therefore, the mass reduction of the particle or combustion rate is decreased. As the moisture and volatile release is decreased, the char shallow initiates to react.

4.7.4 Devolatization of Coal Solid Fuels

When the drying is complete, the temperature increases, and the coal solid fuel activates to decompose and discharge volatiles. Then the volatiles stream out of the coal solid over the apertures; oxygen from outside cannot enter the particle, and therefore devolatilization is stated as the pyrolysis phase. The frequency of pyrolysis and

devolatilization of the product is contingent on the temperature and kind of fuel. The pyrolysis produces, then burns, proceeds, and flares around the particle as oxygen disperses into the products. The flare heats the particle, producing improved devolatilization. If water vapor is still streaming out of the holes, the flare temperature will be short and the flare will be weak, but after all the water vapor has disappeared, the flare will be warmer. For larger fuel particles, a substantial period is essential to heat the particles to pyrolysis temperatures; afterward, they are introduced into the combustor, and the process slowly enters the particle.

The burning of coal-solid fuels can happen either by combustion of the fixed carbon on the surface of the fuel or by the combustion of volatiles in the periphery film around the particle. Which operation essentially arises first is reliant on the degree of radiative and convective heat transference to the particle. If the radiative heat transference is higher so that the shallow carbon rapidly warms up to the burning temperature, or if the degree of convective heating is higher so that the shallow carbon quickly warms and the volatiles are removed earlier, a combustible composite can gather and, the burning will happen first at the shallow. Further, if shallow heating is lower, then the volatiles might burn first; meanwhile, they have lower burning temperatures than the carbon burning period, which is contingent upon particle dimension and thermal diffusivity along with heating degree and the pyrolysis ratio. Burning times for crushed fuels are typically a few milliseconds; however, under furnace conditions, a larger particle could take several seconds. The burning delay can last several minutes for larger particles if the temperature is barely above the burning temperature. Moisture causes the burning temperature to increase, which can be a major problem when designing combustors for pulverized fuels.

4.7.5 Char Combustion

The last phase in the coal-solid fuel-burning procedure is char combustion. Once devolatilization is completed, the char and ash remain. Char is highly porous; after no further volatiles are evading from the char, oxygen (O_2) can be drawn out over the exterior periphery film and interior escaping of O_2. The shallow reaction mainly produces CO, and

after the response, the particle produces CO_2. The degree of char burning relies on the O_2 concentration, Reynolds number, gas temperatures, char dimension, and permeability.

4.7.6 Ash Formation

As char combusts, the minerals that are disseminated as ions and submicrons in the fuel particles are transformed into a film of ash on the char surface. In higher-temperature crushed coal burning, the ash is likely to form hollow, glossy circles termed ecospheres. At a lower temperature, the ash tends to persist leniently. The ash layer can have an important consequence on the heating capability, radiative heat transference, and catalytic shallow responses, along with the outcome in enlarged diffusivity confrontation with O_2, particularly delay in the char burning period. In burning systems, the ash, which is made from mineral substance, might slag on radiant heat transference shells and foul convective heat transference shells if the particle temperature is too high. According to US-EPA, the residual byproduct ash may be dumped or recycled to make further goods utilized in porcelain or cement collective, used on mine sites to fill the pits, create or amend the soil, and as a low-permeability or high alkalinity material, roofing materials, and bricks.

Coal solid fuel particles in the burning environment start dehydrating, devolatilization, and char burn. The degree of these progressions depends on the fuel category, fuel moisture content, magnitude and mass, and heat transference to the particle. For smaller particles, the three stages occur in series, whereas for bigger particles, they occur simultaneously. Drying is fastest for smaller particles, but char burning is longer than devolatilization. For large fuel units, char burn is the rate-limiting phase and is reduced by the progress of the moisture. Devolatilization is a kinematic procedure that is frequently modeled as a first-order reaction. The volatiles contain H_2, CO, CO_2, H_2O, hydrocarbon gases, and tars, which blend with O_2 and combust in the vapor part. Char has a permeable carbon content with a lesser volume of hydrogen combined with inorganic compounds. Char burning contains the dispersal of O_2 to the shallow and the chemical reaction at the shallow. Because of the surface reaction, the char is warmer than the surrounding gas. As

char combusts, small inorganic particles develop on the surface of the char, and ash particulates are made.

4.7.8 Modelling of the Riser/Combustor

Coal is burned using a variety of risers or combustors, and combustion techniques. The primary combustor is separated into three areas, mainly the drying area, the combusting area, and the burnout area. As stated in the combustion mechanism of coal fuels above, the first stage would be the drying grate, where hot air at a temperature below the ignition of volatiles is introduced to the fuel. The velocity of the air should be higher than the rest to spread the vapors out of the fuel. The main purpose of this grate is to reduce as much moisture from the coal as possible. This is to improve the whole combustion process. With less moisture, the rate of combustion of coal can be made faster and more efficient. Since coal is heterogeneous and not in a pulverized state, we would expect to have some devolatilization at this stage. The main purpose is to eliminate free water rather than bound water.

The combustion grate, where all three stages of combustion occur, is the next: the elimination of bound water, devolatilization, and char burning. At this stage, devolatilization is the major reaction where the pyrolysis products are burned. Hot air at higher temperatures and lower speeds is introduced into the fuel. This is to make sure all the volatiles can be extracted fully and combusted efficiently. At the end of this stage, there would be more char than volatiles. Moving onto the final stage, the burnout grate, the remaining char is fully combusted with an inlet of high oxygen-filled hot air.

For the geometries of the risers/combustors, we have to consider the three different types according to their respective geometries. First, there is the center flow, counter flow, and parallel flow, as shown in Figure 4.17. In Figure 4.18, the graphs depict the basic profile of heat release from across the grate.

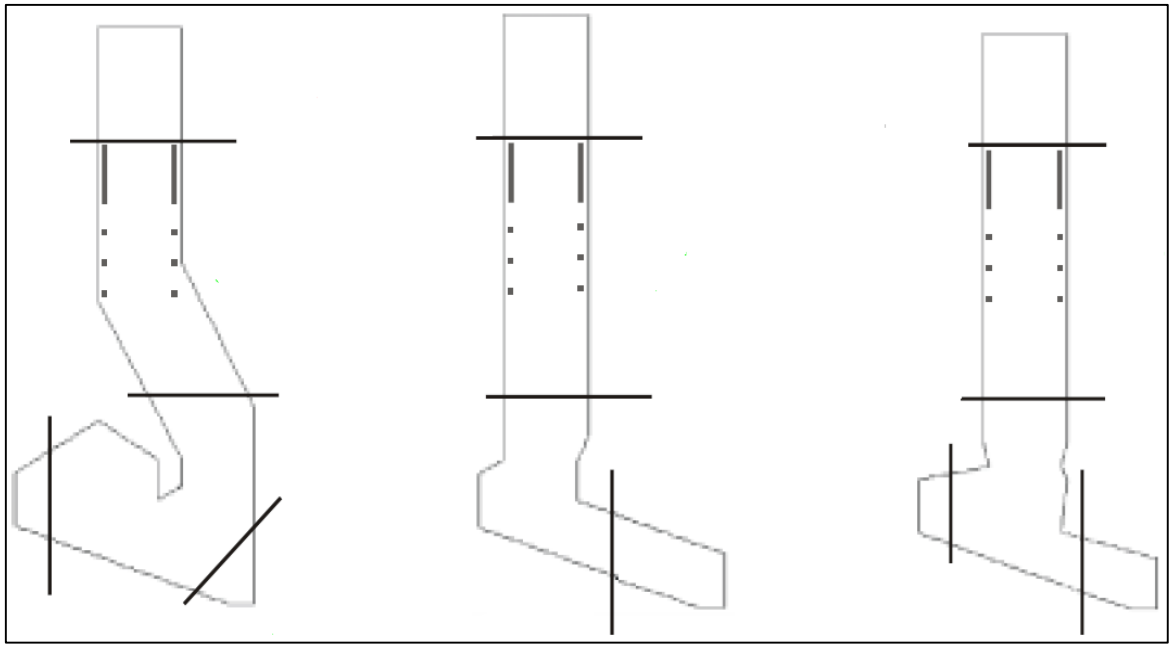

Parallel Flow Counter Flow Center Flow

(a) **(b)** **(c)**

Figure 4.17: Three Types of Geometries (a) Parallel (b) Counter(c) Center

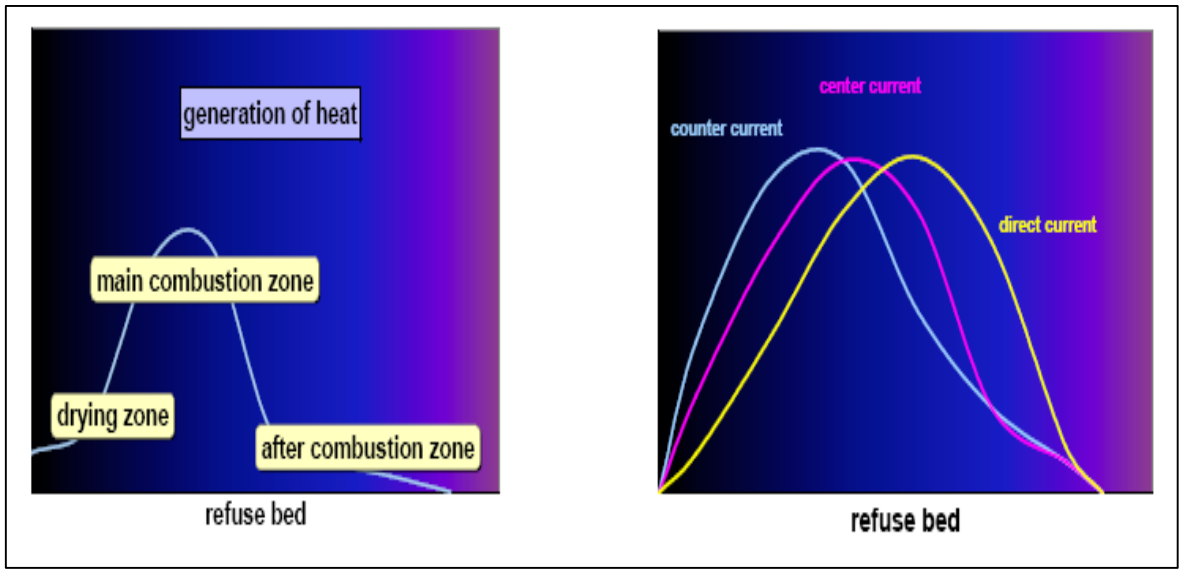

(a) (b)

Figure 4.18: (a) Heat discharge over the grate (outline) (b) Heat discharge outlines reliant on the plant Furnace geometry strategy

4.7.9 Modeling Approach

The above flow chart describes the complete work strategy for this simulation task. Models of coal-solid combustors were first created in Solid Works. The models are imported into ANSYS FLUENT to mesh and specify the types of boundary restrictions after being protected as a *.STEP file. The precisely meshed file is subsequently sent as a *.MSH file, which is suitable for ANSY FLUENT once this task is accomplished.

At a similar time, the bed or solid burning simulation is also completed by utilizing fluid dynamic incinerator code (FLIC) to model the bed burning to acquire the appropriate constraints to transfer into FLUENT to track the burning gas stream and burning, as depicted in Figure 4.19.

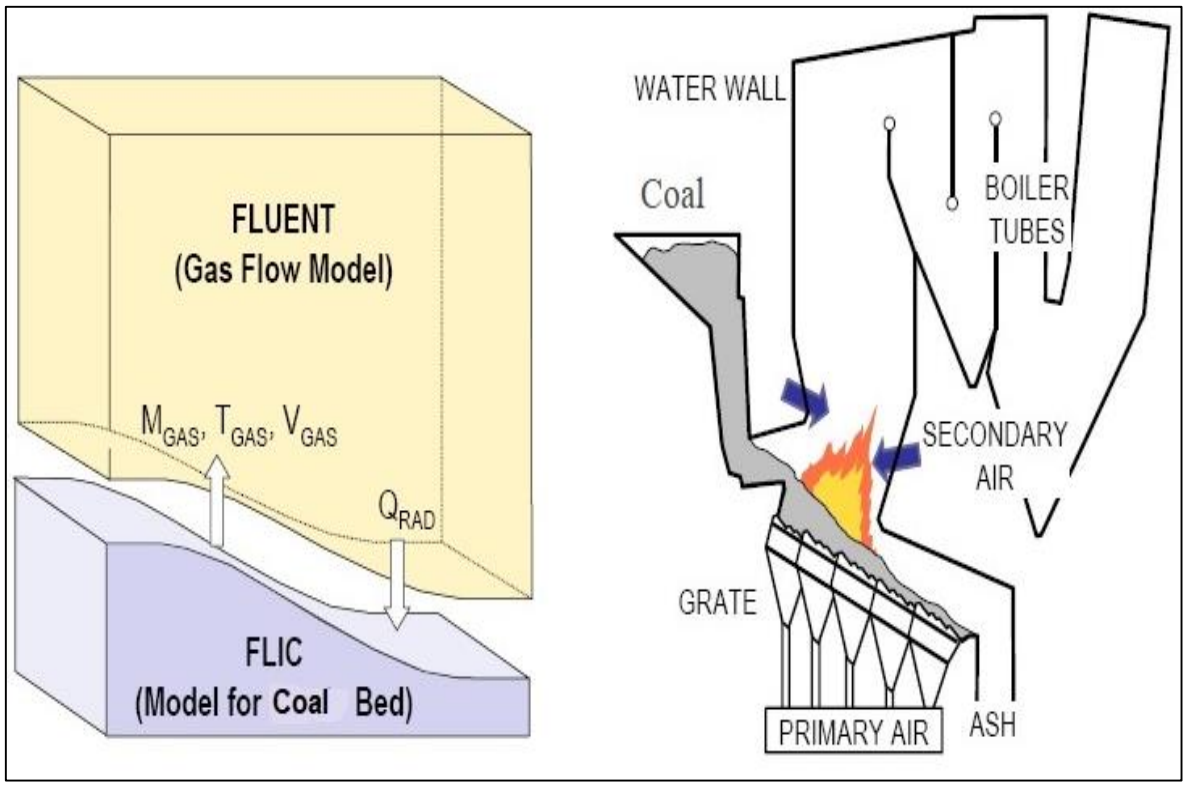

Figure 4.19: An Illustration of using FLIC for coal bed burning and FLUENT for gas movement modeling Geometries of the proposed coal fluidized bed combustor were modeled using SolidWorks and saved as *.STEP files.

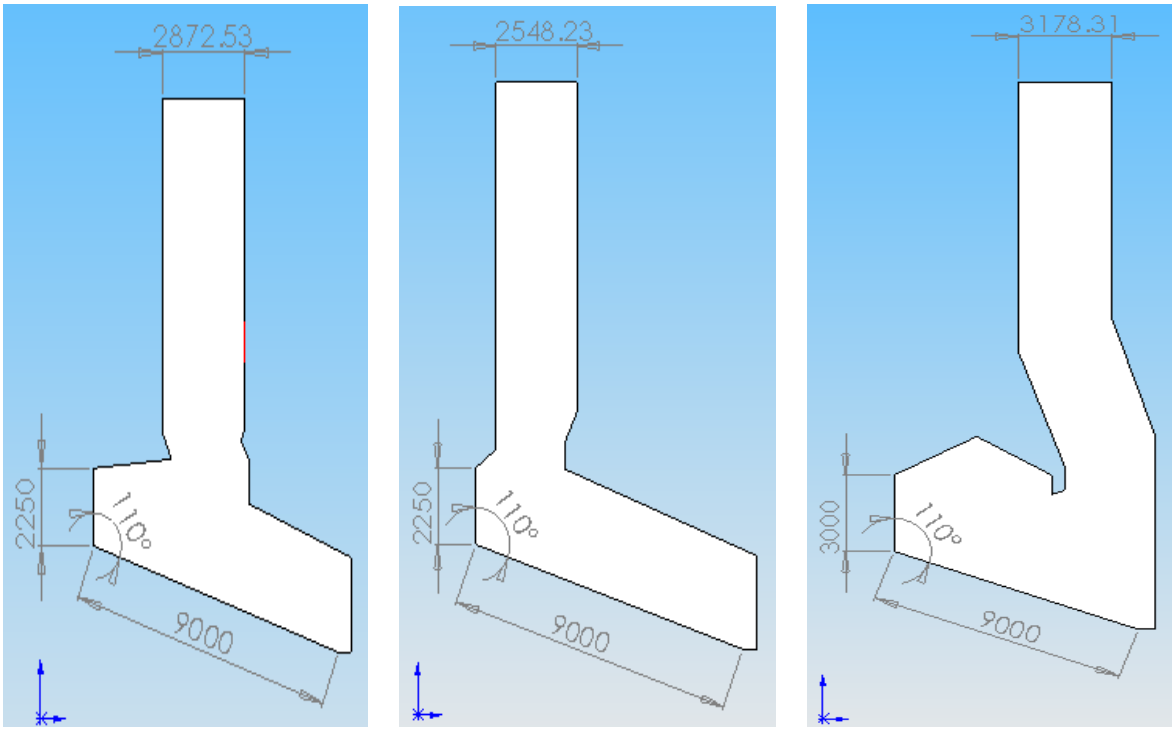

(a) Center Flow (b) Counter Flow (c) Parallel Flow

Figure 4.20: Geometries of the CFB Combustors (mm)

4.7.10 Solid Bed Combustion Simulation (FLIC)

To model coal bed combustion, FLIC, a code built by the Sheffield University Center of Waste Incineration, is employed. Figure 4.21 depicts the many stages of combustion that can be described with FLIC, and Figure 4.22 depicts the basic profile of bed combustion in a typical grate riser/combustor.

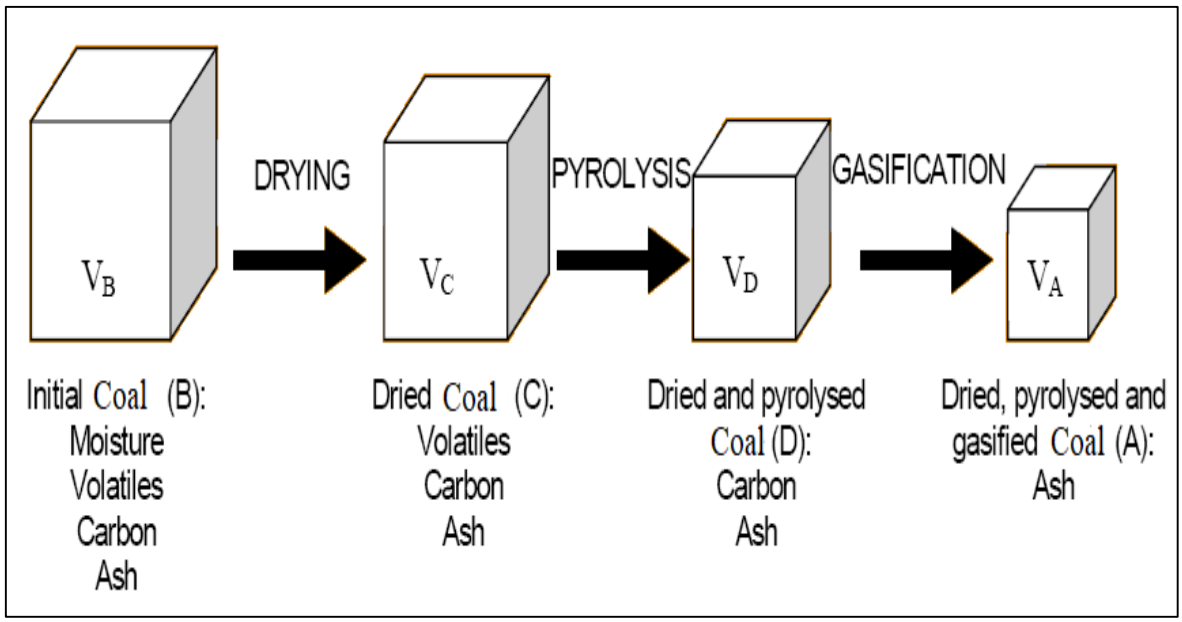

Figure 4.21: Stages change model for the coal solid volume during combustion

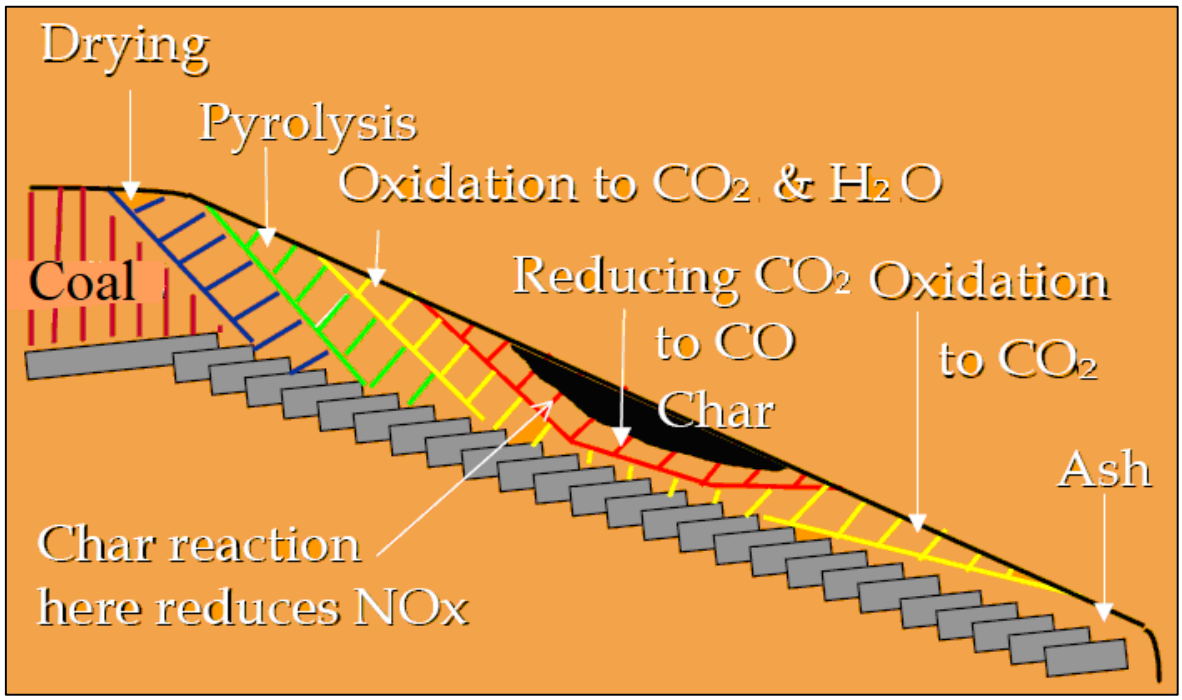

Figure 4.22: Profile of the coal solid bed combustion

Firstly, a new project is created using the latest version of FLIC Ver.2.3c. The composition of the Thar Block-II coal is inputted as follows:

Table 4.10: Composition of Thar Block-II Coal

Proximate Analysis	**Weight (%)**
Moisture	46.26
Volatile Matter	28.85
Fixed Carbon	18.47
Ash	6.42
Ultimate analysis (DAF)	**Weight (%)**
Carbon	67.29
Hydrogen	4.30
Nitrogen	0.52
Oxygen	26.01
Sulfur	1.88
Calorific Value	**kcal/Kg**
Calorific/Heating Value	3030.0

DAF= Moisture and Ash Free Basis

The iterations were calculated at an approximate time of 1 hour and 36 minutes. Once the models have been created in SolidWorks, they are exported as *.STEP files and imported into GAMBIT 2.2.3 to do the meshing. The grids are created using tri-elements with an interval count of 10. All the boundaries are also defined.

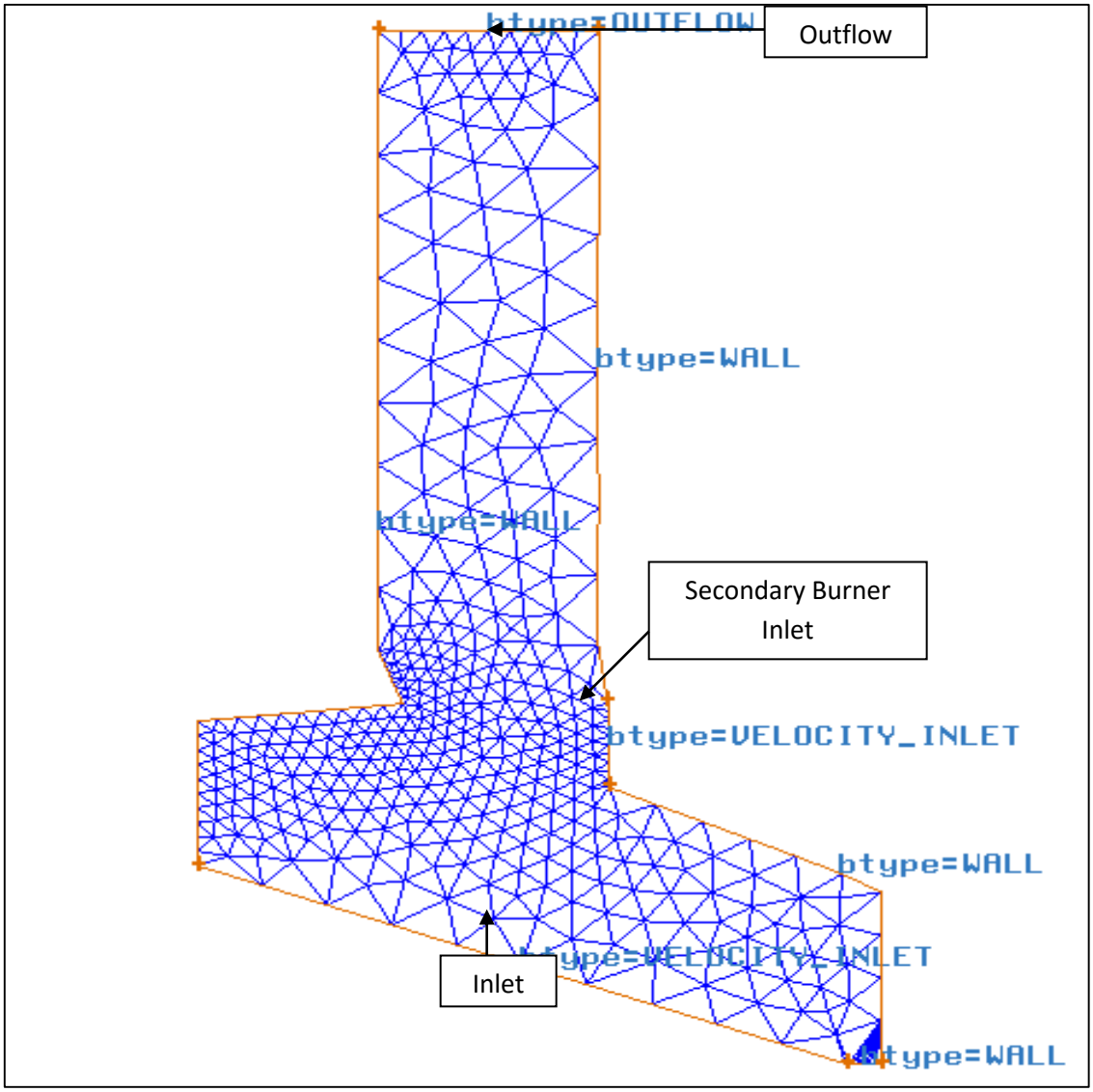

Figure 4.23: Center Geometry Coal Solid Fuel Combustor

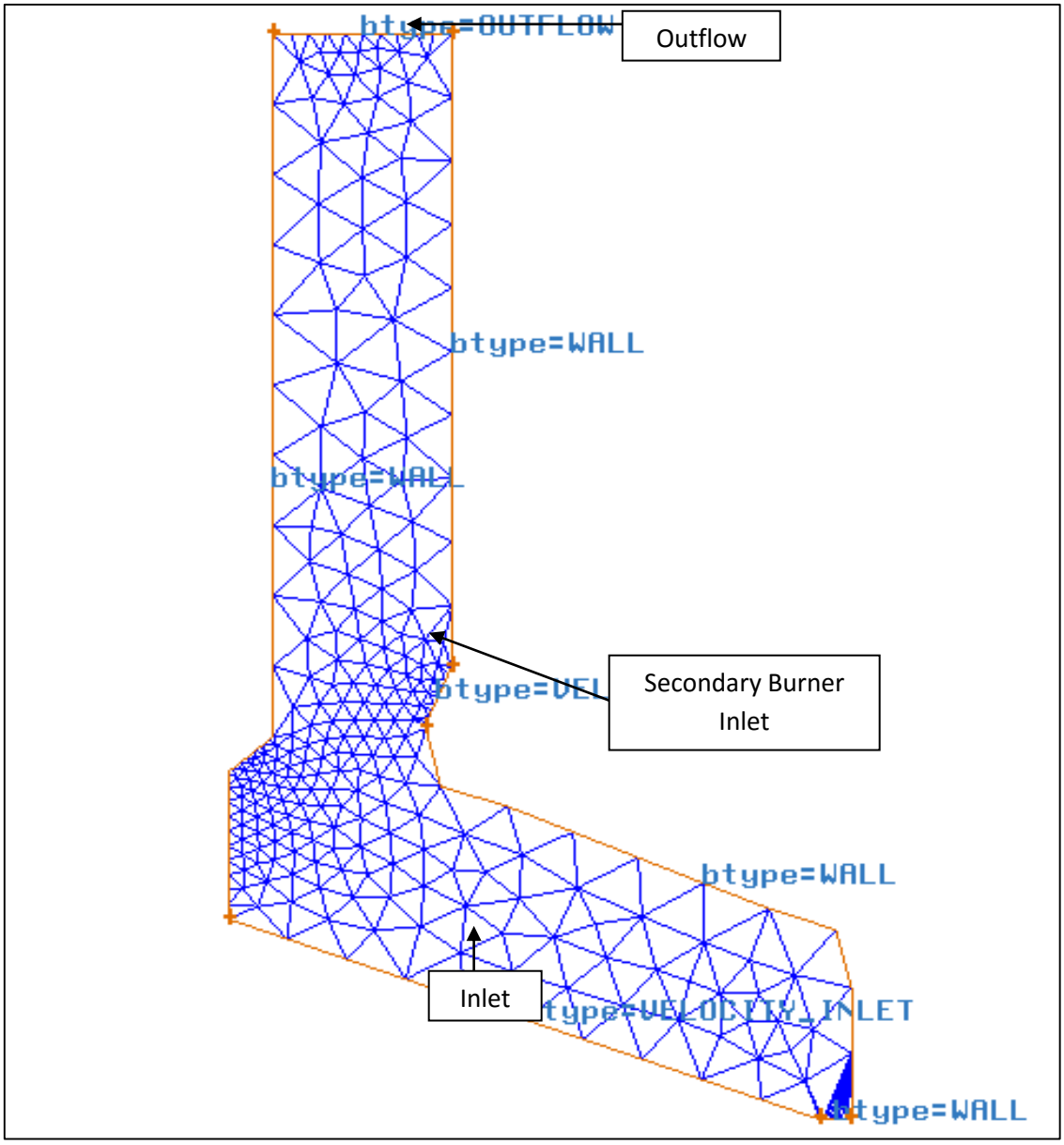

Figure 4.24: Counter Geometry Coal Solid Fuel Combustor

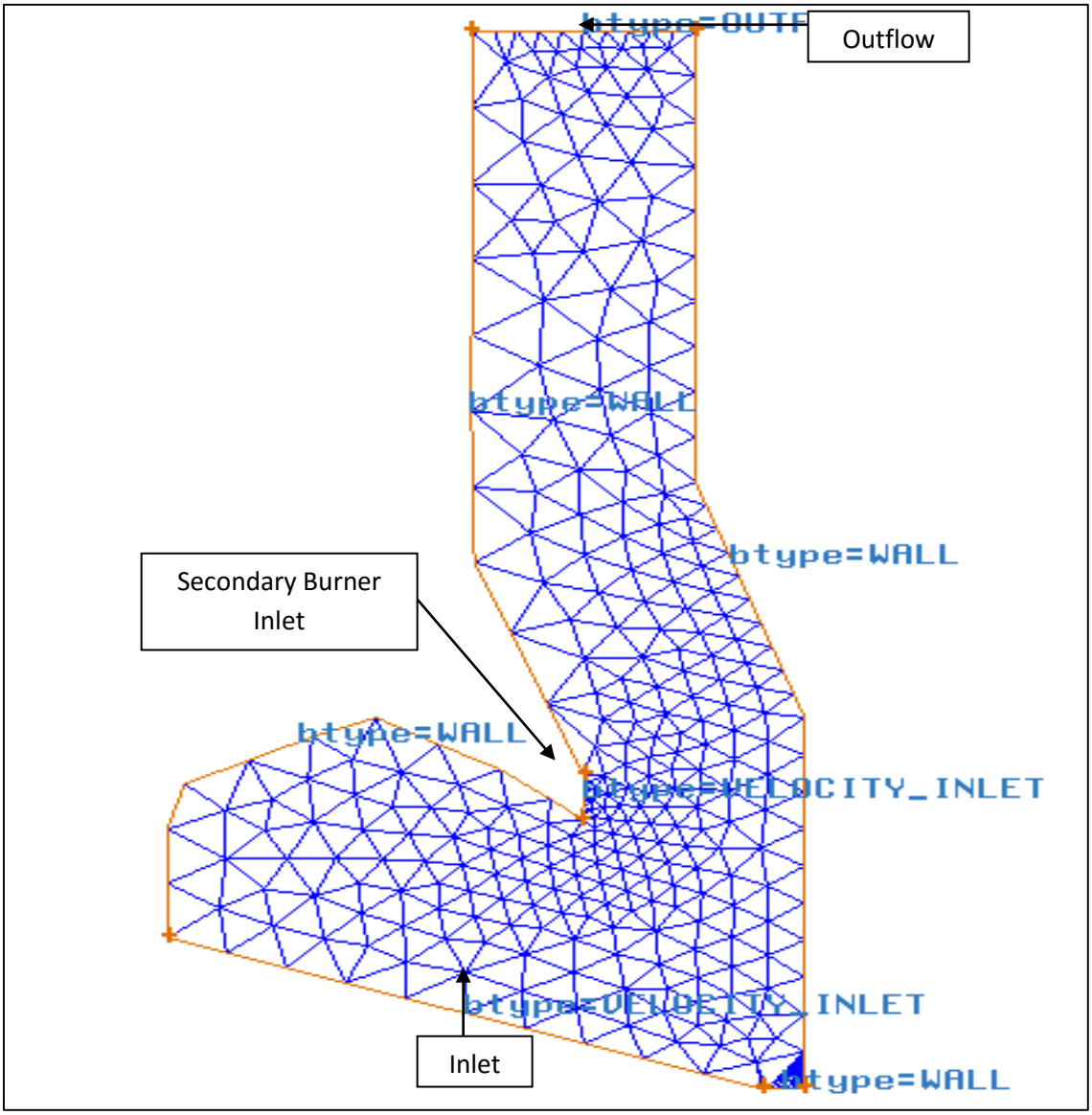

Figure 4.25: Parallel Geometry Coal Solid Fuel Combustor

4.7.11 CFD Modeling Techniques

In the CFD Code, there are four types of combustion models: widespread premixed, non-premixed, semi-premixed, and finite-rate. All have different principles and ranges of implementation. However, we only considered one type of model as the most suitable for this scheme of modeling for a riser/combustor because it was supposed to be the best option. This is for the reason that the burnings in the premixed and semi-premixed models

happen at the molecular level, similar to a flare-up, and it cannot be employed with the contaminants (i.e., soot and NOx).

4.7.12 Generalized Finite-Rate Model

This method is based on solving transportation equations for species mass sections using a well-defined chemical reaction contrivance. The reaction rates are calculated using Arrhenius rate terms from the Magnussen and Hjertager eddy dissipation model, or the EDC model. Nonetheless, mathematical modeling is required as is complete and progressive computer software that can anticipate not just the burn-out of numerous solid fuels but also the establishment of main contaminants and toxic constituents (Chernetskiy and Dekterev, 2011). Most previous studies, on the other hand, were more experiential and were unable to provide spatial specifics of combustion progressions inside the fluidized beds. The present research examines modeling on a much larger scale. The entire freeboard area and bed are distributed into numerous smaller capacities, and the transport equations for the solid and gas phases flow, heat transfer, and burning, are discretized across these cells and resolved iteratively above the entire computation environment. The computation yields result for temperature, waste constituent dispersions, gas species dispersions, and other parameters together inside the bed and in the freeboard area. Further features of the research comprise imagining the controlling consequences and investigating the transitory properties of altering solid fuel participation or further bed working circumstances (Meneses et al., 2004).

In the FLUENT modeling, three-dimensional cover equations for momentum, mass, and energy are used. The Finite Volume Method is used to discretize the differential equations, and the SIMPLE algorithm is used to solve them. As a turbulence model, the k-turbulence model was utilized, which includes two transport equations for turbulent kinetic energy and its rate of dissipation. The FLUENT code discretizes the conservation equations for mass, momentum, and energy using an unstructured, non-uniform mesh. The k-model establishes a compromise between turbulent quantity resolution and computing time by defining turbulent kinetic energy and its rate of dissipation (Wang et al., 2021).

In order to simulate the burning of solid fuel, the models utilized in ANSYS FLUENT are shown in Table 4.11.

Table 4.11: ANSYS FLUENT Models that were used in the simulation

Model	Setting
Space	2D
Time	Steady
Viscous	Standard k-epsilon turbulence model
Wall Treatment	Standard Wall Function
Heat Transfer	Enabled
Radiation Model	P1 Model
Species Transport	Generalized Finite Rate
Reaction Model	Eddy Dissipation
NOx Model	Thermal and Prompt

To represent the flow of gaseous discharges from the coal bed burning, the pattern of the surface of the bed was transferred from the FLIC program and translated into FLUENT.

4.7.13 NOx Modeling

The FLUENT NOx model is used to simulate NOx formation in combustion systems owing to thermal, rapid, and fuel combustion, as well as NOx utilization in combustion processes due to burning. FLUENT uses a transport equation for nitric oxide (NO) content to estimate NOx discharges. A particular flow state and burning response are used to calculate the NOx transport equations. To put it another way, NOx is treated after a combustion simulation. As a result, an appropriate combustion strategy is required for NOx estimation. Once the flame temperature is around 2200 K, for example, thermal NOx generation doubles with every 90 K temperature rise. To obtain the correct thermophysical components and boundary condition parameters for the combustion model, special attention must be taken. Chemistry, turbulence, radiation, and other sub-models are essential to be

utilized appropriately. To be accurate, the result may only be as precise as the statistics and object models used as input. NOx fluctuation patterns can usually be predicted quite accurately, but NOx concentrations cannot.

4.7.13.1 NOx Production and Reduction in Flames

The generation of NOx in laminar flames, as well as at the molecular level in turbulent flames, can be characterized by four chemical kinetic procedures: thermal NOx generation, rapid NOx generation, fuel NOx generation, and intermediary N_2O generation. Thermal NOx is produced when ambient nitrogen in the burning air is oxidized.

The oxidation of nitrogen in the fuel produces fuel NOx, whereas elevated reactions close to the flame tip produce quick NOx. NOx can also be produced from molecular nitrogen (N_2) by N_2O under high pressures and oxygen-rich environments. The burning decreases the whole NOx generation by accounting for the response of NO to hydrocarbons and ammonia, correspondingly.

4.7.13.2 Fuel NOx from Coal

4.7.13.2.1 Nitrogen in Char and in Volatiles

To study the coal's nitrogen content, Pohl and Sarofim (1977) used dispersed, crushed lignite coal particles that were heated quickly to temperatures between 1000 and 2100 K. With the notable exception that little nitrogen was released until 10 to 15 percent of the coal had been devolatilized, nitrogen evolution was similar to the pattern of the total volatiles. The nitrogen pyrolysis data had a pseudo-first-order rough fit, and the rate constant was $9.3\ 10^3$ exp (22,700/RT) sec^{-1}. When HCN is employed as the transitional species, two different fuel processes for coal are combined, similar to how NO_X is created from coal via HCN. Fuel nitrogen is assumed to be dispersed among the volatiles and char.

4.7.13.2.2 Coal Fuel NOx Arrangement A

The first HCN process converts all of the nitrogen to HCN, which is then partially transformed to NO.

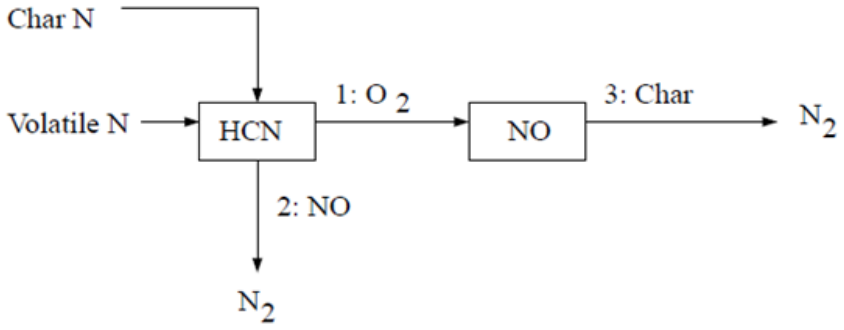

(4.1)

The first technique transforms all char-bound nitrogen to HCN. Thus,

$$S_{char,HCN} = \frac{S_c Y_{N,char} M_{w,HCN}}{M_{w,N} V} \tag{4.2}$$

$$S_{char,NO} = 0$$

where

S_c = char burnout rate (kg/s)

$Y_{N,char}$ = mass fraction of nitrogen in char

V = cell volume (m^3)

4.7.13.2.3 Coal Fuel NOx Arrangement B

The following HCN process assumes that all char N is transformed to NO immediately.

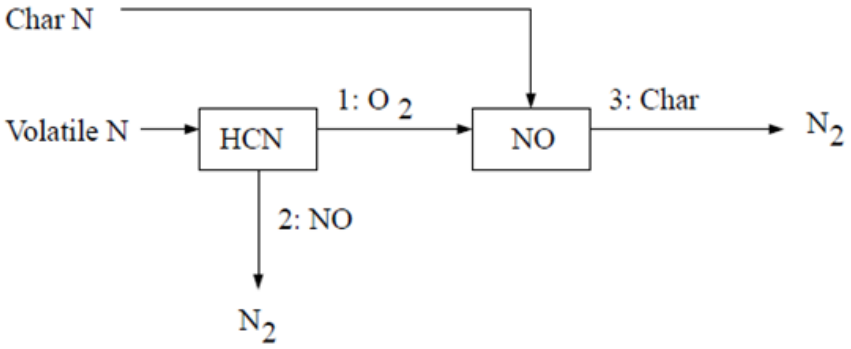

(4.3)

As a decomposition result from oxidation char nitrogen atoms, char nitrogen is released straight to the gas section as NO. If the above technique is followed,

$$S_{char,HCN} = 0$$

$$S_{char,NO} = \frac{S_c Y_{N,char} M_{w,NO}}{M_{w,N} V} \quad (4.4)$$

4.7.13.2.4 Reduced NOx on Char Surface

The following is a prediction of the heterogeneous effect of NO decrease on the char surface:

$$\mathcal{R}_3 = A_3 e^{-E_3/R\overline{T}}\overline{p}_{NO} \tag{4.5}$$

where

$\mathcal{R}_3$ = rate of NO reduction $(\mathrm{mol}/\mathrm{m}^2_{\mathrm{BET}} - \mathrm{s})$

$\overline{p}_{NO}$ = mean NO partial pressure (atm)

E_3 = 142737.485 J/mol

A_3 = 230 $\mathrm{mol}/\mathrm{m}^2_{\mathrm{BET}} - \mathrm{s} - \mathrm{atm}$

$\overline{T}$ = mean temperature (K)

The partial pressure $\overline{p}_{NO}$ is calculated using Dalton's law:

$$\overline{p}_{NO} = \overline{p}X_{NO} \tag{4.6}$$

The rate of NO consumption due to reaction 3 will then be

$$S_{NO-3} = c_s A_{BET} M_{w,NO} \mathcal{R}_3 \tag{4.7}$$

where

A_{BET} = BET surface area $(\mathrm{m}^2/\mathrm{kg})$

c_s = concentration of particles $(\mathrm{kg}/\mathrm{m}^3)$

S_{NO-3} = NO consumption $(\mathrm{kg}/\mathrm{m}^3 - \mathrm{s})$

4.7.13.2.5 Coal Fuel NOx Arrangement C

The first NH_3 trend indicates that all of the nitrogen is transformed to NH_3, which could then be partly turned to NO.

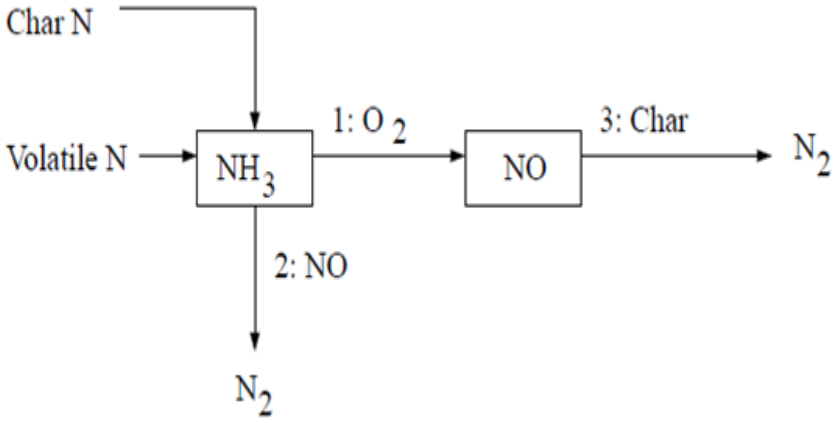

(4.8)

All char-bound nitrogen is converted to NH_3 in this configuration. Hence,

$$S_{char,NH_3} = \frac{S_c Y_{N,char} M_{w,NH_3}}{M_{w,N} V} \tag{4.9}$$

$$S_{char,NO} = 0$$

where

S_c = char burnout rate (kg/s)

$Y_{N,char}$ = mass fraction of nitrogen in char

V = cell volume (m^3)

4.7.13.2.6 Coal Fuel NOx Scheme D

In the second NH_3 process, every char N is instantly converted to NO.

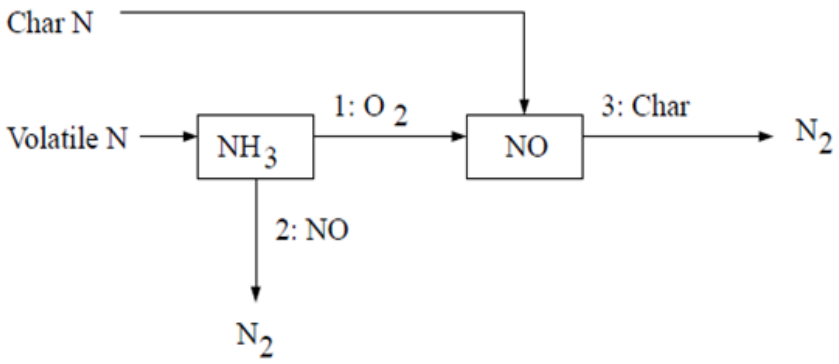

(4.10)

As a decomposition outcome from oxidation char nitrogen atoms, char nitrogen is directly discharged to the gas stage as NO. If this plan is implemented,

$$S_{char,NH_3} = 0$$

$$S_{char,NO} = \frac{S_c Y_{N,char} M_{w,NO}}{M_{w,N} V} \quad (4.11)$$

4.7.14 SOx Modeling

For fuels with a greater sulfur ratio, the SO_X concentration field would be computed using either of the ANSYS FLUENT response models in conjunction with the main burning control. The post-processing function, which solves transport equations for H_2S, SO_2, SO, SH, and SO_3, can be employed when the sulfur content of the fuel is minimal. The following steps are included in the SO_X model:

Step-I: The release of sulfur from the fuel

In the case of coal, the procedure is more complicated; currently, some sulfur is dissolved into the gas segment by devolatilization as H_2S, COS, SO_2, and CS_2, although a portion of the sulfur is reserved in the char to be oxidized later. The amount of sulfur reserved in char is determined by the coal type.

Step-II: In the gaseous state, the sulfur reaction

SO, SO_2, and SO_3 are the most common sulfur forms in oxygen-rich combustion. H_2S, S_2, and SH exist in substantial proportions at lower oxygen levels, but SO_3 develops insignificantly.

Step-III: Retention of sulfur in sorbents

Sulfur pollutants might be absorbed by sorbent material, which could be introduced anywhere in the system, including in the post-flame portion. SO_2 may be generated straight at a similar % as char burnout for the char S. H_2S, SO_2, SO, SH, and SO_3 transport equations are coupled, and a suitable reaction is established.

ANSYS FLUENT is used to solve the mass transport equations for the species, which take into consideration diffusion, convection, production, and utilization of the associated species. This approach is entirely generic due to the fundamental idea of mass conservation. The convection relations in the governing equations inscribed in the Eulerian orientation frame incorporate the outcome of residence time in mechanisms, a Lagrangian orientation setting idea. Only the species transfer equation is needed if all fuel sulfur is supposed to shift and all other products and transitional species are supposed to be unimportant.

SO_X formation mechanisms, as stated in Reaction Mechanisms for Sulfur Oxidation, include a variety of interactions involving numerous species, with trailing sulfur-containing intermediate species being particularly important. In addition to the SO_2 model, ANSYS FLUENT solves transport equations for H_2S, SO_3, SO, and SH species to forecast the mean.

4.7.14.1 SOx Production and Reduction in Flames

Sulfur is found in coal in the forms of organic sulfur, sulfates, and pyretic, with a mass % ranging from 0.5 to 3 percent. The oxidation of fuel-bound sulfur produces complete discharges.

Fuel sulfur is converted to SO_2 and SO_3 during the burning process. At high temperatures (>1273 K), sulfur compounds react with oxygen to create SO_2. In the ash, however, a part of the sulfur remains unburned. In addition, SO_2 can be oxidized further to generate SO_3. A portion of the vapor will condense on the particles, discharging water and forming sulfuric acid, or it will react more vigorously, producing sulfates. While releases are the major cause of acid rain, they also cause particle discharges and the erosion of burn apparatus.

Sulfur pollutants can be stopped during the burning process or afterward using techniques like wet or dry scrubbing. Coal-fired boilers are by far the most common source of output, accounting for more than half of all discharges.

4.7.14.2 SOx Transport Governing Equations

Only the species transfer equation is necessary if all fuel sulfur is expected to convert directly to SO_2, and other products and transition species are assumed to be minimal.

$$\frac{\partial}{\partial t}\left(\rho Y_{SO_2}\right) + \nabla \cdot \left(\rho \vec{v}\, Y_{SO_2}\right) = \nabla \cdot \left(\rho \boldsymbol{\mathcal{D}} \nabla Y_{SO_2}\right) + S_{SO_2} \tag{4.12}$$

ANSYS FLUENT solves transport equations for H_2S, SO_3, SO, and SH species:

$$\frac{\partial}{\partial t}\left(\rho Y_{H_2S}\right) + \nabla \cdot \left(\rho \vec{v}\, Y_{H_2S}\right) = \nabla \cdot \left(\rho \boldsymbol{\mathcal{D}} Y_{H_2S}\right) + S_{H_2S} \tag{4.13}$$

$$\frac{\partial}{\partial t}\left(\rho Y_{SO_3}\right) + \nabla \cdot \left(\rho \vec{v}\, Y_{SO_3}\right) = \nabla \cdot \left(\rho \boldsymbol{\mathcal{D}} Y_{SO_3}\right) + S_{SO_3} \tag{4.14}$$

$$\frac{\partial}{\partial t}\left(\rho Y_{SO}\right) + \nabla \cdot \left(\rho \vec{v}\, Y_{SO}\right) = \nabla \cdot \left(\rho \boldsymbol{\mathcal{D}} Y_{SO}\right) + S_{SO} \tag{4.15}$$

$$\frac{\partial}{\partial t}\left(\rho Y_{SH}\right) + \nabla \cdot \left(\rho \vec{v}\, Y_{SH}\right) = \nabla \cdot \left(\rho \boldsymbol{\mathcal{D}} Y_{SH}\right) + S_{SH} \tag{4.16}$$

Where Y_{SO_2}, Y_{H_2S}, Y_{SO_3}, Y_{SO} and Y_{SH} are mass fractions of SO_2, H_2S, SO_3, SO and SH in the gas phase.

4.7.14.3 Coal-Based SO_2 Production

Sulfur is supposed to be distributed among the volatiles and char in coal. Meanwhile, instead of supposing that S is evenly distributed across the volatiles and char, the fraction of S in the volatiles and char would be given individually.

SO_2 from Char The rate of char burning is related to the source of SO_2 from the char:

$$S_{char,i} = \frac{S_c Y_{S,char} M_{w,i}}{M_{w,S} V} \tag{4.17}$$

where

S_c = char burnout rate (kg/s)

$S_{char,i}$ = source of i $(kg/m^3 - s)$ in char, where $i = SO_2$ or H_2S

$Y_{S,char}$ = mass fraction of sulfur in char

V = cell volume (m^3)

4.7.14.4 SO_2 Produced by Volatiles

The rate of volatile emission is related to the source of SO_2 from volatiles:

$$S_{vol,i} = \frac{S_{vol} Y_{S,vol} M_{w,i}}{M_{w,S} V} \tag{4.18}$$

where

$S_{vol,i}$ = source of volatiles originating from the coal particles into the gas phase (kg/s), where $i = SO_2$ or H_2S

$Y_{S,vol}$ = mass fraction of sulfur in the volatiles

V = cell volume (m^3)

4.7.15 Model Discussion

Riser departures may negatively impact a CFB's overall performance. If additional solids congregate near the riser departure, the return line will have fewer solids. The solids volume fraction in the riser and connection may be decreased because of the reduced solids rotation. The solids volume fraction might be higher if the solids accretion nearby the riser exits outspreads into these mechanisms. Systems that might evaluate for an uneven stream in the departure area include inner/outer gesture, first-order secondary flows, cavity development, and tangential acceleration/deceleration near riser departures. The solids volume % is added or kept persistent at the bottom half of the riser, as indicated by a blind T riser departure and a right-angle exit with interior perplexes. As revealed in Figure 4.26, the blind T exit showed a substantial gain in solid volume percent with elevation in the upper half, but the right angle exits with the inside baffle showed a drop. The riser departure strategy has a big impact on the magnitude and form of the upstream exit area.

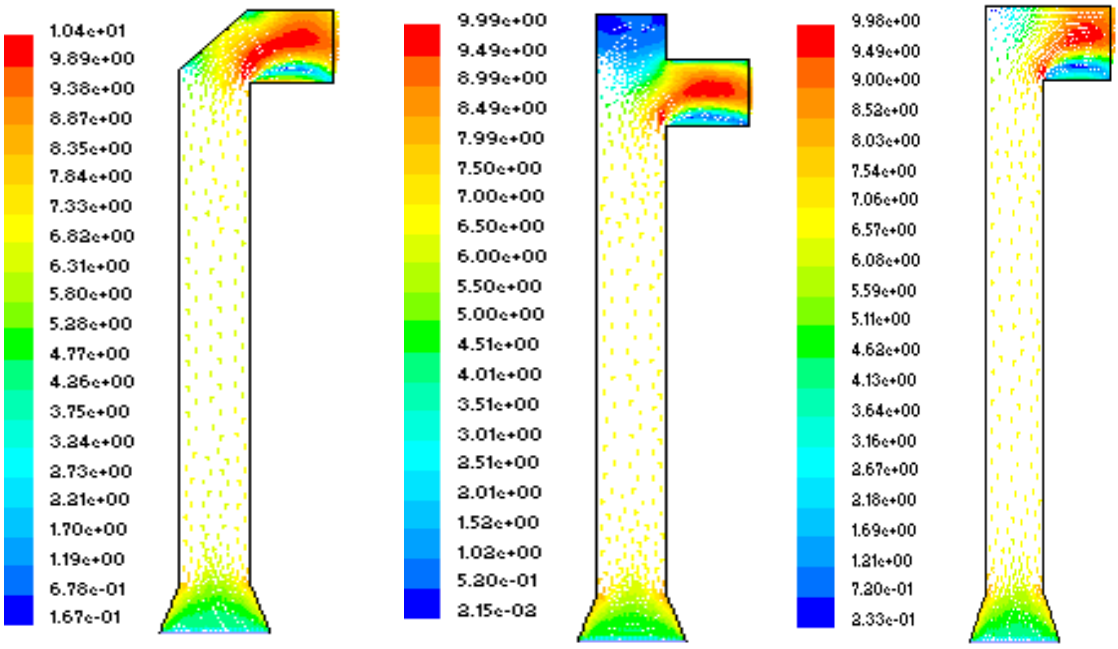

Figure 4.26: Velocity contours in exit geometries

The extended-radius curve exit gathered more solids than the right-angle departure. The blind T exit accumulated more materials and generated a higher solid volume fraction in the riser than the right-angle exit. For the departure with a perplex, the solids grip-up is bigger. The blind T exit shows a rise in solids volume fraction with height in the upper half of the riser and greater solids volume fractions along the whole riser elevation. The solids volume fraction remains constant at the departure with inner perplex, but for the right angle and blind T departures, it rises with height in the upper half of the riser, as revealed in Figure 4.27.

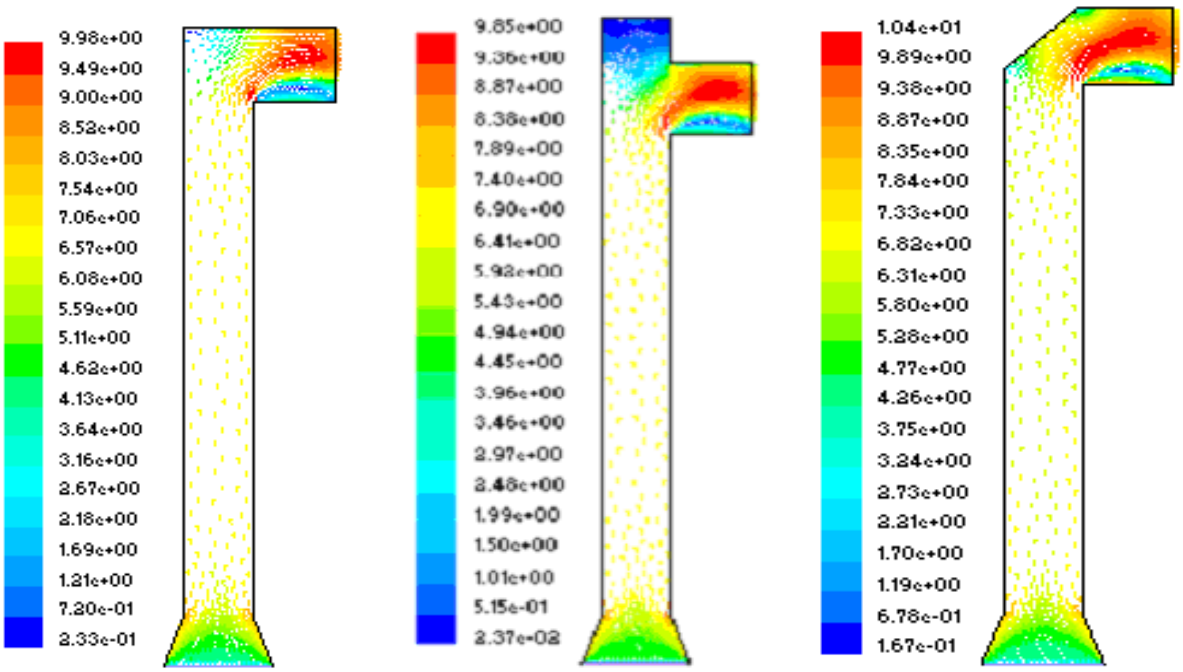

Figure 4.27: Contours of velocity by volume fraction of sand

The disconnecting outlets and the departure with interior perplex raise the condensed solids volume segment's top departure area. There is little or no upstream departure area with this curve departure. As demonstrated in Figure 4.26, the blind T departure, right-angle exit, and departures with an inlet or outlet perplex all cause an upstream departure area with an enlarged solids volume fraction. Greater blind T allowance elevations might raise a larger upstream departure area, as long as they

persist underneath a serious postponement elevation. Middle-size inside or outside perplexes might yield larger upstream departure areas than large or minor perplexes.

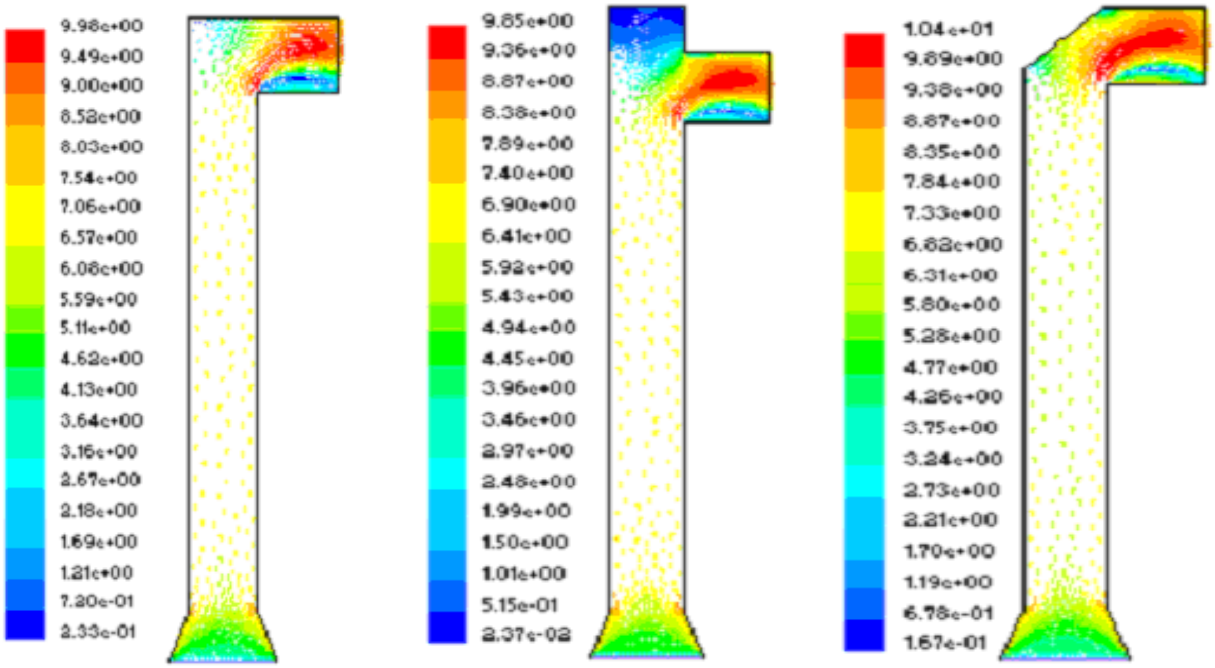

Figure 4.28: Velocity contours by volume fraction of air

As shown in the motion of a particle in an exit bend figure, a particle in the center of a bend departure practices a radial acceleration ($\bar{u}_{st}^2 / R$) corresponding to the radial module of the acceleration due to gravity (g cos 45° or g /$\sqrt{2}$), i.e. $\bar{u}_{st}^2 / R = g / \sqrt{2}$. This form proposes that radial slip is lessened by about $Fr_R = 1/\sqrt{2}$. Greater values Fr_R might yield further motion of solids to the exterior of the riser departure and condensed Froude numbers to the internal side of the riser departure.

The internal/external motion of solids in a riser depart is reduced to a Froude number $Fr_R = 1/\sqrt{2}$ according to a radial acceleration equilibrium. Greater FrR values result in more motion to the outside of the riser exit, whereas lower values result in more motion to the inside. The average departing velocity in the right-angle departure

bend is around 10 m/s, as shown in Figure 4.28, resulting in FrR well over the $1/\sqrt{2}$ value. As a result, the elements' primary motion is independent of the riser's departure. A similar pattern can be seen with other exits. The right angle exits with the baffle, on the other hand, producing more perceptible motion outside the riser exit. Blind T appears to have a slight extension height result when it comes to right-angle departure. The slip is particularly relevant at the departure bends, according to Figure 4.29. Right-angle departure changes the slip circulation, and perplex displays have a larger slip than blind T exits.

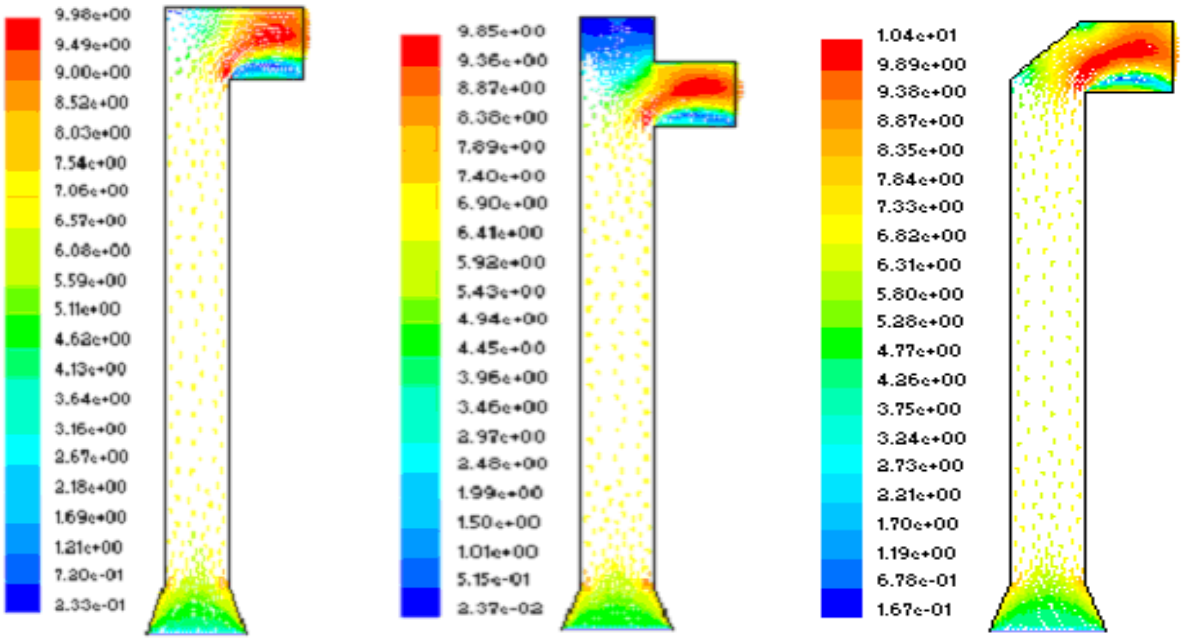

Figure 4.29: Slip velocity contours

After that, it was operated to a bed combustion time of approximately 1 hour and 40 minutes. The following outcomes were achieved.

According to Bai et al. (2017), coal with different particle sizes, shapes, and motion exhibits distinctly different combustion behaviors in the riser. For the large coal particle (150–212 μm), the combustion of volatiles and char takes place sequentially, with clear fragmentation at the early stage of the char combustion. For the small coal particle (106–

150 μm), the combustion of volatiles and char occurs simultaneously with no clear fragmentation. The size of the two burning particles shows a decreasing trend, with periodic variation attributed to the rapid rotations of the particles.

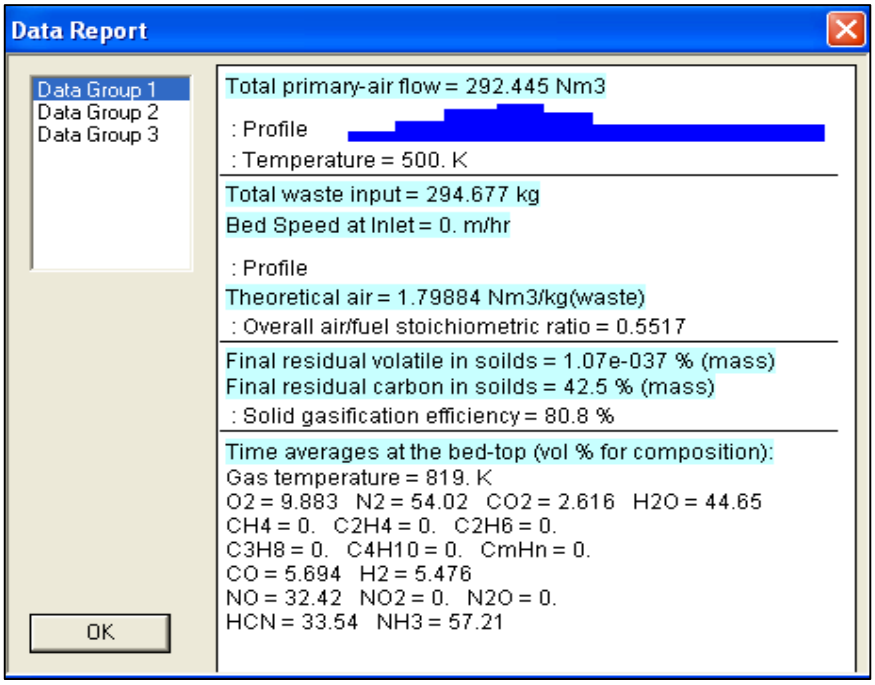

Figure 4.30: Data Group 1

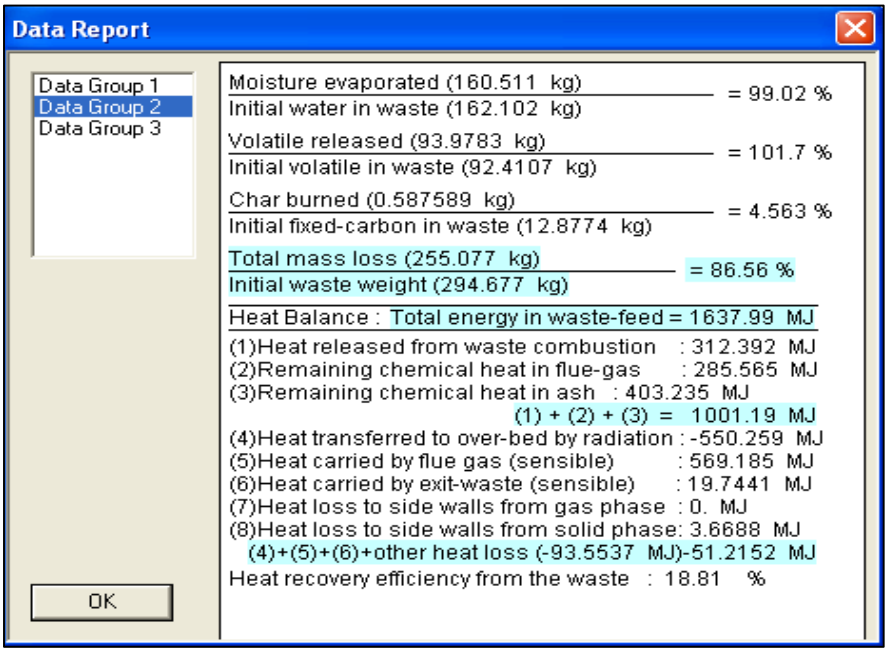

Figure 4.31: Data Group 2

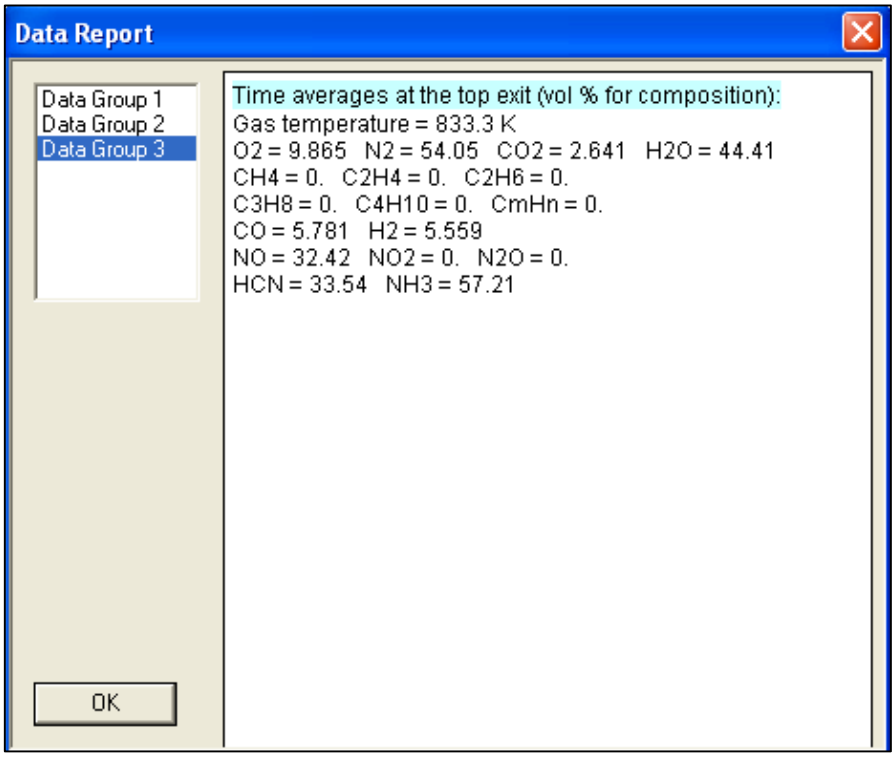

Figure 4.32: Data Group 3

From Data Group 1, we can see the configuration of the gaseous discharge at the bed top. In Data Group 2, we can see the amount of moisture evaporated, volatiles released, and char ignited. In the bed, we can see the entire mass loss along with the heat energy balance. In Data Group 3, the results of the composition at the bed top exit are shown. Take note that these are just averaged values across the bed. Next, we move on to the profiles of the fluidized bed.

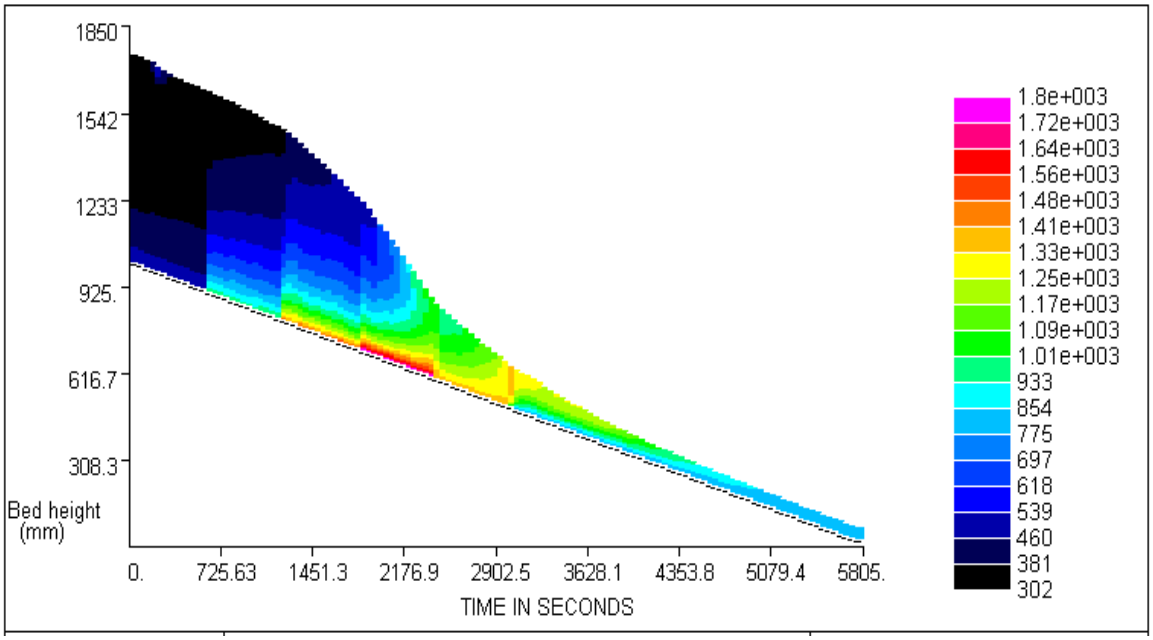

Figure 4.33: Gas Temperature (K) along the bed

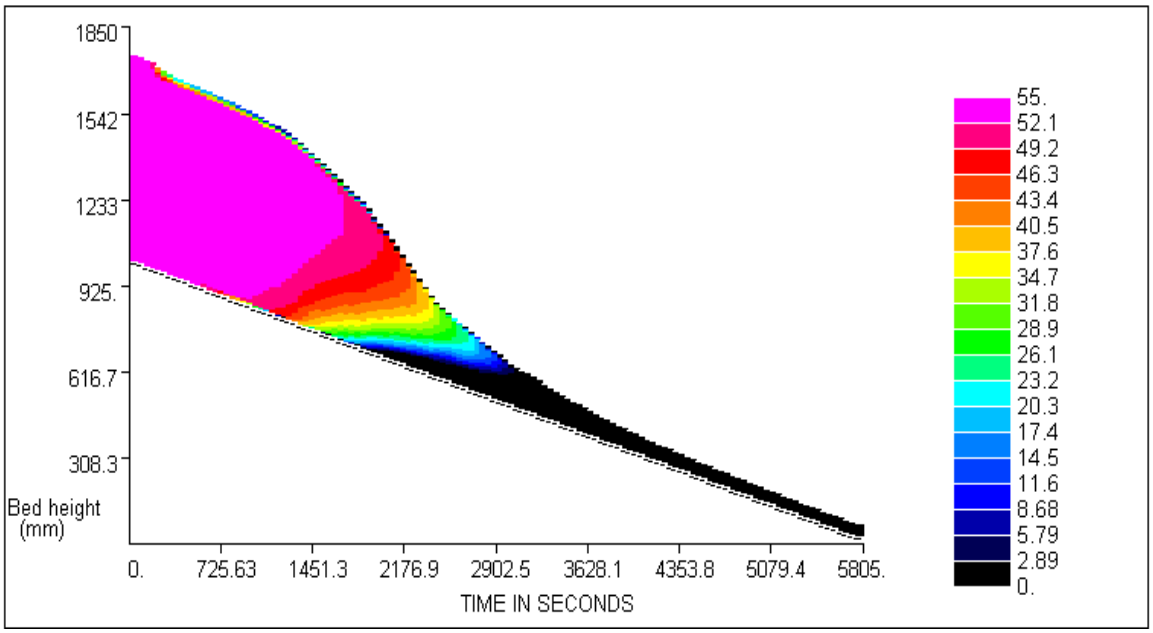

Figure 4.34: Water left in solid after bed combustion

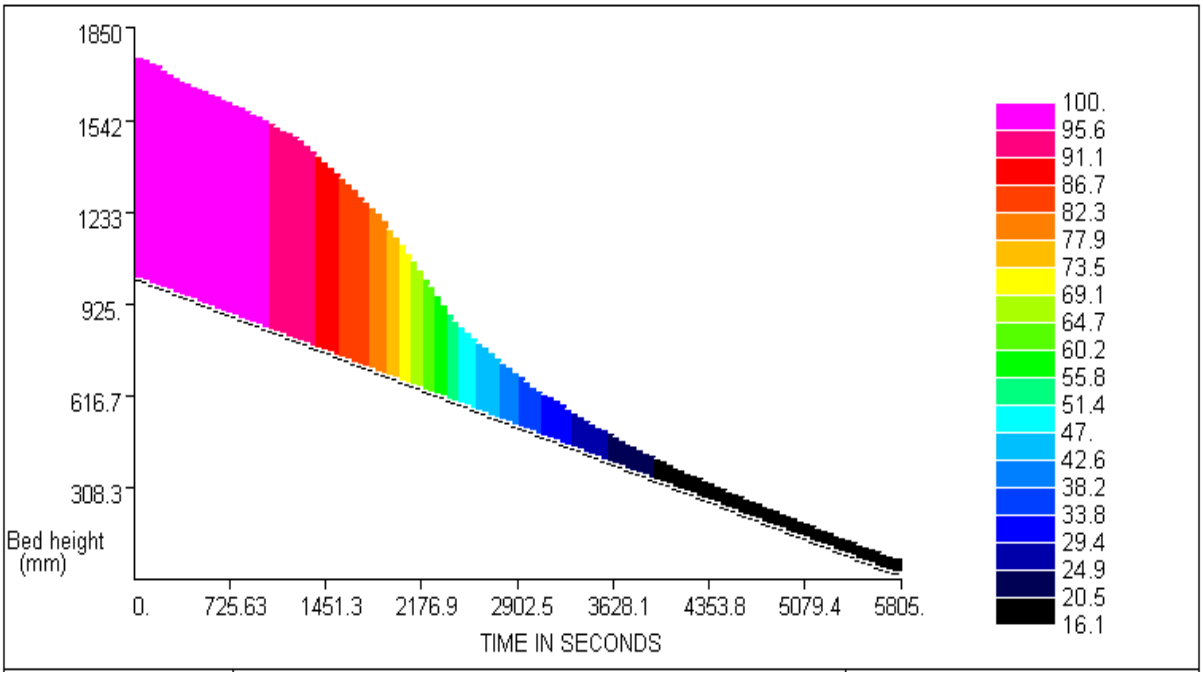

Figure 4.35: Mass left on bed after combustion

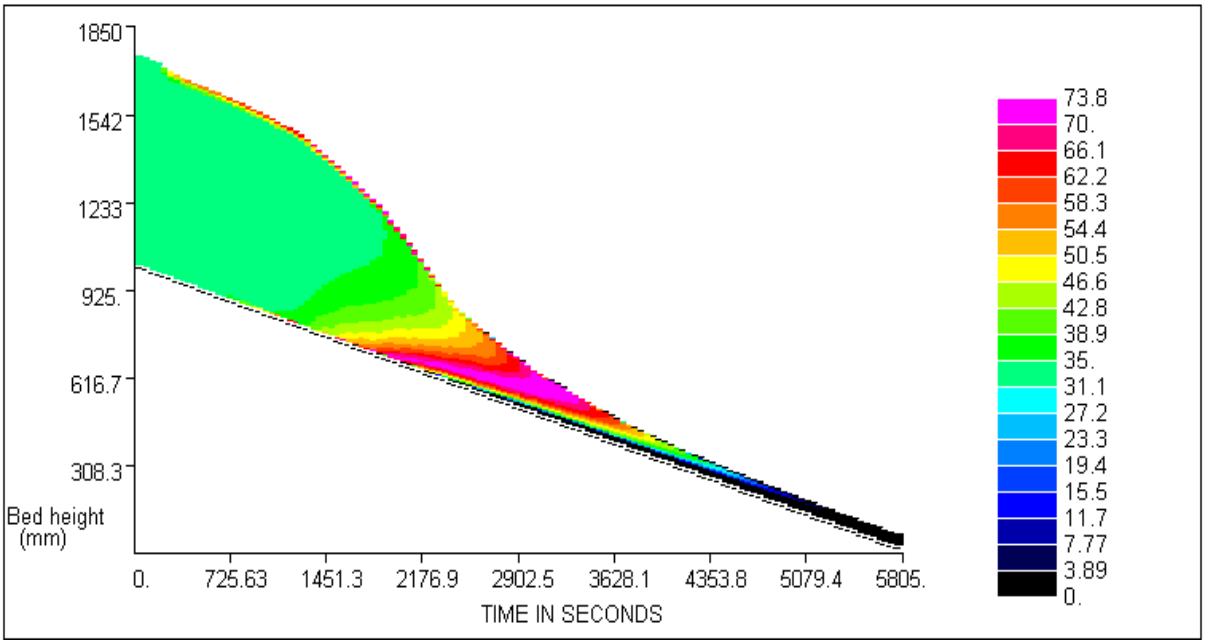

Figure 4.36: Volatiles left in solid after gasification

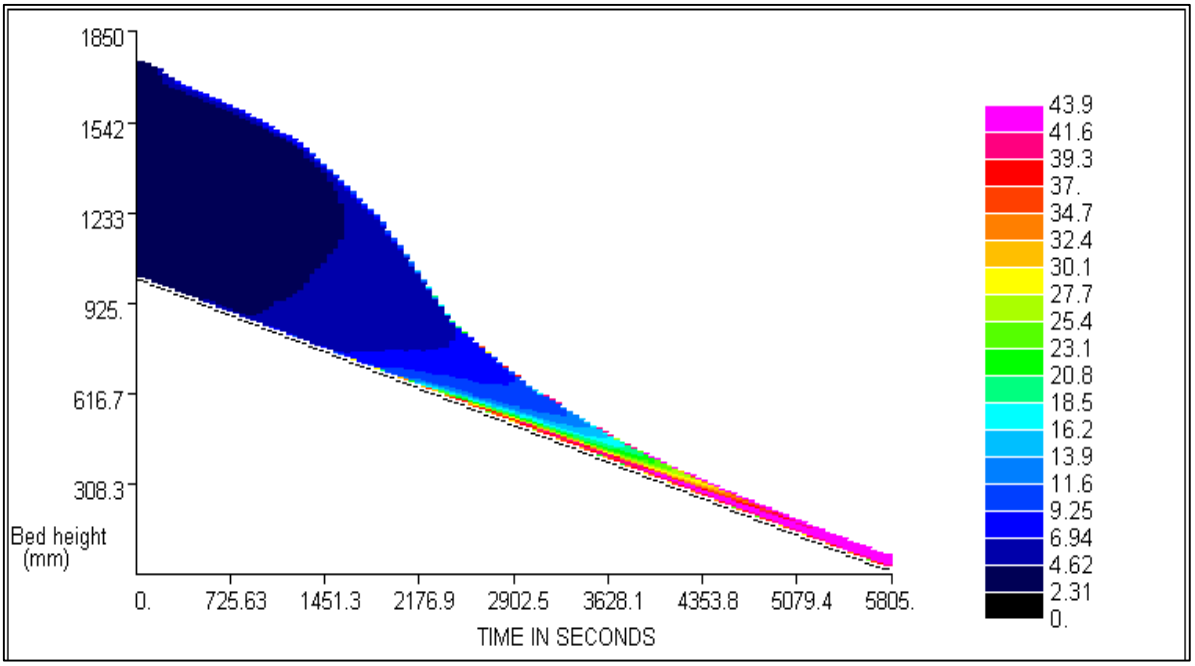

Figure 4.37: Amount of pure carbon content along bed length

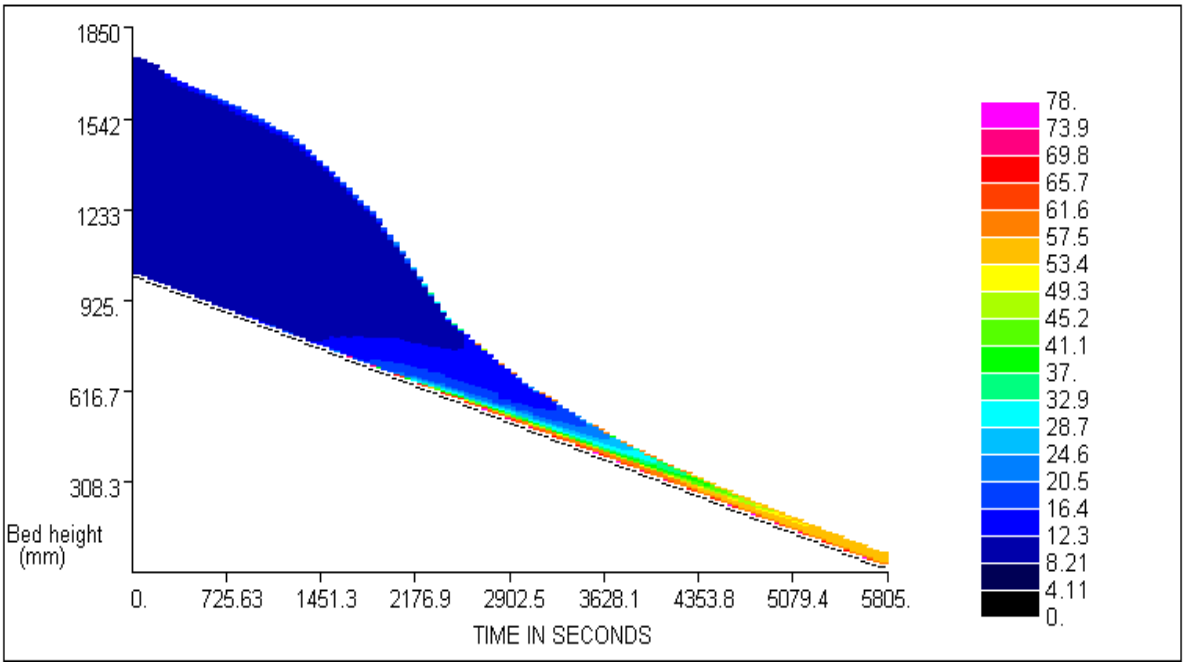

Figure 4.38: % of ash after combustion

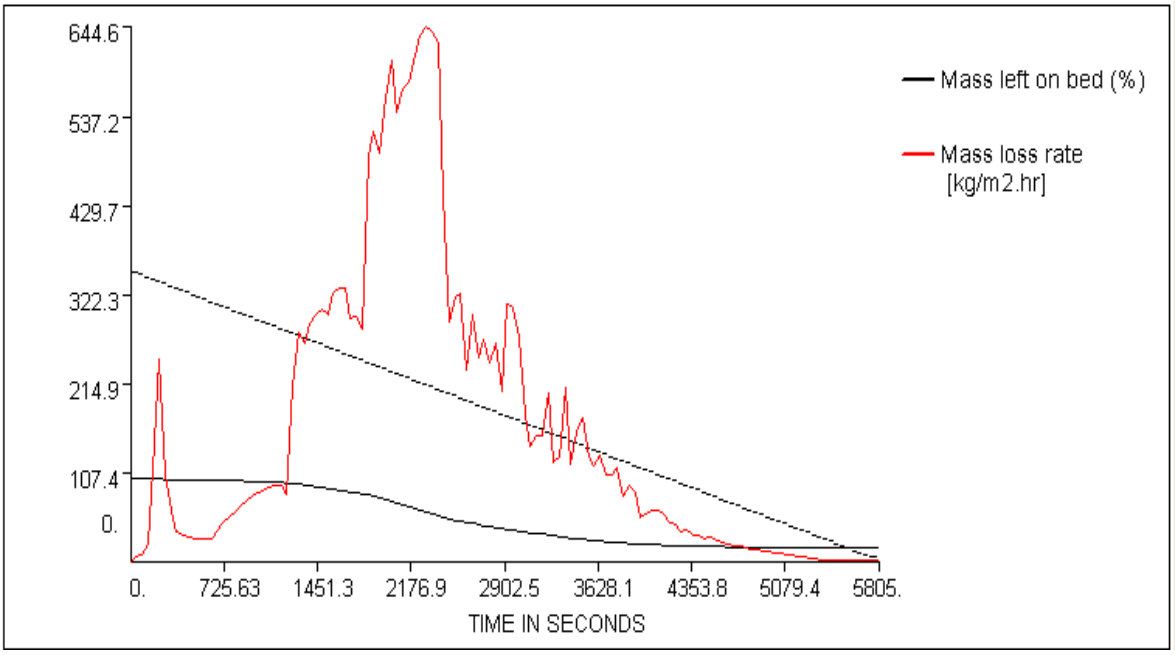

Figure 4.39: Plot of mass left on bed and mass loss rate along bed length

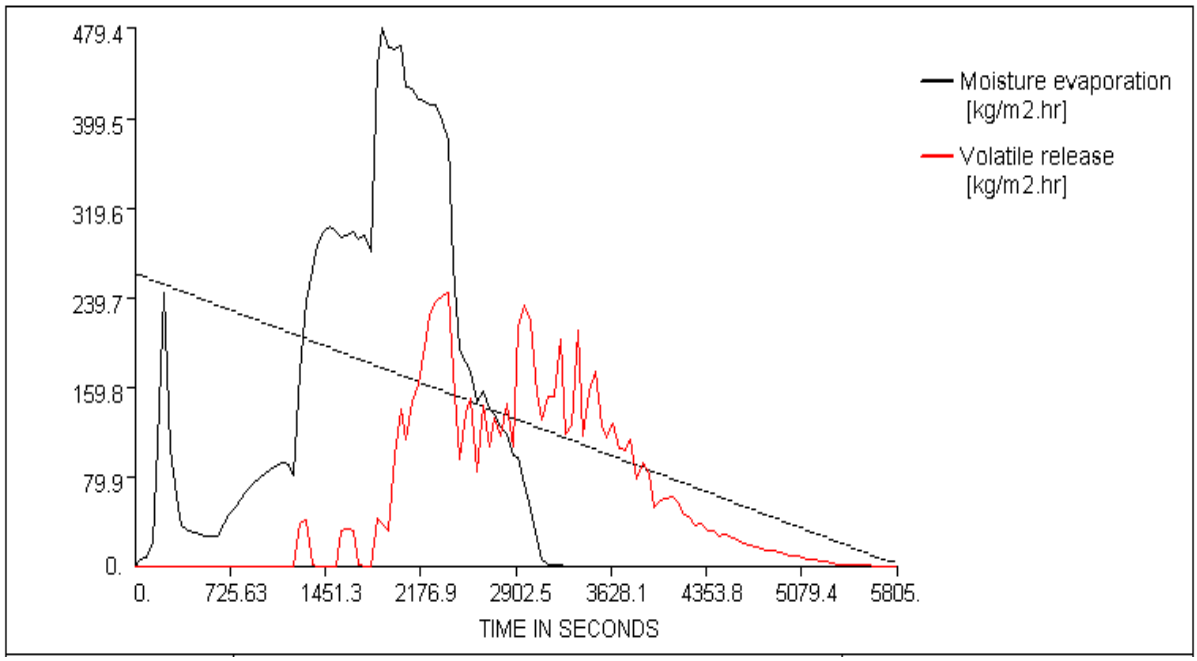

Figure 4.40: Plot of moisture evaporation and volatile release

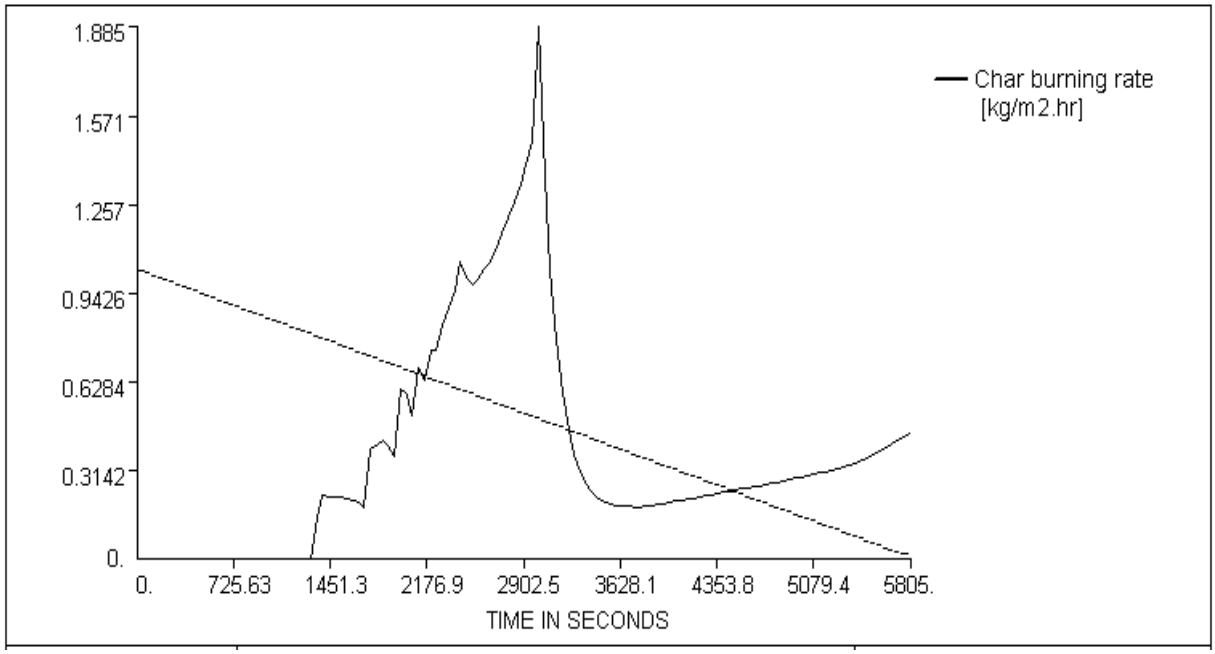

Figure 4.41: Plot of Char burning rate

The characteristics of gaseous emittance and bed temperature are transferred into the FLUENT application to begin gas flow modeling. From the results shown, it is clearly shown all the processes included in combustion, i.e., drying, devolatilization, char burning, and ash formation. Each simulation takes about 4000 to 8000 iterations to converge.

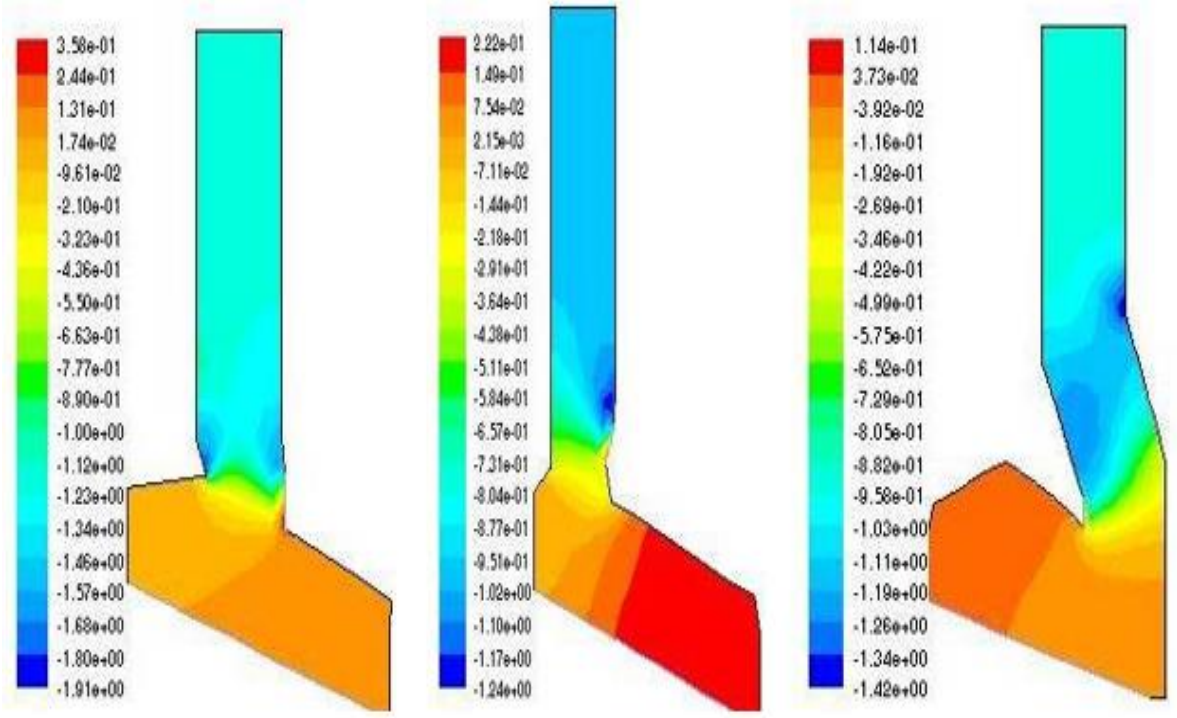

(a) (b) (c)

Figure 4.42: Contours of Static Pressure (a) Center (b) Counter (c) Parallel

Here, we obtain a maximum static pressure of 0.36 pascal to 0.11 pascal and a minimum of -1.9 pascal to -1.24 pascal from the static pressure contours in all three geometries. These statistics are small in comparison to atmospheric pressure; hence, we can determine that the term strategy pressure in the compartment won't cause any trouble.

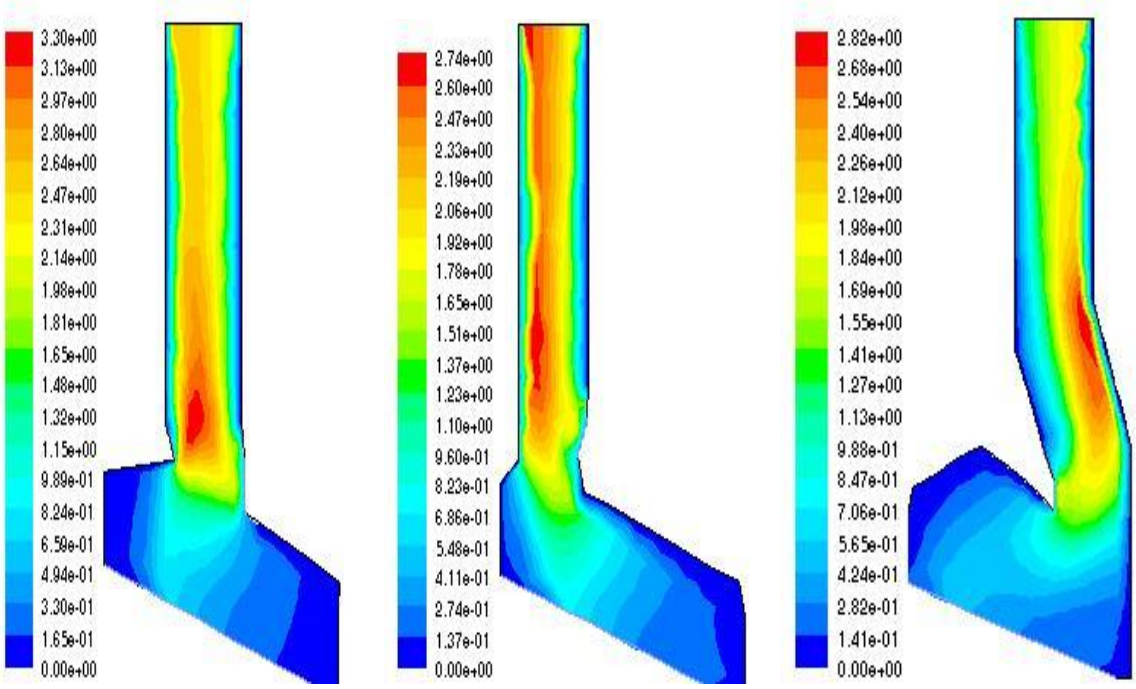

(a) (b) (c)

Figure 4.43: Contours of Velocity (a) Center (b) Counter (c) Parallel

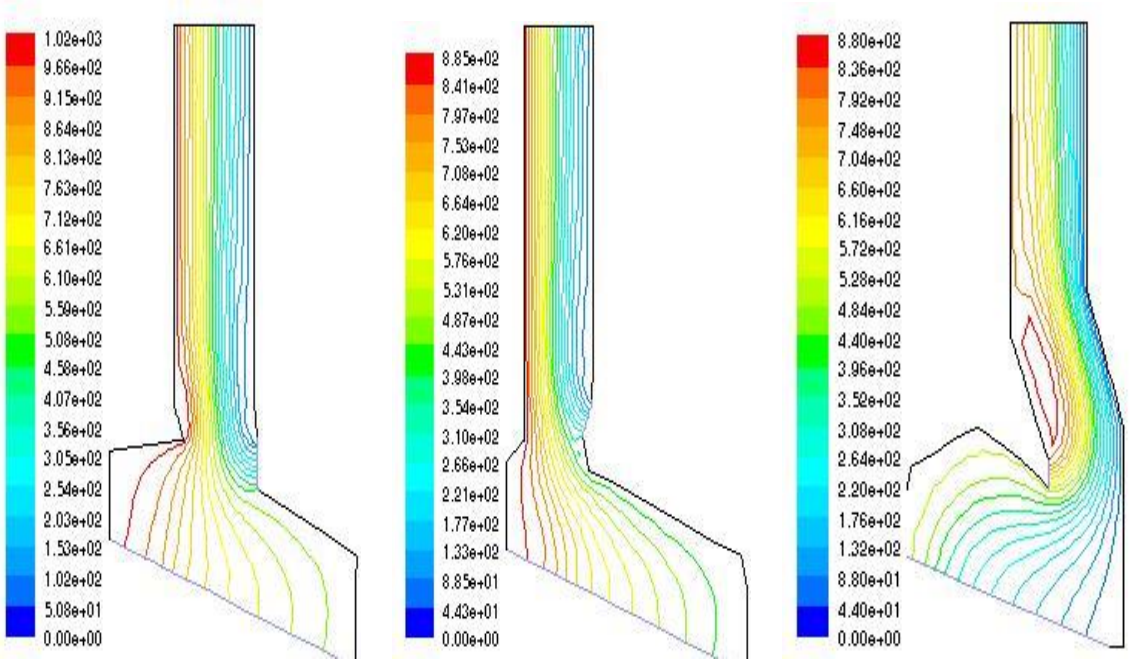

(a) (b) (c)

Figure 4.44: Contours of Velocity Stream (a) Center (b) Counter (c) Parallel

The peak value at the center-oriented riser/combustor maximum velocity is 3.3 m/s, according to the velocity contours. We can see that all three velocities are at their highest at the neck area when flue gases leave the primary chamber. The velocity stream contours reveal that in the counter scenario, fouling, slagging, and corrosion on the left-side wall near the neck area may cause problems.

In the third circumstance, we may experience a similar difficulty on the right side of the neck wall. This is because the gas discharge stream is focused near the wall.

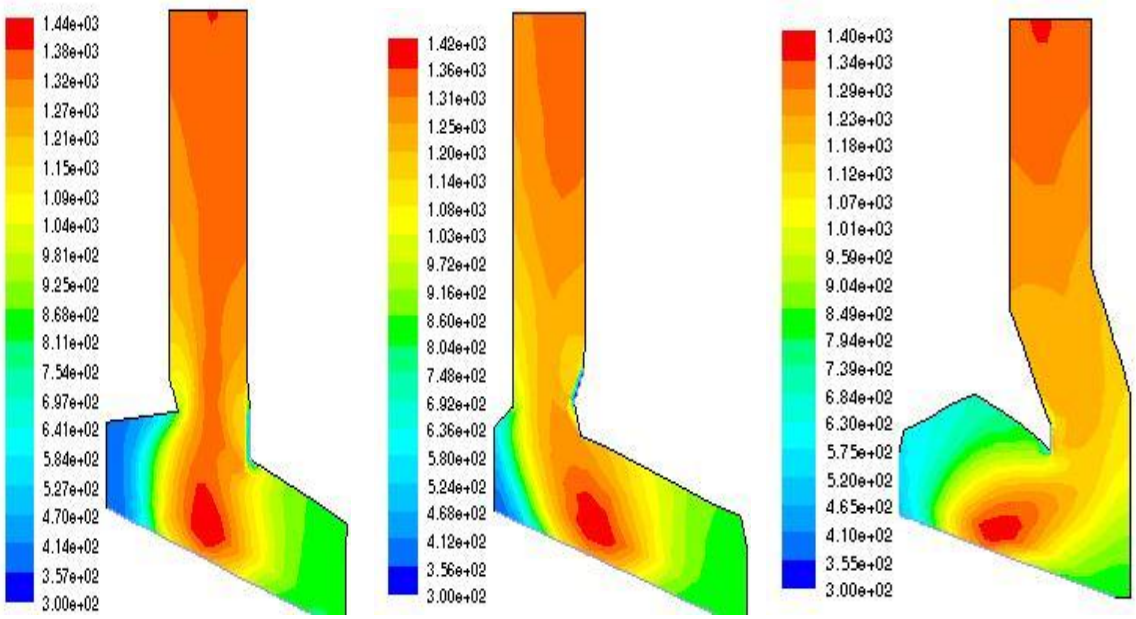

(a) (b) (c)

Figure 4.45: Contours of Static Temperature (a) Center (b) Counter (c) Parallel

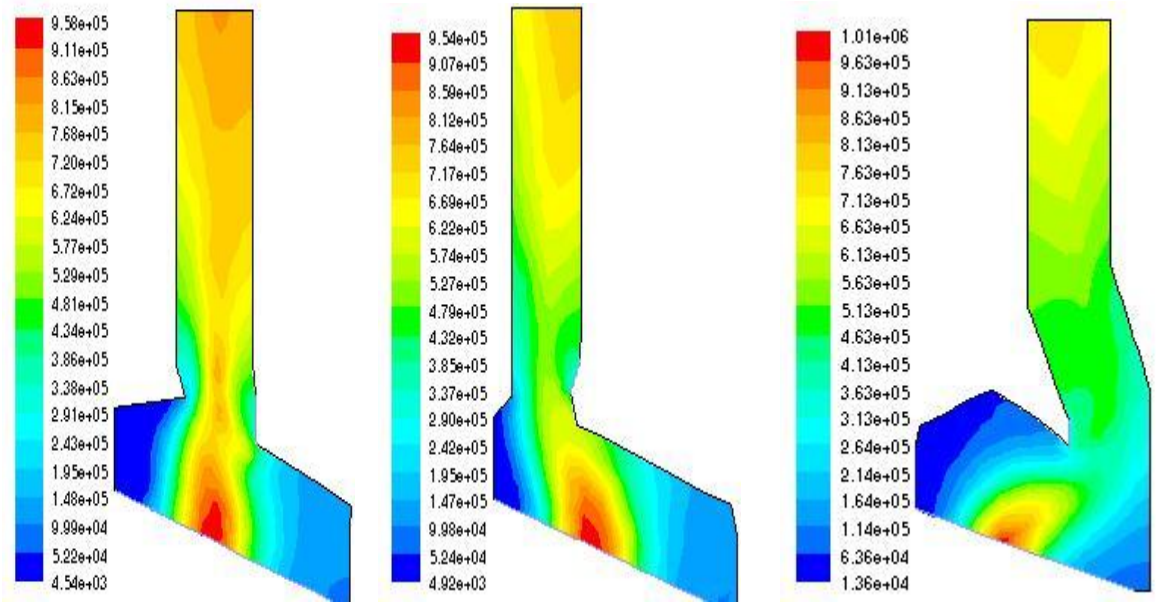

(a) (b) (c)

Figure 4.46: Contours of Radiation (a) Center (b) Counter (c) Parallel

The extreme temperature in all three cases is between 1400K and 1440K, with the middle area of the grate receiving the most heat. This is the area where, due to the high temperature, volatiles are burned. We can see from the radiation contours that the most heat may be recovered from solid fuel in the combustor's middle zone, where the maximum incident radiation is around 960 kW/m2 to 1000 kW/m2.

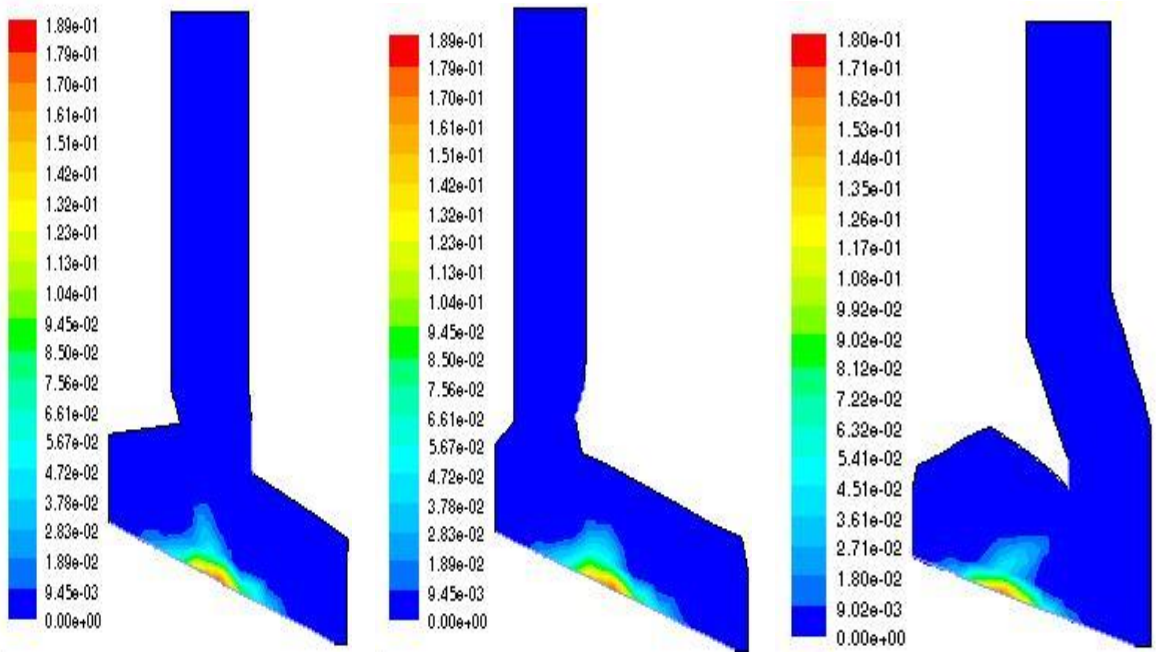

(a) (b) (c)

Figure 4.47: Contours of Mass Fraction of CO (a) Center (b) Counter (c) Parallel

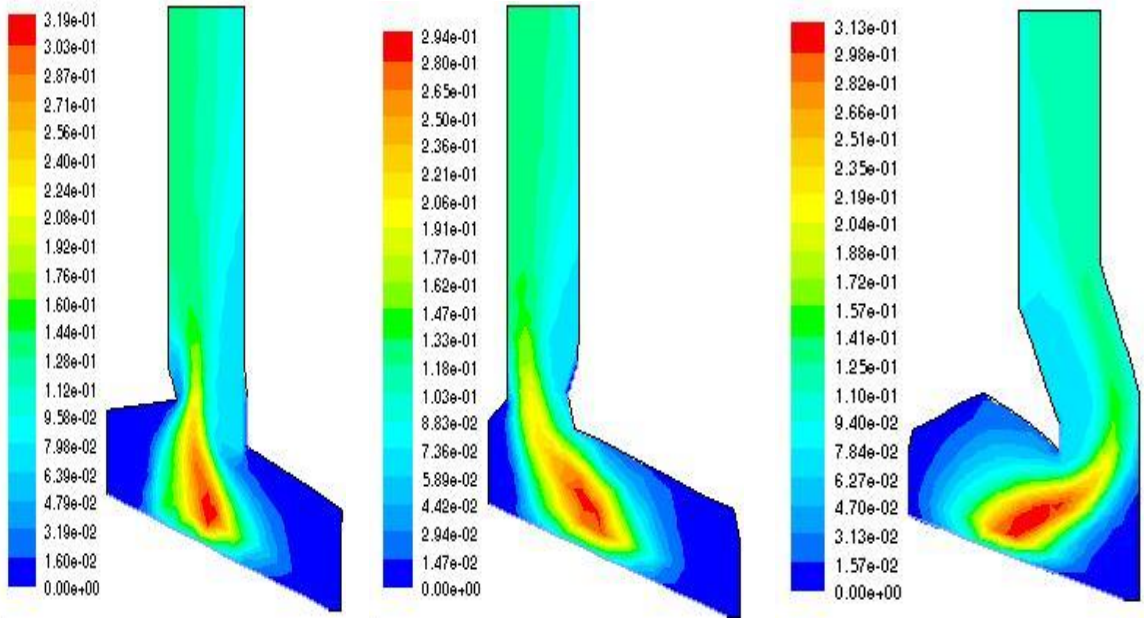

(a) (b) (c)

Figure 4.48: Contours of Mass Fraction of CO_2 (a) Center (b) Counter (c) Parallel

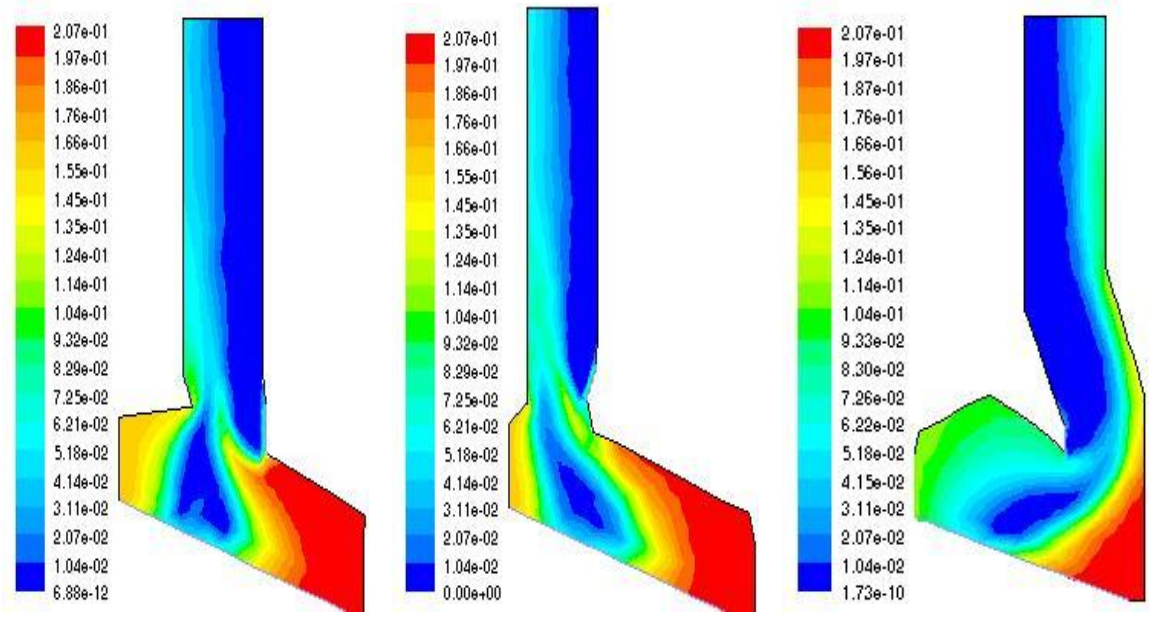

(a) (b) (c)

Figure 4.49: Contours of Mass Fraction of O_2 (a) Center (b) Counter (c) Parallel

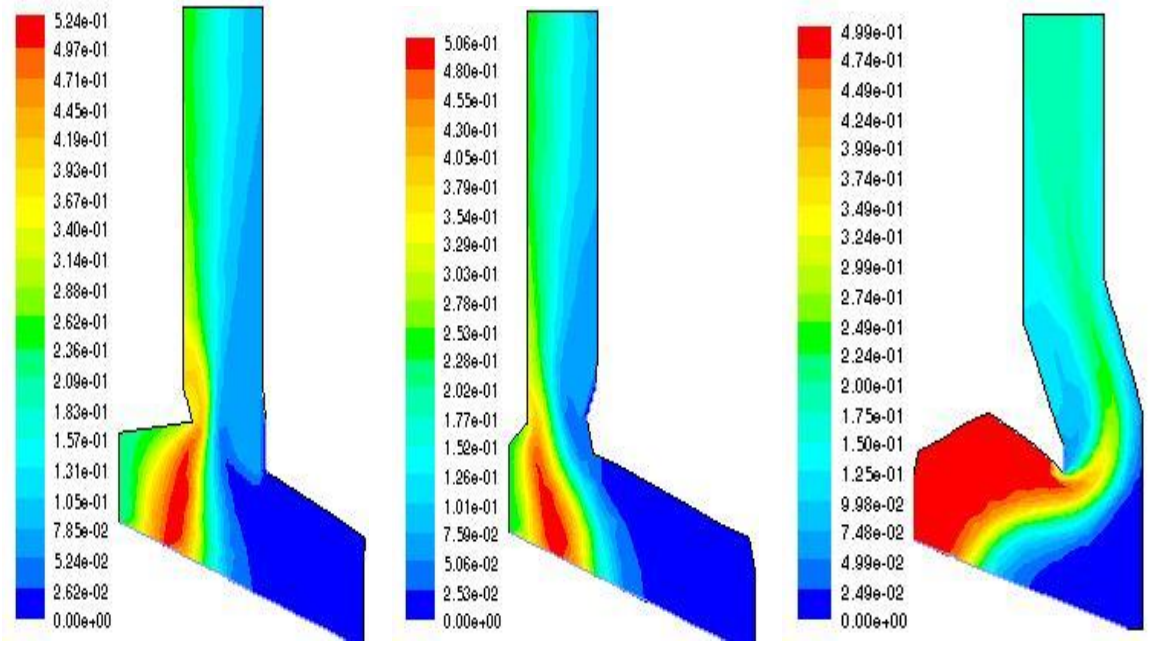

(a) (b) (c)

Figure 4.50: Contours of Mass Fraction of H_2O (a) Center (b) Counter (c) Parallel

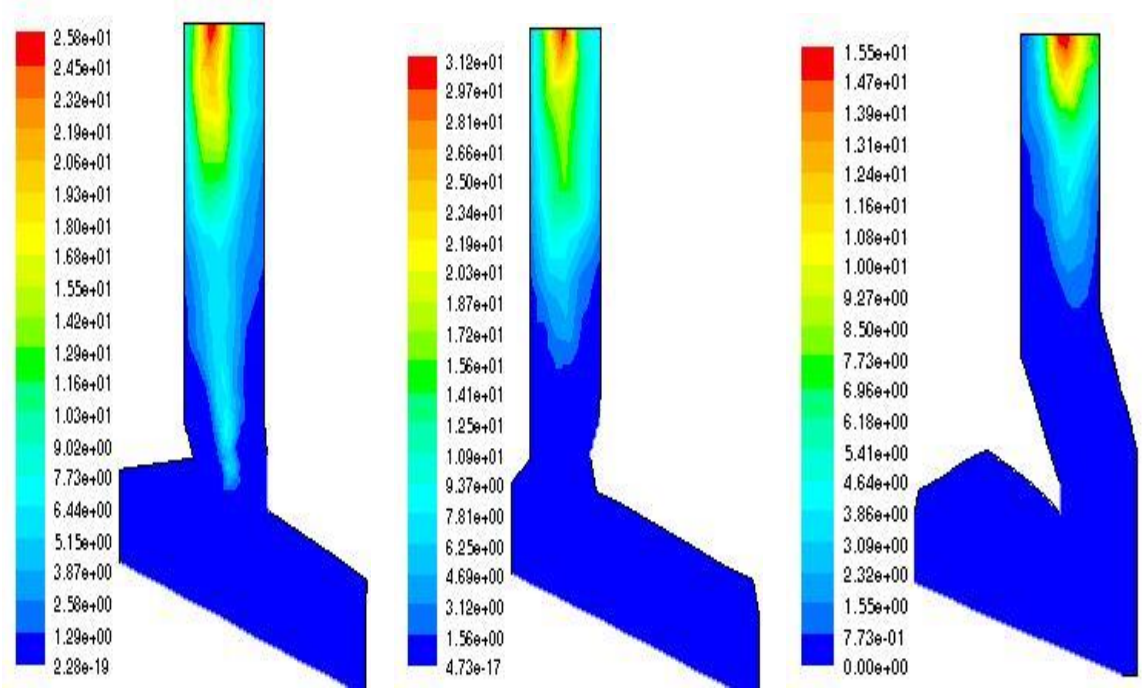

(a) (b) (c)

Figure 4.51: Contours of NOx (ppm) (a) Center (b) Counter (c) Parallel

The burning of the volatiles is defined in two reactions equations (I and II):

$2CO + O_2 \rightarrow 2CO_2$ (I)

&

$CH_4 + 2O_2 \rightarrow CO_2 + 2H_2O$ (II)

The CO mass fraction contours demonstrate that it is concentrated in the grate's central section, where devolatilization from the waste bed happens. CO_2 is then produced by combusting it with oxygen. The center section has the highest CO_2 concentration and the lowest O_2 concentration. At the secondary combustor area at the neck, we can see the reduction of O_2, having responded with CH_4 to produce CO_2 and H_2O. In the contours that display the mass fraction of H_2O, we can see that it is focused at the starting area of the grate, where the dehydrating of the solid fuel happens.

The contours indicating the amount of NOx in ppm highlight the area of the geometry where it is frequently focused in the upper region. The counter geometry establishes the highest level at around 31 ppm, while the parallel geometry establishes the lowest level at around 15 ppm.

4.7.16 Combustion of Coal Blends

Federal rules in the United States addressing the release of air pollutants have become more stringent due to public health and environmental concerns. The 1990 EPA New Source Performance Standards (NSPS) mandate a 50 percent decrease in acid rain-causing pollutants (i.e., NOx and SO_2). Numeral approaches and procedures have been presented for decreasing NOx, SO_2, and CO_2 gaseous emissions from fossil fuel burning while also lowering the costs of these moderation practices. Certain controller measures are costly, which raises manufacturing costs. Co-firing has become popular among electric utility producers as a less expensive alternative. Co-firing is described as the combustion of a renewable fuel (such as biomass) alongside a primary fuel (natural gas, coal, furnace oil, etc.). Current investigations in Europe and the United States (Reid et al., 2020; Rather et al., 2022) have found that combustion of biomass with fossil fuels has a favorable influence on the environment and electricity generation costs. In most co-firing studies, SO_2 and NOx emissions decreased. Since biomass is deemed CO_2-neutral, the net CO_2 generation was also lower. Besides, in some cases, overall fuel charges might be decreased if biomass handling charges (transport, grinding, etc.) are lower on an energy source than main fuel processing charges.

For several reasons, biomass fuels are deliberately environmentally pleasant. For starters, burning biomass does not result in a net increase in CO_2 (i.e., fossil-produced CO_2). During its growth, biomass consumes a similar volume of CO_2 that is discharged through burning. Consequently, combining coal with biomass fuels can minimize fossil-based CO_2 releases (Xu et al., 2020; Patrizio et al., 2021). Co-firing biomass residues instead of energy crops reduces greenhouse gas emissions by preventing CH_4 leakage from the land-filled biomass. In terms of global warming, CH_4 is thought to be 21 times more

powerful than CO_2 (EPA, 2020). Because most biomass fuels contain little or no sulfur, co-firing coal and biomass can also minimize net SO_2 emissions. When co-combustion with higher sulfur coal occurs, this feature is especially advantageous (Kanwal et al., 2021).

Pakistan has a large amount of biomass waste, of which rice husk waste has the lagest share. In addition to biomass, Pakistan is blessed with huge coal reserves, although they are sub-bituminous in nature. After doing the basic thermogravimetric and kinetic studies of coal blends, it is also important to perform co-firing studies using blends of Thar coal biomass waste. It is also important to identify the burning and discharge behavior in the fluidized bed combustor.

In this study, the co-firing of biomass with Thar coal was modeled using the FLIC and ANSYSFLUENT codes mentioned earlier. The feed rate of fuel could be varied to flow rates of 1.0, 2.0, and 2.5 kg/hr. In the fluidized bed riser, the primary air flow rate was adjusted, and emission and temperature patterns were observed. The variance of NOx in the riser for various coal blends is shown in Figure 4.52. In comparison to other particle sizes, coal particles of 600 microns produced the least amount of NOx.

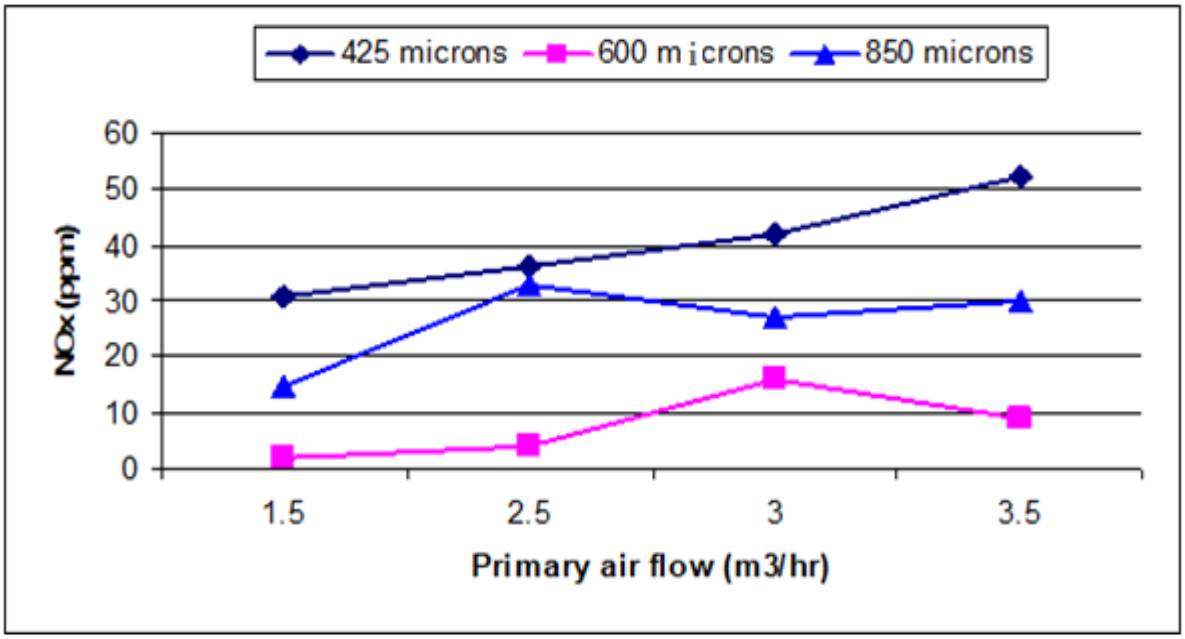

Figure 4.52: Variation of NOx as a function of primary air flow rate for different particle sizes of Thar coal blended with 10% Biomass

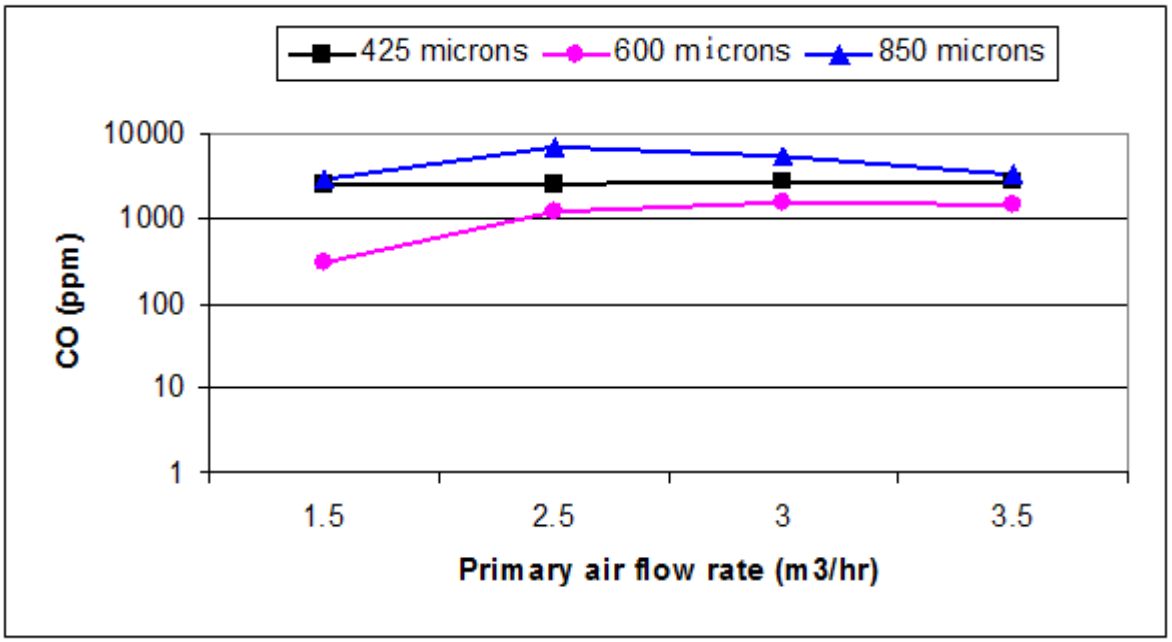

Figure 4.53: Variation of CO as a function of primary air flow rate for different particle sizes of Thar coal blended with 10% Biomass

The studies were carried out in the same way as those for a coal blend with biomass. The effects of coal blending, from 10 to 60 percent, were documented on the burning scenario for temperature observation. For various coal blends, the biomass feed rate was set at a flow rate of 1.00 kg/hr. In the fluidized bed combustor, the primary air flow rate was changed, and discharge and temperature results were noted. Figure 4.53 displays the dissimilarity of the average maximum riser temperature for different blending ratios. A blending fraction of 40% gives rise to the extreme riser temperature of 900°C.

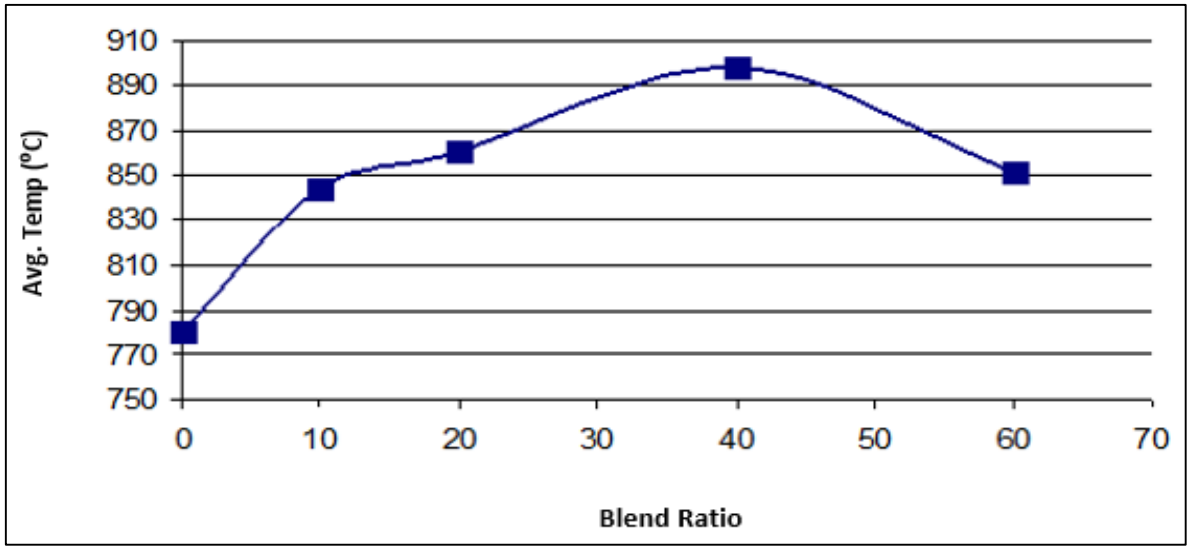

Figure 4.54: Variation of maximum average temperature of riser for various blending ratios at constant fed rate.

In the next part of the experiment, the primary fluidization airflow was fixed at 1.5 m^3/hr, and the feed rate was varied so that the effect of the feed rate on emissions could be obtained. Figure 4.54 shows the variation of the average maximum riser temperature for different blending ratios. Also, in this case, a blending fraction of 40% gives rise to the extreme CFBC temperature of 876°C.

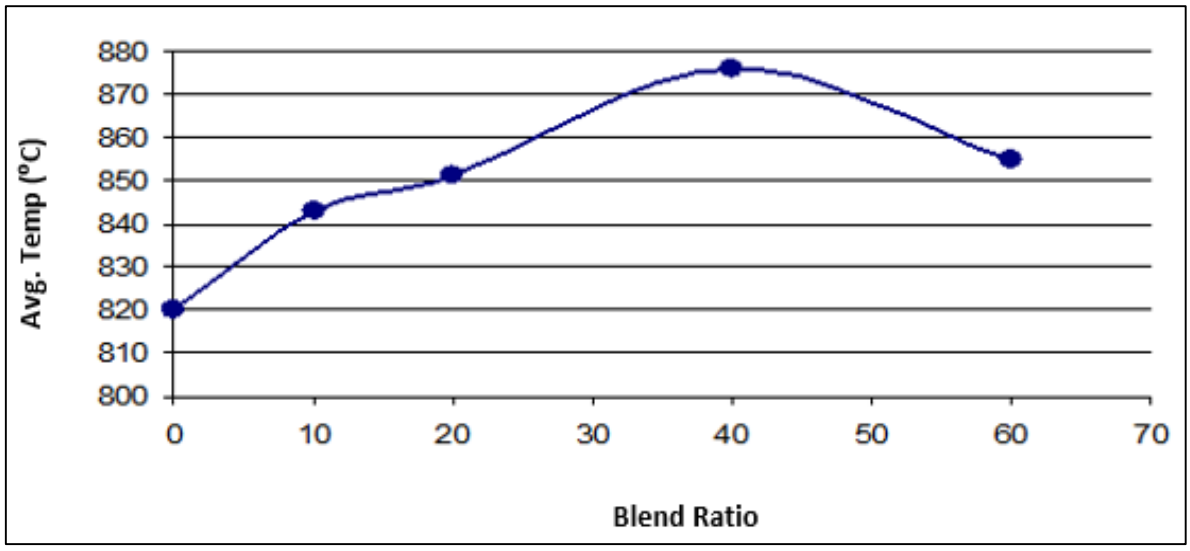

Figure 4.55: Variation of maximum average temperature of riser for various blending ratios at constant primary air flow rate

Figure 4.56 displays the CO and NOx emission behavior for numerous coal mixtures, and it might be deduced that raising the blending ratio reduces CO and NOx releases. Figure 4.57 demonstrates that when the blending ratio increases, SO_2 levels decrease significantly, setting the upper limit for coal blending ratios in CFB combustors. Figures 4.55 and 4.56 show that a blending fraction of 40% is best for achieving an upper riser temperature while 30% lowers NOx, SO_2, and CO levels.

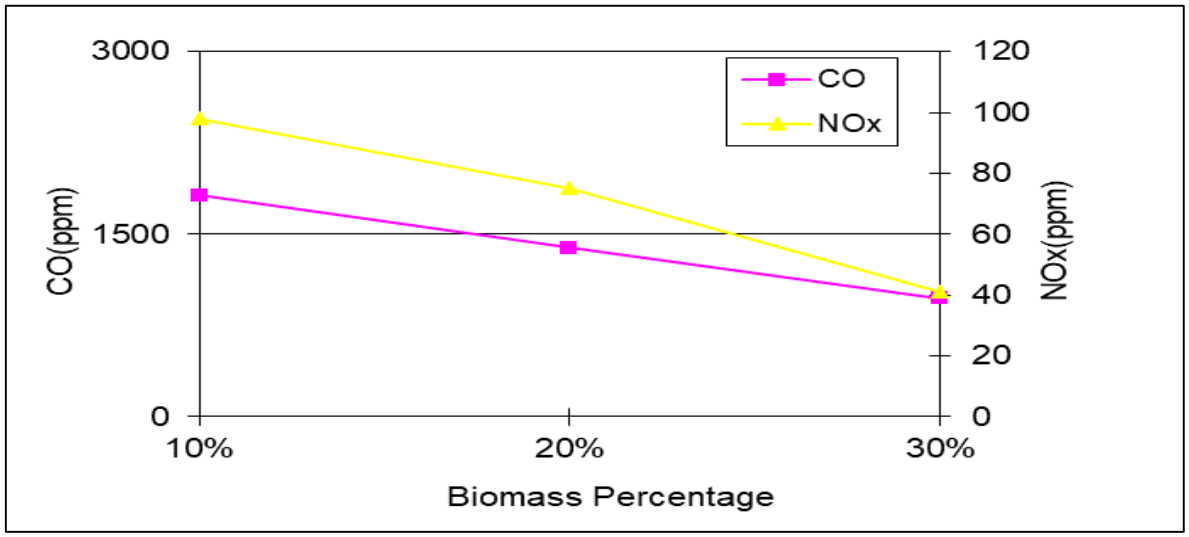

Figure 4.56: CO and NOx Emission profiles for several coal blending fractions

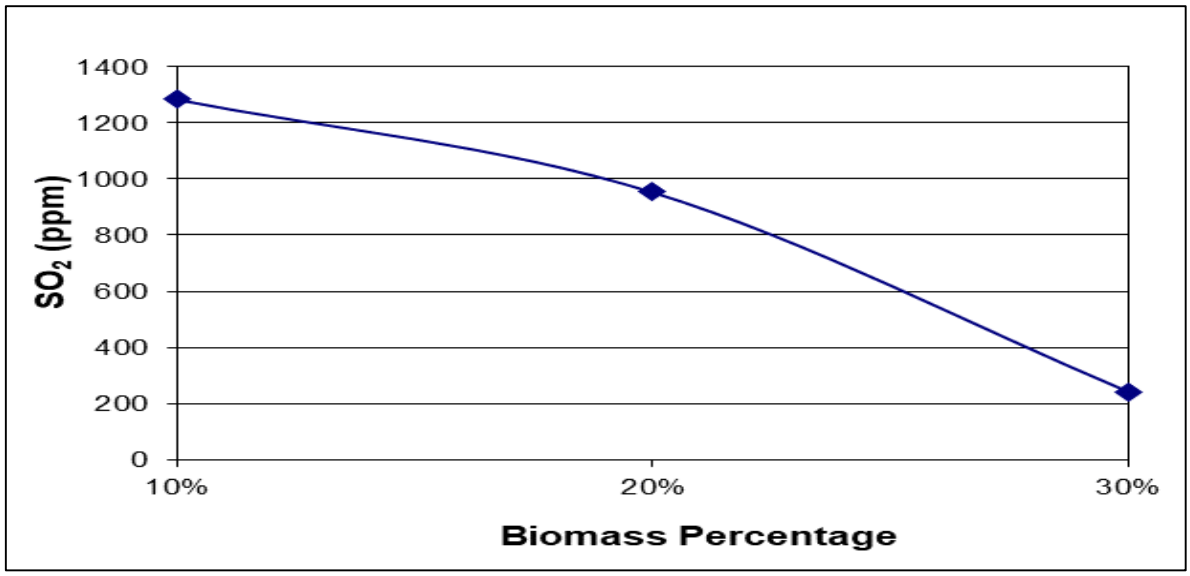

Figure 4.57: Distinction of SO_2 as a purpose of blend fraction

CHAPTER 5

CONCLUSIONS

5.1 Conclusions

The characteristics of coal are important for burning and are expressed as the basis for the technology selected for the power plant. According to the values obtained in the Thar Block-II coal assessment, moisture is found to be higher in all samples, and volatile matter values are found at low to medium levels. Those variables indicate that energy values are dependent on volatile matter, while a higher moisture content will decrease the efficiency of power production. The low to medium calorific value of local coals shows their potential as a future fuel. The sulfur and carbon content in Thar coal Block II was also found to be low to medium levels. In the coal ash composition, it can be realized that most ash contents are comprised of inorganic compounds such as SiO_2, Fe_2O_3, Al_2O_3, and CaO, as well as lower quantities of Na_2O and K_2O.

In the co-combustion, it was found that rice husk comprises a higher content of volatile matter, lower moisture, and sulfur with higher ash contents. By adding the biomass rice husk to Thar coal, its basic configuration changed and provided less sulfur and other content as related to the coal. This study explores the coal-rice husk blending effects on coal configuration and emission gases. It was observed that the blending fraction decreased discharges of SO_2 and NOx. A decline in SO_2 and NOx discharges was found by increasing the blending ratio. NOx and SOx emissions were reduced from 89 ppm (CRh-1) to 34 ppm (CRh-3) and 828 ppm (CRh-1) to 169 ppm (CRh-3), respectively, by increasing the

blending percentage from 10 to 30%. The outcome of the current work illustrates the optimum values for the Thar low-ranking coal-rice husk blends. In comparison to other blended samples, samples of coal-rice husk blend (70:30%) (CRh-3) were found to be suitable from the perspective of power production due to their low gas emissions, high calorific value, high volatile matter content, low moisture, and ash content. Furthermore, this combination has a low sulfur content, making it a viable contender for power generation under environmental friendly conditions and support to fulfill the requirements of the UN SDG 7 goal (Affordable and Clean Energy) and also suitable for power generation at the district level.

Using the Thermogravimetric (TGA) analysis, the pyrolytic heating rate and temperature were established, which have a significant effect on the pyrolysis of Thar coal. Kinetic constraints (frequency factor and activation energy) were obtained by curve-fitting the TGA data. A one-step global model was utilized to forecast the pyrolytic transition using these kinetic limitations. It might be concluded that the pyrolysis reaction is kinetically controlled, and that’s greatly dependent on the temperature of the reaction.

A CFD model was developed to simulate the hydrodynamics of gas-solid flow in a circulating fluidized bed riser using the ANSYS FLUENT software. The effect of several exit shapes of the riser was modeled using a parametric investigation of the two-phase gas-solid stream hydrodynamics of a CFB riser. The CFD model for the gas segment and the viscosity of static particles in the solids segment with a k-ϵ turbulence model for evaluating mixing performance. For combustion modeling, the FLIC code was found to be precise in simulating coal bed combustion, and the FLIC code's outcomes were imported into the FLUENT database. The maximum temperature inside the compartment, according to the FLUENT results, is around 1440K (1166°C) at the primary burning sector in the bed center. The peak value in the center-oriented riser/combustor is 3.3 m/s, as determined from velocity contours. The CO and CO_2 mass fraction contours show that it is concentrated in the center geometry, and a lower CO concentration is found in the parallel geometry. The contours indicate the amount of NOx at the highest level of around 31 ppm, while the

parallel geometry establishes the lowest level at around 15 ppm. It is concluded that the most favorable and effective technology for power production from Thar lignite coal is the Circulating Fluidized Bed Combustor (CFBC), which uses suitable Clean Coal Technologies (CCT) plus supercritical (SC) and ultra-supercritical (USC) plants to permit cleaner and cost-effective coal consumption to reduce emissions.

5.2 Future Research Directions

The below suggestions are being made for further investigations of combustion modeling of fluidized beds concerning this research study:

a. Measurements of intermediates like HCN, NH_3, NH_2, and Particulate Matter (PM) could also be taken along the riser elevation to understand the mechanism of generation and decrease of NOx discharges in the CFBC for the co-combustion processes.

b. Further research into the solid particle residence period inside the riser is needed to understand the complicated hydrodynamics of CFB cluster development and annihilation.

c. To see the effect of an increase in the blending of biomass in coal-fired power plants, examine the hydrodynamics and emission levels. Other biomasses, such as bagasse and wheat straw, could be studied as well, with an emphasis on agglomeration and segregation issues.

d. To better anticipate gaseous emissions, a thorough model of co-combustion in a CFBC, including the depth of devolatilization kinetics and biomass burning performance, must be developed.

e. The development and validation of the dynamic system model using an unsteady state need to be studied in the future.

f. This study is limited to Thar Block-II coal; further CFD studies and research may be conducted for other coal reserves in Pakistan.

REFERENCES

Abaide, E.R., Tres, M.V., Zabot, G.L., Mazutti, M.A. (2019). Reasons for processing of rice coproducts: reality and expectations. *Biomass Bioenergy*, 120: 240–256. ISSN 0961-9534. https://doi.org/10.1016/j.biombioe.2018.11.032.

Abbasi, K.R., Hussain, K., Abbas, J., Adedoyin, F.F., Shaikh, P.A., Yousaf, H., Muhammad, F. (2021). Analyzing the role of industrial sector's electricity consumption, prices, and GDP: A modified empirical evidence from Pakistan. *AIMS Energy*, 9 (1): 29–49. Doi: 10.3934/energy.2021003.

Abdeshahian, P., Lim, J.S., Ho, W.S., Hashim, H., Lee, C.T. (2016). Potential of biogas production from farm animal waste in Malaysia. *Renewable and Sustainable Energy Reviews*, 60: 714–723. ISSN 1364-0321. https://doi.org/10.1016/j.rser.2016.01.117.

Abdullah, (2007). *Control of oxides of Nitrogen and Sulfur from a Coal fired Circulating Fluidized Bed Combustor*. A Ph.D. thesis, Faculty of Engineering and Technology, University of Punjab, Quaid-e-Azam Campus Lahore, Pakistan. Available at: http://prr.hec.gov.pk/jspui/handle/123456789//4364.

Aboyade, A. O., Gorgens, F. J., Carrier, M., Meyer, L.E., Knoetze, H. J. (2013). Thermogravimetric study of Pyrolysis characteristics and kinetics of coal blends with corn and sugarcane residues. *Fuel Processing Technology*, 106: 310-320. ISSN 0378-3820. https://doi.org/10.1016/j.fuproc.2012.08.014.

Adamczyk, W. P. Wecel, G. Klajny, M. Kozolub, P. Klimanek, A. Bialecki, R. (2014). Modeling of particle transport and combustion phenomena in a large-scale circulating fluidized bed boiler using a hybrid Euler–Lagrange approach. *Particuology*, 16: 29–40. ISSN 1674-2001. https://doi.org/10.1016/j.partic.2013.10.007.

Adams, D., Lockwood, T., Baruya, P., Wiatros-Motyka, M. Qian, Z. Q. (2021). *A Pathway to Reducing Emissions from Coal Power in India*. CCC/297, London, UK, International Centre for Sustainable Carbon/CIAB, 157 pp. Available at: https://www.sustainable-carbon.org/login/?download-id=36316.

AHL, (2021). *Pakistan Power Sector.* Arif Habib Limited, 25 Jan 2021. Available at: https://arifhabibltd.com/downloads/Daily_Call/PowerGenerationDec-20-2021-01-25.pdf. (Accessed 11th December 2021).

Ahmad, A., Hakimi, M.H. & Chaudhry, M.N. (2015). Geochemical and organic petrographic characteristics of low-rank coals from Thar coalfield in the Sindh Province, Pakistan. *Arab J Geosci* 8, 5023–5038. https://doi.org/10.1007/s12517-014-1524-6.

Ahmed S., Ali, A., Kumar, D., Malik, Z. M., Memon A. H. (2019). China Pakistan Economic Corridor and Pakistan's Energy Security: A Meta-Analytic Review. *Energy Policy*, 127: 147–54. https://doi.org/10.1016/j.enpol.2018.12.003.

Aho, M. J. and Pirkonen, P.M. (1995). Effects of Pressure, Gas Temperature and CO2 and O-2 Partial Pressures on the Conversion of Coal-Nitrogen to No, N_2O and NO_2. *Fuel*, 74 (11): 1677-1681. ISSN 0016-2361. https://doi.org/10.1016/0016-2361(95)00169-6.

Aized T., Shahid, M., Bhatti, A., Saleem, M., Anandarajah, G. (2018). Energy Security and Renewable Energy Policy Analysis of Pakistan. *Renewable and Sustainable Energy Reviews*, 84: 155–69. ISSN 1364-0321. https://doi.org/10.1016/j.rser.2017.05.254.

Akbar, A., Riaz, A., Hassan, M. T. (2021). Energy Crisis in Pakistan (2008-2018): Impact on Industrial Sector. *Global Regional Review*, VI (I), 145-153. https://doi.org/10.31703/grr.2021(VI-I).16.

Akhtar, J., Yaqub, M., Iqbal, J., Sheikh, N., Saba T. (2018). Way forward in meeting energy challenges in Pakistan. *International Journal of Ambient Energy,* 39 (8): 904–908. DOI: 10.1080/01430750.2017.1341430.

Akhtar, K. S., Hussain, S., Khan, R., Ijaz, A. (2013). Thermochemical Studies and Fluidized Bed Combustion of Low-Grade Pakistani Coal Blends. *Life Science Journal*, 10 (4): 3358-3362. (ISSN: 1097-8135).

Akhtar, N. A. (1995). *Gaseous emissions control from a coal fired circulating fluidized bed*. A Ph. D. Thesis, Chemical Engineering, The University of Leeds, UK.

Akowuah J.O., Kemausuor F., Mitchual S.J. (2012). Physico-Chemical Characteristics and Market Potential of Sawdust Charcoal Briquettes. *Int J Energy Environ Eng.* 3 (20). https://doi.org/10.1186/2251-6832-3-20.

Al-Abbas, A. H. (2012). *Computational Fluid Dynamics (CFD) Modelling of Oxy-Fuel Combustion Technique for Power Plants*. A Ph.D. thesis, Faculty of Engineering and Industrial Science, Swinburne University of Technology, Australia.

Ali, J. (2019). *Chemical Analysis of Arsenic and Mercury in Coal of Thar Coal Field and Their Interaction with Adjoining Aquifer Water and Solid Matrices: An Environmental Impact Study*. A Ph.D. Thesis Submitted to National Centre of Excellence in Analytical Chemistry, University of Sindh, Jamshoro Pakistan.

Ali, Y., Memoona, A., Socci, C., Saleem S. B. (2018). Can coal replace other fossil fuels to fulfil the energy demand in Pakistan? An environmental impact analysis. *Asia-Pacific Journal of Regional Science*. https://doi.org/10.1007/s41685-018-0096-y.

Aliman I. and Pasek A. D. (2018). The evaluation of experimental and numerical study of combustion process on mini traveling chain grate furnace (incinerator) by computational fluid dynamics method. AIP Conference Proceedings 1984, 030005 (2018); https://doi.org/10.1063/1.5046626.

Almuttahar, A. Taghipour, F. (2008). Computational fluid dynamics of high density circulating fluidized bed riser: Study of modeling parameters. *Powder Technology,* 185 (1): 11-23. ISSN 0032-5910. https://doi.org/10.1016/j.powtec.2007.09.010.

Amand, L. E., Andersson, S. (1989). Emissions of nitrous oxide from fluidized bed boilers. In A. Manaker (Ed.), *Proceedings of 10th International Conference on Fluidized Bed Combustion* (pp. 49–56). New York: ASME.

Anderson, S. and Newell, R. (2004). Information programs for technology adoption: the case of energy-efficiency audits. *Resource and Energy Economics,* 26 (1): 27-50. ISSN 0928-7655. https://doi.org/10.1016/j.reseneeco.2003.07.001.

Anjum, G., Khan, M.N. (2017). The Power Generation from Coal in Pakistan: Assessment of Physicochemical Pollutant Indicators in Indigenous Reserves in Comparison to the Foreign Coal. *Pakistan Journal of Analytical & Environmental Chemistry* 18 (1):54-63. ISSN 2221-5255. DOI: http://dx.doi.org/10.21743/pjaec/2017.06.05.

Anshar, M., Ani, F. N. and Kader, Ab. S. (2016). Electrical Energy Potential of Rice Husk as Fuel for Power Generation in Indonesia. *ARPN Journal of Engineering and Applied Sciences,* 11 (6): 3616-3624. ISSN 1819-6608.

Anukam, A. I., Mamphweli, S. N., Mabizela, P., S., Meyer, E., L. (2016). Blending Influence on the Conversion Efficiency of the Co-gasification Process of Corn Stover and Coal. *Hindawi Publishing Corporation. Journal of Chemistry,* Vol 2016, Article ID 3910986, 8 pages http://dx.doi.org/10.1155/2016/3910986.

Arena, U., Camarote, A., Massimilla, L., Sicilliano, L., and Basu, P., (1990). Carbon attrition during combustion of a char in a circulating fluidized bed. *Combustion Science and Technology,* 73 :(1-3): 383-394. https://doi.org/10.1080/00102209008951658.

Arenillas, A., Rubiera, F., Arias, B., Pis, J. J., Faúndez, J. M., Gordon, A. L. and García, X. A. (2004). A TG/DTA study on the effect of coal blending on ignition behavior. *Journal of Thermal Analysis and Calorimetry*, 76: 603–614. https://doi.org/10.1023/B:JTAN.0000028039.72613.73.

Argus Media, (2021). *Pakistan power-sector coal demand growth set to slow*. Available from: https://www.argusmedia.com/en/news/2173778-pakistan-powersector-coal-demand-growth-setto-slow.

Armesto, L., Boerrigter, H., Bahillo, A., and Otero, J. (2003). N_2O emissions from fluidized bed combustion. The effect of fuel characteristics and operating conditions. *Fuel*. 82 (15-17): 1845-1850. ISSN 0016-2361. https://doi.org/10.1016/S0016-2361(03)00169-8.

Asai, M., Aoki, K., Shimoda, H., Makino, K., and Omata, K. (1990). Optimization of circulating fluidized bed combustion. *Proceeding of the 3rd International Conference on Circulating Fluidized Bed Combustion*. Nagoya, Japan, 379.

Ataei, A., Simin S., Aliraz A., Sahand B. K., Maryam F., Abari M.F., and Hadi R. (2012). Energy Analysis of co-gasification System Based on Rice husk and Bagasse. *The 1ST International and 4thNational Congress on Recycling of Organic Waste in Agricultural, 26 – 27 April 2012* in Isfahan, Iran. https://crowa.khuisf.ac.ir/DorsaPax/userfiles/file/pazhohesh/crowa91/1.pdf.

Atimtay AT (2003) A global outlook to the carbon dioxide emissions in the world and emission factors of the thermal power plants in turkey. *Water, Air, and Soil Pollution Focus* 3(5-6):335-345. http://dx.doi.org/10.1023/A:1026086002856.

Atimtay, A.T. and Topal, H.s., (2004). Co-combustion of olive cake with lignite coal in a circulating fluidized bed. Fuel, 83(7-8), p. 859-867. DOI: 10.1016/j.fuel.2003.09.015.

Baiyu G. (2020). China relaxes restrictions on coal power expansion for the third year running. Available at: https://www.chinadialogue.net/article/show/single/en/11966-China-relaxes-restrictions-on-coal-power-expansion-for-third-year-running. China Dialogue Trust, London, UK, 2 pp.

Bai X., Lu G., Bennet T., Sarroza, A., Eastwick C., Liu H., Yan Y. (2017). Combustion behavior profiling of single pulverized coal particles in a drop tube furnace through high-speed imaging and image analysis. Experimental Thermal and Fluid Science, 85; (322-330). https://doi.org/10.1016/j.expthermflusci.2017.03.018.

Balasubramanian, S., Sudhindra, K., Bhat, S., (2021). An Insight into Advanced Technology in Circulating Fluidised Bed Combustion Steam Generators. *Banalore: TATA Consulting Engineers Ltd*. Available at: (Accessed 13 February 2022). https://www.academia.edu/34881373/An_Insight_into_Advanced_Technology_in_Circulating_Fluidised_Bed_Combustion_Steam_Generators.

Balat, M. (2007). Coal-fired power generation: proven technologies and pollution control systems. *Energy Sources, Part A: Recovery, Utilization, and Environmental Effects* 30(2): 132–140. https://doi.org/10.1080/00908310600628313.

Bampenrat, A., Sukkathanyawat, H., and Seangwattana, T. (2021). Coal/biomass co-combustion investigation by thermo gravimetric analysis. *E3S Web of Conferences 302*, 01002, https://doi.org/10.1051/e3sconf/202130201002.

Banerjee, S. and Hughes, R. (2020). *Biomass Combustion in a Circulating Fluidized Bed Combustor.* DOE.NETL-2020.2148; NETL Technical Report Series; U.S. Department of Energy, National Energy Technology Laboratory: Morgantown, WV; p 32. DOE: 10.2172/1659115.

Barca, S. (2011). Energy, property, and the industrial revolution narrative. *Ecological Economics* 70(7): 1309–1315. https://doi.org/10.1016/j.ecolecon.2010.03.012.

Bariani M., Boix E., Cassella F., Cabrera M.N., (2020). Furfural production from rice husks within a biorefinery framework. *Biomass Conversion and Biorefinery*: 1–14. DOI:10.1007/s13399-020-00810-1.

Barisic, V., Klingstedt, F., Kilpinen, P., and Hupa, M. (2005). Kinetics of the catalytic decomposition of N_2O over bed materials from industrial circulating fluidized-bed boilers burning biomass fuels and wastes. *Energy Fuels,* 19 (6): 2340-2349. https://doi.org/10.1021/ef050110x.

Barnes, I. (2012). *Understanding pulverized coal, biomass and waste combustion.* CCC/205, London, UK. IEA Clean Coal Centre, 57 pp.

Basak, A. K., Sitkiewitz, S. D., Friedman, M. A. (1991). Emission performance summary from the circulating fluidized bed boiler demonstration project. *Proceeding of the 11th International Conference on Fluidized Bed Combustion*. Montreal, Canada, 211.

Basu S. and Debnath A. K. (2019). *Chapter 3 - Plant P&ID (Process) Discussions*. Power Plant Instrumentation and Control Handbook (Second Edition), Academic Press, 2019, Pages 149-250, ISBN 9780128195048, https://doi.org/10.1016/B978-0-12-819504-8.00003-2.

Basu, P. (2006). *Combustion and Gasification in Fluidized Beds*, 1st ed.; CRC Press: Boca Raton, FL, USA.

Basu, P. (2015). *Circulating Fluidized Bed Boilers Design, Operation and Maintenance. Springer International Publishing Switzerland*. ISBN 978-3-319-06172-6. DOI 10.1007/978-3-319-06173-3.

Baumann, H., and Moller, P. (1991). Pyrolysis of Hard Coals under Fluidized Bed Combustor Conditions. *Erdol Kohle-Erdgas Petrochem,* (44): 29-33.

Benyahia, S., Arastoopour, H., Knowlton, T. M., Massah, H. (2000). Simulation of particles and gas flow behavior in the riser section of a circulating fluidized bed using the kinetic theory approach for the particulate phase. *Powder Technology,* 112 (1-2): 24- 33. ISSN 0032-5910. https://doi.org/10.1016/S0032-5910(99)00302-2.

Bhattacharyya, M., Shadangi, K. P., Mahanta, P., Mohanty, K. (2021). Co-pyrolysis of coal-biomass: study on reaction kinetics and thermodynamics. Society of Chemical Industry and John Wiley & Sons, Ltd. *Biofuels, Bioprod & Bioref*. 16 (3): 725-742. https://doi.org/10.1002/bbb.2333.

Bhutta, M. M. A., Rehman, S., Shah, A. N., Kamran, M. S., Naveed, A., Rehman, S. S. M. (2021). Optimization of multi variant process parameters to reduce emissions of high sulfur coal during combustion in fluidized bed facility. *Advances in Mechanical Engineering*. 13 (9): 1–12. https://doi.org/10.1177/16878140211044659.

Bhutta, Zafar, (2020). *Installed power production capacity rises*. The Express Tribune. Available at: https://tribune.com.pk/story/1989618/installed-power-production-capacity-rises. Retrieved 4 June 2020.

Bhutto, A. W., Bazmi, A. A., Zahedi, G. (2011). Greener energy: Issues and challenges for Pakistan—Biomass energy prospective. *Renewable and Sustainable Energy Reviews*, 15 (6): 3207–3219. ISSN 1364-0321. https://doi.org/10.1016/j.rser.2011.04.015.

Bhutto, A. and Karim, S. (2005). Coal gasification for sustainable development of the energy sector in Pakistan. *Energy For Sustainable Development,* 9(4): 60–67. https://doi.org/10.1016/S0973-0826(08)60500-1.

Blaszczuk, A. and Nowak, W. (2014). Bed-to-wall heat transfer coefficient in a supercritical CFB boiler at different bed particle sizes. *International Journal of Heat*

and Mass Transfer, 79: 736–749. ISSN 0017-9310. https://doi.org/10.1016/j.ijheatmasstransfer.2014.08.080.

Boerrigter, H. and Reinhard R. (2006). *Review of application of gasses from biomass gasification*. Chap. 10 in Hand book Biomass gasification, by H. A. M. Knoef, 211-230. Viena: Biomass Technology Group (BTG), Viena University of Technology, Institute of Chemical Engineering.

Bolkan, Y., Franco B., Jesse Z., and Bruce, M. (2003). Hydrodynamic Modeling of CFB Risers and Downers. *International Journal of Chemical Reactor Engineering*, 1 (1): 1115. https://doi.org/10.2202/1542-6580.1115.

BP (British Petroleum Company), (2020). *Annual BP Statistical Review of World Energy, 2020.* 69th edition. Available from: https://www.bp.com/content/dam/bp/business-sites/en/global/corporate/pdfs/energy-economics/statistical-review/bp-stats-review-2020-full-report.pdf. 65 pp.

BP, (2021). *Statistical review of world energy*. Available from: https://www.bp.com/content/dam/bp/business-sites/en/global/corporate/pdfs/energyeconomics/.

Breault, R. (2006). A review of gas-solid dispersion and mass transfer coefficient correlations in circulating fluidized beds. *Powder Technology*, 163 (1-2): 9-17. ISSN 0032-5910. https://doi.org/10.1016/j.powtec.2006.01.009.

Cai R., Ke X., Lyu1 J., Yang1 H., Zhang M., Guangxi Yue1 and Wen Ling (2017). Progress of circulating fluidized bed combustion technology in China: a review. *Clean Energy*, 1 (1): 36–49. https://doi.org/10.1093/ce/zkx001.

Cai, J., and Y. Chen (2012). Iterative linear integral iso- conversion method theory and application. *Bioresource Technology*, 103 (1):309-12. DOI: 10.1016/j.biortech.2011.10.008.

Cai, R., Huang, Y., Li, Y., Wu, Y., Zhang, H., Zhang, M., Yang, H., & Lyu, J. (2019). Effects of the Limestone Particle Size on the Sulfation Reactivity at Low SO_2 Concentrations Using an LC-TGA. *Materials (Basel, Switzerland)*, 12 (9): 1496. https://doi.org/10.3390/ma12091496.

Cardozo, E., Erlich, C., Alejo, L., Fransson, T.H. (2016). Comparison of the thermal power availability of different agricultural residues using a residential boiler. Biomass Conversion and Biorefinery, 6 (4): 435–447. DOI:10.1007/s13399-016-0200-3.

Cebrucean, D., Cebrucean, V., Ionel, I. (2020). Modeling and performance analysis of subcritical and supercritical coal-fired power plants with biomass cofiring and CO_2 capture. *Clean Technologies and Environmental Policy*, 22 (1): 153-169. https://doi.org/10.1007/s10098-019-01774-1.

Chang, J., Wang, X., Zhou, Z., Chen, H., Niu, Y. (2021). CFD modelling of hydrodynamics, combustion and NOx emission in a tangentially fired pulverized-coal boiler at low load operating conditions. *Advanced Powder Technology,* 32 (2): 290–303. ISSN 0921-8831. https://doi.org/10.1016/j.apt.2020.12.008.

Changkook, R., Yao-Bin, Y., Hisaki, Y., Vida, N., & Swithenbank, J. (2007). Integrated FLIC/FLUENT Modelling of Large Scale MSW Incineration Plants. *Sheffield University Waste Incineration Centre, Department of Chemical and Process Engineering, Mapping Street, S1 3JD.*

Chapman, G. (2022). *Global Thermal Coal Supply Fundamentals. International Centre for Sustainable Carbon*. ICSC Report # ICSC/318. ISBN 978–92–9029–641-6. Available at: https://www.sustainable-carbon.org/login/?download-id=40758.

Chen, J. M., Ju, W., Cihlar, J., Price, D., Liu J., Chen W., Pan, J., Black A., Barr A. (2003). Spatial distribution of carbon sources and sinks in Canada's forests. *Tellus B: Chemical and Physical Meteorology,* 55 (2): 622-641. https://doi.org/10.3402/tellusb.v55i2.16711.

Chen, Wei-Hsin & Kuo, Po-Chih. (2011). Isothermal Torre faction kinetics of hemicellulose, cellulose, lignin and xylan using thermo-gravimetric analysis. *Energy,* 36 (11): 6451-6460. DOI: 10.1016/j.energy.2011.09.022.

Chernetskiy, M. & Dekterev, A. (2011). Mathematical model for heat transfer and combustion in a pulverized coal flame. *Combustion Explosion and Shock Waves*. 47 (3): 280-288. DOI:10.1134/S001050821103004X.

Chieng, S. and Kuan, S.H. (2020). Harnessing bioenergy and high value-added products from rice residues: a review. *Biomass Conversion and Biorefinery,* 1–25. https://doi.org/10.1007/s13399-020-00891-y.

Chokphoemphuna, S., Eiamsa-ardb, S., Promvongec, P., Chuwattanakulc,V. (2019). Rice husk combustion characteristics in a rectangular fluidized-bed combustor with triple pairs of chevron-shaped discrete ribbed walls. *Case Studies in Thermal Engineering,* 14 (2019): 100511. https://doi.org/10.1016/j.csite.2019.100511.

Choudry, M. A. F., Nergis, Y., Sharif, M., Mahmood, A. A., Abbasi, H. N. (2010). Composition, Trace Element Contents and Major Ash Constituents of Thar Coal, Pakistan. *American Journal of Scientific Research,* 11 (2010): 92-102. ISSN 1450-223X.

Cláudio, C. J., Danielle, G. Glauton, D. Glaucia, A. P. (2019). Evaluation of Biomass Properties for the Production of Solid Biofuels. *Floresta Ambient.* 26 (2) Seropédica. http://dx.doi.org/10.1590/2179-8087.043318.

Cocco, R., Reddy, S. B., Knowlton, K. T. (2014). *Introduction to Fluidization*. American Institute of Chemical Engineers (AIChE). Particulate Solid Research, Inc. (PSRI). Available at : https://www.aiche.org/sites/default/files/cep/20141121.pdf.

Collot, A. G., Y. Zhuo, D. R. Dugwell, and R. Kandiyoti (1999). Co-pyrolysis and co-gasification of coal and biomass in bench scale fixed bed gasifier and fluidized bed reactors. Fuel 78(6): 667-679. ISSN/ISBN: 0016-2361. DOI: 10.1016/s0016-2361(98)00202-6.

Cordero, T., Rodriguez-Mirasol, J., Pastrana, J., Rodriguez, J.J. (2004). Improved solid fuels from co-pyrolysis of a high-sulphur content coal and different lignocellulosic wastes. *Fuel (Elsevier)* 83, no. 11-12: 1585–1590. https://doi.org/10.1016/j.fuel.2004.02.013.

Cornelissen, J. T., Taghipour, F., Escudié, R., Ellis, N., Grace, J. R. (2007). CFD modeling of a liquid– solid fluidized bed. *Chemical Engineering Science*; 62 (22): 6334–6348. https://doi.org/10.1016/j.ces.2007.07.014.

CPEC, (2017). China-Pakistan Economic Corridor. Available at: (Accessed 10 February 2021). http://www.cpecinfo.com/energy-generation.

Czakiert, T., Sztekler, K., Karski, S., Markiewicz, D., Nowak, W. (2010). Oxy-fuel circulating fluidized bed combustion in a small pilot-scale test rig. *Fuel Processing Technology*. 91. 1617-1623. DOI:10.1016/j.fuproc.2010.06.010.

Damartzis, Th., D. Vamvuka, S. Sfakiotakis, and A. Zabaniotou (2011). Thermaldegradation studies and kinetic modeling of cardoon (Cynara cardunculus) pyrolysis using thermo-gravimetric analysis (TGA). *Bio resource Technol.* 102 (10): 6230-6238. ISSN 0960-8524. https://doi.org/10.1016/j.biortech.2011.02.060.

Danish, M., Naqvi, M., Farooq, U., Naqvi, S. (2015). Characterization of South Asian agricultural residues for potential utilization in future 'energy mix'. *Energy Procedia*, 75: 2974 – 2980. ISSN 1876-6102. https://doi.org/10.1016/j.egypro.2015.07.604.

Daood, S.S., Javed, M.T., Rizvi A.H., Nimmo, W. (2014). Combustion of Pakistani lignite (Thar coal) in a pilot-scale pulverized fuel down-fired combustion test facility. *Energy and Fuels*, 28 (2). 1541 - 1547. http://dx.doi.org/10.1021/ef402362t.

Daryus, A., Siswantara, A. I., Budiarso, Gunadi, G. G. R., Pujowidodo, H. (2019). CFD Simulation of Multiphase Fluid Flow in a Two- Dimensional Gas-Solid Fluidized Bed Using Two Different Turbulence Models. *AIP Conf. Proc.* 2062, 020016-1–020016-13; https://doi.org/10.1063/1.5086563.

DeMartini, N., Murzin, D.Y., Forssen, M., Hupa, M. (2004). Kinetics of cyanide decomposition in alkaline solutions of high ionic strength: The catalytic effect of bicarbonate. *Industrial & Engineering Chemistry Research*, 43 (16): 4815-4821. https://doi.org/10.1021/ie034189+.

Demirbas, A (2005) Biomass co-firing for boilers associated with environmental impacts. Energy Sources 27(14):1385-1396. DOI: https://doi.org/10.1080/009083190523217.

Di Natale, F., Nigro, R., Scala, F. (2013). *Heat and mass transfer in fluidized bed combustion and gasification systems. In Fluidized Bed Technologies for Near-Zero Emission Combustion and Gasification.* Scala, F., Ed.; Woodhead Publishing: Sawston, UK, pp. 177–253.

Diego Perrone, (2015a). A study of an oxy-coal combustion with wet recycle using CFD modeling. *ATI 2015. Energy Procedia*, 82: 900-907. ISSN 1876-6102. https://doi.org/10.1016/j.egypro.2015.11.837.

Diego, L.F., Londono, C.A., Wang, X.S., and Gibbs, B.M. (1996b). Influence of operating parameters on NOx and N_2O axial profiles in a circulating fluidized bed combustor. *Fuel*, 75 (8): 971-978. ISSN 0016-2361. https://doi.org/10.1016/0016-2361(96)00045-2.

Dong X. (2021). Optimization of the operational controllable factor for firing lignite blend at the bituminous coal-fired boiler. *In Workshop on coal blending technology and fuel intelligence for coal-fired power plants.* Zhibo, Shangdong, China, 27-29 Apr 2021. 30 pp (Apr 2021 in Chinese).

Dooley, B. and Mason, P. E. (2018). *Supply chain costs of biomass cofiring. CCC/286, London, UK.* IEA Clean Coal Centre. ISBN 978-92-9029-609-6, 85 pp. Available at : http://unia-ups.pl/wp-content/uploads/2018/06/Za%C5%82.3_Supply-chain-biomass-ExecSum.pdf.

Downmore, M., Jambwa, S. D., and Kusaziwa K. P. (2015). Trends in the control of NOx and SOx combustion emissions: Implications to the design of fluidized bed combustion operations. *Proceedings of the Institution of Mechanical Engineers, Part E: Journal of Process Mechanical Engineering,* 231 (3):349-358. Doi:10.1177/0954408915601296.

Dwivedi, K. K., Karmakar, M. K., Pramanick, A. K. and Chatterjee, P. K. (2019). A Brief Review on Hydrodynamic Behavior Analysis of Coal Gasification in a Circulating Fluidized Bed Gasifier. *International Journal of Heat and Technology,* 37 (3): 792-802. https://doi.org/10.18280/ijht.370316.

EIU Report. (2017) http://www.eiu.com/industry/arti cle/825415066/betting-on-coal-to-solve-the-electricity-shortage/2017-05-11. The Economist Intelligence Unit (Accessed 11th May 2017).

Elsukov, V. and Latushkina, S. (2020). Features of formation and reduction of sulfur dioxide emissions when burning brown coal in boilers with liquid slag removal. *E3S*

Web of Conferences 209, 03012 (2020) ENERGY-21. https://doi.org/10.1051/e3sconf/202020903012.

Emami, M. D., Shahbazian, H., Sunden, B. (2019). Effect of Operational Parameters on Combustion and Emissions in an Industrial Gas Turbine Combustor. *J. Energy Resour. Technol*. 141 (1): 012202. DOI: https://doi.org/10.1115/1.4040532.

Emérita, D., Miguel, Q. Juan, P. Hector, A. Borja, V. (2020). Estimation of the Energy Consumption of the Rice and Corn Drying Process in the Equatorial Zone. Appl. Sci. 10 (21): 7497; https://doi.org/10.3390/app10217497.

EPA, (2020). *Overview of Greenhouse Gases*. U.S. Environmental Protection Agency, Washington, DC, USA. https://www.epa.gov/ghgemissions/overview-greenhouse-gases.

Ersoy, L E., Golriz, M. R., Koksal, M. F., Hamdullahpur. (2004). Circulating fluidized bed hydrodynamics with air staging: an experimental study. *Powder Technology*. 145 (1): 25-33. ISSN 0032-5910. https://doi.org/10.1016/j.powtec.2004.05.008.

Eudarson, C. M. and Allison, M. G. (1994). Control of NOx & N_2O emissions from circulating fluidized bed boilers. *Proceeding in 4th International Conference on Circulating Fluidized Beds.* Halifax, Nova Scotia, Canada.

Farooqui, S. Z. (2014). Prospects of renewable penetration in the energy mix of Pakistan. *Renewable and Sustainable Energy Reviews,* 29: 693–700. ISSN 1364-0321. https://doi.org/10.1016/j.rser.2013.08.083.

Fatai, K., Oxley, L., Scrimgeour, F. G. (2004). Modelling the causal relationship between energy consumption and GDP in New Zealand, Australia, India, Indonesia, The Philippines and Thailand. *Mathematics and Computers in Simulation,* 64 (3–4): 431–445. https://doi.org/10.1016/S0378-4754(03)00109-5.

Fernandez, M. J. and Lyngfelt, A. (2001). Concentration of sulphur compounds in the combustion chamber of a circulating fluidized bed boiler. *Fuel,* 80 (3): 321-326. ISSN 0016-2361. https://doi.org/10.1016/S0016-2361(00)00104-6.

Fernando, R. (2012). *Cofiring high ratios of biomass with coal*. CCC/194, London, UK, IEA Clean Coal Centre, 64 pp. ISBN 978-92-9029-514-3. Available at:

https://usea.org/sites/default/files/012012_Cofiring%20high%20ratios%20of%20biomass%20with%20coal_ccc194.pdf.

Feugier, A., Gaulie, C., and Martin, G. (1986). Some aspects of hydrodynamics, heat transfer and gas combustion in circulating fluidized beds. *Proceeding in 9th International Conference on Fluidized Bed Combustion*. San Diego, CA, USA.

Fluent, (2013). *ANSYS Fluent User's Guide*. Release 15.0. Available at: http://www.pmt.usp.br/academic/martoran/notasmodelosgrad/ANSYS%20Fluent%20Users%20Guide.pdf.

Frank, L. (2018). High efficiency biomass CFB boilers for the Asian market. *Conference Paper in Asia power week, POWER-GEN, 18-20 September 2018.* Jakarta, Indonesia.

Fuertes, A. B.; Fernandez, M. J. (1995). Kinetics of the Calcium-Sulfate Decomposition. *Chemical Engineering Research & Design*, 73 (A7): 854-862.

Gautam, N., RAM, K.V., Chaurasia A. (2020). Study on chemical kinetics and characterization of nano-silica from rice husk and rice straw in the fixed-bed pyrolysis process. *Biomass Conversion and Biorefinery,* 12: 1435–1448. https://doi.org/10.1007/s13399-020-00838-3.

Gavin, D.G. and Dorrington, M.A. (1993). Factors in the conversion of fuel nitrogen tonitric and nitrous oxides during fluidized bed combustion. *Fuel,* 72 (3); 381-388. https://doi.org/10.1016/0016-2361(93)90057-9.

Gera D., Gautam M., Tsuji Y., Kawaguchi T.T. (1998). Computer simulation of bubbles in large-particle fluidized beds. Powder Technology, 98 (1); 38-47. ISSN 0032-5910. https://doi.org/10.1016/S0032-5910(98)00017-5.

Gidaspow, D., Bezburuah, R. and Ding J. (1992). Hydrodynamics of Circulating Fluidized Beds, Kinetic Theory Approach. *In: Potter, O.E. and Nicklin, D.J., Eds., Fluidization VII, Proceedings of the 7th Engineering Foundation Conference on Fluidization, Engineering Foundation*, New York, 75-82.

Gielen, D., Boshell, F., Saygin, D., Bazilian, M. D., Wagner, N., Gorini, R. (2019). The role of renewable energy in the global energy transformation. *Energy Strategy Reviews,* 24: 38-50, ISSN 2211-467X. https://doi.org/10.1016/j.esr.2019.01.006.

Göğebakan, Y. (2006). *Simulation of Circulating Fluidized Bed Combustors*. A Ph.D. Thesis, Middle East Technical University, Ankara, Turkey.

Gómez-Barea, A., Leckner, B. (2010). Modeling of biomass gasification in fluidized bed. *Prog. Energy Combust. Sci*., 36 (4), 444–509. ISSN 0360-1285. https://doi.org/10.1016/j.pecs.2009.12.002.

GoP, (2015). *Private Power & Infrastructure Board. Ministry of Water & Power.* Government of Pakistan, Islamabad. Power Generation Policy. Available at: https://www.ppib.gov.pk/Power%20Generation%20Policy%202015%20small.pdf.

Greg, K. and Paul, B. (2022). *The Role of Low Emission Coal Technologies in a Net Zero Asian Future*. International Centre for Sustainable Carbon (ICSC). The International Energy Agency's (IEA). Coal Industry Advisory Board (CIAB). https://www.sustainable-carbon.org/team/greg-kelsall/.

Gulyurtlu, I., Abelha, P., Boavida, D., Lopes, H., Cabrita, I. (2004a). In Consideration for mixing different biomass fuels and non-toxic waste during fluidized bed combustion. *Proceeding in 2nd World Conference on Biomass for Energy, Industry and Climate Protection*, Rome, Italy, pp 1297-1300.

Gulyurtlu, I., Abelha, P., Gregorio, A., Garcia-Garcia, A., Boavida, D., Crujeira, A., Cabrita, I. (2004b). The emissions of VOCs during co-combustion of coal with different waste materials in a fluidized bed. *Energy & Fuels*, 18 (3): 605-610. https://doi.org/10.1021/ef0340155.

Gungor, A. and Eskin, N., (2008). Two-dimensional coal combustion modeling of CFB. *International Journal of Thermal Sciences*, 47 (2): 157-174. DOI: 10.1016/j.ijthermalsci.2007.01.017.

Gungor, A., (2007). Hydrodynamic modeling of a circulating fluidized bed. *Power Technology*, 172 (1): 1–13. ISSN 0032-5910. https://doi.org/10.1016/j.powtec.2006.10.035.

Gungor, A., (2009). Prediction of SO2 and NOx emissions for low-grade Turkish lignite's in CFB combustors. *Chemical Engineering Journal*, 146 (3): 388-400. DOI10.1016/j.cej.2008.06.019.

Gungor, A., (2012). Effects of Operational Parameters on SO_2 Emission in a Circulating Fluidized Bed Combustor. *Niğde Üniversitesi Mühendislik Bilimleri Dergisi*, 1 (1): 1-11. https://dergipark.org.tr/tr/download/article-file/207851.

Guo, F., He Yi., Hassanpour, A., Gardy J., Zhong Z. (2020). Thermo gravimetric analysis on the co-combustion of biomass pellets with lignite and bituminous coal. *Energy*, 197: 117147. ISSN 0360-5442. https://doi.org/10.1016/j.energy.2020.117147.

Haas, J., Tamura, M., Weber, R. (2001). Characterization of coal blends for pulverized fuel combustion. *Fuel*, 80 (9): 13l7-23. ISSN 0016-2361. https://doi.org/10.1016/S0016-2361(00)00216-7.

Hagler Bailly, (2014). *Environmental and Social Impact Assessment (ESIA).* Thar Coal power project block II final report. Hagler Bailly Pakistan. 1: 6-1 – 6-24. Available at : https://urckarachi.org/wp-content/uploads/2020/07/EIA-report-vol-1-330MW-Thar-Energy-HubPower-Company-2.compressed.pdf.

Hamalainen, J. P., Aho, M. J., and Tummavuori, J. L. (1994). Formation of Nitrogen-Oxides from Fuel-N through HCN and NH_3 - a Model-Compound Study. *Fuel*, 73 (12): 1894-1898. ISSN 0016-2361. https://doi.org/10.1016/0016-2361(94)90218-6.

Hameed, Z., Naqvi, S. R., Naqvi, M., Ali, I., Taqvi, A. S. A., Gao, N., Hussain, S. A., and Hussain, S. (2020). A Comprehensive Review on Thermal Co-conversion of Biomass, Sludge, Coal, and Their Blends Using Thermo gravimetric Analysis. *Hindawi Journal of Chemistry*, Volume 2020, Article ID 5024369, 23 pages. https://doi.org/10.1155/2020/5024369.

Hansen, K. G., Madsen, J., Ibsen, C. H., Solberg T. & Hjertager B. H. (2002). An experimental and computational study of a gas-particle flow in a scaled circulating fluidized bed. *Presented at WCP74, World Congress on Particle Technology, 21-25 July*, Sydney, NSW, Australia.

Harris, A., Davidson, J. & Thorpe, R. B. (2003). Influence of Exit Geometry in Circulating Fluidized-Bed Risers. *AIChE Journal*, 49 (1): 52 - 64. https://doi.org/10.1002/aic.690490107.

Hartge, E. U., Ratschow, L., Wischnewski, R.., Werther, J. (2009). CFD-Simulation of a Circulating Fluidized Bed Riser. *Particuology*, 7 (4): 283-296. ISSN 1674-2001. https://doi.org/10.1016/j.partic.2009.04.005.

Hashmi, S. A. M., Sabir, R., Ahmed, A. (2021). Modelling and Optimization of a Carbon Capturing Membrane Using Computational Fluid Dynamics with Case Study. *International Journal of Electrical Components and Energy Conversion*. 7 (1): 23-34. doi: 10.11648/j.ijecec.20210701.14.

Hassid, A., Klinger, M., Krzack, S., & Cohen, H. (2022). TGA-DSC Combined Coal Analysis as a Tool for QC (Quality Control) and Reactivity Patterns of Coals. *ACS omega*, *7*(2), 1893–1907. https://doi.org/10.1021/acsomega.1c05296.

HDIP, (2014). *Pakistan Energy Year Book*. Hydrocarbon Development Institute of Pakistan Available at: https://books.google.com.pk/books?id=RIGqE82osn8C&source=gbs_book_other_versions

Hina, A., Liu J., Mazher, A., Mojo, D., Muhammad, I. and Fu, C. (2018). Willingness to Pay for Improved Water Services in Mining Regions of Developing Economies: Case Study of a Coal Mining Project in Thar Coalfield, Pakistan. *Water 2018*, 10: 481. Doi:10.3390/w10040481.

Hong, B.D., Slatick, E.R. (1994). *Energy Information Administration* (DC Quarterly Coal Report, Washington, DC.) January–April 1994, DOE/EIA-0121(94/Q1) (Washington, DC, August 1994), 1–8. 2.

https://books.google.com.pk/books?id=RIGqE82osn8C&source=gbs_book_other_versions.

https://ir.lib.uwo.ca/etd/1572.

Huilin, L., Guangbo, Z., Rushan, B., Yongjin, C., Gidaspow, D. (2000). A coal combustion model for circulating fluidized bed boilers. *Fuel*, 79 (2); 165-172, ISSN 0016-2361, https://doi.org/10.1016/S0016-2361(99)00139-8.

Hupa, M. (2005). Interaction of fuels in co-firing in FBC. *Fuel*, 84 (10): 1312-1319. ISSN 0016-2361. https://doi.org/10.1016/j.fuel.2004.07.018.

Hussain, A. (2006). *Hydrodynamic and Thermo gravimetric Studies of Palm Shell Waste and Coal Blends in a Circulating Fluidized Bed Riser*. A PhD thesis by Ahmed Hussain, Department of Mechanical Engineering, University Technology Malaysia, Johor Bharu, Malaysia.

Hussain, A. and Nasir, F. (2005). The effect of riser exit geometry on hydrodynamics of a circulating fluidized bed. *MURJET*, 24 (2): 141-148.

Hussain, A., Junejo, F., Qureshi, M. N., Haque, A., (2018). Hydrodynamic and combustion behavior of low-grade coals in the riser of a circulating fluidized bed combustor. *NUST Journal of Engineering Sciences*, 11 (1): 1-11.

Hussain, S., (2015). *Factors Influencing the Formation of Producer Gas from Coal and Biomass in Circulating Fluidized Bed Gasifier*. A Ph.D. Thesis, Institute of Chemical Engineering and Technology, University of the Punjab, Pakistan. Available at: http://prr.hec.gov.pk/jspui/handle/123456789/13079

Hyunbin, Jo, Kang, K., Park, J., Ryu, C., Ahn, H., Go, Y. (2020). Detailed assessment of mesh sensitivity for CFD simulation of coal combustion in a tangential-firing boiler. *Journal of Mechanical Science and Technology*, 34 (2): 917-930. https://doi.org/10.1007/s12206-020-0141-4.

Iannello, S., Morrin, S., Materazzi, M. (2020). Fluidized Bed Reactors for the Thermochemical Conversion of Biomass and Waste. *KONA Powder and Particle Journal*, 37: 114-131. https://doi.org/10.14356/kona.2020016.

IEA, (2009). *21st Century Coal Advanced Technology and Global Energy Solutions*. Paris, IEA Coal Industry Advisory Board (CIAB).

IEA, (2020). *Global Energy & CO2 Status Report 2020*. https://www.iea.org/geco/.& https://www.iea.org/countries/pakistan. Accessed on 5th January 2021.

IEA, (2021a). *Coal 2021, Analysis and forecast to 2024 Report.* International Energy Agency: https://www.iea.org/reports/coal-2021. Accessed on 5th January 2022.

IEA, (2021b). *Net Zero by 2050- a roadmap for the global energy sector*. Available from: https://www.iea.org/reports/net-zero-by-2050. IEA special report, Paris, 222 pp.

IEA, (2022). *Electricity Market Report*. International Energy Agency Report January, 2022. Available at: https://iea.blob.core.windows.net/assets/d75d928b-9448-4c9b-b13d-6a92145af5a3/ElectricityMarketReport_January2022.pdf.

IEP, (2022). Pakistan Energy Outlook Report 2021-2030. Integrated Energy Planning for Sustainable Development. Ministry of Planning, Development & Special Initiatives Government of Pakistan. https://www.pc.gov.pk/uploads/report/IEP_Report_FINAL.pdf.

IPCC, (2018). *Intergovernmental Panel on Climate Change (IPCC) United Nation*. Available at: http://klimatsans.com/2018/10/24/omojligt-mal-i-ipcc-special-report-2018/.

Iqbal, T., Dong, C., Lu, Q. Ali, Z. Khan, I. Hussain, Z. Abbas, A. (2018). Sketching Pakistan's energy dynamics: Prospects of biomass energy. *J. Renewable Sustainable Energy*, 10 (2): 023101. https://doi.org/10.1063/1.5010393.

Irfan M., Zhao Z., Panjwani M. K., Mangi F. H., Li H., Jan A., Ahmad M., Rehman A. (2020a). Assessing the energy dynamics of Pakistan: Prospects of biomass energy. Energy Reports, 6; 80-93, ISSN 2352-4847, https://doi.org/10.1016/j.egyr.2019.11.161.

Irfan, M., Zhao, Z.Y., Mukeshimana, M.C., Ahmad, M. (2019b). Wind energy development in south asia: status, potential and policies. *Proceeding in 2nd International Conference on Computing, Mathematics and Engineering Technologies (ICoMET) 2019 Jan 30*. IEEE, pp. 1–6.

Jaffri, G. R. (2018). Thermodynamic analysis of release volatile species during high pressure gasification of biomass. *International Journal of Scientific & Engineering Research*, 9 (11): 503-508. ISSN 2229-5518.

Jallil, R., Tasirin, S., Takriff, M. S. (2002). Computational Fluid Dynamics (CFD) in Fluidized Bed column: effect of Internal Baffles. *The proceedings of RSCE Oct 2002*, Malaysia.

Jia, L., Tan, Y., Anthony, E. (2010). Emissions of SO_2 and NOx during oxy-fuel CFB combustion tests in a mini-circulating fluidized bed combustion reactor. *Energy Fuel*. 24 (2), 910–915. https://doi.org/10.1021/ef901076g.

JICA, (2013). *Data Collection Survey on Thar Coal Field in Pakistan*. Final Report, Japan international cooperation agency. Available at: https://openjicareport.jica.go.jp/pdf/12113221_01.pdf.

Johansson, T.B., McCormick, K., Neij, L., Turkenburg, W. (2004). The potentials of renewable energy. *In Proceedings for the International Conference for Renewable Energies, 1 to 4 June 2004*, Bonn, Germany. p. 40.

Jong, W.d. (2005). *Nitrogen compounds in pressurized fluidized bed gasification of biomass and fossil fuels.* A PhD thesis submitted in faculty of Design, Engineering and Production, Technical University Delft, Delft. Available at: http://resolver.tudelft.nl/uuid:10922fbb-6891-4ddd-9971-d3c8e3d22e05.

Kanwal, F., Ahmed, A., Jamil, F., Rafiq, S., Ayub, H. M. U., Ghauri, M., Khurram, M. S., Munir, S., Inayat, A., Abu Bakar, M. S. (2021). Co-Combustion of Blends of Coal and Underutilized Biomass Residues for Environmental Friendly Electrical Energy Production. *Sustainability*, 13, 4881. https://doi.org/10.3390/su13094881.

Kanwal, S., Khan, B., Qasim R. M. (2020). Infrastructure of sustainable energy development in Pakistan: A review. *Journal of Modern Power Systems and Clean Energy*, 8 (2): 206–218. DOI: 10.35833/MPCE.2019.000252.

Kaplan, S. (2021). *CCUS: Big Opportunities and Hard Questions*. Available at: https://www.powermag.com/ccus-big-opportunity-and-hard-questions/.

Kaushal, P., Pröll, T., Hofbauer, H. (2007). Modelling and simulation of the biomass fired dual fluidized bed gasifier at Guessing/Austria. *Renewable Energy and Power Quality Journal*, 1: 300-306. DOI:10.24084/repqj05.279.

Kaynak, B., Topal, H., Atimtay, A. T. (2005). Peach and apricot stone combustion in a bubbling fluidized bed. *Fuel Processing Technology*, 86 (11): 1175-1193.

Kazanc F. (2013). *Gaseous and Particulate Emissions from Pulverized Coal and Biomass Combustion under Different O_2/N_2 and O_2/CO_2 Environments*. A Thesis by Feyza Kazanc, The Department of Mechanical and Industrial Engineering, Northeastern University, Boston, Massachusetts.

Kazuhiro, K., Hanaoka, T., Fujimoto, S., Minowa, T., Sakanishi, K. (2007). Co-gasification of woody biomass and coal with air and steam. *Fuel*, 86 (5-6): 684-689.

Kelsall, G. (2020). *Carbon capture utilisation and storage status barriers and potential.* CCC/304, London, UK. International Centre for Sustainable Carbon, 99 pp. ISBN 978–92–9029–627-0. Available at: https://www.sustainable-carbon.org/login/?download-id=34008.

Khan, A.A. (2007). *Combustion and co-combustion of biomass in a bubbling fluidized bed boiler.* A PhD thesis by Atif Ahmed Khan. Technische Universiteit Delft, Netherland.

Khan, A.A., Aho, M., de Jong, W., Vainikka, P., Jansens, P.J., and Spliethoff, H. (2008). Scale-up study on combustibility and emission formation with two biomass fuels (B quality wood and pepper plant residue) under BFB conditions. *Biomass and Bioenergy,* 32 (12): 1311-1321.

Khan, W. A., Shahzad, k, Saleem M., Akhtar, N. A. and Tahir, S. (2011). Radial heat transfer investigation in a circulating fluidized bed burning makarwal coal. *Journal of Faculty of Engineering & Technology,* 18 (1): 59-70.

Khan, W.A., Shahzad K., Akhtar N.A. (2009). Hydrodynamics of Circulating Fluidized Bed Combustor: A review. *Journal of Pakistan institute of Chemical Engineering,* XXXVII: 90-94.

Khan S., Shah S. A., Ali S, Ali A., Almas L. K., Shaheen S. (2022). Technical Efficiency and Economic Analysis of Rice Crop in Khyber Pakhtunkhwa: A Stochastic Frontier Approach. *Agriculture*, 12 (4): 503. https://doi.org/10.3390/agriculture12040503.

Khatami, R., Levendis, Y. A. (2016). An overview of coal rank influence on ignition and combustion phenomena at the particle level. *Combust Flame*, 164: 22–34. Doi:10.1016/j.combustflame.2015.10.031.

Kishore S. N., Rao T. V., Kumar M. L.S. D. (2017). Furnace design of 210 mw circulating fluidized bed boiler-numerical investigation. *International Journal of Mechanical Engineering and Technology (IJMET),* 8 (3) :442–455. http://iaeme.com/Home/issue/IJMET?Volume=8&Issue=3.

Kishore, S. N., Kumar, M.L.S.D., Rao, T. V. (2021). Selection of Ca/S ratio and bed temperature for Indian lignite based CFBC boiler using simplified sulfur capture

model. *Case Studies in Chemical and Environmental Engineering*, 3: 100094. https://doi.org/10.1016/j.cscee.2021.100094.

Krzywanski, J. and Nowak, W. (2016). Artificial Intelligence Treatment of SO_2 Emissions from CFBC in Air and oxygen-enriched Conditions. *Journal of Energy Engineering*, 142 (1). https://doi.org/10.1061/(ASCE)EY.1943-7897.0000280.

Kullendorff, A. and Andersson, S. (1985). A general review on combustion in circulating fluidized beds. *Proceeding in 1st International Conference on Circulating Fluidized Beds. Halifax,* Nova Scotia, Canada.

Kumar, A., Kumar, N., Baredar, P., Shukla, A. (2015). A review on biomass energy resources, potential, conversion and policy in India. Renewable and Sustainable Energy Reviews, 45: 530–539. ISSN 1364-0321. https://doi.org/10.1016/j.rser.2015.02.007.

Kumar, H., Mohapatra, S. K., Singh, R. I. (2017). Review on CFD Modelling of Fluidized Bed Combustion Systems based on Biomass and Co-firing. *Journal of the Institution of Engineers (India)* 99(1). DOI 10.1007/s40032-017-0361-2.

Kumar, R. and Pandey, K.M. (2012). CFD Analysis of Circulating Fluidized Bed Combustion. *IRACST–Engineering Science and Technology: An International Journal (ESTIJ)*, 2 (1). ISSN: 2250-3498,

Kumar, R., Navindgi, M.C., Srinivas, G. (2016). Performance Guarantee Test Assessment of CFBC Boiler. *IJISET - International Journal of Innovative Science, Engineering & Technology*, 3 (7). ISSN (Online) 2348 – 7968.

Kumar, S. S., Sathyabalan, P. (2018). CFD Analysis of 500 MWe Tangentially Fired Boiler Furnace. Journal of Chemical and Pharmaceutical Sciences (JCPS), 11 (1): 25-28. ISSN (Online 2349-8552).

Kurose, R., Ikeda, M., Makino, H., Kimoto, M., Miyazaki, T. (2004). Pulverized coal combustion characteristics of high-fuel-ratio coals. *Fuel*, 83 (13): 1777-1785. ISSN 0016-2361. https://doi.org/10.1016/j.fuel.2004.02.021.

Kwong, P.C.W., Chao, C.Y.H., Wang, J.H., Cheung, C.W., and Kendall, G. (2007). Co-combustion performance of coal with rice husks and bamboo. *Atmospheric Environment*. 41 (35): 7462-7472.

Lackner, M., Loeffler, G., Totschnig, G., Winter, F., and Hofbauer, H. (2004). Carbon conversion of solid fuels in the freeboard of a laboratory-scale fluidized bed combustor-application of in situ laser spectroscopy. *Fuel*, 83 (10): 1289-1298.

Leckner, B. (2015). Developments in fluidized bed conversion of solid fuels. *Therm. Sci*., 20 (00): 135-135. DOI:10.2298/TSCI150703135L.

Leckner, B., Amand, L.E., Lucke, K., and Werther, J. (2004). Gaseous emissions from co-combustion of sewage sludge and coal/wood in a fluidized bed. *Fuel,* 83 (4-5): 477-486.

Leckner, B., Karlsson, M., Mjornell, M., and Hagman, U. (1992). Emissions from a 165-Mw (Th) Circulating Fluidized-Bed Boiler. *Journal of the Institute of Energy*, 65 (464): 122-130.

Leckner, B.; Karlsson, M. (1993). Gaseous Emissions from Circulating Fluidized-Bed Combustion of Wood. *Biomass & Bioenergy*, 4 (5): 379-389.

Lee, S. Y., Sankaran, R., Chew, K. W., Tan, C. H., Krishnamoorthy, R., Chu, D.T., Show, P. L. (2019). Waste to bioenergy: a review on the recent conversion technologies. *BMC Energy*, 1, 4. https://doi.org/10.1186/s42500-019-0004-7.

Levendis, Y.A., Joshi, K., Khatami, R., Sarofim, A.F. (2011). Combustion behavior in air of single particles from three different coal ranks and from sugarcane bagasse. *Combust Flame*; 158:452–65. https://doi.org/10.1016/j.combustflame.2010.09.007.

Li, S., Chen X., Liu A., Li W., and Yu G. (2014). Study on co-pyrolysis characteristics of rice straw and shenfu bituminous coal blends in fixed bed reactor. *Bio resource Technology (Elsevier)* 155 (0): 252-257.

Li, S., Wu, A., Deng, S., and Pan, W. P. (2008). Effect of co-combustion of chicken litter and coal on emissions in a laboratory-scale fluidized bed combustor. *Fuel Processing Technology*, 89 (1): 7-12.

Liang, D. Li, Y. Zhou, Z. (2022). Numerical Study of Thermochemistry and Trace Element Behavior during the Co-Combustion of Coal and Sludge in Boiler. *Energies*, 15, 888. https://doi.org/10.3390/en15030888.

Lim, M. Tzeng, S. P., Justin N. (2012). Investigation of solids circulation in a cold model of a circulating fluidized bed. *Powder Technology,* 226 (0): 57-67.

Liu, D.; Li, W.; Li, S.; Song, W.; Liu, D. Kong, R. (2019b). Transformation characteristics of sodium, chlorine and sulfur of Zhundong coal during O_2/CO_2 combustion in circulating fluidized bed. *Energy*, 185: 254–61.

Liu, H. and Gibbs, B.M., (1998). Influence of limestone addition at different positions on gaseous emissions from a coal fired circulating fluidized bed combustor. *Fuel*, 77 (14): 1569-1577.

Liu, X., Yang, H., Lyu, J., (2020a). Optimization of Fluidization State of a Circulating Fluidized Bed Boiler for Economical Operation. *Energies*, 13 (376). Doi: 10.3390/en13020376.

Liu, X., Zhang, M., Zhang, S., Ding, Y., Huang, Z., Zhou, T., Yang, H., Yue, G. (2022). Measuring Technologies for CFB Solid Circulation Rate: A Review and Future Perspectives. *Energies*,15: 417. https://doi.org/10.3390/en15020417.

Liu, Y., Huo P., Li X., Qi H. (2020b). Numerical analysis of the operating characteristics of a large-scale CFB coal-gasification reactor with the QC-EMMS drag model. *Can. J. Chem. Eng.* 99:1390–1403. DOI: 10.1002/cjce.23911.

Liu, Y., Jiang, L., & Zhang, Y. (2021b). Hydrodynamic Modeling of Turbulence Modulation by Particles in a Swirling Gas-Particle Two-Phase Flow. *ACS Omega*, 6 (15), 10106–10118. https://doi.org/10.1021/acsomega.1c00085.

Liu, Y., Liu, S., Li, Y., He, J. (2021a). Influence of Operating Parameters on Chlorine Release and Pollutant Emission Characteristics of a 130 t/h BCFB Combustion System. *ACS Omega* 6: 12530−12540. https://doi.org/10.1021/acsomega.1c00270.

Liu, Y., Peng, J., Kansha, Y., Ishizuka, M., Tsutsumi, A., Jia, D., Bi, X.T., Lim, C.J., Sokhansanj, S. (2014). Novel fluidized bed dryer for biomass drying. *Fuel Processing Technology*, 122: 170–175. DOI:10.1016/j.fuproc.2014.01.036.

Liu, Z., Ma, S., Pan, X., Chen, J. (2019a). Experimental study on the load response rate under the dynamic combined combustion of PC coal and CFB coal in a CFB boiler. *Fuel*, 236: 445-451.

Liukkonen, M., Heikkinen, M., Alikk, E. H., Hiltunen, T., Hiltunen, Y.O., (2010). Analysis of Flue Gas Emission Data from Fluidized Bed Combustion Using Self-

Organizing Maps. *Applied Computational Intelligence and Soft Computing*, 2010, Article ID 932467, 8 pages, https://doi.org/10.1155/2010/932467.

Lockwood, T. (2013). *Techno-Economic Analysis of PC Versus CFB Combustion Technology*. Report CCC/226; IEA Clean. Coal Centre: London, UK, 2013.

Lu, C.Y., Yan, X.P., Zhang, Z.P., Wang, Z.P., Liu, L.W. (2004). Flow injection on-line sorption pre-concentration coupled with hydride generation atomic fluorescence spectrometry using a polytetrafluoroethylene fiber-packed microcolumn for determination of Se (IV) in natural water. *Journal of Analytical Atomic Spectrometry*, 19: 277-281.

Luecke, K., Hartge, E., Werther, J. (2004). A 3D model of combustion in large-scale circulating fluidized bed boilers. *International Journal of Chemical Reactor Engineering,* 2 (1). DOI: 10.2202/1542-6580.1135.

Lundqvist, R., Basak, A. K., Smedley, J., Boyd, T. J. (1991). An evaluation of process performance and scale up effects for Ahlstrom Pyro flow circulating fluidized bed boiler. *Proceeding in 11th International Conference on Fluidized Bed Combustion*. Montreal, Canada.

Lyngfelt, A. and Leckner, B. (1999). Combustion of wood-chips in circulating fluidized bedboilers -- NO and CO emissions as functions of temperature and air-staging. *Fuel*, 78 (9): 1065-1072.

Madejski, P. and Mondinski, N. (2019). Numerical investigation using two different CFD codes of pulverized-coal combustion process characteristic in an industrial power plant boiler. *E3S Web of Conferences 82, 01009, ICBT Poland*. https://doi.org/10.1051/e3sconf/20198201009.

Madhiyanon, T., Sathitruangsak, P., and Soponronnarit, S. (2009). Co-combustion of rice husk with coal in a cyclonic fluidized-bed combustor ([psi]-FBC). *Fuel*, 88 (1): 132-138.

Magalhães, D., Panahi, A., Kazanç, F., Levendis, Y. A. (2019). Comparison of single particle combustion behaviors of raw and terrified biomass with Turkish lignite's. *Fuel*, 241:1085–94. Doi:10.1016/j.fuel.2018.12.124.

Magalhães, D., Panahi, A., Kazanç, F., Levendis, Y.A. (2019). Comparison of single particle combustion behaviours of raw and torrefied biomass with Turkish lignite's. *Fuel*, 241:1085–94. https://doi.org/10.1016/j.fuel.2018.12.124.

Mahar, R. B. (2010). *Converting Waste Agricultural Biomass into Energy Source*. Online available: http://www.unep.or.jp/ietc/GPWM/data/T3/AB_4_1_BaselineReport.pdf. Accessed. pag. 26, 27.

Maitlo, G., Kandhro, G. A., Korai, R. M., Shah, A. K., Maitlo, I. (2019). Computational Fluid Dynamic (CFD) Simulation of Thar Lignite Coal and Sugarcane Bagasse in Entrained Flow Gasifier. *Pak. J. Anal. Environ. Chem*. 20 (2): 141–150. http://doi.org/10.21743/pjaec/2019.12.18.

Mal, V., Abro, M., Brohi, K. M., Memon, A. S., Unar, I. N. (2021). Investigating the Effects of Different Operating Parameters on the Performance of Biomass Gasification Mixed with Coal in Multi-Opposite Burner (MOB) Gasifier. *Engineering Science and Technology International Research Journal*, 5 (1): 74-81. ISSN (e) 2520-7393.

Malik, S., Qasim, M., Saeed, H., Chang, Y., Taghizadeh-Hesary, F. (2019). Energy Security in Pakistan: A Quantitative Approach to a Sustainable Energy Policy. *ADBI Working Paper 1024. Tokyo: Asian Development Bank Institute*. Available: https://www.adb.org/publications/energy-security-pakistan-sustainable-energy-policy.

Malkani, M. S. (2012). A Review of Coal and Water Resources of Pakistan. *Journal of Science, Technology and Development*, 31 (2): 202-218. ISSN: 0254-6418.

Manook, M. (2021). *Stop wordsmithing around coal. Financial Times*. Available at: https://www.ft.com/content/30fc0408-3d7a-4490-ab09-81ff2393305a. (Subscription required).

Mashi A. 2018. Thar Coalfield: Sustainable Development and an Open Sesame to the Energy Security of Pakistan. *IOP Conf. Series: Journal of Physics: Conf. Series, 989, 012004, Chiyi, Taiwan*; DOI: http://dx.doi.org/10.1088/1742-6596/989/1/012004.

Meer, E. H., Thorpe, R. B., Davidson, J. F. (2000). Flow patterns in the square cross-section riser of circulating fluidized bed and the effect of riser exit design. *Chemical Engineering Science*, 55 (19): 4079-4099.

Meer, E.H. (1997). *Riser Exits and Scaling of Circulating Fluidized Beds*. Ph.D. dissertation. University of Cambridge, United Kingdom.

Mehdi, M., Siddiqi, M. H. (2020). Study of Hydrothermally Lignite and Rice Husk blend: Thermo gravimetric Analysis. *IOP Conf. Series: Materials Science and Engineering*, 738 012022; Doi:10.1088/1757-899X/738/1/012022.

Mehrabian, R., Scharler, R., and Obernberger, I. (2012). Effects of pyrolysis conditions on the heating rate in biomass particles and applicability of TGA kinetics parameters in practical thermal conversion modeling. *Fuel,* 93 (1):567–575. DOI:10.1016/j.fuel.2011.09.054.

Memon T. A., Harijan K., Soomro M. I., Meghwar S., Valasai G. D., Khoharo H. (2017). Potential of Electricity Generation from Rice Husk-A Case Study of Rice Mill. *Sindh Univ. Res. Jour. (Sci. Ser.),* 49 (3): 495-498.

Meneses. M., Schuhmacher. M., Domingo, J.L. (2004). Health risk assessment of emissions of dioxins and furans from a municipal waste incinerator: comparison with other emission sources. *Environment International,* 30 (4): 481– 489. DOI: 10.1016/j.envint.2003.10.001.

Mengal, A., Mirjat, N. H., Walasai, G. D., Khatri, S. A., Harijan, K., Uqaili, M. A. (2019). Modeling of Future Electricity Generation and Emissions Assessment for Pakistan. *Processes*, 7 (4): 212. https://doi.org/10.3390/pr7040212.

Miccio, F., Raganati, F., Ammendola, P., Okasha, F., Miccio, M. (2021). Fluidized Bed Combustion and Gasification of Fossil and Renewable Slurry Fuels. *Energies*, 14 (22):7766. https://doi.org/10.3390/en14227766.

Miller, J. A., Bowman, C. T. (1989). Mechanism and modeling of nitrogen chemistry in combustion. *Progress in Energy & Combustion Science*, 15 (4): 287-338. https://doi.org/10.1016/0360-1285(89)90017-8.

Mills, S. (2021). Potential Markets for High Efficiency, Low Emissions Coal-Fired Power Plants. *International Centre for Sustainable Carbon*. ICSC Report # ICSC/312. ISBN 978–92–9029–635-5.

Mirani, A. A., Ahmad, M. Kalwar, S. A. Ahmad, T. (2013). A Rice Husk Gasifier for Paddy Drying. *Sci., Tech. and Dev*., 32 (2): 120-125.

Mirjat, N. H., Uqaili, M. A., Harijan, K., Valasai, G. D., Shaikh, F., & Waris, M. (2017). A review of energy and power planning and policies of Pakistan. *Renewable and Sustainable Energy Reviews*, 79: 110–127. https://doi.org/10.1016/j.rser.2017.05.040.

Mirza, U.K., Ahmad, N. and Majeed, T. (2008). An Overview of Biomass Energy Utilization in Pakistan. *Renewable and Sustainable Energy Reviews*, 12 (7): 1988-1996. https://doi.org/10.1016/j.rser.2007.04.001.

Mohanta, S., Meikap, B., Chakraborty, S. (2015). Impact of coal quality on thermal power plant savings: A case study for an Indian thermal power plant. *South African Journal of Chemical Engineering*, 20 (2): 56-68.

Mohiuddin, O., Mohiuddin, A. Obaidullah, M. Ahmed, H. Asumadu-Sarkodie, S. (2016). Electricity production potential and social benefits from rice husk, a case study in Pakistan. *Civil & Environmental Engineering*, 3 (1): 1177156.

Moller, P., Bauman, H., Juntgen, H. (1988). Coal combustion studies in fluidized bed in VGB Konferenz. *Forschung in der Kraftwerkstechnik*. Essen.

Monceaux, L., Azzi, M., Molodtsof, Y., Large, J.F. (1985). *Overall and local characterization of flow regimes in a circulating fluidized bed, in Circulating Fluidized Bed Technology*. Basu, P. and Editor. Pergamon Press, Toronto. p. 185-191.

Morrison, G. F. (1980). *Nitrogen oxides from combustion abatement and control*. London: IEA Coal Research. Report no ICTIS/TRII.

Mortaria, A., Avila D., Santosa, D.A.M., Crnkovica, P.M. (2010). Study of thermal decomposition and ignition temperature of bagasse, coal and their blends. *Thermal Engineering,* 9 (1): 81-88.

Moti L. M., Hemendra C. S., Richa S. (2012). Estimates of Emissions from Coal Fired Thermal Power Plants in India. *Paper presented at the 2012 international emission inventory conference, Tampa,* Florida, USA.

Munir, S. (2010). A review on Biomass-Coal Co-combustion: current state of knowledge. *Proceedings of Pakistan Academy of Sciences*, 47 (4): p. 265-287.

Munir, S. (2011). Co-combustion of Coal with Biomass: Energy for a Clean Environment. *VDM Verlag Dr. Müller.* ISBN-10: 3639327985.

Munir, S., Daood S.S., Nimmo W., Cunliffe A.M., and Gibbs B.M. (2009). Thermal analysis and devolatilization kinetics of cotton stalk, sugar cane bagasse and Shea meal under nitrogen and air atmospheres. Bioresou. Technol., 100 (3): 1413-1418.

Munir, S., Nimmo W., and Gibbs B. (2010).Co-combustion of agricultural residues with coal: turning waste into energy. *Energy & Fuels*, 24 (3): 2146-2153.

N_2O1 emission formation in an oxy-fired fluidized bed boiler. *Chinese Journal of Chemical Engineering*, 27 (2): 426-443. https://doi.org/10.1016/j.cjche.2018.06.033.

Naseem Aziz, (2015). Biomass energy potential in Pakistan. *The Free Library* (April, 12), https://www.thefreelibrary.com/BIOMASS ENERGY POTENTIAL IN PAKISTAN-a0412300568 (Accessed May 25 2021)

Naseem, I. and Khan, J. (2015). Impact of Energy Crisis on Economic Growth of Pakistan. *International Journal of African and Asian Studies,* 7: 33-42. An International Peer-reviewed Journal. ISSN 2409-6938.

Nazar, M., Yasar, A., Raza, S. A., Ahmad, A., Rasheed, R., Shahbaz, M., Tabinda, A. B. (2021). Techno-economic and environmental assessment of rice husk in comparison to coal and furnace oil as boiler fuel. *Biomass Conversion and Biorefinery*, 1-9. https://doi.org/10.1007/s13399-020-01238-3.

Nergis, Y., Khan, M. J., Mughal, N. A., Shareef, M., Butt, J. A. (2018). Management of Ground Water Hazard: A Case Study from Thar Coal Mines, Pakistan. *Int. J. Econ. Environ. Geol.*, 9 (4): 68-73. DOI: https://doi.org/10.46660/ijeeg.Vol9.Iss4.2018.191.

Ngampradit, N., Piumsomboon, P., Sajjakulnukit, B. (2004). Simulation of a Circulating Fluidized Bed Combustor with Shrinking Core and emission model. *Science Asia*, 30 (4): 365-374. DOI:10.2306/scienceasia1513-1874.2004.30.365.

Nguyen, T. D. B., Seo, M. W., Lim, Y-II., Song, B-H., Kim, S-D. (2012). CFD simulation with experiments in a dual circulating fluidized bed gasifier. *Compute. Chem. Eng*., 36, 48-56. ISSN 0098-1354. https://doi.org/10.1016/j.compchemeng.2011.07.005.

Noor, N. A. W. M., Hasini, H., Samsuri, M. S. H. M., Zulkifli, M. M. F. M. (2020). CFD Analysis on the Effects of Different Coal on Combustion Characteristics in Coal-fired Boiler. *CFD Letters,* 12 (10), 128-138. https://doi.org/10.37934/cfdl.12.10.128138.

NTDC, (2021). *Indicative Generation Capacity Expansion Plan IGCEP 2021-30*. National Transmission and Dispatch Company. Power System Planning Report, May 2021. https://nepra.org.pk/Admission%20Notices/2021/06%20June/IGCEP%202021.pdf.

Nussbaumer, T., (2003). Combustion and Co-combustion of Biomass: Fundamentals, Technologies, and Primary Measures for Emission Reduction. *Energy & Fuels,* 17 (6): 1510-1521. https://doi.org/10.1021/ef030031q.

Oka, S. (2003). *Fluidized Bed Combustion*. Thermal Science, 7 (2): 105-107. Published by Marcel Dekker, Inc.: New York, USA. https://doi.org/10.2298/TSCI0302105G.

Oka, S., & Anthony, E. J. (2004). *Fluidized bed combustion*. In Harmful matter emission from FBC boilers. Chap. 7, vol. 162, pp. 505–580). New York: CRC Press, Marcel Dekker, Inc.

Oloruntoba, A., Zhang, Y., Hsu, C.S. (2022). State-of-the-Art Review of Fluid Catalytic Cracking (FCC) Catalyst Regeneration Intensification Technologies. *Energies*, 15, 2061. https://doi.org/10.3390/en15062061.

Otero, M., Gomez, X., Garcia, A., Moran A. (2008). Non-isothermal thermo-gravimetric analysis of the combustion of two different carbonaceous materials coal and sewage sludge. *J. Therm. Anal. Calorim.*, 9: 619-26. https://doi.org/10.1007/s10973-007-8415-y.

Özer, B. (2019). *A Study on Coal Combustion: Experiments and Modelling*. A MS Thesis Submitted to Mechanical Engineering Department, Middle East Technical University, Turkey.

Pan, Y. G., Velo, E., Roca, X., Manya, J. J. Puigianer, L. (2000). Fluidized bed co-gasification of residual biomass /poor coal blends for fuel gas production. *Fuel*, 79 (11): 1317-1326. https://doi.org/10.1016/S0016-2361(99)00258-6.

Patel, V.R., Patel, R.N., Rao, V.J. Kinetic Study of Indian Lignite by Model-Free Methods. *J. Inst. Eng. India Ser. C* 103, 837–845 (2022). https://doi.org/10.1007/s40032-022-00859-z.

Patra, C. (2013). *CFD Simulation of Fluidized Bed Biomass Gasification*. A MS thesis, submitted to Department of Chemical Engineering, National Institute of Technology Rourkela, Odisha, India.

Patrizio, P., Fajardy, M., Bui, M., Dowell, N. M. (2021). CO_2 mitigation or removal: The optimal uses of biomass in energy system decarbonization. *iScience*, 24 (7). 102765, ISSN 2589-0042. https://doi.org/10.1016/j.isci.2021.102765.

Paweł, M. (2018). Numerical study of a large-scale pulverized coal-fired boiler operation using CFD modeling based on the probability density function method. *Applied Thermal Engineering*, 145: 352-363. https://doi.org/10.1016/j.applthermaleng.2018.09.004.

Pedersen, L. S., Nielsen, H. P., Kiil, S., Hansen, L. A., et al. (1996). Full-scale co-firing of straw and coal. *Fuel*, 75 (13): 1584–1590. ISSN 0016-2361. https://doi.org/10.1016/0016-2361(96)82642-1.

Peng, B., Zhu, J. Zhang, C. (2012). A new approach to specify the inlet boundary conditions for computational fluid dynamics (CFD) modeling of hydrodynamic behavior of a circulating fluidized bed (CFB) riser. *Ind. Eng. Chem. Res*., 51 (4): 2152 – 2165. https://doi.org/10.1021/ie200916c.

Peng, J., Sun, W., Han, H., Xie, L. (2021). CFD Modeling and Simulation of the Hydrodynamics Characteristics of Coarse Coal Particles in a 3D Liquid-Solid Fluidized Bed. *Minerals*, 11 (6): 569. https://doi.org/10.3390/min11060569.

PES (2021). *Pakistan Economic Survey 2020-21*. Retrieved from: http://www.finance.gov.pk/survey/chapters_21/14-Energy.pdf. On 20 March 2022.

Peters, J., May, J., Ströhle, J., Epple, B. (2020). The flexibility of CFB Combustion: An Investigation of Co-Combustion with Biomass and RDF at Part Load in Pilot Scale. *Energies*, 13 (8): 4665. https://doi.org/10.3390/en13184665.

Pohl J. H., Sarofim A. F. (1977). Devolatilization and oxidation of coal nitrogen. Symposium (International) on Combustion, 16 (1): 491-501. https://doi.org/10.1016/S0082-0784(77)80346-9.

PPIB, (2017). *About Pakistan. Private Power and Infrastructure Board*. Retrieved 3, February 2017. https://www.ppib.gov.pk/pakistan.html.

Prins, M. J., Ptasinski K. J., Janssen F.J.J.G. (2007). From coal to biomass gasification: Comparison of thermodynamic efficiency. Energy, 32 (7): 1248-1259. ISSN 0360-5442. https://doi.org/10.1016/j.energy.2006.07.017.

Procter, R. (2017). Cutting carbon emissions from electricity generation. *The Electricity Journal*, 30 (2): 41–46.

Prokhorova D.A. and Piralishvilib S. A., (2020). Numerical Simulation of Pulverized Coal Combustion and Comparison with In-furnace Measurements. *AIP Conf. Proc. 2211, 040008-1–040008-7.* https://doi.org/10.1063/5.0000688.

Puig-Arnavat, M., Bruno, J.C., Coronas, A. (2010). A Review and analysis of biomass gasification models. Renew. Sustain. *Energy*, 14 (9): 2841–2851. ISSN 1364-0321. https://doi.org/10.1016/j.rser.2010.07.030.

Qi, S. Z., Wang, Z., Costa, M., He, Y., Cen, K. (2021). Ignition and combustion of single pulverized biomass and coal particles in N2/O2 and CO_2/O_2 environments. *Fuel*, 283: 118956. ISSN 0016-2361. https://doi.org/10.1016/j.fuel.2020.118956.

Querol, X., Alastuey, A., Puicercus, J. A., Mantilla, E., Ruiz, C.R., Lopez-Soler, A., Plana, F., Juan, R., Atmos, J. (1998). Seasonal evolution of suspended particles around a large coal-fired power station: particulate levels and sources. *Atmos. Environ*. 32 (11): 1963-1978. ISSN 1352-2310. https://doi.org/10.1016/S1352-2310(97)00504-9.

Quispe, I., Navia, R. Kahhat, R. (2017). Energy potential from rice husk through direct combustion and fast pyrolysis: A review. *Waste Management,* 59: 200–210. ISSN 0956-053X. https://doi.org/10.1016/j.wasman.2016.10.001.

Raheem, A., Abbasi, S. A., Memon, A., Samo, S. R., Taufiq, Y. H., Danquah, M. K., Harun R. (2016). Renewable energy deployment to combat energy crisis in Pakistan. *Energy, Sustainability and Society*, 6 (1). DOI 10.1186/s13705-016-0082-z.

Rajat Walia (2022). CFD Process. Available at: https://www.linkedin.com/posts/rajat-walia_mechanicalengineering-cfd-simulation-activity-7001071427214819328-5YSX?trk=public_profile_like_view.

Rajan, R. R., Krishnan, R., and Wen, C. Y. (1978). Simulation of fluidized bed combustors: Coal devolatilization and sulfur retention. *Symposium series no.176, AlChE. p. 112.*

Rather, R. A., Wani, A. W., Mumtaz, S., Padder, S. A., Khan, A. H., Almohana, A. I., Almojil, S. F., Alam, S. S., Baba, T. R. (2022). Bioenergy: a foundation to environmental sustainability in a changing global climate scenario. *Journal of King Saud University Science*, 34 (1): 101734. ISSN 1018-3647. https://doi.org/10.1016/j.jksus.2021.101734.

Raza, M. A., Khatri, K. L., Memon, M. A., Rafique, K., Haque, M. I. U., Mirjat, N.H. (2022). Exploitation of Thar coalfield for power generation in Pakistan: A way forward to sustainable energy future. *Energy Exploration & Exploitation*. 1–24. Doi: 10.1177/01445987221082190.

Rehman, A., Ma, H. Radulescu, M. Sinisi, C.I. Yousaf, Z. (2021). Energy Crisis in Pakistan and Economic Progress: Decoupling the Impact of Coal Energy Consumption in Power and Brick Kilns. *Mathematics*, 9 (17): 2083. https://doi.org/10.3390/math9172083.

Rehman, M. (2020). *Pakistan's electricity generation has increased over time. So why do we still not have uninterrupted supply*? DAWN.COM. Retrieved 4 June 2020. https://www.dawn.com/news/1430728.

Rehman, S. M. (2018). *Clean Coal Technologies for Power Sector and their Scope in SAARC Member States.* SAARC Energy Center Report.

https://www.saarcenergy.org/wp-content/uploads/2018/06/Report-of-CCTs-Study.pdf.

Rehman, S., Cai, Y., Mirjat, N. H., Walasai, G. D., Shah, I. A., Ali, S. (2017). The future of sustainable energy production in Pakistan: A system dynamics-based approach for estimating Hubbert Peaks. *Energies,* 10 (11): 1858. https://doi.org/10.3390/en10111858.

Reid, W. V., Ali, M. K., & Field, C. B. (2020). The future of bioenergy. *Global change biology*, 26 (1): 274–286. https://doi.org/10.1111/gcb.14883.

Riaza, J., Khatami, R., Levendis, Y. A., Álvarez, L., Gil, M. V., Pevida, C. (2014). Single particle ignition and combustion of anthracite, semi-anthracite and bituminous coals in air and simulated oxy-fuel conditions. *Combust Flame*, 161 (4): 1096–108. Doi:10.1016/j.combustflame.2013.10.004.

Rizvi, A. H, Daood, S. S, Javed, M. T, Munir, S., Pourkashanian, M., Nimmo, W. (2015). Reactivity Analysis of Pakistani Thar Lignite Reserves in Oxidizing Thermogravimetric Analysis Atmospheres. *Energy Fuels*, 29 (8): 5349−5360. DOI: https://doi.org/10.1021/acs.energyfuels.5b00748.

Sáez-Martínez, F., Lefebvre, G., Hernández, J. J., Clark, J. H. (2016). Drivers of sustainable cleaner production and sustainable energy options. *Journal of Cleaner Production,* 138 (1): 1–7. https://doi.org/10.1016/j.jclepro.2016.08.094.

Safi, M. J., Mishra I. M., Prasad B. (2004). Global degradation of pine needles in air. *Thermochimica Acta*, 412 (1-2): 155-162. https://doi.org/10.1016/j.tca.2003.09.017.

Sahu, R. K., Rao, G. I., Maurya, K. (2015). Energy Performance Assessment of CFBC Boiler. *International Journal of Engineering Research & Technology (Ijert)*. *ISNCESR-2015 Conference Proceedings*, 3 (20). ISSN: 2278-0181.

Sahu, S.G., Chakraborty N., Sarkar P. (2014). Coal–biomass co-combustion: An overview. *Renewable and Sustainable Energy Reviews*, 39: 575-586. https://doi.org/10.1016/j.rser.2014.07.106.

Saini, J.K., Saini, R. & Tewari, L. (2015). Lignocellulosic agriculture wastes as biomass feedstocks for second-generation bioethanol production: concepts and

recent developments. *3 Biotech*, 5: 337–353. https://doi.org/10.1007/s13205-014-0246-5.

Salahi, S. (2012). *Automated Process and Geometry Design Optimization of a Coal Combustion Reactor*. A PhD Thesis submitted to Graduate School, New Brunswick Rutgers, Mechanical and Aerospace Engineering, The State University of New Jersey, USA. https://doi.org/doi:10.7282/T3MG7NJ6.

Sanger, M., Werther, J., Ogada, T. (2001). NOx and N_2O emission characteristics from fluidized bed combustion of semi-dried municipal sewage sludge. *Fuel*, 80 (2):167-177. https://doi.org/10.1016/S0016-2361(00)00093-4.

Sarofim, A. F., & Beer, J. M. (1979). Modeling of fluidized bed combustion. *In 17th Symposium (International) on Combustion (pp. 189–204). Combustion Institute.*

Sarwar, A., Khan, M. N. & Azhar, K. F., (2014). The Physicochemical Characterization of a Newly Explored Thar Coal Resource. *Energy Sources, Part A: Recovery, Utilization, and Environmental Effects*, 36 (5): 525-536. https://doi.org/10.1080/15567036.2010.542447.

Sarwar, A., Khan, M. N., Azhar, K. F. (2012). Kinetic studies of pyrolysis and combustion of Thar coal by thermogravimetry and chemometric data analysis. *J Therm Anal Calorim*, 109: 97–103. DOI 10.1007/s10973-011-1725-0.

Sasongko, D., Wulandari, W., Rubani, I. S., Rusydiansyah, R. (2017). Effects of Biomass Type, Blend Composition, and Co-pyrolysis Temperature on Hybrid Coal Quality. *AIP Conference Proceedings 1805, 040009 (2017)*. https://doi.org/10.1063/1.4974430.

Sathitruangsak, P. and Madhiyanon, T. (2017). Effect of Operating Conditions on the Combustion Characteristics of Coal, Rice Husk, and Co-firing of Coal and Rice Husk in a Circulating Fluidized Bed Combustor. *Energy & Fuels*, 31 (11). DOI:10.1021/acs.energyfuels.7b01513.

Senneca, O., Salatino, P., Chirone, R. (1999). A fast heating-rate Thermogravimetric study of the pyrolysis of scrap tyres. Fuel (Elsevier) 78 (13): 1575-1581. https://doi.org/10.1016/S0016-2361(99)00087-3.

Seo, M. W., Goo, J. H., Kim, S. D., Lee, S. H., Choi Y. C. (2010). Gasification characteristics of coal/biomass blend in a dual circulating fluidized bed reactor. *Energy Fuels*, 24 (5): 3108-3118. https://doi.org/10.1021/ef100204s.

Seville, J. P. K., Ding, Y. L., Stein, M. (2005). Particle Motion in Bubbling Fluidized Beds. *Proceedings of the 3rd European Conference on Fluidization, Toulouse*, 44: 717- 736.

Shabbir, A., (2018). Towards Pakistan's Energy Security and Competitiveness. Pakistan Economic Forum – Energy Panel, Centre of Excellence in Responsible Business. Retrieved from: https://policycommons.net/artifacts/1546438/towards-pakistans-energy-security-and-competitiveness-pakistan-economic-forum/2236273/ on 25 May 2021. CID: 20.500.12592/83v6bm.

Shah, S. A., Soomar, M., Hussain, A. (2016). Comparative Emission Analysis of Bituminous Coal, Sugarcane Bagasse and Rice Husk. *Sindh Univ. Res. Jour. (Sci. Ser.)*, 48 (3): 685-688.

Shahbaz, M., Al-Ansari, T., Aslam, M., Khan, Z., Inayat, A., Athar, M., Naqvi, S. R., Ahmed, M. A., McKay, G. (2020). A state-of-the-art review on biomass processing and conversion technologies to produce hydrogen and its recovery via membrane separation. *Int J. Hydrog Energy*, 45 (30): 15166–15195. https://doi.org/10.1016/j.ijhydene. 2020.04.009.

Shahzad, K., Saleem, M., Ghauri, M., Akhtar, J., Ali, N., Akhtar N. A. (2015). Emissions of NO_X, SO_2 and CO from co-combustion of wheat straw and coal under fast fluidized bed condition. *Combustion Science and Technology*, 187 (7): 1079-1092. https://doi.org/10.1080/00102202.2014.1002561.

Shaikh, S., (2016), Thar coal separating facts from fiction. Tribune the Express, https://tribune.com.pk/story/1069526/thar-coal-separating-facts-from-fiction/. (Accessed 21 March 2020).

Sheikh, K. El., Khan, M. J., Mahar D. H., et al. (2019). Advances in reduction of NOx and

Shen, C.H., Wei-H.C., Heng-W. H., Jieh-Y. S., Tzu-H. H. (2012). Co-gasification performance of coal and petroleum coke blends in a pilot-scale pressurized

entrained-flow gasifier. *Int. J. Energy Res. (Wiley),* 36 (4): 499-508. https://doi.org/10.1002/er.1821.

Shen, D.K., Gu, S., Luo, K.H., Bridgwater, A.V., Fang, M.X. (2009). Kinetic study on thermal decomposition of woods in oxidative environment. Fuel (Elsevier) 88 (6): 1024-1039. https://doi.org/10.1016/j.fuel.2008.10.034.

Shimizu, F., Satoh, M., Sato, K., Tonsho, M., and Inagaki, N. (2002). Simultaneous reduction of SO_2 and N_2O from fluidized bed combustor using sorbent circulation. *7th Conference on Circulating Fluidized Bed. Ontario, Canada.*

Siddiqi, H., Hussain, M. A., Iqbal, T., Tabish, A.N., Mahmood, W., Qureshi, T. (2018). Combustion and Pyrolysis Study of Pakistani Coal, Rice Husk, and Their Blends via TGA Analysis. *International Conference on Energy Conservation and Efficiency (ICECE),* 43-48. DOI:10.1109/ECE.2018.8554987.

Siddique, M., Amin, M., Soomro, S. A., Kakar, E., Bacha, S. (2013). Thermogravimetric Analysis (TGA) of Lignite Coal, Tree Leaves and Their blend. *J. App. Em. Sc.*, 4 (2): 118-121.

Singh, R. I., Brink, A., Hupa, M. (2013). CFD modeling to study fluidized bed combustion and gasification. *Appl. Therm. Eng*., 52 (2): 585-614. https://doi.org/10.1016/j.applthermaleng.2012.12.017.

Skreiberg, Ø., Li, T., Vantaggiato, E., Wang, L., Bugge, M., Løvås ,T. (2019). An evaluation of effects of operational parameters on NOx emissions through detailed chemical kinetics simulations. *Energy Procedia*, 158: 103-110, ISSN 1876-6102, https://doi.org/10.1016/j.egypro.2019.01.053.

Smith, K. L., Smoot, L. D., Fletcher, T. H., Pugmire, R. J. (1994). Introduction. In: *The Structure and Reaction Processes of Coal*. The Plenum Chemical Engineering Series (PCES). The Springer Chemical Engineering Series. Springer, Boston, MA. ISBN: 978-1-4899-1322-7. https://doi.org/10.1007/978-1-4899-1322-7_1.

Solomon, P.R. and colket, M.B. (1978). Coal emissions studies in fluidized bed. *Fuel*, 57: 749-756.

Sonibare, O. O., Ehinola, O. A., Egashir, R., Giap, L.K. (2005). An investigation into thermal decomposition of Nigerian coal. *Journal of Applied Science*, 5 (1): 104-107. DOI:10.3923/jas.2005.104.107.

Sonobe, T. **and** Worasuwannarak, N. (2006). Pyrolysis Characteristics of blend of Agricultural Residues with Lignite. *Asian Journal of Energy and Environment*, 7 (03): 347-355.

Spinti, J.P., Pershing, D.W. (2003). The fate of char-N at pulverized coal conditions. *Combust Flame*, 135 (3): 299–313. DOI: 10.1016/S0010-2180(03)00168-8.

Spörla, D. R., Maiera, D. J., Scheffknechta, T. G. (2013). Sulphur Oxide Emissions from Dust-Fired Oxy-Fuel Combustion of Coal. *Energy Procedia*, 37: 1435 – 1447. https://doi.org/10.1016/j.egypro.2013.06.019.

Sudheer and Nagaraj, M. R. (2016). CFD Simulation of Circulating Fluidized Bed Combustion. *International Journal for Scientific Research & Development,* 4 (06): 947-953. ISSN (online): 2321-0613. Avilable at: https://ijsrd.com/Article.php?manuscript=IJSRDV4I60512.

Sun, Z., Zhang, C., Zhu J. (2022). Numerical investigations on gas–solid flow in circulating fluidized bed risers using a new cluster-based drag model. *Particuology*, 63: 9-23, ISSN 1674-2001. https://doi.org/10.1016/j.partic.2021.05.008.

Sweeten, J. M. (2003). Co-firing of coal and cattle feedlot biomass (FB) fuels. Part I. Feedlotbiomass (cattle manure) fuel quality and characteristics. *Fuel*, 82 (10): 1167-1182. https://doi.org/10.1016/S0016-2361(03)00007-3.

Taghipour, F., Ellis, N., & Wong, C. (2003). CFD modeling of a two-dimensional fluidized-bed reactor. In Ollivier-Gooch, C. (Ed.). *Eleventh annual conference of the CFD Society of Canada (CFD 2003) Proceedings, (p. 132 Megabytes).* Canada: CFD Society of Canada.

Tahir, M., and Ayaz, M. (2018). Energy Security and Economic Growth in Pakistan. *Pakistan Journal of Applied Economics*, 28(1): 47–64.

Tareen, W.U.K., Dilbar, M.T., Farhan, M., Ali, N. M., Durrani, A.W., Memon, K.A., Mekhilef, S., Seyedmahmoudian, M., Horan, B., Amir, M., Aamir, M. (2020). Present Status and Potential of Biomass Energy in Pakistan Based on Existing and

Future Renewable Resources. *Sustainability*, 12 (1): 249. https://doi.org/10.3390/su12010249.

Tarelho, L.A.C., Matos, M., Pereira, F.J.M.A. (2005). The influence of operational parameters on SO_2 removal by limestone during fluidized bed coal combustion. Fuel Processing Technology, 86 (12-13): 1385-1401. DOI:10.1016/j.fuproc.2005.03.002.

TCEB, (2017). http://www.shamrockconferences.net/energy2017/presentations/energy17-04.pdf. Thar Coal Energy Board. (Accessed on March 2020).

TCEB, (2021) https://www.tceb.gos.pk/thar-coalfield/. Thar Coal Energy Board. (Accessed 13 March 2021).

Tchapda, A. H. and Pisupati S. V. (2014). A review of thermo conversion of coal and biomass/ waste. Energies (MDPI), 7 (3): 1098-1148. ISSN 1996-1073. DOI: 10.3390/en7031098.

Tian, Z. F., Witt, P. J., Schwarz M. P. and Yang W. (2016). *Numerical Modelling of Pulverized Coal Combustion*. Springer Nature Singapore Pvt. Ltd. G.H. Yeoh (ed.), Handbook of Multiphase Flow Science and Technology. DOI 10.1007/978-981-4585-86-6_9-1.

Tillman, D. A. (2000). Biomass cofiring: the technology, the experience, the combustion consequences. *Biomass and Bioenergy*, 19 (6): 365-384. https://doi.org/10.1016/S0961-9534(00)00049-0.

Tiwari, P. and Deo, M. (2012). Compositional and Kinetics analysis of oil shale pyrolysis using TGA-MS. Fuel, 94: 333-341. ISSN 0016-2361. https://doi.org/10.1016/j.fuel.2011.09.018.

Tomeczek, J. (1994). *Coal Combustion*. Krieger Publishing Company. United States. 167 pp. ISBN 0 89464 6516.

Tora, E. A. and Dahliquest, E. (2015). CFD ANSYS Fluent Simulation of Prevention of Dioxins Formation via Controlling Homogeneous Mass and Heat Transfer within Circulated Fluidized Bed Combustor. *Energy Procedia*, 75: 130- 136. https://doi.org/10.1016/j.egypro.2015.07.236.

Trinks, W., Mawhinney, M.H., Shannon, R.A., Reed, R.J., Garvey, J.R. (2004). *Industrial Furnaces.* John Wiley & Sons, Inc.: Hoboken, NJ, USA, 2004. ISBN: 978-0-471-38706-0.

Ullah, S.M., Zahid, U., Masood, T., (2019). Ultimate and Proximate Analysis of Coal Samples from Different Regions in Pakistan for their Future Utilization. Journal of Heterocyclics, 1 (1): 39-41. ISSN: 2639-6734. https://doi.org/10.33805/2639-6734.106.

Usto, M. A., Jarwar, A. I., Maitlo, G., Qureshi, S. A., Abbasi, S. A., Alam, S., Hashmi, Z., Shah, A. K., Shah, A. A., Jatoi, A. S., Kandharo, G. A., Memon, S. R. (2021). Desulfurization of Thar Lignite by Oxidative Alkali Leaching Under Pressure. *International Journal of Coal Preparation and Utilization*. DOI: 10.1080/19392699.2021.1965589.

Valasai, G. D, Uqaili, M. A, Memon, H. R., Samoo S. R., Mirjat, N. H., Harijan, K. (2017). Overcoming electricity crisis in Pakistan: A review of sustainable electricity options. Renewable and Sustainable *Energy Reviews*, 72: 734–745. https://doi.org/10.1016/j.rser.2017.01.097.

Vatanakul, M., Zheng, Y., Jia, L., Zhang, K. (2005). Regime transition in a gas-liquid-solid fluidized bed. *Chemical Engineering Journal*, 108 (1–2): 35–45. ISSN 1385-8947. https://doi.org/10.1016/j.cej.2004.12.035.

Vejahati, F., Xu, Z., and Gupta, R. (2010). Trace elements in coal: Associations with coal and minerals and their behavior during coal utilization–A review. *Fuel*, 89 (4): 904-911. ISSN 0016-2361. https://doi.org/10.1016/j.fuel.2009.06.013.

Vivekananda, M., Anantharaman, N. and Premalatha, M. (2019). The Hydrodynamics Studies on Loop Seal in CFBC Boiler Using CFD Analysis. Chemical Product and Process Modeling. *Chemical Product and Process Modeling.* 15 (1). DOI: 10.1515/cppm-2019-0031.

Vuthaluru, H. B. (2004). Investigations into the pyrolytic behavior of coal/biomass blends using Thermogravimetric blends. Bioresource Technology 92 (2): 187-195. https://doi.org/10.1016/j.biortech.2003.08.008.

Vyas, V. D. and Jani, D. B. (2017). CFD Simulation of Air Flow in CFBC Boiler under Different Geometry of Nozzle Grid. *International Journal for Research in Applied Science & Engineering Technology (IJRASET)*, 5 (V): 437-443. ISSN: 2321-9653.

Wahab A., Sattar H., Ashraf A., Hussain S. N., Saleem M., Munir S. (2020). Thermochemical, kinetic and ash characteristics behaviour of Thar Lignite, agricultural residues and synthetic polymer waste (EVA). *Fuel*, (266), 117151. https://doi.org/10.1016/j.fuel.2020.117151.

Walter, H. and Epple, B. (Eds.) (2017). *Numerical Simulation of Power Plants and Firing Systems.* Springer-Verlag Wien, Vienna. ISBN: 978-3-7091-4855-6. https://doi.org/10.1007/978-3-7091-4855-6.

Wang, C. (2013). *High density gas-solids circulating fluidized bed riser and downer reactors*. Electronic Thesis and Dissertation Repository. 1572. The University of Western Ontario.

Wang, G., Yang, F., Wu, K., Ma, Y., Peng C., Liu, T., Wang, L. P. (2021). Estimation of the dissipation rate of turbulent kinetic energy: A review. *Chemical Engineering Science*, 229: 116133. ISSN 0009-2509. https://doi.org/10.1016/j.ces.2020.116133.

Wang, M., Lan, X., Wang, C., Gao, J., Yu, A., Kuang, S. (2021). Numerical simulation of the pilot-scale high-density circulating fluidized bed riser. *Industrial and Engineering Chemistry Research*, 60 (7), 3184–3197. https://doi.org/10.1021/acs.iecr.1c00170.

Wang, P., Hedges, S. W., Casleton, K., Guenther, C. (2012). Thermal behavior of coal and Biomass blends in inert and oxidizing gaseous environments. International Journal of Clean Coal and Energy, 1 (3): 35-42. http://dx.doi.org/10.4236/ijcce.2012.13004.

Wang, X. S., Gibbs, B. M., J., R. M. and Akhtar, N.A. (1993). Fate of NOx in a circulating fluidized bed burning coal. *Institute of Energy's, in the proceedings of the First International Conference on Combustion and Emissions Control*. Cardiff, UK.

Wang, Y., Yan, L. (2008). CFD studies on biomass thermo chemical conversion. *Internationals journal of molecular sciences*, 9 (6): 1108 – 1130. DOI:10.3390/ijms9061108.

Wang, Z. & Li, J. (2018). Numerical study of rice husk and coal co-combustion characteristics in a circulating fluidized bed. *IOP Conference Series: Earth and Environmental Science. 113 (1): 012233*, Harbin, China. DOI:10.1088/1755-1315/113/1/012233.

Wankhede, U.S., Adgulkar D. D. (2008). CFD Simulations of heat transfer in a bubbling fluidized bed for different materials. *1st International Conference on Emerging Trends in Engineering and Technology* (Nagpur, India): 1094–1098.

Waters, P. L. (1975). Factors influencing fluidized combustion of low-grade solid and liquid fuels. *Symposium Series 1, Institute of Fuel*, London, p.C6-3.

WCA, (2021). *Coal & electricity*. World Coal Association. https://www.worldcoal.org/coal-facts/coal-electricity/. (Accessed on 5th January 2022).

WEC, (2004). World Energy Council in Survey of energy resources. World Energy Council. Available at: https://www.worldenergy.org/assets/downloads/PUB_Survey-of-Energy-Resources_2004_WEC.pdf.

Wei, C., Siva, S. Thanapal, K., Annamalai, R., James, A., Mustafa M. (2013). Co-Gasification of Mesquite and Coal Blend in an Updraft Fixed Bed Gasifier. *Journal of Sustainable Bioenergy Systems (SCIRP),* 3 (0): 234-241. DOI: 10.4236/jsbs.2013.33032.

Werther, J., Ogada, T., and Philippek, C. (1995). N_2O Emissions from the Fluidized-Bed Combustion of Sewage Sludge's. *Journal of the Institute of Energy*, 68 (475): 93-101.

Werther, J., Senger, M., Hartge, E.U., Ogada, T., and Siagi, Z. (2000). Combustion of agricultural residues. *Progress in Energy and Combustion Science*, 26 (1): 1-27.

Wijayanto, R. M., Sudarmanta, B., Syaifudin, A. and Nugroho, G. (2018). CFD Simulation of Circulating Fluidized Bed Boiler 30 MW: Effect of Primary and Secondary Air Distribution on Fluidization Behavior. *Proceedings of the 3rd*

International Conference on Mechanical Engineering (ICOME 2017), AIP Conf. Proc. 1983: 020018-1–020018-9. https://doi.org/10.1063/1.5046214.

Williams, A., backreedy, R., Habib, R., Jones, M., Porkashanian, M. (2002). Modeling coal combustion: the current position. Fuel 81 (5): 605-618. ISSN 0016-2361. https://doi.org/10.1016/S0016-2361(01)00158-2.

Williams, A., Pourkashanian M., Jones J. (2001).Combustion of pulverized coal and biomass. *Progress in Energy and Combustion Science*, 27 (6): 587-610. ISSN 0360-1285. https://doi.org/10.1016/S0360-1285(01)00004-1.

World Bank, (2016). *Biomass Resource Mapping in Pakistan*: Final Report on Biomass Atlas. World Bank, Washington, DC. https://openknowledge.worldbank.org/handle/10986/24918. License: CC BY 3.0 IGO.

World Coal Association, (2021). *Coal Facts*. Available at: https://www.worldcoal.org/coal-facts/.

Xie, J., Zhong, W., Jin, B., Shao, Y., Huang, Y. (2013). Eulerian–Lagrangian method for three-dimensional simulation of fluidized bed coal gasification. *Advanced Powder Technology*, 24 (1) :382-392. https://doi.org/10.1016/j.apt.2012.09.001.

Xie, J., Zhong, W., Yu, A. (2018). MP-PIC modelling of CFB risers with homogeneous and heterogeneous drag models. *Advanced Powder Technology*, 29 (11): 2859–2871. https://doi.org/10.1016/j.apt.2018.08.007.

Xu, L., Cheng, L., Ji, J., Wang, Q. A. (2019). Comprehensive CFD combustion model for supercritical CFB boilers. *Particuology*, 43: 29–37. https://doi.org/10.1016/j.partic.2017.11.012.

Xu, S., Zhou Z., Gao X., Yu G., Gong X. (2009). The gasification reactivity of unburned carbon present in gasification slag from entrained-flow gasifier. *Fuel Processing Technology*, 90 (9): 1062-1070. ISSN 0378-3820. https://doi.org/10.1016/j.fuproc.2009.04.006.

Xu, Y., Yang, K., Zhou, J., Zhao, G. (2020). Coal-Biomass Co-Firing Power Generation Technology: Current Status, Challenges and Policy Implications. *Sustainability*, 12 (9): 3692. https://doi.org/10.3390/su12093692.

Yan, Y., Liu, Y., Huang, L., Li, J. (2018). Effects of Inlet Parameters on Combustion Performance in Gas Turbine Combustor. *International Journal of Turbo & Jet-Engines*, 35 (4): 339-350. https://doi.org/10.1515/tjj-2016-0058.

Yang, N., Wang, W., Ge, W., Li, J. (2003). CFD Simulation of Con-current-up Gas-Solid Flow in Circulation Fluidized Beds with Structure-Dependent Drag Coefficient. Chemical Engineering Journal, 96 (1-3): 71-80. ISSN 1385-8947. https://doi.org/10.1016/j.cej.2003.08.006.

Yang, N., Wang, W., Ge, W., Wang, L., Li, J. (2004). Simulation of Heterogeneous Structure in a Circulation Fluidized-Bed Riser by Combining the Two-Fluid Model with the EMMS Approach. *Industrial & Engineering Chemistry Research*, 43 (18): 5548-5561. https://doi.org/10.1021/ie049773c.

Yang, R. T., Krishana, C. R., Steinburg, M. (1977). Fluidized bed coal combustion with lime additives. The Phenomenon of Peaking of Sulfur Retention at a Certain Temperature. *Industrial & Engineering Chemistry Fundamentals*, 16 (4): 465-467. https://doi.org/10.1021/i160064a012.

Yang, S. and Wang, S. (2020). Shape Effect of the Riser Cross Section on the Full-Loop Hydrodynamics of a Three-Dimensional Circulating Fluidized Bed. *ACS Omega*, 5 (11): 5784-5795. https://doi.org/10.1021/acsomega.9b03903.

You, C.F. and Xu, X.C. (2010). Coal combustion and its pollution control in China. *Energy*, 35 (11): 4467-4472. https://doi.org/10.1016/j.energy.2009.04.019.

Youchou, L. and Kwauk, M. (1980). *The dynamics of fast fluidization*. In: Grace, J.R., Matsen, J.M. (eds) Fluidization. Springer, Boston, MA. ISBN 978-1-4684-1047-1. https://doi.org/10.1007/978-1-4684-1045-7_57.

Yuan Y., He Y., Tan J., Wang Y., Kumar S., Wang Z. (2021). Co-Combustion Characteristics of Typical Biomass and Coal Blends by Thermo gravimetric Analysis. *Frontiers in Energy Research*, 9:753622. ISSN=2296-598X. https://doi.org/10.3389/fenrg.2021.753622.

Yuan L.Y., Zhong W.Q., Chen X., Li J., Liu G.Y., Tian W.J. (2019). Three-dimensional numerical simulation of variable load combustion of supercritical coal-

fired boiler for deep peak load regulation. *JSEU (Natural Science Edition)*, 49: 535–541.

Yurdakul, Y. S. and Atimtay A. T. (2009). Investigation of combustion kinetics of treated and untreated wood waste samples with thermogravimetric analysis. *Fuel Processing Technology*, 90 (7-8): 939-946. ISSN 0378-3820. https://doi.org/10.1016/j.fuproc.2009.02.010.

Zabetta, E.C., Hupa, M., Saviharju, K. (2005). Reducing NOx emissions using fuel staging, air staging, and selective no catalytic reduction in synergy. *Industrial & Engineering Chemistry Research*, 44 (13): 4552-4561. https://doi.org/10.1021/ie050051a.

Zaigham, N. A. and Nayyar, Z., (2005). Prospects of renewable energy sources in Pakistan. *Renewable Energy Technologies and Sustainable Development*, pp. 65-86.

Zhang, N., Lu, B., Wang, W., Li, J. (2010). 3D CFD simulation of hydrodynamics of a 150MWe circulating fluidized bed boiler. *Chemical Engineering Journal*, 162 (2): 821–828. DOI: 10.1016/j.cej.2010.06.033.

Zhang, X. (2019). *Support mechanisms for cofiring biomass with coal*. CCC/294, London, UK, IEA Clean Coal Centre, 60 pp.

Zhang, X. (2021a). *Blended Firing of Coal and Lignite. International Centre for Sustainable Carbon*. International Centre for Sustainable Carbon. ICSC Report # ICSC/316. ISBN 978–92–9029–639-3.

Zhang, X. and Meloni, S. (2020). *Technology Developments in The Cofiring of Biomass*. IEA Clean Coal Center. IEACCC Report # CCC/305. ISBN 978–92–9029–628-7.

Zhang, Y., Lei, F. and Xiao, Y. (2015). Computational fluid dynamics simulation and parametric study of coal gasification in a circulating fluidized bed reactor. *Asia-Pac. J. Chem. Eng.*, 10 (2): 307–317. https://doi.org/10.1002/apj.1878.

Zhang, Y., Ren, P., Li, W., Yu, K. (2021b). Turbulent mass transfer model for the simulation of liquid-solid CFB risers and its verification. *Powder Technology*, 377: 847-856, ISSN 0032-5910. https://doi.org/10.1016/j.powtec.2020.09.050.

Zhao, J, Grace, J. R., Lim, C.J., Brereton C. M. H., Legros,R. (1994). The influence of operating parameters on NOx emission from a circulating fluidized bed combustor. Fuel, 73 (10): 1650-1657. ISSN 0016-2361. https://doi.org/10.1016/0016-2361(94)90146-5.

Zhao, Jiangming (2021). *Novel Peridynamic Models for Material Degradation and Mass Transport*. Mechanical and Materials Engineering, Doctoral Dissertation, University of Nebraska-Lincoln. https://digitalcommons.unl.edu/mechengdiss/179.

Zheng L. (2011). Oxy-fuel combustion for power generation and carbon dioxide (CO_2) capture. 1st Edition, Woodhead Publishing Limited. ISBN: 978-1-84569-671-9.

Ziqu, O., Wen, L., Jianguo, Z., Jingzhang, L., Chengbo, M. (2018). Experimental research on combustion characteristics of coal gasification fly ash in a combustion chamber with a self-preheating burner. Fuel, 215: 378-385. https://doi.org/10.1016/j.fuel.2017.11.047.

Zixiang L., Zhengqing M., Xusheng S., Jiangtao Li. (2018). Effects of momentum ratio and velocity difference on combustion performance in lignite-fired pulverized boiler. *Energy*, 165 (A): 825-839. ISSN 0360-5442. https://doi.org/10.1016/j.energy.2018.09.082.

Zuo H., Geng W., Zhang J., Wang G. (2015). Comparison of kinetic models for isothermal CO2 gasification of coal char–biomass char blended char. *Int. J. Miner. Metall. Mater*., 22 (4): 363. https://doi.org/10.1007/s12613-015-1081-3.

APPENDIX A

Proximate Analysis Block-II Data					
Sample No.	As Received (AR) Basis %				Gross Calorific Value kcal/Kg
	Moisture	Ash	Volatile Matter	Fixed Carbon	
1	43.91	5.52	31.82	18.75	2871.0
2	45.96	5.40	30.39	18.25	2964.0
3	44.08	5.49	29.91	20.52	2027.0
4	45.43	6.43	27.36	20.78	2348.0
5	46.11	5.25	30.09	18.55	2916
6	47.46	5.38	28.06	19.10	2764.0
7	45.84	5.83	30.59	17.74	3178
8	48.71	7.78	26.97	16.54	2461.9
9	48.45	6.74	27.76	17.05	2571.9
10	43.94	4.79	31.34	19.93	2665.8
11	50.08	5.62	27.88	16.42	2768.0
12	45.37	8.01	28.78	17.84	2218.4
13	42.06	5.38	30.99	21.57	3184.7
14	43.32	6.81	30.52	19.35	2980.2
15	44.04	5.14	33.05	17.77	3118.6
16	42.10	4.80	32.08	21.02	2956.3
17	47.54	6.41	28.67	17.38	2729.7
18	48.40	4.99	30.26	16.35	2785.2
19	44.06	6.57	27.52	21.85	2959.7
20	45.99	6.61	28.55	18.85	2684.7
21	46.18	9.54	25.25	19.03	3608.0
22	44.48	7.25	29.15	19.12	3351.7

23	42.33	5.59	34.37	17.71	3350.2
24	47.30	5.45	29.13	18.12	3687.6
25	45.37	5.04	31.95	17.64	3652.7
26	47.34	8.26	27.92	16.48	2846.9
27	45.08	4.98	30.18	19.76	3189.7
28	44.26	4.26	28.62	22.86	3394.2
29	43.89	7.18	29.42	19.51	2440.2
30	46.15	6.48	30.68	16.69	3118.6
31	46.6	8.77	27.96	16.67	2688.5
32	45.55	10.38	27.31	16.76	2859.1
33	48.97	6.71	27.38	16.94	3273.3
34	42.47	6.15	29.82	21.56	3429.2
35	45.27	9.56	28.43	16.74	2567.4
36	48.01	6.02	28.99	16.98	3391.4
37	45.32	6.01	31.28	17.39	3230.3
38	43.92	5.31	32.05	18.72	3241.4
39	46.80	5.53	30.59	17.08	3281.9
40	46.47	8.34	27.82	17.37	3132.5
41	45.82	7.02	28.63	18.53	2945.2
42	46.67	5.35	28.27	19.71	3107.8
43	45.46	8.10	27.83	18.61	2786.1
44	49.33	5.37	27.87	17.43	2906.3
45	44.84	8.57	27.58	19.01	3007.1
46	43.31	6.54	30.27	19.88	3064.0
47	45.30	8.25	27.75	18.70	3096.8
48	46.95	4.77	27.02	21.26	3314.7
49	47.03	8.33	25.86	18.78	3430.9
50	43.92	6.12	29.11	20.85	3170.2
51	42.52	7.66	28.50	21.32	2976.8
52	46.80	6.90	28.38	17.92	3318.0
53	47.59	5.31	29.09	18.01	3451.7
54	46.75	10.21	25.65	17.39	2887.3
55	43.49	6.74	29.71	20.06	2918.1
56	45.91	7.16	29.14	17.79	2755.2
57	46.31	5.13	28.18	20.38	2945.2
58	47.47	5.46	30.05	17.02	3708.9
59	50.15	6.52	26.36	16.97	3257.1
60	42.09	4.82	35.05	18.04	3442.6
61	46.82	5.54	30.58	17.06	3495.7
62	47.60	5.29	29.02	18.09	2981.8
63	42.96	5.07	27.05	24.92	2955.1
64	47.50	5.34	30.22	16.94	3577.0

65	48.23	7.65	27.32	16.80	2804.9
66	45.89	4.84	29.21	20.06	3460.5
67	47.98	5.20	29.91	16.91	3499.8
68	46.81	6.20	28.18	18.81	3284.5
69	49.45	7.88	25.67	17.00	2833.3
70	50.01	5.37	26.53	18.09	2999.9
71	47.21	8.14	28.37	16.28	2563.9
72	50.62	5.33	25.49	18.56	2974.2
73	48.66	5.35	26.34	19.65	3459.8
74	47.43	6.27	27.62	18.68	3025.8
75	50.10	7.28	25.56	17.06	2706.7
76	48.30	9.11	26.33	16.26	2539.3
77	47.47	7.34	28.07	17.12	2879.2
78	46.36	6.07	30.92	16.65	2638.5
79	50.07	5.34	27.38	17.21	3067.4
80	49.16	4.80	26.84	19.20	3273.6
Min.	**42.06**	**4.26**	**25.25**	**16.26**	**2027.0**
Max.	**50.62**	**10.38**	**35.05**	**24.92**	**3708.9**
Mean	**46.26**	**6.42**	**28.85**	**18.47**	**3030.0**

APPENDIX B

Ultimate Analysis Block-II Data					
As Received (AR) Basis %					
Sample No.	**Carbon**	**Hydrogen**	**Nitrogen**	**Sulfur**	**Oxygen**
1	35.89	7.22	0.31	2.04	37.84
2	35.0	6.67	0.48	1.66	38.57
3	35.83	6.10	0.45	1.64	37.63
4	37.71	7.83	0.34	0.92	38.19
5	38.45	6.7	0.53	0.63	36.45
6	37.68	6.89	0.38	1.57	38.08
7	38.39	6.94	0.49	0.54	43.86
8	40.79	7.92	0.27	0.60	37.34
9	36.29	6.55	0.46	0.59	40.10
10	37.69	6.71	0.44	0.54	39.80
11	38.89	7.1	0.41	0.60	40.46
12	37.56	7.12	0.37	0.48	40.48
13	38.92	7.2	0.35	0.49	39.87
14	37.98	6.51	0.44	0.59	40.03
15	30.41	5.9	0.26	1.29	40.61
16	28.98	5.54	0.24	1.33	43.59
17	34.61	6.43	0.29	1.03	35.22
18	32.54	7.46	0.31	2.39	39.99
19	35.54	6.5	0.22	2.17	34.51
20	33.42	6.54	0.18	1.21	34.47
21	37.01	7.53	0.20	0.51	41.24
22	35.14	7.13	0.17	0.57	37.99

23	33.56	6.69	0.43	1.01	41.06
24	36.73	7.53	0.58	1.51	35.38
25	35.68	6.96	0.23	0.66	41.11
26	37.97	6.63	0.19	1.46	35.40
27	37.77	6.82	0.25	2.01	35.70
28	33.55	7.36	0.21	0.44	40.24
29	32.08	7.55	0.20	0.55	48.01
30	34.97	7.47	0.19	0.72	41.47
31	34.37	6.15	0.24	0.98	41.93
32	29.22	5.66	0.12	0.65	48.01
33	33.52	7.09	0.19	0.67	41.47
34	33.61	6.67	0.13	0.52	42.89
35	28.91	5.63	0.26	0.70	48.86
36	34.84	6.98	0.30	1.30	35.90
37	27.12	5.01	0.21	0.70	43.31
38	26.71	6.05	0.19	2.02	39.14
39	29.65	6.88	0.29	1.53	42.81
40	33.01	7.37	0.11	2.43	43.94
41	31.87	6.86	0.13	1.76	37.67
42	32.36	6.94	0.11	1.05	42.81
43	28.83	6.26	0.18	0.52	39.03
44	34.41	7.21	0.18	1.49	36.66
45	32.07	6.84	0.17	2.90	37.85
46	30.75	7.19	0.18	0.65	41.02
47	35.08	7.09	0.18	1.04	33.44
48	31.74	7.44	0.16	1.77	44.34
49	32.42	6.77	0.15	0.69	39.86
50	34.08	7.16	0.24	1.42	39.76
51	32.84	7.61	0.13	0.70	44.08
52	27.42	7.05	0.16	0.46	44.50
53	36.18	7.25	0.21	0.86	37.86
54	34.84	7.37	0.24	0.62	37.60
55	34.34	7.83	0.22	0.55	43.54
56	30.63	7.10	0.33	0.58	42.10
57	33.55	7.56	0.37	0.92	44.13
58	36.73	7.40	0.18	0.84	35.35
59	36.67	7.58	0.20	0.46	40.73
60	34.47	7.97	0.19	0.58	47.44
61	35.32	7.99	0.15	0.56	46.44
62	33.67	7.77	0.15	0.90	44.76
63	32.85	8.00	0.17	0.70	48.82
64	31.22	7.74	0.25	0.66	48.31

65	32.04	7.46	0.19	0.69	40.94
66	30.40	7.90	0.22	0.89	48.29
67	27.19	7.20	0.15	0.61	47.94
68	29.78	6.08	0.25	0.81	41.06
69	31.18	8.19	0.31	0.37	49.80
70	33.51	7.63	0.34	1.57	40.50
71	32.96	6.45	0.26	0.73	44.32
72	31.47	6.15	0.28	0.61	49.28
73	30.90	8.23	0.29	0.26	46.70
74	32.70	6.24	0.29	0.49	48.92
75	38.36	5.58	0.33	0.62	45.27
76	36.98	5.43	0.35	0.50	44.70
77	38.30	5.66	0.34	0.51	46.90
78	30.52	7.88	0.34	0.28	47.80
79	32.52	5.6	0.27	0.52	44.15
80	30.03	7.61	0.31	0.41	48.59
Min.	**26.71**	**5.01**	**0.11**	**0.26**	**33.44**
Max.	**40.79**	**8.23**	**0.58**	**2.90**	**49.80**
Mean	**33.76**	**6.95**	**0.26**	**0.95**	**41.70**

APPENDIX C

Ash Analysis Thar Block-II DATA							
Sample No.	**SiO_2**	**Al_2O_3**	**Fe_2O_3**	**CaO**	**MgO**	**Na_2O**	**K_2O**
1	15.68	9.54	7.16	7.78	2.27	8.94	0.81
2	24.89	13.82	11.14	4.39	3.17	5.94	1.02
3	26.55	17.43	16.29	5.18	2.92	3.41	0.82
4	32.10	24.56	11.29	9.27	3.67	0.48	0.62
5	33.14	22.64	9.37	6.28	4.32	1.38	0.47
6	31.84	16.96	18.84	7.71	3.86	2.37	0.23
7	33.91	23.24	11.14	7.08	5.10	3.37	0.17
8	19.41	12.53	9.87	8.22	5.96	3.25	0.54
9	33.93	18.37	7.77	8.53	4.80	4.73	0.39
10	27.15	17.50	18.50	5.00	3.10	3.00	0.32
11	36.08	6.76	7.23	1.95	1.58	6.38	0.59
12	18.80	7.54	13.1	4.45	1.45	4.20	0.53
13	32.54	16.62	4.23	0.50	0.43	4.51	0.59
14	21.54	7.73	20.35	1.79	2.22	5.62	0.89
15	22.07	14.83	3.15	4.62	4.59	8.35	1.01
16	39.58	22.93	3.03	0.16	0.14	2.07	0.73
17	26.24	17.74	14.62	2.09	2.60	7.30	0.89
18	18.79	6.81	17.52	5.63	3.25	5.88	0.77
19	32.77	20.55	15.35	2.9	2.78	4.21	2.03
20	14.75	8.63	19.53	1.32	1.14	0.58	0.68
21	22.53	16.50	19.89	0.43	0.34	1.91	0.62
22	25.56	24.27	17.73	1.72	3.46	5.15	0.74
23	22.24	13.03	4.02	0.24	0.55	2.02	0.71
24	25.47	16.39	4.00	0.28	0.68	3.81	0.41

25	41.88	21.56	16.76	1.57	1.80	5.77	1.44
26	25.71	13.76	8.21	1.26	1.43	4.22	0.83
27	17.47	7.06	15.37	2.03	2.71	4.24	0.57
28	13.84	7.60	5.92	2.16	2.86	5.06	0.76
29	38.48	25.95	3.30	0.53	0.68	7.01	0.52
30	13.45	6.41	13.79	3.19	3.28	2.67	0.56
31	30.05	17.01	12.71	0.37	0.41	3.97	0.43
32	16.77	11.50	20.9	1.03	1.41	4.23	0.58
33	16.56	9.15	20.93	1.12	1.42	6.33	0.46
34	27.31	12.65	20.4	0.99	0.97	5.75	0.52
35	22.78	14.51	9.75	0.67	0.56	4.33	0.47
36	13.25	8.62	15.14	2.04	2.84	6.61	0.49
37	38.54	13.55	12.77	1.88	2.21	7.97	0.69
38	31.86	7.41	10.95	1.37	1.29	6.62	0.62
39	22.97	16.86	11.02	2.39	3.25	9.85	0.61
40	14.56	10.51	8.8	9.24	5.61	9.79	0.96
41	47.04	12.54	7.16	1.78	1.27	8.94	0.81
42	19.02	12.79	13.85	3.68	3.65	9.62	1.09
43	27.36	22.57	4.62	0.35	0.11	3.55	0.44
44	33.16	21.34	12.13	0.62	0.15	3.99	0.46
45	23.18	15.34	7.75	1.99	2.86	5.16	0.59
46	31.91	17.00	14.11	0.87	0.42	4.35	0.55
47	36.65	12.97	20.21	2.24	1.48	7.85	0.86
48	24.18	14.73	6.48	0.73	0.40	4.33	0.44
49	36.86	24.47	9.09	0.42	0.19	3.83	0.5
50	15.33	10.43	3.42	0.94	0.76	4.74	0.46
51	18.78	6.86	6.37	1.74	0.48	1.62	0.35
52	15.20	8.36	6.76	0.5	0.31	1.15	0.35
53	14.93	8.48	3.08	0.78	0.76	2.51	0.43
54	12.16	12.38	7.88	0.69	0.62	2.8	0.41
55	22.92	22.22	5.67	0.3	0.16	1.84	0.55
56	15.88	12.98	12.28	3.21	4.00	7.59	1.15
57	13.82	9.29	3.45	0.8	0.80	3.00	0.50
58	17.65	16.5	3.79	6.33	4.08	7.02	0.41
59	14.53	14.9	18.16	3.35	5.84	7.22	0.91
60	20.88	19.97	8.48	2.26	3.75	6.19	1.07
61	33.06	25.34	7.74	0.57	0.72	4.70	0.51
62	14.36	23.11	5.18	0.29	0.09	3.19	0.51
63	15.64	8.11	17.58	0.58	0.28	2.79	0.35
64	12.14	10.11	6.90	0.56	0.36	3.78	0.33
65	24.34	22.05	20.19	0.61	0.40	4.43	0.40
66	31.32	19.91	7.39	0.48	0.26	4.12	0.39

67	26.46	11.8	15.8	1.26	0.92	5.55	0.47
68	18.24	8.18	6.51	7.72	5.48	6.68	0.55
69	17.55	7.65	6.07	2.3	2.45	5.56	0.41
70	13.54	11.71	3.12	3.37	3.23	9.03	0.76
71	16.38	14.49	12.53	7.01	6.17	8.14	0.89
72	24.50	14.2	10.52	3.97	4.90	9.36	0.94
73	12.37	8.44	20.65	5.38	4.36	5.95	0.68
74	18.51	11.85	7.90	2.4	3.58	6.64	0.51
75	18.44	14.77	12.08	4.33	5.19	7.12	0.54
76	28.69	20.67	10.46	1.05	1.48	6.27	0.55
77	32.18	21.96	20.92	0.77	1.02	5.09	0.49
78	12.16	8.93	12.22	2.54	3.07	6.00	0.46
79	13.50	9.62	4.07	6.59	5.27	6.83	0.56
80	19.57	11.53	5.71	6.39	5.86	8.45	0.65
Min.	**12.14**	**6.41**	**3.03**	**0.16**	**0.09**	**0.48**	**0.17**
Max.	**47.04**	**25.95**	**20.93**	**9.27**	**6.17**	**9.85**	**2.03**
Mean	**23.59**	**14.52**	**11.00**	**2.76**	**2.30**	**5.13**	**0.63**